B. Cameron Reed

The Physics
of the Manhattan
Project

Second Edition

 Springer

The Physics of the
Manhattan Project

B. Cameron Reed

The Physics of the Manhattan Project

B. Cameron Reed
Alma College
Department of Physics
Alma, Michigan 48801
USA
reed@alma.edu

Cover illustration: Mushroom cloud of the Trinity test, Monday, July 16, 1945. The yield of this im-plosion-triggered plutonium fission bomb is estimated at 21 kilotons. This is the only color photograph taken of the Trinity test. Photo by Jack Aeby courtesy of the Los Alamos National Laboratory.

Cover design: eStudio Calamar S.L.

Printed on acid-free paper

This work is dedicated to my wife Laurie,
whose love knows no half-life.

Preface

The scientific, social, political, and military implications of the development of nuclear weapons under the auspices of the United States Army's "Manhattan Project" in World War II drove much of world geopolitical strategy for the last half of the twentieth century. These implications remain with us today in the form of ongoing concerns and debates regarding issues such as weapons stockpiles and deployments, proliferation, fissile material security and test-ban treaties. For better or worse, the historical legacy of Los Alamos, Oak Ridge, Hanford, *Trinity*, *Little Boy*, *Fat Man*, Hiroshima and Nagasaki will influence events for decades to come even as the number of nuclear weapons in the world continues to decline.

While even a casual observer of the world situation cannot help but be aware that the idea of terrorists or unstable international players being able to acquire enough "fissile material" to assemble the "critical mass" necessary to construct a nuclear weapon is of concern, popular understanding of the history and science of nuclear weapons is extremely limited. Even most physics and engineering graduates probably have no deeper appreciation of the science underlying these weapons than a typical high-school student. Why is there is such a thing as a critical mass in the first place, and how can one determine it? How does a reactor differ from a weapon? Why can't a nuclear weapon be made with a common metal such as aluminum or iron as its "active ingredient"? How did the properties of various uranium and plutonium isotopes lead in World War II to the development of "gun-type" and "implosion" weapons? How can one estimate the energy yield of these devices? How does one arrange to assemble the critical mass at just the time when a bomb is to be detonated?

This book is an effort to address such questions. It covers, at about the level of a junior-year undergraduate physics major, the basic physics underlying fission weapons as they were developed during the Manhattan Project.

This work has grown out of three courses that I have taught at Alma College. One of these is a conventional undergraduate sophomore-level "modern physics" class for physics majors which contains a unit on nuclear physics, the second is an algebra-level general-education class on the history of the making of atomic bombs

in World War II, and the third a junior-level topics class for physics majors that uses the present volume as its text. My motivation in preparing this book was that there seemed to be no one source available for a reader with a college-level background in physics who desired to learn something of the technical aspects of the Manhattan Project in more detail than is typically presented in conventional modern/nuclear texts or popular histories. Readers are often left wondering about the details of questions such as outlined above. As my own knowledge of these issues grew, I began assembling an informal collection of derivations and results to share with my students and which have evolved into the present volume. I hope that readers will discover, as I did, that studying the physics of nuclear weapons is not only fascinating in its own right but also an excellent vehicle for reinforcing understanding of foundational physical principles such as energy, electromagnetism, dynamics, statistical mechanics, modern physics, and of course nuclear physics.

This book is consequently neither a conventional text nor a work of history. I assume that readers are already familiar with the basic history of some of the physics that led to the Manhattan Project and how the project itself was organized (Fig. 1). Excellent background sources are Richard Rhodes' masterful *The Making*
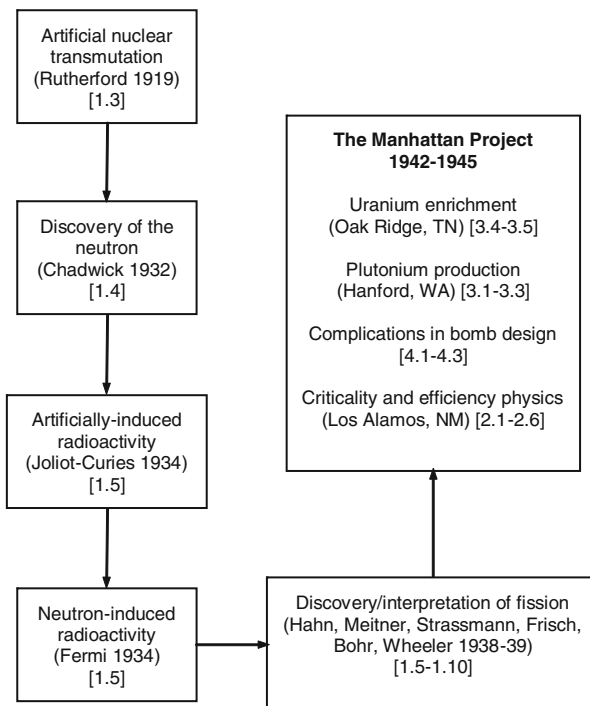

Fig. 1 Concept map of important discoveries in nuclear physics and the organization of the Manhattan Project. Numbers in *square brackets* indicate sections in this book where given topics are discussed

of the Atomic Bomb (1986) and F. G. Gosling's *The Manhattan Project: Making the Atomic Bomb* (1999). While I include some background material for sake of a reasonably self-contained treatment, it is assumed that within the area of nuclear physics readers will be familiar with concepts such as reactions, alpha and beta decay, Q-values, fission, isotopes, binding energy, the semi-empirical mass formula, cross-sections, and the concept of the "Coulomb barrier." Familiarity with multi-variable calculus and simple differential equations is also assumed. In reflection of my own interests (and understanding), the treatment here is restricted to World War II-era fission bombs. As I am neither a professional nuclear physicist nor a weapons designer, readers seeking information on postwar advances in bomb and reactor design and related issues such as isotope separation techniques will have to look elsewhere; a good source is Garwin and Charpak (2001). Similarly, this book does not treat the *effects* of nuclear weapons, for which authoritative official analyses are available (Glasstone and Dolan 1977). For readers seeking more extensive references, an annotated bibliography appears in Appendix I of the present book.

This book comprises 27 sections within five chapters. Chapter 1 examines some of the history of the discovery of the remarkable energy release in nuclear reactions, the discovery of the neutron, and characteristics of the fission process. Chapter 2 details how one can estimate both the critical mass of fissile material necessary for a fission weapon and the efficiency one might expect of a weapon that utilizes a given number of critical masses of such material. Aspects of producing the fissile material by separating uranium isotopes and synthesizing plutonium are taken up in Chap. 3. Chapter 4 examines some complicating factors that weapons engineers need to be aware of. Some miscellaneous calculations comprise Chap. 5. Useful data are summarized in Appendices A and B. Some background derivations are gathered in Appendices C–G. For readers wishing to try their own hand at calculations, Appendix H offers a number of questions, with brief answers provided. A bibliography for further reading is offered in Appendix I, and some useful constants and conversion factors appear in Appendix J. The order of the main chapters, and particularly the individual sections within them, proceeds in such a way that understanding of later ones sometimes depends on knowledge of earlier ones.

It should be emphasized that there is no material in the present work that cannot be gleaned from publicly-available texts, journals, and websites: I have no access to classified material.

I have developed spreadsheets for carrying out a number of the calculations described in this work, particularly those in Sects. 1.4, 1.7, 1.10, 2.2–2.5, 4.1, 4.2, and 5.3. These are freely available at a companion website, http://www.manhattanphysics.com. When spreadsheets are discussed in the text they are referred to in **bold** type. Users are encouraged to download these, check calculations for themselves, and run their own computations for different choices of parameters. A number of the problems in Appendix H are predicated on using these spreadsheets.

This book is the second edition of this work. The first edition was self-published with Trafford Publishing, and I am grateful for their very professional work. The present edition includes a number of new and revised sections. A discussion of

numerically estimating bomb yield and efficiency (Sect. 2.5), an analysis of Rudolf Peierls' criticality parameter (Sect. 2.6), development of a model for estimating Pu-240 production in a reactor (Sect. 5.3), and a formal derivation of the Bohr–Wheeler spontaneous fission limit (Appendix E) are completely new, as is a bibliography of books, articles, and websites dealing with the Manhattan Project (Appendix I). The discussion of predetonation probability as a consequence of spontaneous fission (Sect. 4.2) has been significantly upgraded, the analysis of estimating the average neutron escape probability from within a sphere has been revised (Appendix D), and some corrections have been made to the discussion of analytically estimating bomb efficiency (Sect. 2.4).

Over several years now, I have benefitted from discussions on this material with Gene Deci, Jeremy Bernstein, Harry Lustig, Carey Sublette, and Peter Zimmerman, and am grateful for their time and patience. I am grateful to John Coster-Mullen for permission to reproduce his beautiful cross-section diagrams of *Little Boy* and *Fat Man* that appear in Chaps. 2 and 4. Students in the first version of my topics class – Charles Cook, Reid Cuddy, David Jack and Adam Sypniewski – served as guinea pigs for these notes and pointed out a number of confusing statements. I owe a great debt of gratitude to Alma College for various forms of professional development support extending over many years.

Finally, I am grateful to the staff of Springer for helping to bring this project to fruition. Their efficiency and professionalism are nothing short of outstanding. Naturally, I claim exclusive ownership of any errors that remain.

Suggestions for corrections and additional material will be gratefully received. I can be reached at: Department of Physics, Alma College, Alma, MI 48801.

Alma, MI, USA   B. Cameron Reed
May 17, 2010

References

Garwin, R. L., Charpak, G.: Megawatts and Megatons: A Turning Point in the Nuclear Age? Alfred A. Knopf, New York (2001)

Glasstone, S., Dolan, P. J.: The Effects of Nuclear Weapons, 3rd edn. United States Department of Defense and Energy Research and Development Administration, Washington (1977)

Gosling, F. G.: The Manhattan Project: Making the Atomic Bomb. United States Department of Energy, Washington. Freely available online at http://www.osti.gov/accomplishments/documents/fullText/ACC0001.pdf (1999)

Rhodes, R.: The Making of the Atomic Bomb. Simon and Schuster, New York (1986)

Contents

Chapter 1
Energy Release in Nuclear Reactions, Neutrons, Fission, and Characteristics of Fission

Abstract This introductory chapter covers the background nuclear physics necessary for understanding later calculations of critical mass, nuclear weapon efficiency and yield, and how fissile materials are produced. It describes how the energy released in nuclear reactions can be calculated, how artificially-produced nuclear transmutations were discovered, the discovery of the neutron, artificially-produced radioactivity, the discovery and interpretation of neutron-induced nuclear fission, why only certain isotopes of uranium and plutonium are feasible for use in nuclear weapons, and how nuclear reactors differ from nuclear weapons.

While this book is not intended to be a history of nuclear physics, it will be helpful to set the stage by briefly reviewing some historically relevant discoveries. To this end, we first explore the discovery of the enormous energy release characteristic of nuclear reactions, work that goes back to Ernest Rutherford and his collaborators at the opening of the twentieth century; this is covered in Sect. 1.2. Rutherford also achieved, in 1919, the first artificial transmutation of an element (as opposed to this happening naturally, such as in an alpha-decay), an issue we examine in Sect. 1.3. Nuclear reactors and weapons cannot function without neutrons, so we devote Sect. 1.4 to a fairly detailed examination of James Chadwick's 1932 discovery of this fundamental constituent of nature. The neutron had almost been discovered by Irène and Frédéric Joliot–Curie, who misinterpreted their own experiments. They did, however, achieve the first instance of artificially inducing radioactive decay, a situation we examine in Sect. 1.5, which also contains a brief summary of events leading to the discovery of fission. In Sects. 1.6–1.10 we examine the release of energy and neutrons in fission, some theoretical aspects of fission, and delve into why only certain isotopes of heavy elements are suitable for use in fission weapons. Before doing any of these things, however, it is important to understand how physicists notate and calculate the energy liberated in nuclear reactions. This is the topic of Sect. 1.1.

1.1   Notational Conventions for Mass Excess and Q-Values

On many occasions we will need to compute the energy liberated in a nuclear reaction. Such energies are known as Q-values; this section develops convenient notational and computational conventions for dealing with such calculations.

Any reaction will involve *input* and *output* reactants. The total energy of any particular reactant is the sum of its kinetic energy and its relativistic mass-energy, mc^2. Since total mass-energy must be conserved, we can write

$$\sum KE_{input} + \sum m_{input}c^2 = \sum KE_{output} + \sum m_{output}c^2, \qquad (1.1)$$

where the sums are over the reactants; the masses are the *rest masses* of the reactants. The Q-value of a reaction is defined as the difference between the output and input kinetic energies:

$$Q = \sum KE_{output} - \sum KE_{input} = \left(\sum m_{input} - \sum m_{output} \right) c^2. \qquad (1.2)$$

If $Q > 0$, then the reaction liberates energy, whereas if $Q < 0$ the reaction demands a *threshold* energy to cause it to happen.

If the masses in (1.2) are in kg and c is in m/s, Q will emerge in Joules. However, rest masses are usually tabulated in atomic mass units (abbreviation: amu or simply u). If f is the number of kg in one amu, then we can put

$$Q = \left(\sum m_{input}^{(amu)} - \sum m_{output}^{(amu)} \right) fc^2. \qquad (1.3)$$

Q-values are conventionally quoted in MeV. If g is the number of MeV in 1 J, then Q in MeV for masses given in amu will be given by

$$Q = \left(\sum m_{input}^{(amu)} - \sum m_{output}^{(amu)} \right) \left(gfc^2 \right). \qquad (1.4)$$

Define $\varepsilon = gfc^2$. Recalling that 1 MeV $= 1.602176462 \times 10^{-13}$ J, then $g = 6.24150974 \times 10^{12}$ MeV/J. Putting in the numbers gives

$$\varepsilon = gfc^2 = \left(6.24150974 \times 10^{12} \frac{\text{MeV}}{\text{J}} \right) \times \left(1.66053873 \times 10^{-27} \frac{\text{kg}}{\text{amu}} \right)$$
$$\times \left(2.99792458 \times 10^8 \frac{\text{m}}{\text{s}} \right)^2 = 931.494 \frac{MeV}{\text{amu}}. \qquad (1.5)$$

More precisely, this number is 931.494013. Thus, we can write (1.4) as

$$Q = \left(\sum m_{input}^{(amu)} - \sum m_{output}^{(amu)} \right) \varepsilon, \tag{1.6}$$

where $\varepsilon = 931.494$ MeV/amu. Equation (1.6) will give Q-values in MeV when the masses are in amu.

Now consider an individual reactant of mass number A. The *mass excess* μ of this species is defined as the number of amu that has to be added to A amu (as an integer) to give the actual mass (in amu) of the species:

$$m^{(amu)} = A + \mu. \tag{1.7}$$

Substituting this into (1.6) gives

$$Q = \left(\sum \left[A_{input} + \mu_{input} \right] - \sum \left[A_{output} + \mu_{output} \right] \right) \varepsilon. \tag{1.8}$$

Nucleon number is always conserved, $\Sigma A_{input} = \Sigma A_{output}$, which reduces (1.8) to

$$Q = \left(\sum \mu_{input} - \sum \mu_{output} \right) \varepsilon. \tag{1.9}$$

The product $\mu \varepsilon$ is conventionally designated as Δ:

$$Q = \left(\sum \Delta_{input} - \sum \Delta_{output} \right). \tag{1.10}$$

Δ-values for various nuclides are tabulated in a number of texts and references and are usually given in units of MeV. The most extensive such listing is published as the *Nuclear Wallet Cards* and is available from Brookhaven National Laboratory at http://www.nndc.bnl.gov; a list of selected values appears in Appendix A. The value of quoting mass excesses as Δ-values is that the Q-value of any reaction can be quickly computed via (1.10) without having to worry about factors of c^2 or 931.494. Various examples of Δ-value calculations appear in the following sections.

For a nuclide of given Δ-value, its mass in atomic mass units is given by

$$m^{(amu)} = A + \frac{\Delta}{\varepsilon}. \tag{1.11}$$

1.2   Rutherford and the Energy Release in Radium Decay

The energy released in nuclear reactions is on the order of a million times or more than that typical of chemical reactions. This vast energy was first quantified by Rutherford and Soddy (1903) in a paper titled "Radioactive Change". In this paper they wrote: "It may therefore be stated that the total energy of radiation during the

disintegration of one gram of radium cannot be less than 10^8 g-cal and may be between 10^9 and 10^{10} g-cal. The union of hydrogen and oxygen liberates approximately 4×10^3 g-cal per gram of water produced, and this reaction sets free more energy for a given weight than any other chemical change known. The energy of radioactive change must therefore be at least 20,000 times, and may be a million times, as great as the energy of any molecular change".

Let us have a look at the situation using modern numbers. ^{226}Ra has an approximately 1,600-year half-life for alpha decay:

$$^{226}_{88}\text{Ra} \rightarrow \, ^{222}_{86}\text{Rn} + \, ^{4}_{2}\text{He}. \tag{1.12}$$

The delta-values here are, in MeV,

$$\begin{cases} \Delta\left(^{226}_{88}\text{Ra}\right) = 23.669 \\ \Delta\left(^{222}_{86}\text{Rn}\right) = 16.374 \\ \Delta\left(^{4}_{2}\text{He}\right) \;\; = 2.425. \end{cases} \tag{1.13}$$

These give $Q = 4.87$ MeV in contrast to the *few eV* typically released in chemical reactions.

The notation used here to designate nuclides, $^{A}_{Z}X$, is standard in the field of nuclear physics. X denotes the symbol for the element, Z its atomic number (= number of protons) and A its nucleon number (= number of neutrons plus number of protons, also known as the atomic weight and the mass number). The number of neutrons N is given by $N = A - Z$.

Rutherford and Soddy expressed their results in gram-calories, which means the number of calories liberated per gram of material. Since $1 \text{ eV} = 1.602 \times 10^{-19}$ J, $4.87 \text{ MeV} = 7.80 \times 10^{-13}$ J. One calorie is equivalent to 4.186 J, so the Q-value of this reaction is 1.864×10^{-13} cal. One mole of ^{226}Ra has a mass of 226 g, so a single atom has a mass of 3.75×10^{-22} g. Hence the energy release per gram is about 4.97×10^8 cal, in line with their estimate of 10^8–10^{10}. The modern figure for the heat of formation of water is 3,790 cal/g; gram-for-gram, therefore, radium decay releases about 131,000 times as much energy as the formation of water from hydrogen and oxygen. We are assuming here that the entire gram of radium is decaying in computing the figure of 5×10^8 cal; in reality, this would take an infinite amount of time and cannot be altered by any human intervention. But the important fact is that individual alpha decays release *millions* of electron-Volts of energy, a fantastic number compared to any chemical reaction.

Another notational convention can be introduced at this point. In this book, reactions will usually be written out in detail as above, but some sources express them in a more compact notation. As an example, in the next section we will encounter a reaction where alpha-particles (helium nuclei) bombard nitrogen nuclei to produce protons and oxygen:

$$^{4}_{2}\text{He} + \, ^{14}_{7}\text{N} \rightarrow \, ^{1}_{1}\text{H} + \, ^{17}_{8}\text{O}. \tag{1.14}$$

This can be written more compactly as

$$^{14}_{7}N\left(^{4}_{2}He,\,^{1}_{1}H\right)^{17}_{8}O. \tag{1.15}$$

In this notation, convention is to have the target nucleus as the first term, the bombarding particle as the first term within the brackets, the lighter product nucleus as the second term within the brackets, and finally the heavier product nucleus outside the right bracket.

1.3 Rutherford's First Artificial Nuclear Transmutation

The discovery that nitrogen could be transformed into oxygen under the action of alpha-particle bombardment marked the first time that a nuclear transmutation had been deliberately achieved (Rutherford 1919). This work had its beginnings in experiments conducted by Ernest Marsden in 1915.

In Rutherford's experiment, alpha particles emitted by radium bombard nitrogen, producing hydrogen and oxygen in the reaction:

$$^{4}_{2}He + {}^{14}_{7}N \rightarrow {}^{1}_{1}H + {}^{17}_{8}O. \tag{1.16}$$

The hydrogen nuclei (protons) are detected via the scintillations they produce when they strike a fluorescent screen. The Δ values for this reaction are:

$$\begin{cases} \Delta\left(^{4}_{2}He\right) = 2.425 \\ \Delta\left(^{14}_{7}N\right) = 2.863 \\ \Delta\left(^{1}_{1}H\right) = 7.289 \\ \Delta\left(^{17}_{8}O\right) = -0.809. \end{cases} \tag{1.17}$$

The Q-value of this reaction is -1.19 MeV. That Q is negative means that this process has a *threshold* of 1.19 MeV, that is, the bombarding alpha must possess at least this much kinetic energy to cause the reaction to happen. This energy emerges from the spontaneous decay of radium which gives rise to the alphas. We saw in the preceding section that decay of ^{226}Ra liberates some 4.87 MeV of energy, more than enough to power the nitrogen-bombardment reaction.

The conditions of energy and momentum conservation relevant to "two body" reactions of the general form $A + B \rightarrow C + D$ are detailed in Appendix C. A companion spreadsheet, **TwoBody.xls**[1], allows a user to input nucleon numbers and Δ-values for all four nuclides, along with an input kinetic energy for reactant A; nucleus B is presumed to be stationary when struck by A. The spreadsheet then

---

[1]All Excel sheets are available at http://www.manhattanphysics.com

computes and displays the Q-value for the reaction and the post-reaction kinetic energies and momenta for the products C and D. This will be put to considerable use in the following section.

1.4   Discovery of the Neutron

Much of the material in this section is adopted from a publication elsewhere by the author (Reed 2007).

James Chadwick's discovery of the neutron in early 1932 was a critical turning point in the history of nuclear physics. Within 2 years Enrico Fermi would generate artificially-induced radioactivity by neutron bombardment, and less than 5 years after that Hahn and Strassmann would discover neutron-induced uranium fission. The latter would lead directly to the *Little Boy* uranium-fission bomb while Fermi's work would lead to reactors to produce plutonium for the *Trinity* and *Fat Man* bombs.

Chadwick's discovery was reported in two papers. The first, titled "Possible Existence of a Neutron," is a brief report dated February 17, 1932 and published in the February 27 edition of *Nature* (Chadwick 1932a). A more extensive follow-up paper dated May 10, 1932 was published on June 1 in the *Proceedings of the Royal Society of London* (Chadwick 1932b). As we work through Chadwick's analysis, these will be referred to as Papers 1 and 2, respectively. The *Nature* paper is reproduced in Andrew Brown's excellent biography of Chadwick [Brown (1997)].

A complete description of the experiments which resulted in the discovery of the neutron would be quite extensive, so only a brief summary of the essentials is given here. A more thorough discussion appears in Chap. 6 of Brown; see also Chap. 6 of Rhodes (1986).

The experiments which lead to the discovery of the neutron were first reported in 1930 by Walther Bothe and his student Herbert Becker, working in Germany. Their research involved studying gamma radiation which is produced when light elements such as magnesium and aluminum are bombarded by energetic alpha-particles emitted in the radioactive decay of elements such as radium or polonium. In such reactions, the alpha particles often interact with a target nucleus to yield a proton (hydrogen nucleus) and a gamma-ray, both of which can be detected in Geiger counters. A good example of such a reaction is the one used by Chadwick's mentor, Ernest Rutherford, to produce the first artificially-induced nuclear transmutation discussed in the preceding section:

$$^{4}_{2}\text{He} + {}^{14}_{7}\text{N} \rightarrow {}^{1}_{1}\text{H} + {}^{17}_{8}\text{O} + \gamma. \tag{1.18}$$
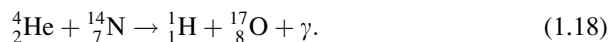
The mystery began when Bothe and Becker found that boron, lithium, and particularly beryllium gave evidence of gamma emission under alpha bombardment *but with no accompanying protons being emitted*. A key point here is that they were

certain that some sort of energetic but electrically neutral "penetrating radiation" was being emitted; it could penetrate foils of metal but could not be deflected by a magnetic field as electrically charged particles would be. Gamma-rays were the only electrically neutral form of penetrating radiation known at the time, so it was natural for them to interpret their results as evidence of gamma-ray emission despite the anomalous lack of protons.

Bothe and Becker's unusual beryllium result was picked up by the Paris-based husband-and-wife team of Frédéric Joliot and Irène Curie, hereafter referred to as the Joliot–Curies. In January 1932 they reported that the presumed gamma-ray "beryllium radiation" was capable of knocking protons out a layer of paraffin wax that had been put in its path. The situation is shown schematically in Fig. 1.1, where the supposed gamma-rays are labeled as "mystery radiation."

The energy (hence speed) of the protons could be deduced by means such as determining what thickness of metal foil they could penetrate through before being stopped or by measuring how many ion pairs they created in a Geiger counter; such measurements were well-calibrated by that time. In comparison to the gargantuan particle accelerators of today these experiments were literally table-top nuclear physics; in his recreation of the Joliot–Curies' work, Chadwick's experimental setup involved polonium deposited on a silver disk 1 cm in diameter placed close to a disk of pure beryllium 2 cm in diameter, with both enclosed in a small vessel which could be evacuated; a photograph appears in Brown's biography.

The alpha-producing polonium decay in Fig. 1.1 can be written as

$$^{210}_{84}\text{Po} \rightarrow {}^{206}_{82}\text{Pb} + {}^{4}_{2}\text{He}. \tag{1.19}$$

This spontaneous decay liberates $Q = 5.407$ MeV of energy to be shared between the lead and alpha nuclei. The masses of the products involved in such reactions are typically such that their speeds are non-relativistic, a feature we will make considerable use of in our analysis. Even if mass is created or lost in a reaction, momentum must always be conserved. If the polonium nucleus is initially stationary then the lead and alpha nuclei must recoil in opposite directions. One can
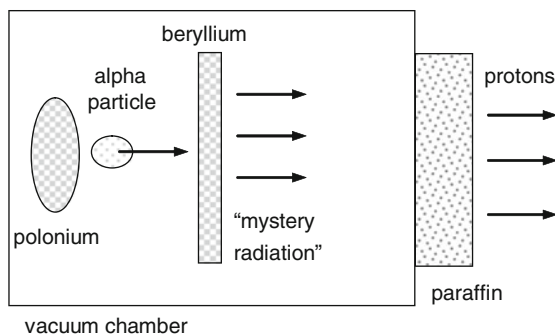
Fig. 1.1 The "beryllium radiation" experiment of Becker, Bothe, the Joliot–Curies and Chadwick

easily show from classical momentum conservation that if the total kinetic energy shared by the two product nuclei is Q, then the kinetic energy of the lighter product nucleus must be

$$K_m = \frac{Q}{1 + m/M},\tag{1.20}$$

where m and M are respectively the masses of the light and heavy product nuclei. Here we have $m/M \sim 4/206$, so the alpha-particle carries off the lion's share of the liberated energy, about 5.3 MeV. The speed of such an alpha-particle is about $0.05c$, justifying the non-relativistic assumption.

We now set up some expressions that will be useful for dissecting Chadwick's analysis.

First, let us assume that Bothe and Becker and the Joliot–Curies were correct in their interpretation that α-bombardment of Be creates gamma-rays. To conserve the number of nucleons involved, they hypothesized that the reaction was

$$_2^4\text{He} + {}_4^9\text{Be} \rightarrow {}_6^{13}\text{C} + \gamma.\tag{1.21}$$

(Strictly speaking, we are cheating here in writing the reaction in modern notation that presumes knowledge of both neutrons and protons, but this has no effect on the analysis.) From left to right the Δ-values for this reaction are 2.425, 11.348, and 3.125, so the Q-value is 10.65 MeV; this energy, when added to the $\sim$5.3 MeV kinetic energy of the incoming alpha, means that the γ-ray can have energy of about 16 MeV at most. But the energy of the supposed gamma-ray is crucial here, so we do a more careful analysis. In Appendix D it is shown that in a collision like this, the energy E_γ of the emergent gamma-ray is given by solving the quadratic equation

$$\alpha E_\gamma^2 + \varepsilon E_\gamma + \delta = 0,\tag{1.22}$$

where

$$\alpha = \frac{1}{2E_C},\tag{1.23}$$

$$\varepsilon = 1 - \frac{\sqrt{2E_{He}K_{He}}}{E_C},\tag{1.24}$$

and

$$\delta = \left(\frac{E_{He}}{E_C}\right)K_{He} - (E_{He} + E_{Be} + K_{He} - E_C),\tag{1.25}$$

Table 1.1 Δ-values and rest energies for the Joliot–Curie γ-reaction

Nucleus	A	Δ	E (MeV)
He	4	2.425	3728.40228
Be	9	11.348	8394.79688
C	13	3.125	12112.55116

Fig. 1.2 A γ-ray strikes a massive, initially stationary particle, which emerges from the collision with kinetic energy K_m. The γ-ray is assumed to recoil backwards

where E_{He}, E_{Be} and E_C represent the mc^2 rest energies (in MeV) of the alpha-particle, Be nucleus and carbon nucleus, respectively, and where K_{He} is the kinetic energy of the incoming alpha-particle. (We assume that the gamma-ray that is produced travels in the forward directio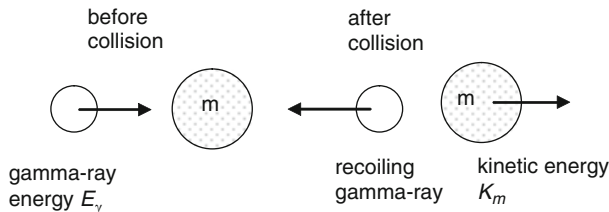n.) These rest energies can be calculated form the corresponding nucleon numbers and Δ-values as $E = \varepsilon A + \Delta$ (Sect. 1.1).

The relevant numbers appear in Table 1.1.

These numbers give (with $K_{He} = 5.3$ MeV) $\alpha = 4.12795 \times 10^{-5}$ MeV^{-1}, $\varepsilon = 0.983587$, and $\delta = -14.316590$ MeV.

Solving the quadratic gives $E_\gamma = 14.55$ MeV; this is a little less than the approximately 16 MeV estimated on the basis of the Q-value alone as the carbon nucleus carries off some momentum. This solution takes the upper sign (+) in the solution of the quadratic; choosing the lower sign leads to a negative value for the kinetic energy of the carbon atom, a result which would be unphysical.

Spreadsheet **TwoBodyGamma.xls** allows a user to investigate reactions of the general form $A + B \rightarrow C + \gamma$. As with **TwoBody.xls**, the user inputs nucleon numbers and Δ-values for nuclides A, B, and C and the input kinetic energy for reactant A; B is presumed to be stationary when struck head-on by A. The spreadsheet computes and displays the possible solutions for the energy of the γ-ray and the kinetic energy and momentum of product C.

The 14.5-MeV gamma-rays then strike protons in the paraffin, setting them into motion. See Fig. 1.2. Such a collision is a problem in both relativistic and classical dynamics; a γ-ray is relativistic whereas the protons can be treated classically (this is justified below).

Suppose that the gamma-ray strikes an initially stationary particle of mass m. In what follows, the symbol E_m is used to represent the Einsteinian rest energy mc^2 of the struck particle, while K_m is used to designate its post-collision classical kinetic energy $mv^2/2$; E_γ again designates the energy of the gamma-ray before the collision. Maximum possible forward momentum will be imparted to the struck particle if the gamma-ray recoils backwards after the collision; we assume that this is the case.

If the energy of the gamma-ray after the collision is E_γ^*, then conservation of mass-energy demands

$$E_\gamma + E_m = E_\gamma^* + E_m + K_m. \tag{1.26}$$

Since we are assuming that the struck particle does not change its identity, the factors of E_m in (1.26) cancel each other. Since the momentum of a photon of energy E is given by E/c, conservation of momentum for this collision can be written as

$$E_\gamma / c = -E_\gamma^* / c + mv, \tag{1.27}$$

where v is the post-collision speed of the struck particle. The negative sign on the right side of (1.27) means that the γ-ray recoils backwards.

It will prove handy to also have on hand expressions for the classical momentum and kinetic energy of the struck particle in terms of its rest energy:

$$mv = \sqrt{2mK_m} = \frac{\sqrt{2mc^2 K_m}}{c} = \frac{\sqrt{2E_m K_m}}{c} \tag{1.28}$$

and

$$K_m = \frac{1}{2} mv^2 = \frac{(mc^2) v^2}{2c^2} = \frac{1}{2} E_m \left(\frac{v}{c}\right)^2. \tag{1.29}$$

With (1.28), a factor of c can be cancelled in (1.27); then, on eliminating E_γ^* between (1.26) and (1.27), we can solve for E_γ:

$$E_\gamma = \frac{1}{2} \left(K_m + \sqrt{2E_m K_m} \right). \tag{1.30}$$

If the kinetic energy of the struck particle (proton) can be measured, we can use (1.30) to figure out what energy the gamma-ray must have had to set it into such motion. On the other hand, if we desire to solve for K_m presuming that E_γ is known, the situation is slightly messier as (1.30) is a quadratic in $\sqrt{K_m}$ that has no neat solution:

$$K_m + \left(\sqrt{2E_m} \right) \sqrt{K_m} - 2E_\gamma = 0. \tag{1.31}$$

Now, the gamma-rays involved here have $E_\gamma \sim 14.6$ MeV, but a proton has a rest energy of about 938 MeV. It is consequently quite reasonable to set $E_m \ll E_\gamma$, in which case this quadratic can be solved approximately, as shown in what follows.

The formal solution of the quadratic is

$$\sqrt{K_m} = \frac{-\sqrt{2E_m} + \sqrt{2E_m + 8E_\gamma}}{2}.$$

Extract a factor of $2E_m$ from under the second radical:

$$\sqrt{K_m} = \frac{-\sqrt{2E_m}\left[1 - \sqrt{1 + 4E_\gamma/E_m}\right]}{2}.$$

We have $4E_\gamma/E_m \ll 1$. Invoking the expansion

$$\sqrt{1 + x} \sim 1 + x/2 - x^2/8 + \ldots \, (x < 1)$$

with $x = 4E_\gamma/E_m$ gives

$$\sqrt{K_m} \sim \frac{1}{2}\left\{-\sqrt{2E_m}\left[1 - \left(1 + 2\frac{E_\gamma}{E_m} - 2\frac{E_\gamma^2}{E_m^2} + \ldots\right)\right]\right\}$$

$$\sim \left\{-\sqrt{2E_m}\left[-\frac{E_\gamma}{E_m} + \frac{E_\gamma^2}{E_m^2} - \ldots\right]\right\}$$

$$\sim \sqrt{2E_m}\left(\frac{E_\gamma}{E_m}\right)\left\{1 - \frac{E_\gamma}{E_m} + \ldots\right\}.$$

Squaring gives

$$K_m \sim 2\left(\frac{E_\gamma^2}{E_m}\right)\left\{1 - 2\frac{E_\gamma}{E_m} + \ldots\right\}. \tag{1.32}$$

Equation (1.32) will prove valuable presently.

Upon reproducing the Joliot–Curie experiments, Chadwick found that protons emerge from the paraffin with speeds of up to about 3.3×10^7 m/s. This corresponds to $(v/c) = 0.11$, so our assumption that the protons can be treated classically is reasonable. The modern value for the rest mass of a proton is 938.27 MeV. From (1.29), these figures give the kinetic energy of the ejected protons as 5.7 MeV, exactly the value quoted by Chadwick on p. 695 of his Paper 2. Equation (1.30) then tells us that if a proton is to acquire this amount of kinetic energy by being struck by a gamma-ray, then the gamma-ray must have an energy of about 54.4 MeV. But we saw in the argument following (1.25) that a gamma-ray arising from the Joliot–Curies' proposed $\alpha + {}^9\text{Be} \rightarrow {}^{13}\text{C}$ reaction has energy of only about 14.6 MeV, a factor of nearly four too small! This represents a serious difficulty with the gamma-ray proposal.

Before invoking a reaction mechanism involving a (hypothetical) neutron, Chadwick devised a further test to investigate the remote possibility that 55-MeV gamma-rays might somehow be being created in the α-Be collision. In addition to having the "beryllium radiation" strike protons, he also directed it to strike a sample

of nitrogen gas. The mass of a nitrogen nucleus is about 14 mass units; at a conversion factor of 931.49 MeV per mass unit, the rest energy of a ^{14}N nucleus is about 13,040 MeV. If such a nucleus is struck by a 54.4-MeV gamma-ray, (1.32) indicates that it should acquire a kinetic energy of about 450 keV. From prior experience, Chadwick knew that when an energetic particle travels through air it produces ions, with about 35 eV required to produce a single ionization (hence yielding "one pair" of ions). A 450 keV nitrogen nucleus should thus generate some 13,000 ion pairs. Upon performing this experiment, however, he found that some 30,000–40,000 ion pairs would typically be produced. These figures imply a kinetic energy of ~1.1–1.4 MeV for the recoiling nitrogen nuclei, which in turn by (1.30) would require gamma-rays of energy up to ~90 MeV, a number completely inconsistent with the ~55 MeV indicated by the proton experiment. Indeed, upon letting the supposed gamma-rays strike heavier and heavier target nuclei, Chadwick found that " ... if the recoil atoms are to be explained by collision with a quantum, we must assume a larger and larger energy for the quantum as the mass of the struck atom increases." The absurdity of this situation led him to write (Paper 2, p. 697) that "It is evident that we must either relinquish the application of conservation of energy and momentum in these collisions or adopt another hypothesis about the nature of the radiation." To be historically correct, the mass of beryllium atoms had not yet been accurately established in 1932, so Chadwick did not know the $E_\gamma = 14.6$ MeV figure for certain. However, he was able to sensibly estimate it as no more than about 14 MeV unless the beryllium nucleus lost an unexpectedly great amount of mass in the reaction, so, as he remarked in his Paper 2 (p. 693), "... it is difficult to account for the production of a quantum of 50 MeV from the interaction of a beryllium nucleus and an α-particle of kinetic energy of 5 MeV."

To summarize to this point, the fundamental problem with the gamma-ray hypothesis is that for the amount of energy Q liberated in the α-Be reaction, any resulting gamma-ray will possess much less momentum than a classical particle of the same kinetic energy; the ratio is $p_\gamma/p_m = \sqrt{Q/2E_m}$, where E_m is the rest energy of the classical particle. Only an extremely energetic gamma-ray can kick a proton to a kinetic energy of several MeV. Chadwick's key insight was to realize that if the protons were in reality being struck billiard-ball style by neutral *material* particles of mass equal or closely similar to that of a proton, then the striking energy need only be on the order of the kinetic energy that the protons acquire in the collision.

This is the point at which the neutron makes it debut. Chadwick hypothesized that instead of the Joliot–Curie reaction of (1.21), the α-Be collision leads to the production of carbon and a neutron via the reaction

$$\,^{4}_{2}\text{He} + \,^{9}_{4}\text{Be} \rightarrow \,^{12}_{6}\text{C} + \,^{1}_{0}\text{n}. \tag{1.33}$$

Note that in this case a ^{12}C atom is produced as opposed to the Joliot–Curies' proposed ^{13}C. Since the "beryllium radiation" was known to be electrically neutral, Chadwick could not invoke a charged particle such as a proton or electron here. Incidentally, the ^{12}C nucleus will likely remain trapped in the Be target and hence go undetected. If the neutron is assumed to have a mass excess identical to that of

a proton, a calculation like that discussed in Appendix C (and carried out with the **TwoBody.xls** spreadsheet) shows that the kinetic energy of the neutron would be about 10.9 MeV if the neutron's true mass and the momentum acquired by the ^{12}C nucleus are accounted for. Chadwick was able to verify this mass presumption experimentally as described below; since neutrons were thought of as being an electron/proton combination, taking the neutron to have a mass excess like that of a proton would have been a reasonable premise. A subsequent neutron/proton collision will be like a collision between equal-mass billiard balls, so it is entirely plausible that a neutron that begins with about 11 MeV of energy will be sufficiently energetic to accelerate a proton to a kinetic energy of ~5.7 MeV even after it (the neutron) batters its way out of the beryllium target and through the window of the vacuum vessel on its way to the paraffin.

As a check on this neutron hypothesis, consider again the nitrogen experiment described above. Instead of a gamma-ray being created in the α-Be collision, now a neutral material particle of mass μ – a neutron – is presumed to be created and which subsequently collides with an initially stationary particle of mass m as illustrated in Fig. 1.3.

This collision can be analyzed with the familiar head-on elastic-collision formulae of basic physics; if the neutron has speed v_μ and kinetic energy K_m, then the post-collision speed and kinetic energy of the struck mass will be

$$v_m = \left(\frac{2\mu}{\mu + m}\right) v_\mu \quad \text{and} \quad K_m = \frac{4\mu m}{(m + \mu)^2} K_\mu. \tag{1.34}$$

Suppose that neutrons emerging from the vacuum vessel do indeed have energies of 5.7 MeV. With neutrons of mass 1 and nitrogen nuclei of mass 14, (1.34) indicates that a nitrogen nucleus should be set into motion with a kinetic energy equal to $56/225 = 0.249$ of that of the incoming neutron, or about 1.4 MeV. This figure is in excellent agreement with the energy indicated by the observed number of ion pairs created by the recoiling nitrogen nuclei!

As Chadwick related in his Paper 2 (p. 698), independent cloud-chamber measurements of the recoiling nitrogen atoms indicated that they acquired speeds of ~4.7×10^6 m/s as a result of being struck by neutrons. Knowing this and the fact that neutron-bombarded protons are set into motion with a speed of about 3.3×10^7 m/s, he was able to estimate the mass of the neutron by a simple classical argument. If the mass of a proton is 1 unit and that of a nitrogen 14 units, (1.34) indicates that the ratio of the speed of a recoiling proton to that of a recoiling nitrogen would be $(\mu + 14)/(\mu + 1)$; the measured speeds lead him to conclude

before collision   after collision

Fig. 1.3 Particle of mass μ strikes a stationary particle of mass m, setting the latter in motion with speed v_m
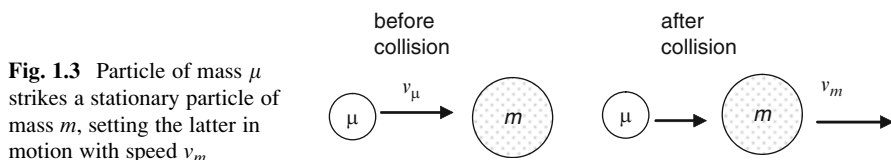
$\mu \sim 1.15$ with an estimated error of 10%. Further experiments with boron targets led Chadwick to report a final estimate of the neutron mass as between 1.005 and 1.008 mass units. The modern figure is 1.00866; the accuracy he achieved with equipment which would now be regarded as primitive is nothing short of awe-inspiring.

In summary, Chadwick's analysis consists of four main points: (1) If the "beryllium radiation" comprises gamma-rays, then they must be of energy ~55 MeV to set protons into motion as observed. (2) Such a high energy is unlikely from an α-Be collision, although not inconceivable if the reaction happens in some unusual way involving considerable mass loss. (3) Letting the same "gamma-rays" strike nitrogen nuclei causes the latter to recoil with energies indicating that the gamma-rays must have energies of ~90 MeV, utterly inconsistent with point (1). (4) If instead the "beryllium radiation" is assumed to be a neutral particle of mass close to that of a proton, consistent results emerge for the proton and particularly the nitrogen recoil energies.

The neutron hypothesis also quickly proved to resolve longstanding issues concerning the spin properties of nuclei; Chadwick was awarded the 1935 Nobel Prize in Physics for his discovery. He further speculated in his Paper 2 that neutrons might represent a complex particle consisting of a proton and an electron, but this proved not to be the case: Heisenberg's uncertainty principle ruled against the possibility of containing electrons within such a small space. Subsequent experiments by Chadwick himself showed that the neutron is a fundamental particle in its own right.

1.5   Artificially-Induced Radioactivity and the Path to Fission

Irène and Frédéric Joliot–Curie misinterpreted the discovery of the neutron in early 1932 but scored a success 2 years later with their discovery that normally stable nuclei could be induced to become radioactive upon alpha-particle bombardment.

Their discovery reaction involved bombarding aluminum with alphas emitted in the decay of polonium, the same source of alphas used in the neutron-discovery reaction:

$$^{210}_{84}\text{Po} \xrightarrow[138 \text{ days}]{\alpha} {}^{206}_{82}\text{Pb} + {}^{4}_{2}\text{He}. \tag{1.35}$$
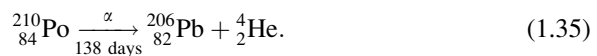
The Q-value of this reaction was found in the preceding section to be 5.41 MeV. These alphas then bombard aluminum, fuse with it, and chip off a neutron to leave phosphorous:

$$^{4}_{2}\text{He} + {}^{27}_{13}\text{Al} \rightarrow {}^{1}_{0}\text{n} + {}^{30}_{15}\text{P}. \tag{1.36}$$

The Δ values here are respectively 2.425, -17.197, 8.071 and -20.201, giving $Q \sim -2.64$ MeV. Despite this threshold the incoming alpha is more than energetic

enough to cause the reaction to proceed. The ^{30}P nucleus subsequently undergoes positron decay to ^{30}Si with a half-life of 2.5 min:

$$^{30}_{15}\text{P} \xrightarrow[2.5 \text{ min}]{\beta^+} {}^{30}_{14}\text{Si}. \tag{1.37}$$
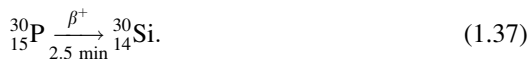
It was this positron emission that alerted the Joliot–Curies to the fact that they had induced radioactivity in aluminum. When the bombarded aluminum was dissolved in acid the small amount of phosphorous created could be separated and chemically identified as such; that the radioactivity carried with the phosphorous and not the aluminum verified their suspicion.

The Joliot–Curies' success stimulated Enrico Fermi to see if he could similarly induce radioactivity by neutron bombardment. He soon succeeded with fluorine:

$$^{1}_{0}\text{n} + {}^{19}_{9}\text{F} \rightarrow {}^{20}_{9}\text{F} \xrightarrow[11.1 \text{ sec}]{\beta^-} {}^{20}_{10}\text{Ne}, \tag{1.38}$$
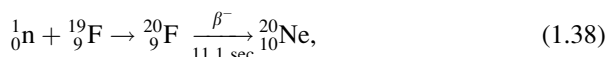
and also with aluminum, discovering a different half-life than had the Joliot–Curies:

$$^{1}_{0}\text{n} + {}^{27}_{13}\text{Al} \rightarrow {}^{1}_{1}\text{H} + {}^{27}_{12}\text{Mg} \xrightarrow[9.5 \text{ min}]{\beta^-} {}^{27}_{13}\text{Al}. \tag{1.39}$$
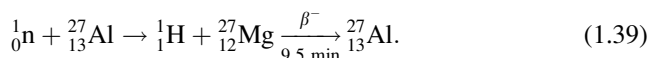
It was not long before Fermi and his collaborators had worked their way up the periodic table to uranium, neutron bombardment of which would lead to the discovery of fission.

The above reaction is not the only one possible when a neutron strikes aluminum. In such reactions, three different *reaction channels* are typically seen: the neutron may chip off a proton as above, but it may also give rise to an alpha-particle or simply be absorbed by the aluminum nucleus. In all cases the product eventually decays by beta-decay to something stable:

$$^{1}_{0}\text{n} + {}^{27}_{13}\text{Al} \rightarrow \begin{cases} {}^{1}_{1}\text{H} + {}^{27}_{12}\text{Mg} \xrightarrow[9.5 \text{ min}]{\beta^-} {}^{27}_{13}\text{Al} \\[2mm] {}^{4}_{2}\text{He} + {}^{24}_{11}\text{Na} \xrightarrow[15 \text{ hr}]{\beta^-} {}^{24}_{12}\text{Mg} \\[2mm] {}^{28}_{13}\text{Al} \xrightarrow[2.25 \text{ min}]{\beta^-} {}^{28}_{14}\text{Si}. \end{cases} \tag{1.40}$$
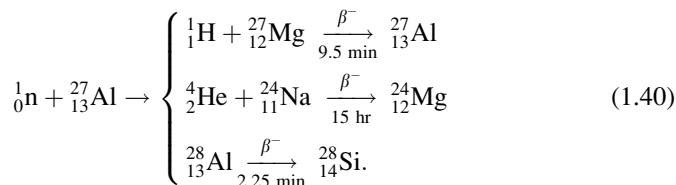
The path from the discovery of artificially-induced radioactivity to the discovery of fission was full of near-misses. A brief description of significant developments is given here as a segue into the next five sections, where the physics of fission is covered in more detail. A good qualitative discussion of this material can be found in Chaps. 8 and 9 of Rhodes (1986); a comprehensive technical discussion of developments between the discovery of the neutron and the discovery of fission appears in Amaldi (1984).

As neutron sources, Fermi and his group used small glass vials containing radon gas mixed with powdered beryllium. Radon alpha-decays with a half-life of 3.8 days and is consequently a copious source of alpha particles; these alphas strike beryllium nuclei and produce neutrons of energy ~11 MeV as in Chadwick's polonium-source experiment. In early 1934 the Rome group began systematically bombarding target elements with neutrons, working their way up through the periodic table. By the spring of 1934 they had come to uranium, for which, at the time, only one isotope was known, ^{238}U. (^{235}U would be discovered by University of Chicago mass spectroscopist Arthur Dempster in 1935.) Upon carrying out the bombardment, they found that β^- activity was induced, with evidence for several half-lives appearing; in particular, they noted one of 13 min. They knew from previous experience with heavy elements that induced beta-decay often resulted from neutron bombardment, so they assumed that in the case of uranium they must be synthesizing a new element, number 93:

$$\, _0^1\text{n} + \, _{92}^{238}\text{U} \rightarrow \, _{92}^{239}\text{U} \xrightarrow{\beta^-} \, _{93}^{239}\text{X} \xrightarrow{\beta^-} ?, \tag{1.41}$$
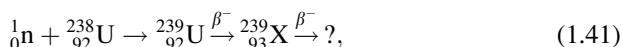
where X denotes a new "transuranic" element which might itself undergo a subsequent beta-decay. Indeed, chemical testing revealed that their beta-emitters were not uranium isotopes or any known element between lead ($Z = 82$) and uranium, a result that strengthened their belief that they were synthesizing new "transuranic" elements. Indeed, it was in part for this work that Fermi was awarded the 1938 Nobel Prize in Physics.

As it happens, ^{238}U is in fact quite fissile when bombarded by very energetic neutrons (see Sect. 1.9). However, the experimental arrangement adopted by Fermi's group precluded their being able to detect the high-energy fission fragments that are so created. In addition to being an alpha-emitter, radon is a fairly prolific gamma-ray emitter, and these gamma-rays would have caused an unwanted background signal for their ionization-chamber detectors if they were placed near neutron sources. Consequently, their procedure was to irradiate target samples and then literally run them down a long hallway to a detector far from the neutron source. Since they were seeking to detect delayed effects (induced half-lives are often on the order of minutes) this procedure would not affect their results. But the fission process occurs on a timescale of about 10^{-15} s, so any fission fragments that they might have detected directly would be long gone by the time the sample arrived at the detector. Fission fragments tend to be neutron rich and hence suffer a succession of beta-decays, and it must have been beta-decays from such fragments remaining in the samples that were being detected and attributed to synthesis of transuranic elements. A common product of fission is barium, and a particular isotope of this element, ^{131}Ba, indeed has a beta-decay half-life of 14.6 min. Because any reaction that had ever been explored involved transmutations of elements by at most one or two places in the periodic table, nobody was expecting fission to happen and so never considered that their experimental arrangement might be biasing them against detecting it. Retrospect is always perfect.

In October 1934 Fermi discovered by accident that if the bombarding neutrons were caused to be slowed ("moderated") before hitting the target element by first having them pass through water of paraffin, the activity of the induced radioactivities could in some cases be drastically increased. Fermi attributed this to the neutrons having more time in the vicinity of target nuclei and hence a greater probability of reacting with them. As a result, the Rome group began re-investigating all those elements which they had previously subjected to *fast* (energetic) neutron bombardment. Uranium was one of many elements which proved to yield greater activity upon *slow* neutron bombardment. Ironically, *slow* neutron bombardment of uranium does create plutonium, as we will see in Sect. 1.9; Fermi initially thought this was happening with *fast* neutron bombardment of uranium, which tends to lead to fission.

The possibility that new elements were being created was treated with some skepticism within the nuclear research community. Among the leaders of that community were Otto Hahn and Lise Meitner at the Kaiser Wilhelm Institute for Chemistry in Berlin, who between them had accumulated years of experience with the chemistry and physics of radioactive elements. In 1935, they and chemist Fritz Strassmann began research to sort out to what elements uranium transmuted under slow neutron bombardment. By 1938 the situation had become extremely muddled, with no less than ten distinct half-lives having been identified. To complicate things further, Irène Curie (Marie and Pierre's daughter) and Paul Savitch, working in Paris, had identified an approximately 3.5-h β half-life resulting from slow neutron bombardment of uranium, an activity which Hahn and his group had not found. Curie and Savitch suggested that the 3.5-h decay might be attributed to thorium, element 90. If this were true it would mean that neutrons slowed to the point of possessing less than an eV of kinetic energy (see Sect. 3.2) were somehow capable of knocking alpha-particles out of uranium nuclei.

Further research by Curie and Savitch showed that the 3.5-h beta-emitter had chemical properties similar to those of element 89, actinium. This observation would eventually be realized as another missed chance in the discovery of fission. To isolate the beta-emitter from the bombarded uranium target, Curie and Savitch used a lanthanum-based chemical analysis. Lanthanum is element 57, which is in the same column of the periodic table as actinium. Chemists were long familiar with the fact that elements in the same column of the table behave similarly as far as their chemical properties are concerned. That the beta emitter "carried" with lanthanum in a chemical separation indicated that it must have chemistry similar to lanthanum, and since the element nearest uranium in the periodic table with such chemistry is actinium, it was assumed that nuclei of that element must be the beta-decayers. The other possibility, that uranium might in fact be transmuting to lanthanum, would have seemed ludicrous as U and La differ by a factor of nearly two in mass. In actuality, Curie and Savitch were in fact detecting ^{141}La, which is now known to have a half-life of 3.9 h.

Hahn, Meitner, and Strassmann resolved to try to reproduce the French work. Tragically, in July 1938, Meitner was forced to flee to Holland. Born into a Jewish

family in Austria, she had assumed that her Austrian citizenship would protect her against German anti-Semitic laws, but this protection ended with the German annexation of Austria in March 1938. Hahn and Strassmann carried on with the work and corresponded with her by letter, but her career was essentially destroyed.

By December of 1938 Hahn and Strassmann had refined their chemical techniques and had become convinced that they were detecting barium (element 56) as a result of slow-neutron bombardment of uranium. Barium is adjacent to lanthanum in the periodic table and is another common product of uranium fission. On December 19 Hahn wrote to Meitner (who by then was settled in Sweden) of the barium result, and 2 days later followed up with a second letter indicating that they were also detecting lanthanum. By chance, Meitner's nephew, physicist Otto Frisch, was then working at Niels Bohr's institute in Copenhagen. He traveled to Sweden to spend Christmas with his aunt and they conceived of the fission process on December 24, working out an estimate of the energy that could be expected to be released. By this time Hahn and Strassmann had already submitted their barium paper to the journal *Naturwissenschaften* (Hahn and Strassmann 1939). Otto Hahn was awarded (solely) the 1944 Nobel Prize in Chemistry; Meitner and Strassmann did not share in the recognition.

Soon after returning to Copenhagen on New Year's Day 1939, Frisch informed Niels Bohr of the discovery of fission. Bohr was about to depart for a semester at Princeton University, and it is he who "carried the word" of the discovery to the New World on the same day (January 16) that Meitner and Frisch submitted a paper to *Nature* with their interpretation of the fission process. This was published on February 11 (Meitner and Frisch 1939), by which time the process had been duplicated in a number of laboratories in Europe and America.

Otto Frisch is credited with borrowing the term "fission" from the concept of cell division in biology to describe this newly-discovered phenomenon. He is also credited with being the first person to set up an experiment to deliberately demonstrate it and measure the energy of the fragments, work he did in Copenhagen on Friday, January 13. After replicating the Hahn and Strassmann uranium results, he also tested thorium. This element proved to act like uranium in that it would fission under bombardment by *fast* neutrons, but at the same time to act curiously unlike uranium in that it did not do so at all when bombarded with *slow* neutrons. This asymmetry catalyzed a crucial revelation on the part of Niels Bohr a few weeks later as to what isotope of uranium is responsible for slow-neutron fission. Uranium consists of two isotopes, the "even/even" (in the sense Z/N) isotope ^{238}U and the much rarer "even/odd" isotope ^{235}U, whereas thorium has only one naturally-occurring isotope, ^{232}Th, an "even/even" nuclide. Bohr realized that, as a matter of pure logic, ^{235}U must be responsible for slow-neutron fission as it is the one "parity" of isotope that thorium does not possess.

The difference in behavior between ^{238}U and ^{235}U under neutron bombardment and how this relates to their nuclear "parity" is examined further in Sect. 1.9. Until then, we examine in more detail the energetics of the fission process itself.

1.6 Energy Release in Fission

Neutron-induced uranium fission can happen in a multiplicity of ways with a wide variety of fission products resulting. Empirically, equal division of the bombarded nucleus is quite unlikely; the most likely mass ratio for the products is about 1.5.

To understand the energy release in fission, consider the splitting of a ^{235}U nucleus into barium and krypton (the Hahn-Strassmann fission-discovery situation) along with the release of three neutrons:

$$\,^{1}_{0}\text{n} + \,^{235}_{92}\text{U} \rightarrow \,^{141}_{56}\text{Ba} + \,^{92}_{36}\text{Kr} + 3\,(^{1}_{0}\text{n}). \tag{1.42}$$
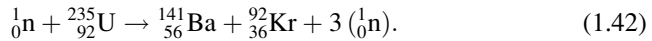
The delta values are

$$\begin{cases} \Delta\left(^{1}_{0}\text{n}\right) = 8.071 \\ \Delta\left(^{235}_{92}\text{U}\right) = 40.921 \\ \Delta\left(^{141}_{56}\text{Ba}\right) = -79.726 \\ \Delta\left(^{92}_{36}\text{Kr}\right) = -68.79, \end{cases} \tag{1.43}$$

hence $Q = 173.3$ MeV.

The fission energy latent in a single kilogram of ^{235}U is enormous. With an atomic weight of 235 g/mol, 1 kg of ^{235}U comprises about 4.26 mol or 2.56×10^{24} atoms. At 173 MeV/reaction the potential fission energy amounts to 4.43×10^{32} eV, or 7.1×10^{13} J. Explosion of 1 ton of TNT liberates about 4.2×10^{9} J, so 1 kg of ^{235}U is equivalent to nearly 17 kt (*kilotons*) of TNT. The explosive yield of the *Little Boy* uranium bomb dropped on Hiroshima has been estimated at 13 kt (Penney et al. 1970), from which we can infer that only some 0.8 kg of ^{235}U actually underwent fission. Upon considering that *Little Boy* contained about 64 kg of ^{235}U (Sect. 2.3), we can appreciate that the first fission weapons were actually rather *inefficient* despite their enormous explosive yields. Weapon efficiency is examined in detail in Sects. 2.4 and 2.5.

In writing the above fission reaction it was assumed that three neutrons were released in the process. If one is to have any hope of sustaining a neutron-moderated chain reaction, it is clear that, on average, *at least one* neutron will have to be liberated per fission event. Soon after the discovery of fission a number of research teams began looking for evidence of these "secondary" neutrons, and proof of their existence was not long in coming. On March 16, 1939, two independent teams at Columbia University submitted letters to *The Physical Review* reporting their discovery: Anderson et al. (1939) and Szilard and Zinn (1939). Both groups estimated about two neutrons emitted per each captured. Their papers were published on April 15. In Paris on April 7, von Halban et al. (1939) submitted a paper to *Nature* in which they reported 3.5 ± 0.7 neutrons liberated per fission; their paper was published on April 22. The modern value for the average number of secondary neutrons liberated by U-235 when it is fissioned by a fast neutron is about 2.6. In an

ingenious experiment carried out about the same time and reported in the April 8 edition of *Nature*, Feather (1939) reported that the fission process must take place within a time of no more than about 10^{-13} s. To researchers in the field of nuclear physics, it was apparent in the spring of 1939 that a rapid, extremely energetic uranium-based neutron-initiated-and-maintained chain reaction was at least a theoretical possibility.

1.7   The Bohr–Wheeler Theory of Fission: The Z^2/A Limit Against Spontaneous Fission

Much of the material in this section is adopted from a publication elsewhere by the author (Reed 2003).

Within a few weeks of the discovery of slow-neutron-induced fission of uranium, Niels Bohr published a paper in which he argued that of the two then-known isotopes of uranium (^{235}U and ^{238}U), it was likely to be the lighter, much rarer one that was undergoing fission whereas the heavier one would likely simply absorb any bombarding neutrons and later decay (Bohr 1939). Experimental verification of this prediction came in early 1940 when Alfred Nier separated a small sample of uranium into its constituent isotopes via mass spectroscopy (Nier et al. 1940). In the meantime, Bohr continued with his work on the theory of nuclear fission, and, in the September 1, 1939 edition of *The Physical Review*, he and John Wheeler of Princeton University published an extensive analysis of the theory of fission (Bohr and Wheeler 1939). In this seminal work they reported two important discoveries: (1) That there exists a natural limit $Z^2/A \sim 48$ beyond which nuclei are unstable against disintegration by spontaneous fission, and (2) That in order to induce a nucleus with $Z^2/A < 48$ to fission, it must be supplied with a necessary "activation energy," a quantity also known as a "fission barrier." Uranium isotopes fall into this latter Z^2/A range.

Bohr and Wheeler's calculations are extremely challenging even for advanced physics students. We can, however, get some idea of what they did by invoking some simplifying approximations and by taking some empirical numbers at face value. This section is devoted to an analysis of the issue of the limiting value of Z^2/A against spontaneous fission. A more formal treatment of the Bohr and Wheeler calculation is presented in Appendix E.

Bohr and Wheeler modeled the nucleus as a deformable "liquid drop" whose shape can be described by a sum of Legendre polynomials configured to conserve volume as the nucleus deforms, and considered the total energy of the nucleus to be the sum of two contributions. These are a "surface" energy U_A proportional to the surface area of the nucleus, and an electrostatic contribution U_C corresponding to its Coulomb self-potential. If a nucleus finds itself deformed from its original spherical shape, U_A will increase due to the consequent increase in surface area, while U_C simultaneously decreases as the nuclear charge becomes more spread out. If $(U_A + U_C)_{deformed} < (U_A + U_C)_{original}$, then the nucleus will be unstable against further

deformation and eventual fission. The surface-energy term originates in the fact that nucleons near the surface of the nucleus are less strongly bound than those inside, while the Coulomb term arises from the mutual repulsion of the protons.

The usual textbook approach to establishing the Z^2/A limit is to quote expressions for the surface and Coulomb energies of nuclei modeled as ellipsoids, and then compute the difference in energy between a spherical nucleus and an ellipsoid of the same volume. We can do an approximate treatment, however, by modeling nuclei as spheres.

Begin with a spherical parent nucleus of radius R_O as shown in Fig. 1.4a. Imagine that this nucleus splits into two spherical product nuclei of radii R_1 and R_2 as shown in part b of the figure; after this, they will repel each other by Coulomb repulsion and fly away at high speed as shown in part c of the figure.

Presuming that the density of nuclear matter is constant, conservation of nucleon number demands that volume be conserved:

$$R_O^3 = R_1^3 + R_2^3. \tag{1.44}$$

Define the mass ratio of the fission products as

$$f = \frac{R_1^3}{R_2^3}. \tag{1.45}$$

This ratio could be defined as the inverse of that adopted here, a point to which we shall return below. In terms of the mass ratio, the radii of the product nuclei are

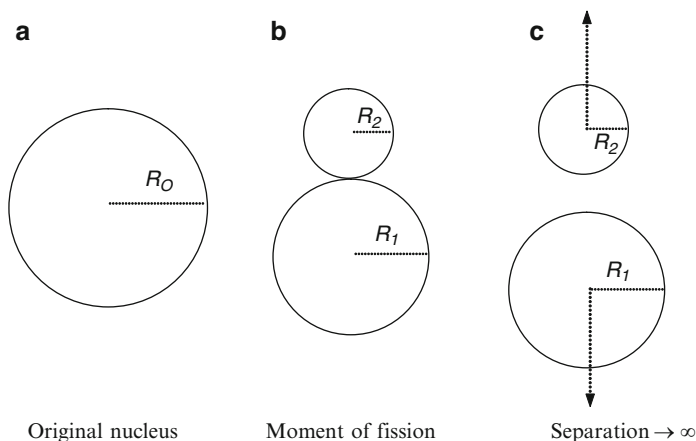$$R_1 = R_O \left(\frac{f}{1+f} \right)^{1/3} \tag{1.46}$$

a **b** **c**

R_O

R_2 R_2

R_1 R_1

Original nucleus   Moment of fission   Separation $\to \infty$

Fig. 1.4 Schematic illustration of the fission process

and

$$R_2 = R_O \left(\frac{1}{1+f} \right)^{1/3}. \tag{1.47}$$

Following Bohr and Wheeler, we take the energy of the system at any moment to comprise two contributions: (1) a surface energy proportional to the surface area of the system, and (2) the Coulombic self-energy of the system. The surface energy of the original nucleus can be written as

$$U_A^{orig} = a_S R_O^2 \tag{1.48}$$

where the coefficient a_S is to be determined. That for the fissioned nucleus will be

$$U_A^{fiss} = a_S \left(R_1^2 + R_2^2 \right) = a_S R_O^2 \alpha, \tag{1.49}$$

where

$$\alpha = \frac{f^{2/3} + 1}{(1+f)^{2/3}}. \tag{1.50}$$

For the Coulomb self-energy, begin with the result that the electrostatic self-energy of a sphere of charge of radius r is given by

$$U_C^{self} = \left(\frac{4\pi\rho^2}{15\,\varepsilon_o} \right) r^5, \tag{1.51}$$

where ρ is the charge density. In the present case, $\rho = 3\,Z\,e/4\,\pi\,R_O^3$ where Z is the atomic number of the *parent* nucleus. This gives $4\pi\rho^2/15\,\varepsilon_o = 3\,Z^2 e^2/20\,\pi\,\varepsilon_o R_O^6$ and hence

$$U_C^{orig} = \left(\frac{3\,e^2\,Z^2}{20\,\pi\,\varepsilon_o\,R_O} \right). \tag{1.52}$$

The electrostatic self-energy of the system at the moment of fission (part b Fig. 1.4) is the sum of that of each of the product nuclei plus that of the point-charge repulsion between them:

$$U_C^{fiss} = \left(\frac{3\,e^2 Z^2}{20\,\pi\,\varepsilon_o R_O^6} \right) \left(R_1^5 + R_2^5 \right) + \frac{Q_1\,Q_2}{4\,\pi\,\varepsilon_o (R_1 + R_2)}, \tag{1.53}$$

where Q_1 and Q_2 are the charges of the *product* nuclei. In terms of the mass ratio f this reduces to

$$U_C^{fiss} = \left(\frac{3\,e^2 Z^2}{20\,\pi\,\varepsilon_o R_O} \right) (\beta + \gamma), \tag{1.54}$$

where

$$\beta = \frac{f^{5/3} + 1}{(1 + f)^{5/3}} \tag{1.55}$$

and

$$\gamma = \frac{(5/3)f}{(1 + f)^{5/3} (f^{1/3} + 1)}. \tag{1.56}$$

The common factor appearing in (1.52) and (1.54) can be simplified. Empirically, nuclear radii behave as $R \sim aA^{1/3}$, where $a \sim 1.2$ fm. Incorporating this approximation and substituting values for the constants gives

$$\frac{3\,e^2\,Z^2}{20\,\pi\,\varepsilon_o\,R_O} \quad \sim \quad 0.72 \left(\frac{Z^2}{A^{1/3}}\right) \text{MeV}. \tag{1.57}$$

If the same empirical radius expression is incorporated into the surface-energy expressions, we can absorb the factor of 1.2 fm into the definition of a_S and write (1.48) and (1.49) as $U_A^{orig} = a_S A^{2/3}$ and $U_A^{fiss} = a_S A^{2/3}\alpha$; the units of a_S will emerge as MeV.

We can now begin to consider the question of the limiting value of Z^2/A. If the total energy of the two nuclei in the fission circumstance shown in Fig. 1.4b is *less* than that for the original nucleus of Fig. 1.4a, then the system will proceed to fission. That is, spontaneous fission will occur if

$$U_A^{orig} + U_C^{orig} > U_A^{fiss} + U_C^{fiss}. \tag{1.58}$$

Substituting (1.48)–(1.50), (1.52) and (1.54)–(1.57) into (1.58) shows that SF will occur for

$$\frac{Z^2}{A} > \frac{a_S\,(\alpha - 1)}{0.72\,(1 - \beta - \gamma)}. \tag{1.59}$$

Estimating the Z^2/A stability limit apparently demands selecting an appropriate mass ratio and knowing the value of a_S. For the latter, we could adopt a value from the semi-empirical mass formula, but it is more satisfying to derive a value for a_S based on some direct physical grounds. We take up this issue now, returning later to the question of an appropriate mass ratio.

To calibrate the value of a_S we appeal to the fact that fission can be induced by slow neutrons, with (in the case of uranium) $Q \sim 170$ MeV of energy being liberated. In the present notation this appears as

$$\left(U_A^{orig} + U_C^{orig}\right) - \left(U_A^{\infty} + U_C^{\infty}\right) = Q, \tag{1.60}$$

where U_A^∞ and U_C^∞ respectively designate the areal and Coulombic energies of the system when the product nuclei are infinitely far apart. Since the areas of the product nuclei do not change following fission, $U_A^\infty = U_A^{fiss}$; see (1.49) and (1.50). U_C^∞ is given by (1.53) without the point–charge interaction term, that is, (1.54) without the γ term. From these we find

$$a_S = \frac{\left(Q/A^{2/3}\right) - 0.72\left(Z^2/A\right)\left(1 - \beta\right)}{\left(1 - \alpha\right)}, \tag{1.61}$$

where A and Z refer to the parent nucleus in the fission reaction, *not* the general Z^2/A spontaneous-fission limit we seek.

Values of a_S derived in this way from a number of fission reactions involving ^{235}U are shown in Table 1.2. The first reaction is representative of the Hahn and Strassmann fission-discovery reaction. The second is concocted to have the masses of the fission products as 139 and 95, values claimed by Weinberg and Wigner (1958, p. 30) to be the most probable mass yields in slow-neutron fission of ^{235}U. The last two reactions are less probable ones chosen to give a sense of how sensitive a_S is to the choice of calibrating reaction. The mass ratios are those of the fission products, neglecting any neutrons emitted. As one might hope if a_S reflects some fundamental underlying physics, its value is fairly *insensitive* to the choice of calibrating reaction. The values of a_S derived here are consistent with those quoted in numerical fits of the semi-empirical mass formula, ~18 MeV.

With a_S in hand we can establish an estimate of the stability limit for Z^2/A against spontaneous fission based on (1.59).

If the limiting value of Z^2/A is to be a matter of fundamental physics, it should be independent of any fission-product mass ratio, a consideration that begs the question of what value of f to use in α, β, and γ in (1.59). In particular, it would make no sense to use the mass ratio for the *induced* reaction used to calibrate a_S to determine a limit against *spontaneous* fission. To resolve this dilemma, recall that f could also have been defined as the inverse of what was adopted in (1.45). The only value of f that is in any sense "unique" is therefore $f = 1$. Indeed, plots of the right side of (1.59) vs. f for fixed values of a_S reveals that a minimum always occurs at $f = 1$, symmetric (in the sense of $f \to 1/f$) about $f = 1$. To establish a lower limit to the spontaneous-fission condition, let us thus take (1.59) evaluated at $f = 1$:

$$\left(Z^2/A\right)_{\text{lim}} \quad \sim \quad 3.356\, a_S. \tag{1.62}$$

Table 1.2 Fission reactions, derived surface energy parameter, and derived spontaneous fission limit

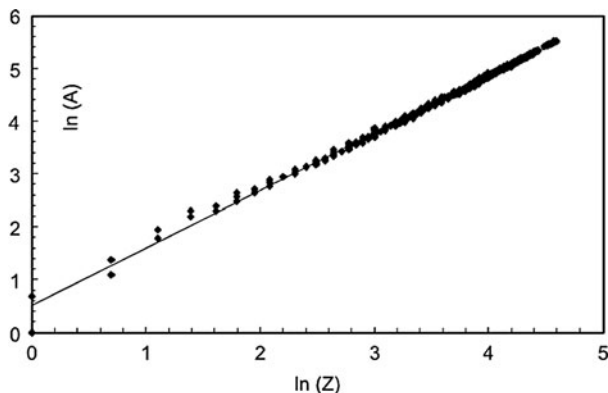| Fission products of ^{1}n + ^{235}U	Q (MeV)	f	a_S (MeV)	$(Z^2/A)_{lim}$
$^{141}_{56}$Ba + $^{92}_{36}$Kr + 3 $\left(^1_0\text{n}\right)$	173.2	1.53	18.3	61.4
$^{139}_{54}$Xe + $^{95}_{38}$Sr + 2 $\left(^1_0\text{n}\right)$	183.6	1.46	17.5	58.6
$^{116}_{46}$Pd + $^{116}_{46}$Pd + 4 $\left(^1_0\text{n}\right)$	177.0	1.00	19.0	63.7
$^{208}_{82}$Pb + $^{26}_{10}$Ne + 2 $\left(^1_0\text{n}\right)$	54.2	8.00	16.3	54.7

Fig. 1.5 ln(A) vs. ln(Z) for 352 nuclides with half-lives >100 years

Limiting values of Z^2/A so calculated are given in the last column of Table 1.2; in each case these are based on the a_S values in the preceding column of the table. While these are somewhat high compared to Bohr and Wheeler value of 48, the agreement is respectable given the simplicity of our model.

Spreadsheet **TwoSphereFission.xls** allows a user to enter mass numbers and delta-values for reactions like those in Table 1.2; the spreadsheet calculates values for $Q, f, \alpha, \beta, \gamma, a_S$, and the limiting value of Z^2/A.

We can estimate the value of Z beyond which nuclei will be unstable against spontaneous fission. From data given in the online version of the *Nuclear Wallet Cards*, one finds that there are 352 isotopes that are either permanently stable or have half-lives >100 years. A plot of A vs. Z for these isotopes can be approximately fit by a power law as shown in Fig. 1.5; the fit is

$$A \sim 1.6864 Z^{1.0870} \quad \left(r^2 = 0.9965 \right). \tag{1.63}$$

This fit slightly underestimates $A(Z)$ for heavy nuclei, giving $A \sim 230$ for $Z = 92$, but is sufficiently accurate for our purposes. For a limiting Z^2/A of 60, (1.63) predicts a maximum stable Z of about 157; the Bohr and Wheeler value of 48 gives a maximum Z of about 123.

1.8 Energy Spectrum of Fission Neutrons

When nuclei fission they typically emit two or three neutrons. These secondary neutrons are not all of the same energy, however; they exhibit a spectrum of kinetic energies. Knowing the average energy of these "secondary" neutrons is important in understanding the relative fissilities of ^{235}U and ^{238}U as discussed in Sect. 1.9.

According to Hyde (1964), the probability of a neutron being emitted with energy between E and $E + dE$ can be expressed as

$$P(E)\,dE = K\sqrt{E}\,e^{-E/\alpha}dE, \tag{1.64}$$

where K is a normalization constant and α is a fitting parameter. For energies measured in MeV, $\alpha \sim 1.29$ MeV in the case of ^{235}U. This distribution is shown in Fig. 1.6.

To determine the normalization factor K, we insist that the sum of the probabilities over all possible energies be unity:

$$\int_0^\infty P(E)\,dE = 1 \Rightarrow K \int_0^\infty \sqrt{E}\,e^{-E/\alpha}\,dE = 1. \tag{1.65}$$

Setting $x = \sqrt{E/\alpha}$ renders this as

$$2K\alpha^{3/2} \int_0^\infty x^2\,e^{-x^2}\,dx = 1. \tag{1.66}$$

This integral evaluates to $\sqrt{\pi}/4$, hence

$$K = \frac{2}{\sqrt{\pi}\,\alpha^{3/2}}. \tag{1.67}$$

To determine the mean neutron energy $\langle E \rangle$ we take a probability-weighted average of E over all possible energies:

$$\langle E \rangle = \int_0^\infty E\,P(E)\,dE = K \int_0^\infty E^{3/2}e^{-E/\alpha}\,dE. \tag{1.68}$$
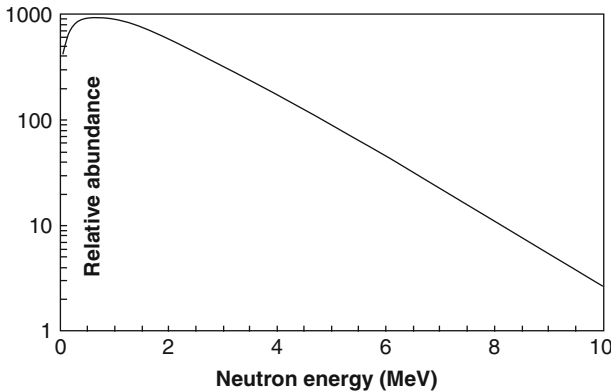

Fig. 1.6 Energy spectrum of neutrons released in fission of ^{235}U

Again setting $x = \sqrt{E/\alpha}$ renders this in a dimensionless form as

$$\langle E \rangle = 2K\alpha^{5/2} \int_0^\infty x^4\, e^{-x^2}\, dx. \tag{1.69}$$

This integral evaluates to $3\sqrt{\pi}/8$; invoking the normalization of (1.67) then gives

$$\langle E \rangle = \frac{3}{2}\alpha. \tag{1.70}$$

For $\alpha \sim 1.29$ MeV, $\langle E \rangle \sim 1.93$ MeV, or, say, about 2 MeV. From kinetic theory, this is equivalent to a $3kT/2$ temperature of $\sim 1.5 \times 10^{10}$ K (see Problem 1.8 in Appendix H).

In considering the question of why ^{238}U does not make an appropriate material for a weapon (Sect. 1.9), it proves helpful to know what fraction of the secondary neutrons are of energy greater than about 1.6 MeV. For the moment, suffice it to say that the reason for this is that the probability of fissioning ^{238}U nuclei by neutron bombardment is essentially zero for neutrons of energy less than this value.

The fraction of neutrons with kinetic energy E greater than some value ε is given by

$$f(E \geq \varepsilon) = \int_\varepsilon^\infty p(E)dE = K \int_\varepsilon^\infty \sqrt{E}e^{-E/\alpha}dE. \tag{1.71}$$

With (1.67) and setting $x = E/\alpha$,

$$f(E \geq \varepsilon) = \frac{2}{\sqrt{\pi}} \int_{\varepsilon/\alpha}^\infty \sqrt{x}e^{-x}dx. \tag{1.72}$$

This integral cannot be solved analytically; it must be evaluated numerically. For $\varepsilon = 1.6$ MeV and $\alpha = 1.29$ MeV, the lower limit of integration becomes $\varepsilon/\alpha = 1.24$. The integral itself evaluates to 0.4243 and the entire expression to 2 $(0.4243)/\pi^{1/2} = 0.4788$. For convenience, we round this off to 0.5. This means that about one-half of the neutrons emitted in the fission of a ^{235}U nucleus would be energetic enough to fission a ^{238}U nucleus. We shall see in the next section, however, that the story is more complicated than this.

1.9 Leaping the Fission Barrier

Much of the material in this section is adopted from a publication elsewhere by the author (Reed 2008).

The isotopes ^{235}U and ^{238}U differ not at all in their chemical properties and yet behave so differently under neutron bombardment. How can this be? While a detailed treatment of fission is very complex and lies beyond the scope of the present text, we can get some idea of why things behave this way from some energy arguments.

Theory indicates that *any* otherwise stable nucleus can be induced to fission under neutron bombardment. However, any specific isotope possesses a characteristic *fission barrier*. This means that a certain minimum energy has to be supplied to deform the nucleus sufficiently to induce the fission process to proceed. This concept is analogous to the *activation energy* for a chemical reaction; the two terms are in fact used synonymously.

This energy can be supplied in two ways: (1) in the form of kinetic energy carried in by the bombarding neutron that initiates the fission, and/or (2) from "binding" energy liberated when the target nucleus absorbs the bombarding particle and so becomes a different nuclide with its own characteristic mass. Both factors play roles in understanding uranium fission.

The smooth curve in Fig. 1.7 shows theoretically-computed fission barrier "heights" in MeV as a function of mass number A; the irregular curve incorporates more sophisticated calculations. Barrier energies vary from a high of about 55 MeV for isotopes with $A \sim 90$ down to a few MeV for the heaviest elements such as uranium and plutonium. For elements heavier than Pu, half-lives for various modes of decay (α and β decays) tend to be so short as to make them impractical candidates for weapons materials despite their low fission barriers.
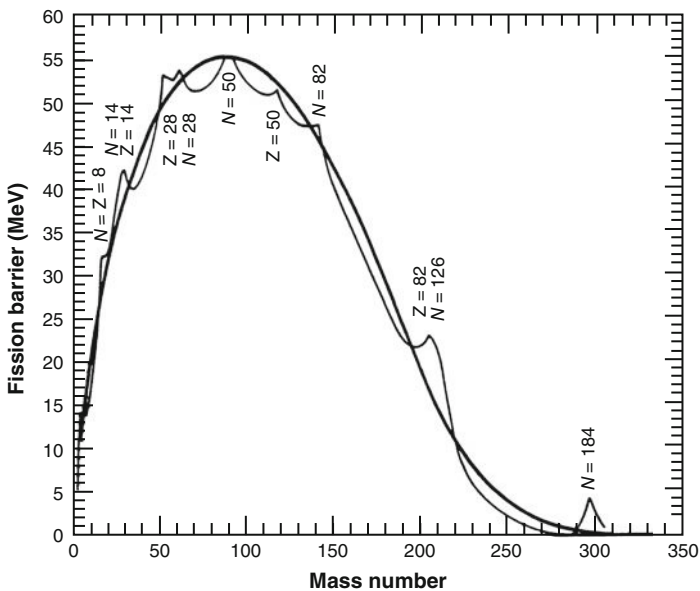

Fig. 1.7 Fission barrier vs. mass number; from Myers and Swiatecki (1966). Reproduced with permission of Elsevier Science

Fission is believed to proceed via formation of an "intermediate" or "compound" nucleus formed when the target nucleus absorbs the incoming neutron. Two cases are relevant for uranium:

$$\,_0^1\text{n} + \,_{92}^{235}\text{U} \rightarrow \,_{92}^{236}\text{U} \tag{1.73}$$

and

$$\,_0^1\text{n} + \,_{92}^{238}\text{U} \rightarrow \,_{92}^{239}\text{U}. \tag{1.74}$$

For reaction (1.73), the Δ values are 8.071, 40.921, and 42.446. The Q-value of this reaction is then 6.546 MeV. For reaction (1.74), the Δ values are 8.071, 47.309, and 50.574, leading to a Q-value of 4.806 MeV. Now imagine that the bombarding neutrons are "slow", that is, that they bring essentially no kinetic energy into the reactions. ("Fast" and "slow" neutron energies are explored in more detail in Sect. 3.2) The nucleus of ^{236}U formed in reaction (1.73) will find itself in an *excited state* with an internal energy of about 6.5 MeV while the ^{239}U nucleus formed in reaction (1.74) will have a like energy of about 4.8 MeV.

Fission barriers for various nuclides are tabulated in Appendix A. For the compound nuclei considered here, ^{236}U and ^{239}U, these are respectively 5.67 and 6.45 MeV. In the case of ^{236}U the Q-value exceeds the fission barrier by nearly 0.9 MeV. Consequently, any bombarding neutron, no matter how little kinetic energy it has, can induce fission in ^{235}U. On the other hand, the Q-value of reaction (1.74) falls some 1.6 MeV short of the fission barrier. To fission ^{238}U by neutron bombardment thus requires input neutrons of at least this amount of energy. ^{235}U is known as a "fissile" nuclide while ^{238}U is termed "fissionable."

Figure 1.8 shows the situation for various U and Pu isotopes; $Q - E_{Barrier}$ is plotted as a function of target mass number A. The upper line is for Pu isotopes while the lower one is for U isotopes.

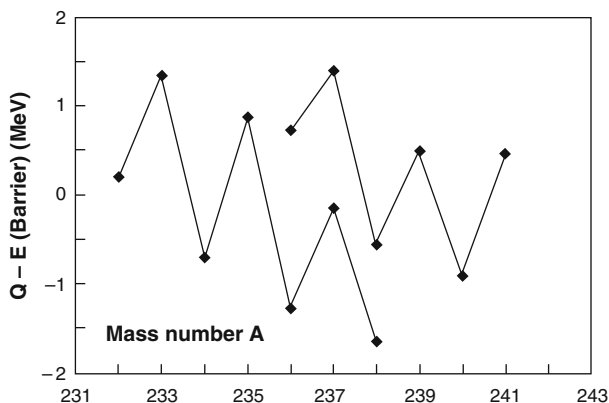**Fig. 1.8** Energy release minus fission barrier for fission of isotopes of uranium (*lower line*) and plutonium (*upper line*). If $Q - E_{Barrier} > 0$, an isotope is said to be "fissile"

From Fig. 1.8, it appears that both ^{232}U and ^{233}U would make good candidates for weapons materials. ^{232}U is untenable, however, as it has a 70-year alpha-decay half-life. For practical purposes, ^{233}U is also not convenient as it does not occur naturally and has to be created by neutron bombardment of ^{232}Th in a reactor that is already producing plutonium (Kazimi 2003). Aside from its fission-barrier issue, ^{234}U has such a low natural abundance as to be of negligible consequence (~0.006%), and ^{236}U does not occur naturally at all. ^{237}U is close to having $Q - E_{Barrier} \geq 0$, but has only a 6.75-day half-life against beta-decay.

In the case of plutonium, mass numbers 236, 237, 238 and 241 have such short half-lives against various decay processes as to render them too unstable for use in a weapon even if one went to the trouble of synthesizing them in the first place (2.87-day alpha-decay, 45-day electron capture, 88-day alpha-decay and 14-day beta-decay, respectively). ^{240}Pu turns out to have such a high spontaneous fission rate that its very presence in a bomb core actually presents a danger of causing an uncontrollable premature detonation; this issue is analyzed in Sect. 4.2. Pu nuclei of mass number 239 are the only ones of this element that are suitable as a weapons material.

A pattern in evident in Fig. 1.8. All stable nuclei have lower masses than one would predict on the naive basis of adding up the masses of their Z protons and A–Z neutrons; the difference goes into binding energy. Nuclear physicists have known for many decades that in this mass-energy sense, so-called even/odd nuclei such as ^{235}U or ^{239}Pu are inherently less stable than even/even nuclei; the underlying cause has to do with the way in which nuclear forces act between pairs of nucleons. In other words, in comparison to even/odd nuclei, even/even nuclei are of even lower mass than the naive mass-addition argument would suggest. Hence, when an even/odd nucleus such as ^{235}U takes in a neutron it becomes an even/even nucleus of "relatively" low mass; the mass difference appears as excitation energy via $E = mc^2$. When an even/even nucleus takes in a neutron it liberates mass-energy as well, but not as much as in the even/odd case; the result is dramatically different $Q - E_{Barrier}$ values. This "parity" effect reveals itself as the jagged lines in Fig. 1.8.

The issue of the unsuitability of ^{238}U as a *weapons* material is, however, more subtle than the above argument lets on. We saw in Sect. 1.8 that the average energy of secondary neutrons liberated in fission of uranium nuclei is about 2 MeV and that about half of these neutrons have energies greater than the ~1.6 MeV excitation energy of the n + ^{238}U → ^{239}U reaction. In view of this it would appear that ^{238}U might make a viable weapons material. Why does it not? The problem turns out to depend on what happens when fast neutrons encounter ^{238}U nuclei.

The fission-spectrum averaged inelastic-scattering cross-section for neutrons against ^{238}U is about 2.6 bn, whereas the average fission cross-section is about 0.31 bn. (*In*elastic scattering means a collision wherein the kinetic energy of the incoming particle is reduced in the collision; in an *elastic* scattering the kinetic energy of the incoming particle is conserved. If the concept of a cross-section is unfamiliar to you, it is discussed in more detail in Sect. 2.1) Thus, a fast neutron striking a ^{238}U nucleus is about eight times as likely to be inelastically scattered as it

is to induce a fission. Experimentally, neutrons of energy 2.5 MeV inelastically scattering from ^{238}U have their energy reduced to a most probable value of about 0.275 MeV as a result of a *single* scattering (Fetisov 1957). The vast majority of neutrons striking ^{238}U nuclei will thus promptly be slowed to energies below the fission threshold. The catch is that below about 1 MeV, ^{238}U begins to have a significant non-fission neutron *capture* cross-section. The relevant cross-sections are shown in Fig. 1.9; see also Fig. 2.3.

In short, the non-utility of ^{238}U as a weapons material is due not to a lack of fission cross-section for fast neutrons but rather to a parasitic combination of inelastic scattering and a fission threshold below which it has an appreciable capture cross-section for slowed neutrons. To aggravate the situation further, the capture cross-section of ^{238}U below about 0.01 MeV is characterized by a dense forest of capture resonances with cross-sections of up to thousands of barns (Hyde 1964; Garwin and Charpak 2001); the curves in Fig. 1.9 terminate at about 0.03 MeV at the low-energy end. The overall result is a rapid suppression of any chain reaction. ^{235}U and ^{239}Pu have cross-sections for inelastic scattering as well, but they differ from ^{238}U in that they have no fission threshold; slowed neutrons will still fission them and fission will in fact always strongly dominate over capture for them. All of these isotopes also *elastically* scatter neutrons but this is of no concern here as this process does not degrade the neutrons' kinetic energies. These cross-section arguments also play a central role in the issue of achieving controlled chain reactions, as is discussed in Sect. 3.1.
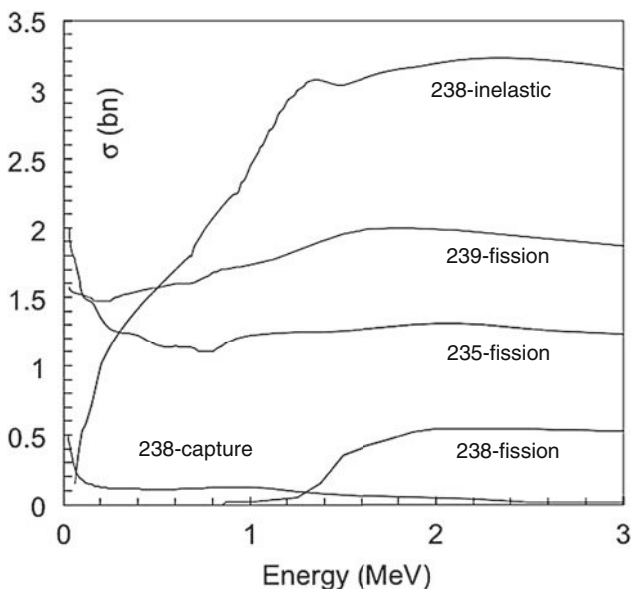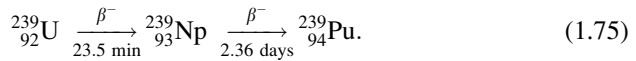

Fig. 1.9 ^{239}Pu, ^{235}U, and ^{238}U fission cross-sections and ^{238}U capture and inelastic-scattering cross-sections as functions of bombarding neutron energy

To put further understanding to this fast-fission poisoning effect of ^{238}U, consider the following numbers. Suppose that 2-MeV secondary neutrons lost only half their energy due to inelastic scattering. At 1 MeV, the fission cross-section of ^{235}U is about 1.22 bn while the capture cross-section of ^{238}U is about 0.13 bn. In a sample of natural U, where the ^{238}U:^{235}U abundance ratio is 140:1, capture would consequently dominate fission by a factor of about 15:1. The net result is that only ^{235}U can sustain a growing fast-neutron chain reaction and it is for this reason that this isotope must be laboriously isolated from its more populous sister isotope if one aspires to build a uranium bomb. Bomb-grade uranium is defined as 90% pure ^{235}U.

Despite its non-fissility, ^{238}U played a crucial role in the Manhattan Project. The ^{239}U nucleus formed in reaction (1.74) sheds its excess energy in a series of two beta-decays, ultimately giving rise to ^{239}Pu:

$$^{239}_{92}\text{U} \xrightarrow[\text{23.5 min}]{\beta^-} {}^{239}_{93}\text{Np} \xrightarrow[\text{2.36 days}]{\beta^-} {}^{239}_{94}\text{Pu}. \tag{1.75}$$

Like ^{235}U, ^{239}Pu is an even–odd nucleus and was predicted by Bohr and Wheeler to be fissile under slow-neutron bombardment. This is indeed the case. The reaction

$$^{1}_{0}\text{n} + {}^{239}_{94}\text{Pu} \rightarrow {}^{240}_{94}\text{Pu} \tag{1.76}$$

has a Q-value of 6.53 MeV, but the fission barrier of ^{240}Pu is only about 6.1 MeV. Fast neutrons thus promptly fission ^{239}Pu. Slow neutron bombardment of Pu-239 can actually lead to two outcomes: fission (cross-section 750 bn) or neutron absorption (cross-section 270 bn) to produce semi-stable Pu-240, which has an α-decay half-life of 6,560 years.

1.10   A Semi-Empirical Look at the Fission Barrier

In this section we extend the model of fission developed in Sect. 1.7 to show how one can "derive" the general trend of fission-barrier energy as a function of mass number as shown in Fig. 1.7. This derivation is not rigorous and will require some interpolation and adoption of a result from Bohr and Wheeler's (1939) paper. Also, as fission barriers are now known to depend in complex ways on nuclear shell effects, pairing corrections, energy levels, and deformation and mass asymmetries, we cannot expect the simple model presented here to capture their detailed behavior.

We saw in Sect. 1.7 that if a nucleus of mass number A and atomic number Z is modeled as a sphere, its total energy U_E can be expressed as

$$U_E^{orig} = a_S A^{2/3} + a_C \left(\frac{Z^2}{A^{1/3}} \right), \tag{1.77}$$

where a_S and a_C are respectively *surface* and *Coulomb* energy parameters of values $a_S \sim 18$ MeV and $a_C \sim 0.72$ MeV. Further, if the fissioning nucleus is modeled as

two touching spheres of mass ratio f ($f > 1$), then the energy of the system at the moment of fission is given by

$$U_E^{fiss} = a_S A^{2/3} \alpha + a_C \left(\frac{Z^2}{A^{1/3}} \right) (\beta + \gamma),$$ (1.78)

where

$$\alpha = \frac{f^{2/3} + 1}{(1 + f)^{2/3}},$$ (1.79)

$$\beta = \frac{f^{5/3} + 1}{(1 + f)^{5/3}},$$ (1.80)

and

$$\gamma = \frac{(5/3)f}{(1 + f)^{5/3} \, (f^{1/3} + 1)}.$$ (1.81)

The difference in energy between the fissioning and original configurations is given by

$$\Delta E = U_E^{fiss} - U_E^{orig} = a_S A^{2/3} (\alpha - 1) + a_C \left(\frac{Z^2}{A^{1/3}} \right) (\beta + \gamma - 1).$$ (1.82)

Typically, $\Delta E > 0$, that is, there is an *energy barrier* that inhibits the fission process. The goal here is to look at the run of ΔE as a function of the mass number A. For a reason that will become clear in a moment, divide through (1.82) by $a_S A^{2/3}$:

$$\frac{\Delta E}{a_S A^{2/3}} = (\alpha - 1) + \frac{a_C}{a_S} \left(\frac{Z^2}{A} \right) (\beta + \gamma - 1).$$ (1.83)

The reason for this manipulation is to set up our expression for ΔE in a form ready to accommodate an important result obtained by Bohr and Wheeler. This is that, in terms of a_S and a_C, they were able to prove that the limiting value of Z^2/A against spontaneous fission is given by

$$\left(\frac{Z^2}{A} \right)_{lim} = 2 \left(\frac{a_S}{a_C} \right).$$ (1.84)

A formal proof of this important result appears in Appendix E. This expression is analogous to (1.62) but is more general as it is entirely independent of the particular shape of the fissioning nucleus. In terms of this limit, we can write (1.83) as

$$\frac{\Delta E}{a_S A^{2/3}} = (\alpha - 1) + 2(\beta + \gamma - 1) x,$$ (1.85)

where x is defined as

$$x = \left(\frac{Z^2}{A}\right) \Big/ \left(\frac{Z^2}{A}\right)_{\text{lim}} \quad (0 \leq x \leq 1). \tag{1.86}$$

Now consider, as Bohr and Wheeler did, fission into equal-mass product nuclei: $f = 1$. In this case we have $\alpha = 1.25992$, $\beta = 0.62996$, and $\gamma = 0.26248$, and hence

$$\frac{\Delta E}{a_S A^{2/3}} = f_{linear}(x) = 0.25992 - 0.21511\, x. \tag{1.87}$$

Equation (1.87) predicts that $\Delta E / a_S A^{2/3}$ will decline linearly with x until it reaches zero at $x = (0.25992/0.21511) = 1.208$; this behavior is shown as the straight line in Fig. 1.10.

That this result predicts a fission barrier of zero for a value of $x > 1$ indicates that our simple "two-sphere" model of fission cannot be an accurate representation of the real shape of a fissioning nucleus; we should have $f(x) \to 0$ as $x \to 1$. Presumably $f(x)$ should have some shape more akin to the smooth curve shown in Fig. 1.10. The precise recipe for the curve shown is elucidated in what follows.

Following Bohr and Wheeler, we develop a plausible interpolating function for $f(x)$. Presuming (as they did) that $f_{\text{linear}}(x)$ accurately models the fission barrier
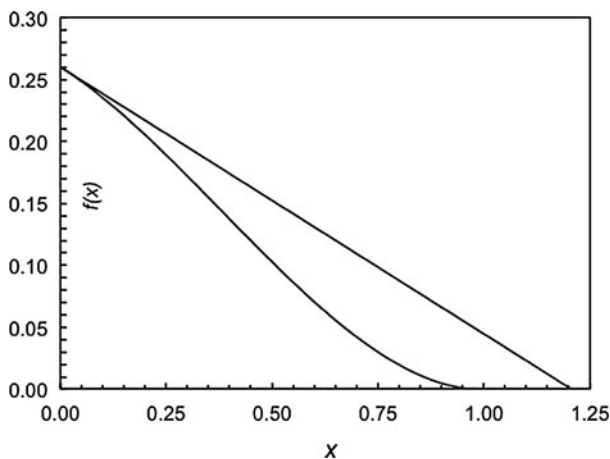

Fig. 1.10 Straight line: fission barrier function $f_{\text{linear}}(x)$ of (1.87). The curved line is the interpolating function of (1.89) and (1.90) designed to give $f_{\text{smooth}}(x) \to 0$ as $x \to 1$

for nuclei with small values of x, we seek an interpolating function that satisfies four criteria:

$$
\begin{aligned}
&\text{(i) } f(x) = (\alpha - 1) \text{ at } x = 0 \\
&\text{(ii) } df/dx = 2(\beta + \gamma - 1) \text{ at } x = 0 \\
&\text{(iii) } f(x) = 0 \text{ at } x = 1 \\
&\text{(iv) } df/dx = 0 \text{ at } x = 1
\end{aligned} \tag{1.88}
$$

Conditions (i) and (ii) demand that $f(x)$ behave as (1.87) for small values of x; condition (iii) is the Bohr and Wheeler limiting condition of (1.86), and condition (iv) ensures that $f(x)$ will approach this limiting condition "smoothly." Apparently, a virtual infinitude of interpolating functions could be conceived. With no physical guide beyond these four criteria to help narrow down a selection, we make a simple choice: a polynomial. The lowest-order polynomial with four adjustable constants is a cubic, that is,

$$
f_{smooth}(x) = Fx^3 + Bx^2 + Cx + D. \tag{1.89}
$$

Fitting the above criteria to this function shows that we must have

$$
\left.
\begin{aligned}
D &= (\alpha - 1) \\
C &= 2(\beta + \gamma - 1) \\
B &= (7 - 3\alpha - 4\beta - 4\gamma) \\
F &= 2(\alpha + \beta + \gamma - 2)
\end{aligned}
\right\}. \tag{1.90}
$$

In their paper, Bohr and Wheeler do not make clear precisely what sort of interpolation they used; they appear to have adopted some interpolating function and calibrated it using the then experimentally-estimated barrier $\Delta E \sim 6$ MeV for ^{238}U.

For $f = 1$, (1.90) gives $(D, C, B, F) = (0.2599, -0.2151, -0.3495, 0.3047)$; this is the smooth curve in Fig. 1.10. With this function that now respects the correct limiting value of Z^2/A, we can write the energy necessary to distort a nucleus to the point of fission as

$$
\Delta E = a_S A^{2/3} f_{smooth}(x). \tag{1.91}
$$

To compare our model with Fig. 1.7 it is desirable to plot ΔE in terms of mass number A. To do this we need some model for how the atomic number Z tracks with mass number A, since $x = (Z^2/A)/(Z^2/A)_{lim}$. If the plot in Fig. 1.5 is reversed, one finds that

$$
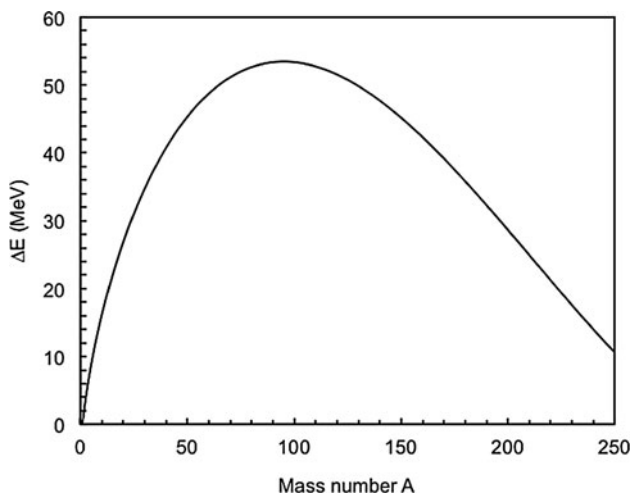Z \sim 0.60679 A^{0.92383} \left(2 \leq Z \leq 98; r^2 = 0.99742 \right). \tag{1.92}
$$

Fig. 1.11 Fission barrier energy of (1.89)–(1.92) for fission-product mass ratio = 1. Compare to Fig. 1.7

Figure 1.11 shows the run of ΔE vs. A for $f = 1$ upon assuming (1.92) and (a_S, a_C) = (18, 0.72) MeV.

In computing Fig. 1.11, a modification was made to (1.91). This is that for $A = 1$, it predicts $\Delta E = 4.65$ MeV. This "offset" value was subtracted from all values of ΔE on the rationale that one cannot fission a nucleus with $A = 1$.

Spreadsheet **BarrierCubic.xls** allows a user to set the mass ratio f and values for the parameters a_S and a_C; the spreadsheet computes and displays the values of α, β, and γ of (1.79)–(1.81) and plots Figs. 1.10 and 1.11, taking into account the $A = 1$ offset.

Figure 1.11 is remarkably similar in shape to Fig. 1.7 in that it displays a broad peak at $A \sim 100$ with $\Delta E \sim 55$ MeV, followed by a decline. The present model predicts $\Delta E \sim 15.8$ MeV for $A = 235$ (for which (1.92) gives $Z = 94.1$), and so is obviously not fully accurate. But it does successfully capture the general trend of barrier energy as a function of A. For elements lighter than uranium the fission barrier is too great to be overcome by release of binding energy alone.

References

Amaldi, E.: From the discovery of the neutron to the discovery of nuclear fission. Phys. Rep. **111** (1–4), 1–332 (1984)

Anderson, H.L., Fermi, E., Hanstein, H.B.: Production of neutrons in uranium bombarded by neutrons. Phys. Rev. **55**, 797–798 (1939)

Bohr, N.: Resonance in uranium and thorium disintegrations and the phenomenon of nuclear fission. Phys. Rev. **55**, 418–419 (1939)

Bohr, N., Wheeler, J.A.: The mechanism of nuclear fission. Phys. Rev. **56**, 426–450 (1939)

Brown, A.: The Neutron and the Bomb: A Biography of Sir James Chadwick. Oxford University Press, Oxford (1997)

Chadwick, J.: Possible existence of a neutron. Nature **129**, 312 (1932a)

Chadwick, J.: The existence of a neutron. Proc. R. Soc. London. **A136**, 692–708 (1932b)

Feather, N.: The time involved in the process of nuclear fission. Nature **143**, 597–598 (1939)

Fetisov, N.I.: Spectra of neutrons inelastically scattered on ^{238}U. Atom. Energ. **3**, 995–998 (1957)

Garwin, R.L., Charpak, G.: Megawatts and Megatons: A Turning Point in the Nuclear Age? Alfred A. Knopf, New York (2001)

Hahn, O., Strassmann, F.: Über den Nachweis und das Verhalten der bei der Bestrahlung des Urans mittels Neutronen entstehenden Erdalkalimetalle. Naturwissenschaften **27**, 11–15 (1939). An English translation appears in Graetzer, H. G.: Discovery of Nuclear Fission. Am. J. Phys. **32**, 9-15 (1964). In English, the title of Hahn and Strassmann's paper is "Concerning the Existence of Alkaline Earth Metals Resulting from Neutron Irradiation of Uranium."

Hyde, E.K.: The Nuclear Properties of the Heavy Elements III. Fission Phenomena. Prentice-Hall, Englewood Cliffs (1964)

Kazimi, M.S.: Thorium fuel for nuclear energy. Am. Sci. **91**, 408–415 (2003)

Meitner, L., Frisch, O.: Disintegration of uranium by neutrons: a new type of nuclear reaction. Nature **143**, 239–240 (1939)

Myers, W., Swiatecki, W.: Nuclear masses and deformations. Nucl. Phys. **81**, 1–60 (1966)

Nier, A.O., Booth, E.T., Dunning, J.R., Grosse, A.V.: Nuclear fission of separated uranium isotopes. Phys. Rev. **57**, 546 (1940)

Penney, W., Samuels, D.E.J., Scorgie, G.C.: The nuclear explosive yields at Hiroshima and Nagasaki. Philos. Trans. R. Soc. Lond. **A266**(1177), 357–424 (1970)

Reed, B.C.: Simple derivation of the Bohr–Wheeler spontaneous fission limit. Am. J. Phys **71**, 258–260 (2003)

Reed, B.C.: Chadwick and the discovery of the neutron. Society of Physics Students Observer. **XXXIX**(1), 1–7 (2007)

Reed, B.C.: A graphical examination of uranium and plutonium fissility. J. Chem. Educ. **85**(3), 446–450 (2008)

Rhodes, R.: The Making of the Atomic Bomb. Simon and Schuster, New York (1986)

Rutherford, E., Soddy, F.: Radioactive change. Philos. Mag. series 6, **v**, 576–591 (1903)

Rutherford, E.: Collision of α particles with light atoms. IV. An anomalous effect in nitrogen. Philos. Mag. series 6, **xxxvii**, 581–587 (1919)

Szilard, L., Zinn, W.H.: Instantaneous emission of fast neutrons in the interaction of slow neutrons with uranium. Phys. Rev. **55**, 799–800 (1939)

von Halban, H., Joliot, F., Kowarski, L.: Number of neutrons liberated in the nuclear fission of uranium. Nature **143**, 680 (1939)

Weinberg, A.M., Wigner, E.P.: The physical theory of neutron chain reactors. University of Chicago Press, Chicago (1958)

This page intentionally left blank

Chapter 2
Critical Mass and Efficiency

Abstract This chapter forms the heart of this book. After deriving the properties of neutron travel through materials, a detailed analysis is presented of how the critical mass of a fissile material, in both "bare" and "tampered" configurations, can be calculated. The calculations are applied to both uranium-235 and plutonium-239. Analytic expressions are developed for estimating bomb energy yield and efficiency. A numerical simulation is developed to analyze conditions of pressure, fission rate, expansion, and energy yield within a fissioning bomb core, and is applied to the Hiroshima *Little Boy* bomb. Spreadsheets for performing the calculations are made available to interested users through a supporting website.

Every atom of separated uranium or plutonium in the Manhattan Project was precious, so estimating the amount of fissile material needed to make a workable nuclear weapon – the so-called critical mass – was a crucial issue for the developers of *Little Boy* and *Fat Man*. Equally important was being able to estimate what efficiency one might expect for a fission bomb. For various reasons, not all of the fissile material in a bomb core actually undergoes fission during a nuclear explosion; if the expected efficiency were to prove so low that one might just as well use a few conventional bombs to achieve the same energy release, there would be no point in taking on the massive engineering challenges involved in making nuclear weapons. In this chapter we investigate these issues.

The concept of critical mass involves two competing effects. As nuclei fission they emit secondary neutrons. A fundamental empirical law of nuclear physics, derived in Sect. 2.1, demands that a certain fraction of these neutrons reach the surface of the mass and escape while the remainder are consumed in fissioning other nuclei. However, if on average more than one neutron is emitted per fission we can afford to let some escape since only one is required to initiate a subsequent fission. For a small sample of material the escape probability is high; as the size of the sample increases, the escape probability declines and at some point will reach a value such that the number of neutrons that fail to escape will number enough to fission every nucleus in the sample. Thus, there is a minimum size (hence mass) of

material at which every nucleus will in principle be fissioned even while some neutrons escape.

The above description of critical mass should be regarded as a purely qualitative one. Technically, the important issue is known as *criticality*. Criticality is said to obtain when the number of free neutrons in a bomb core is increasing with time. A full understanding of criticality demands familiarity with time-dependent diffusion theory. Application of diffusion theory to this problem requires understanding a concept known as the *mean free path* (MFP) for neutron travel, so this is developed in Sect. 2.1. Section 2.2 takes up a time-dependent diffusion theory treatment of criticality. Section 2.3 addresses the effect of surrounding the fissile core with a *tamper*, a metallic casing which has the effects of decreasing the critical mass and improving the efficiency of the explosion. Sections 2.4 and 2.5 take up the issue of bomb efficiency through analytic approximations and a numerical simulation, respectively. Section 2.6 presents an alternate treatment of untamped criticality that has an interesting historical connection.

For readers interested in further sources, an excellent account of the concept of critical mass appears in Logan (1996); see also Bernstein (2002).

2.1 Neutron Mean Free Path

See Fig. 2.1. A thin slab of material of thickness s (ideally, one atomic layer) and cross-sectional area Σ is bombarded by incoming neutrons at a rate R_o neutrons/ $(\text{m}^2 \text{ s})$.

Let the bulk density of the material be ρ g/cm^3. In nuclear reaction calculations, however, density is usually expressed as a *number density* of nuclei in the material, that is, the number of nuclei per cubic meter. In terms of ρ this is given by
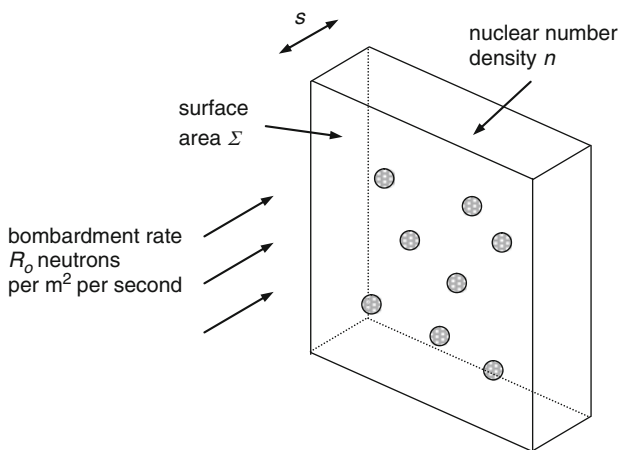

Fig. 2.1 Neutrons penetrating a thin target foil

$$n = 10^6 \left(\frac{\rho N_A}{A} \right), \tag{2.1}$$

where N_A is Avogadro's number and A is the atomic weight (g/mol) of the material; the factor of 10^6 arises from converting cm^3 to m^3.

Assume that each nucleus presents a total reaction cross-section of σ square meters to the incoming neutrons. Cross-sections are usually measured in barns (bn), where 1 bn $= 10^{-28}$ m^2. The first question we address is: "How many reactions will occur per second as a consequence of the bombardment rate R_o?" The volume of the slab is Σs, hence the number of nuclei contained in it will be Σsn. If each nucleus presents an effective cross-sectional area σ to the incoming neutrons, then the total area presented by all nuclei would be $\Sigma sn\sigma$. The *fraction* of the surface area of the slab that is available for reactions to occur is then $(\Sigma sn\sigma/\Sigma) = sn\sigma$. The rate of reactions R (reactions/s) can then sensibly be assumed to be the rate of bombarding particles over the entire surface area of the slab times the fraction of the surface area available for reactions:

$$\begin{pmatrix} Reactions \\ per\ second \end{pmatrix} = \begin{pmatrix} incident\ neutron \\ flux/second \end{pmatrix} \begin{pmatrix} fraction\ of\ surface\ area \\ occupied\ by\ cross-section \end{pmatrix}$$

or

$$R = (R_o \Sigma)(s\,n\,\sigma). \tag{2.2}$$

The *probability P* that an individual incident neutron precipitates a reaction is then

$$P_{react} = \frac{\begin{pmatrix} reactions \\ per\ second \end{pmatrix}}{\begin{pmatrix} incident\ neutron\ flux \\ per\ second \end{pmatrix}} = s\,n\,\sigma. \tag{2.3}$$

For our purposes, more directly useful is not the probability that a neutron will be consumed in a reaction, but rather that it will pass through the slab to escape out the back side:

$$P_{escape} = 1 - P_{react} = 1 - s\,n\,\sigma. \tag{2.4}$$

Now consider a block of material of macroscopic thickness x. As shown in Fig. 2.2, we can imagine this to be comprised of a large number of thin slabs each of thickness s placed back-to-back.

Fig. 2.2 Neutrons penetrating a thick target
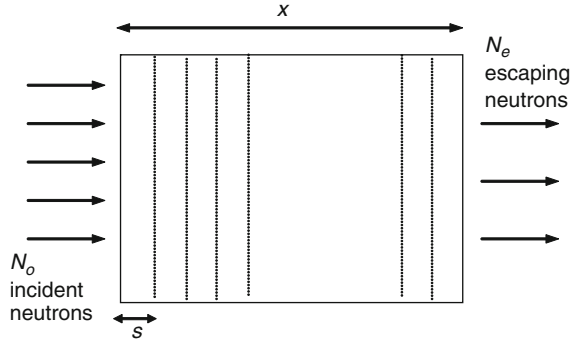
The number of slabs is $\eta = x/s$. If N_o neutrons are incident on the left side of the block, the number that would survive to emerge from the first thin slab would be $N_o P$, where P is the probability in (2.4). These neutrons are then incident on the second slab, and the number that would emerge unscathed from that passage would be $(N_o P)P = N_o P^2$. These neutrons would then strike the third slab and so on. The number that survive passage through the entire block to escape from the right side would be $N_o P^{\eta}$, or

$$N_{esc} = N_o (1 - s n \sigma)^{x/s}. \tag{2.5}$$

Define $z = -sn\sigma$. The number that escape can then be written as

$$N_{esc} = N_o (1 + z)^{-\sigma n x/z} = N_o \left[(1 + z)^{1/z}\right]^{-\sigma n x}. \tag{2.6}$$

Now, ideally, s is very small, which means that $z \to 0$. The definition of the base of the natural logarithms, e, is $e = \lim_{z \to 0} (1 + z)^{1/z}$, so we have

$$N_{esc} = N_o e^{-\sigma n x},$$

or

$$P_{direct\ escape} = \frac{N_{esc}}{N_o} = e^{-\sigma n x}. \tag{2.7}$$

Equation (2.7) is the fundamental escape probability law. In words, it says that the probability that a bombarding neutron will pass through a slab of material of thickness x depends exponentially on x, on the number density of nuclei in the slab, and on the reaction cross-section of those nuclei to incoming neutrons. If $\sigma = 0$, all of the incident particles will pass through unscathed. If $(\sigma n x) \to \infty$, *none* of the incident particles will make it through.

In practice, (2.7) is used to experimentally establish values for cross-sections by bombarding a slab of material with a known number of incident particles and then seeing how many emerge from the other side; think of (2.7) as effectively *defining* σ. Due to quantum-mechanical effects, the cross-section is not the geometric area of the nucleus.

The total cross section had in mind here can be broken down into a sum of cross-sections for individual processes such as fission, elastic scattering, inelastic scattering, non-fission capture and the like:

$$\sigma_{total} = \sigma_{fission} + \sigma_{elastic\ scatter} + \sigma_{inelastic\ scatter} + \sigma_{capture} + \dots . \qquad (2.8)$$

In practice, cross-sections can depend very sensitively on the energy of the incoming neutrons; such energy-dependence plays a crucial role in the contrast between how nuclear reactors and nuclear weapons function. As an example, Fig. 2.3 (see also Fig. 1.9) shows the variation of the fission cross-section for ^{235}U under neutron bombardment for neutrons in the energy range 1–10 eV; note the dramatic resonance effects at certain energies. This graph shows only a small fraction of the energy range over which the cross-section for the ^{235}U(n, f) reaction has been measured; measurements from 10^{-5} eV to 20 MeV are available from the source listed in the figure caption.

A very important result that derives from this escape-probability law is an expression for the *average* distance that an incident neutron will penetrate into the slab before being involved in a reaction. Look at Fig. 2.4, where we now have a slab of thickness L and where x is a coordinate for any position within the slab. Imagine also a small slice of thickness dx whose front edge is located at position x.
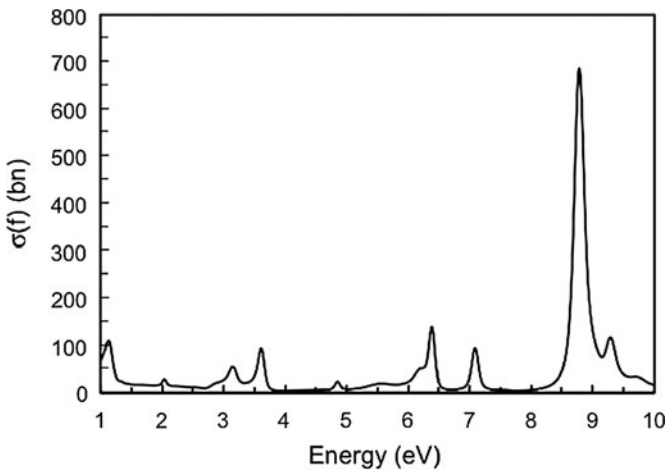

Fig. 2.3 Cross-section for the ^{235}U(n, f) reaction over the energy range 1–10 eV. At 0.01 eV, the cross-section for this reaction is about 930 bn. Data from National Nuclear Data Center
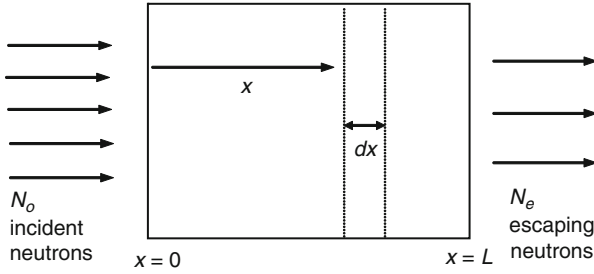
Fig. 2.4 Neutrons penetrating a target of thickness L

From (2.7), the probability that a neutron will penetrate through the entire slab to emerge from the face at $x = L$ is $P_{emerge} = e^{-\sigma nL}$. This means that the probability that a neutron will be involved in a reaction and *not* travel through to the face at $x = L$ will be $P_{react} = 1 - e^{-\sigma nL}$. If N_o neutrons are incident at the $x = 0$ face then the number that will be consumed in reactions within the slab will be $N_{react} = N_o(1 - e^{-\sigma nL})$. We will use this result in a moment.

Also from (2.7), the number of neutrons that penetrate to x and $x + dx$, respectively, is give by

$$N_x = N_o e^{-\sigma nx} \tag{2.9}$$

and

$$N_{x+dx} = N_o e^{-\sigma n(x+dx)}. \tag{2.10}$$

Some of the neutrons that reach x will be involved in reactions before reaching $x + dx$, that is, $N_x > N_{x+dx}$. The number of neutrons consumed between x and $x + dx$, designated as dN_x, is given by

$$dN_x = N_x - N_{x+dx} = N_o e^{-\sigma nx}\left(1 - e^{-\sigma n\,dx}\right). \tag{2.11}$$

If dx is infinitesimal, then $(\sigma n\,dx)$ will be very small. This means that we can write $e^{-\sigma n(dx)} \sim 1 - \sigma n(dx)$, and hence write dN_x as

$$dN_x = N_o e^{-\sigma nx}(\sigma n\,dx), \tag{2.12}$$

a result equivalent to differentiating (2.7) above.

Now, these dN_x neutrons penetrated distance x into the slab before being consumed in a reaction, so the total travel distance accumulated by all of them in doing so would be $(x dN_x)$. The average distance that a neutron destined to be consumed in a reaction will travel before being consumed is given by integrating accumulated travel distances over the length of the slab and dividing by the number

of neutrons consumed in reactions within the slab, that is, $N_{react} = N_o(1 - e^{-\sigma nL})$ from above:

$$\langle x \rangle = \frac{1}{N_{react}} \int_0^L x \, dN_x = \frac{1}{N_o(1 - e^{-\sigma nL})} \int_0^L (N_o \sigma n) \, x \, e^{-\sigma nx} dx$$

$$= \frac{1}{\sigma n} \left[\frac{1 - e^{-\sigma nL}(1 + \sigma nL)}{1 - e^{-\sigma nL}} \right]. \tag{2.13}$$

If we have a slab of infinite thickness, or, more generally, one such that the product σnL is large, then $e^{-\sigma nL}$ will be small and we will have

$$\langle x \rangle_{(\sigma nL)large} \rightarrow \frac{1}{\sigma n}. \tag{2.14}$$

This quantity is known as the *characteristic length* or *mean free path* for the particular reaction quantified by σ. This quantity will figure prominently in Sects. 2.2 through 2.6. If it is computed for an individual cross section such as $\sigma_{fission}$ or $\sigma_{capture}$, one speaks of the mean free path for fission or capture. Such lengths are often designated by the symbol λ. As an example, consider fission in ^{235}U. The nuclear number density n is 4.794×10^{28} m^{-3}, and the fission cross section is $\sigma_f = 1.235$ bn $= 1.235 \times 10^{-28}$ m^2. These numbers give $\lambda_f = 16.9$ cm, or about 6.65 in.

Finally, it should be emphasized that the derivations in this section do not apply to bombarding particles that are *charged*, in which case one has very complex ionization issues to deal with.

2.2 Critical Mass: Diffusion Theory

We now consider critical mass per se. Qualitatively, the concept of critical mass derives from the observation that some species of nuclei fission upon being struck by a bombarding neutron and consequently release secondary neutrons. In a sample of fissile material these secondary neutrons can potentially go on to induce other fissions, resulting in a chain reaction. However, the development in the preceding section indicates that we can expect a certain number of neutrons to reach the surface of the sample and escape, particularly if the sample is small. If the density of neutrons within the sample is increasing with time, *criticality* is said to obtain. Whether or not this condition is fulfilled depends on quantities such as the density of the material, its cross-section for fission, and the number of neutrons emitted per fission, which is designated by the symbol v.

To explore the time-dependence of the number of neutrons in the core requires the use of time-dependent *diffusion theory*. In this section we use this theory to calculate the critical masses of so-called "bare" spherical assemblies of ^{233}U, ^{235}U, ^{237}Np, ^{239}Pu, and ^{241}Am, the five isotopes that one can feasibly consider for use in nuclear weapons. Of these, ^{235}U and ^{239}Pu are used in practice. The term "bare" refers to an *untamped* core. More correctly, we compute critical *radii* which can be transformed into equivalent critical *masses* upon knowing the density of the material involved.

The development presented here is based on the development in Appendix G of a differential equation which describes the spatiotemporal behavior of the neutron number density N, that is, the number of neutrons per cubic meter within the core. The derivation in Appendix G depends upon on some material developed in Sect. 3.5; it is consequently recommended that both those sections be read in advance of this one. Also, be sure not to confuse n and N; the former is the number density of fissile *nuclei* while the latter is the number density of *neutrons*; both play roles in what follows. Note also that the definition of N here differs from that in the previous section, where it represented a number of neutrons.

Before proceeding, an important limitation of this approach needs to be made clear. Following Serber et al. (1992), I model neutron flow within the bomb core by use of a diffusion equation. A diffusion approach is appropriate if neutron scattering is isotropic. Even if this is not so, a diffusion approach will still be reasonable if neutrons suffer a large enough number of scatterings so as to effectively erase non-isotropic angular effects. Unfortunately, neither of these conditions are fulfilled in the case of a uranium core: fast neutrons elastically scattering against uranium show a strong forward-peaked effect, and the mean free path of a fast neutron in ^{235}U, about 3.6 cm, is only about half of the 8.4-cm bare critical radius (see Table 2.1 below). I adopt a diffusion-theory approach for a number of reasons, however. As much of the physics of this area remains classified or at least not easily accessible, we are forced to settle for an approximate model; diffusion theory has the advantage of being analytically tractable at an upper-undergraduate level. Also, despite these various limitations, a comparison of critical radii as predicted by diffusion theory

Table 2.1 Threshold critical radii and masses (untamped)

Quantity	Unit	^{235}U	^{239}Pu	^{233}U	^{237}Np	^{241}Am
A	g/mol	235.04	239.05	233.04	237.05	241.06
ρ	g/cm^3	18.71	15.6	18.55	20.25	13.67
σ_f	bn	1.235	1.800	1.946	1.335	1.378
σ_{el}	bn	4.566	4.394	4.447	4.965	4.833
v	–	2.637	3.172	2.755	2.81	2.5
n	10^{22} cm^{-3}	4.794	3.930	4.794	5.144	3.415
$\lambda_{fission}$	cm	16.89	14.14	10.72	14.56	21.25
$\lambda_{elastic}$	cm	4.57	5.79	4.69	3.92	6.06
λ_{total}	cm	3.60	4.11	3.26	3.09	4.71
R_O	cm	8.37	6.346	5.676	6.736	11.307
M_O	kg	45.9	16.7	14.2	25.92	82.8

with those of an openly-published more exact treatment shows that the two agree within about 5% for the range of fissility parameters of interest here (Reed 2008).

Central to any discussion of critical radius are the *fission* and *transport* mean free paths for neutrons, respectively symbolized as λ_f and λ_t. These are given by (2.14) as

$$\lambda_f = \frac{1}{\sigma_f n} \tag{2.15}$$

and

$$\lambda_t = \frac{1}{\sigma_t n}, \tag{2.16}$$

where σ_t is the so-called transport cross-section. If neutron scattering is isotropic (which we assume), the transport cross-section is given by the sum of the fission and elastic-scattering cross-sections:

$$\sigma_t = \sigma_f + \sigma_{el}. \tag{2.17}$$

We do not consider here the role of *in*elastic scattering, which affects the situation only indirectly in that it lowers the mean neutron velocity. To keep the treatment simple we will also not deal at this point with the effect of any external tamper/neutron reflector.

In a spherical fissioning bomb core, the diffusion theory of Appendix G provides the following differential equation for the neutron number density:

$$\frac{\partial N}{\partial t} = \frac{v_{neut}}{\lambda_f} (v - 1) N + \frac{\lambda_t v_{neut}}{3} \left(\nabla^2 N \right), \tag{2.18}$$

where v_{neut} is the average neutron velocity and the other symbols are as defined earlier.

Now, let r represent the usual spherical radial coordinate. Upon assuming a solution for $N(t, r)$ of the form $N(t, r) = N_t(t)N_r(r)$, (2.18) can be separated as

$$\frac{1}{N_t} \left(\frac{\partial N_t}{\partial t} \right) = \left(\frac{v - 1}{\tau} \right) + \frac{D}{N_r} \left[\frac{1}{r^2} \frac{\partial}{\partial r} \left(r^2 \frac{\partial N_r}{\partial r} \right) \right], \tag{2.19}$$

where D is the so-called diffusion coefficient,

$$D = \frac{\lambda_t v_{neut}}{3}, \tag{2.20}$$

and where τ is the mean time that a neutron will travel before causing a fission:

$$\tau = \frac{\lambda_f}{v_{neut}}. \tag{2.21}$$

If the separation constant for (2.19) is defined as α/τ (that is, the constant to which both sides of the equation must be equal), then the solution for the time-dependent part of the neutron density emerges directly as

$$N_t(t) = N_o e^{(\alpha/\tau)t} \tag{2.22}$$

where N_o represents the neutron density at $t = 0$. N_o would be set by whatever device is used to initiate the chain-reaction. Note that we could have called the separation constant just α, but this form will prove a little more convenient for subsequent algebra. With this definition of the separation constant, the radial part of (2.19) appears as

$$\left(\frac{v-1}{\tau}\right) + \frac{D}{N_r}\left[\frac{1}{r^2}\frac{\partial}{\partial r}\left(r^2\frac{\partial N_r}{\partial r}\right)\right] = \frac{\alpha}{\tau}. \tag{2.23}$$

The first and last terms in (2.23) can be combined (this is why the separation constant was defined as α/τ); on dividing (2.23) by D, we find

$$\frac{1}{d^2} + \frac{1}{N_r}\left[\frac{1}{r^2}\frac{\partial}{\partial r}\left(r^2\frac{\partial N_r}{\partial r}\right)\right] = 0, \tag{2.24}$$

where

$$d = \sqrt{\frac{\lambda_f\,\lambda_t}{3\,(-\alpha + v - 1)}}. \tag{2.25}$$

Now define a new dimensionless coordinate x according as

$$x = \frac{r}{d}. \tag{2.26}$$

This brings (2.24) to the form

$$\frac{1}{N_r}\left[\frac{1}{x^2}\frac{\partial}{\partial x}\left(x^2\frac{\partial N_r}{\partial x}\right)\right] = -1. \tag{2.27}$$

Aside from a normalization constant, the solution of this differential equation can easily be verified to be

$$N_r(r) = \left(\frac{\sin x}{x}\right). \tag{2.28}$$

To determine a critical radius R_C, we need a boundary condition to apply to (2.28). As explained in Appendix G, this takes the form

$$N(R_C) = -\frac{2}{3}\frac{\lambda_t}{3}\left(\frac{\partial N}{\partial r}\right)_{R_C} = -\frac{2}{3}\frac{\lambda_t}{d}\left(\frac{\partial N}{\partial x}\right)_{R_C}. \tag{2.29}$$

On applying this to (2.28), one finds that the critical radius is given by solving the transcendental equation

$$x\cot(x) + x/\eta - 1 = 0, \tag{2.30}$$

where

$$\eta = \frac{2\lambda_t}{3d} = 2\sqrt{\frac{\lambda_t(-\alpha + v - 1)}{3\lambda_f}}. \tag{2.31}$$

With fixed values for the density and nuclear constants for some fissile material, (2.30) and (2.31) contain two variables: the core radius r and the exponential factor α, and they can be solved in two different ways. For both approaches, assume that we are working with material of "normal" density, which we designate as ρ_o. For the first approach, start by looking back at (2.22). If $\alpha = 0$, the neutron number density is neither increasing nor decreasing with time; in this case one has what is called *threshold criticality*. To determine the so-called threshold bare critical radius R_o, set $\alpha = 0$ in (2.25) and (2.31), set the density to ρ_o, solve (2.30) for x, and then get r ($=R_o$) from (2.26). The corresponding threshold bare critical mass M_o then follows from $M_o = (4\pi/3)R_o^3\rho_o$. It is this mass that one usually sees referred to as *the* critical mass; this quantity will figure prominently in the discussion of efficiency in Sects. 2.4 and 2.5.

The second type of solution begins with assuming that one has a core of some radius $r > R_o$. In this case one will find that (2.30) will be satisfied by some value of $\alpha > 0$, with α increasing as r increases. That is, since $x/\eta = 3r/2\lambda_t$ in (2.30) is independent of α, we can set r to some desired value; (2.30) can then be solved for x, which gives d from (2.26), and hence α from (2.25). With $\alpha > 0$ the reaction will grow exponentially in time until all of the fissile material is used up, a situation known as "supercriticality." To see why increasing the radius demands that α must increase, implicitly differentiate (2.30) to show that $d\eta/dx = (\eta/x)^2(1 - x^2/\sin^2 x)$, which demands $d\eta/dx < 0$ for all values of x. From the definition of x, an increase in r (and/or in the density, for that matter) will cause x to increase. To keep (2.30) satisfied means that η must decrease, which, from (2.31), can happen only if α increases.

We come now to a very important point. This is that the condition for threshold criticality can in general be expressed as a constraint on the product ρr where ρ is the mass density of the fissile material and r is the core radius. The factor η in (2.30) is independent of the density, depending only on the cross-sections and secondary neutron number v. Hence, for $\alpha = 0$, (2.30) will be satisfied by some unique value of x which will be characteristic of the material being considered. Since $x = r/d$ and d itself is proportional to $1/\rho$ [see (2.25)], we can equivalently say that the solution of (2.30) demands a unique value of ρr for a given combination of σ and v values. If as above R_o is the bare threshold critical radius for material of normal density ρ_o, then any combination of r and ρ such that $\rho r = \rho_o R_o$ will also be threshold critical,

and any combination with $\rho r > \rho_o R_o$ will be supercritical. For a sphere of material of mass M, the mass, density, and radius relate as $M \propto \rho r^3$, which means that the "criticality product" ρr can be written as $\rho r \propto M/r^2$. This relationship underlies the concept of *implosion* weapons. If a sufficiently strong implosion can be achieved, then one can get away with having less than a "normal" critical mass by starting with a sphere of material of normal density and crushing it to high density by implosion; such weapons are thus inherently more efficient than those that depend on a non-implosive "gun" mechanism to assemble subcritical components. As described in Sect. 4.2, the implosion technique also helps to overcome predetonation issues with spontaneous fission. The key point here is that there is no *unique* critical mass for a given fissile material.

Table 2.1 shows calculated critical radii and masses for five nuclides usually considered for use in nuclear weapons; due to short alpha or beta half-lives and/or high spontaneous fission rates, no nuclides beyond those listed in the Table are likely to be suitable candidates for weapons materials.

Sources for the fission and elastic-scattering cross-sections appearing in the Table are given in Appendix B; the values quoted therein are used as they are averaged over the fission-energy spectra of the nuclides. The v values were adopted from the Evaluated Nuclear Data Files (ENDF) maintained by the National Nuclear Data Center at Brookhaven National Laboratory (http://www.nndc.bnl.gov). For ^{235}U and ^{239}Pu, the v values are for prompt neutrons of energy 2 MeV, about the average energy of fission neutrons. The v value for ^{233}U refers to neutrons of energy 2.5 MeV; that for ^{237}Np was adopted from Hyde (1964) for neutrons of energy 1.4 MeV, and that for ^{241}Am is assumed. The densities for ^{235}U and ^{233}U are respectively (235/238) and (233/238) times the density of natural uranium, 18.95 g/cm^3.

Spreadsheet **CriticalityAnalytic.xls**[1] allows users to carry out these calculations for themselves. This spreadsheet is actually used for the calculations developed in this section and in Sects. 2.3 and 2.4. In its simplest use – corresponding to this section – the user enters the relevant parameters: the core density, atomic weight, fission and scattering cross-sections, and the number of secondary neutrons per fission. The "Goal Seek" function then allows one to solve (2.30) and (2.31) for x (assuming $\alpha = 0$), from which the bare critical radius and mass are computed.

In practice, having available only a single critical mass of fissile material will not produce much of an explosion. The reason for this is that fissioning nuclei give rise to fission products with tremendous kinetic energies. The core consequently very rapidly – within microseconds – heats up and expands, causing its density to drop below that necessary to maintain criticality. In a core comprised of but a single critical mass this will happen at the moment fissions begin, so the chain reaction will quickly fizzle as α falls below zero. To get an explosion of appreciable efficiency one must start with more than a single critical mass of fissile material or implode an initially subcritical mass to high density before initiating the explosion. If the core is surrounded by a massive tamper that is imploded to crush the

---

[1]All Excel sheets are available at http://www.manhattanphysics.com

core, the tamper will resist the expansion to some extent and can also serve to reflect some of the escaped neutrons back into the core to cause more fissions. The issue of using more than one critical mass to enhance weapon efficiency is examined in more detail in Sects. 2.4 and 2.5.

To close this section, it is interesting to look briefly at a famous *mis*calculation of critical mass on the part of Werner Heisenberg. At the end of World War II a number of prominent German physicists including Heisenberg were interned for 6 months in England and their conversations secretly recorded. This story is detailed in Bernstein (2001); see also Logan (1996) and Bernstein (2002). On the evening of August 6, 1945, the internees were informed that an atomic bomb had been dropped on Hiroshima and that the energy released was equivalent to about 20,000 tons of TNT (in actuality, the yield was about 13,000 tons). Heisenberg then estimated the critical mass based on this information and a subtly erroneous model of the fission process.

We saw in Sect. 1.6 that complete fission of 1 kg of ^{235}U liberates energy equivalent to about 17 kt TNT. Heisenberg predicated his estimate of the critical mass on the basis of assuming that about 1 kg of material did in fact fission. One kilogram of ^{235}U corresponds to about $\Omega \sim 2.56 \times 10^{24}$ nuclei. Assuming that on average $v = 2$ neutrons are liberated per fission, then the number of fission generations G necessary to fission the entire kilogram would be $v^G = \Omega$. Solving for G gives $G = \ln(\Omega)/\ln(v) \sim 81$, which Heisenberg rounded to 80. So far, this calculation is fine. Heisenberg then argued that as neutrons fly around in the bomb core they will randomly bounce between nuclei, traveling a mean distance λ between each collision; λ here is the mean free path between fissions as in (2.15) above. From Table 2.1 we have $\lambda \sim 17$ cm for U-235, but, at the time, Heisenberg took $\lambda \sim 6$ cm. Since a random walk of G steps where each is of length λ will take one a distance $r \sim \lambda\sqrt{G}$ from the starting point, he estimated a critical radius of $r \sim (6cm)\sqrt{80} \sim 54$ cm. This would correspond to a mass of some 12,500 kg, roughly 13 U.S. tons! Given that only one kilogram actually underwent fission, this would be a fantastically inefficient weapon. Such a bomb and its associated tamper, casing, and instrumentation would represent an unbearably heavy load for a World War II-era bomber.

The problem with Heisenberg's calculation was that he imagined the fission process to be created by a single neutron that randomly bounces throughout the bomb core, begetting secondary neutrons along the way. Further, his model is too stringent; there is no need for every neutron to cause a fission; many neutrons escape. In the days following August 6 Heisenberg revised his model, arriving at the diffusion theory approach described in this section.

2.3   Effect of Tamper

In the preceding section we saw how to calculate the critical mass of a sphere of fissile material. In that development we neglected the effect of any surrounding *tamper*. In this section we develop a simple model to account for the presence of a

tamper. The discussion here draws from the preceding section and from Bernstein (2002), Serber (1992), and especially Reed (2009).

The idea behind a tamper is to surround the fissile core with a shell of dense material, as suggested in Fig. 2.5. This serves two purposes: (i) it reduces the critical mass, and (ii) it slows the inevitable expansion of the core, allowing more time for fissions to occur until the core density drops to the point where criticality no longer holds. The reduction in critical mass occurs because the tamper will reflect some escaped neutrons back into the core; indeed, the modern name for a tamper is "reflector", but I retain the historical terminology here. This effect is explored in this section; estimating the distance over which the core expands before criticality no longer holds in taken up in the next section. This slowing effect is difficult to model analytically, but can be treated with an approximate numerical model, which is done in Sect. 2.5.

The discussion here parallels that in Sect. 2.2. Neutrons that escape form the core will diffuse into the tamper. To describe the behavior of neutrons in the tamper we can use (2.18) without the term corresponding to production of neutrons, that is, the first term on the right side of (2.18); we are assuming that the tamper is not made of fissile material:

$$\frac{\partial N_{tamp}}{\partial t} = \frac{\lambda_{trans}^{tamp} v_{neut}}{3} \left(\nabla^2 N_{tamp} \right), \tag{2.32}$$

where N_{tamp} is the number density of and λ_{trans}^{tamp} the transport mean free path for neutrons in the tamper. v_{neut} is the average neutron speed within the tamper, which we will later assume for sake of simplicity to be the same as that within the core. We are assuming that the tamper does not absorb neutrons; otherwise, we would have to add a term to (2.32) represent that effect.

Superscripts and subscripts *tamp* will be used liberally here as it will be necessary to join *tamper* physics to *core* physics via suitable boundary conditions.
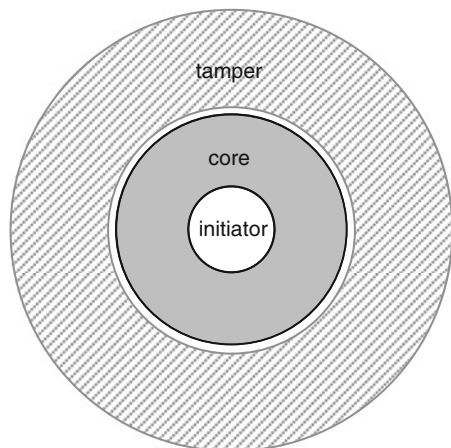

Fig. 2.5 Tamped bomb core

As was done in Sect. 2.2, take a trial solution for N_{tamp} of the form $N_{tamp}(t, r) = N_t^{tamp}(t) N_r^{tamp}(r)$ where $N_t^{tamp}(t)$ and $N_r^{tamp}(r)$ are respectively the time-and space dependences of N_{tamp}; r is the usual spherical radial coordinate. Upon substituting this into (2.32) we find, in analogy to (2.19),

$$\frac{1}{N_t^{tamp}} \left(\frac{\partial N_t^{tamp}}{\partial t} \right) = \left(\frac{\lambda_{trans}^{tamp} v_{neut}}{3} \right) \frac{1}{N_r^{tamp}} \left[\frac{1}{r^2} \frac{\partial}{\partial r} \left(r^2 \frac{\partial N_r^{tamp}}{\partial r} \right) \right]. \tag{2.33}$$

Define the separation constant here to be δ/τ where τ is the mean time that a neutron will travel *in the core* before causing a fission, that is, as defined in (2.21):

$$\tau = \frac{\lambda_{fiss}^{core}}{v_{neut}}. \tag{2.34}$$

This choice renders (2.33) as

$$\frac{1}{N_t^{tamp}} \left(\frac{\partial N_t^{tamp}}{\partial t} \right) = \left(\frac{\lambda_{trans}^{tamp} v_{neut}}{3} \right) \frac{1}{N_r^{tamp}} \left[\frac{1}{r^2} \frac{\partial}{\partial r} \left(r^2 \frac{\partial N_r^{tamp}}{\partial r} \right) \right] = \frac{\delta}{\tau}. \tag{2.35}$$

It may seem strange to invoke a *core* quantity when dealing with diffusion in the *tamper*, but we can define the separation constant however we please. In principle, δ may be different from the exponential factor α of Sect. 2.2, but we will find that boundary conditions demand that they be equal. This choice of separation constant is advantageous in that the neutron velocity v_{neut}, which we assume to be the same in both materials, cancels out.

The solution of (2.35) depends on whether δ is positive, negative, or zero; the latter choice corresponds to threshold criticality in analogy to $\alpha = 0$ in Sect. 2.2. The situations of practical interest will be $\delta \geq 0$, in which case the solutions have the form

$$N_{tamp} = \begin{cases} \dfrac{A}{r} + B & (\delta = 0) \\[2ex] e^{(\delta/\tau)t} \left\{ A \dfrac{e^{r/d_{tamp}}}{r} + B \dfrac{e^{-r/d_{tamp}}}{r} \right\} & (\delta > 0), \end{cases} \tag{2.36}$$

where A and B are constants of integration (different for the two cases), and where

$$d_{tamp} = \sqrt{\frac{\lambda_{trans}^{tamp} \lambda_{fiss}^{core}}{3 \, \delta}}. \tag{2.37}$$

The situation we now have is that the neutron density in the core is described by (2.22) and (2.28) as

$$N_{core} = A_{core}e^{(\alpha/\tau)t}\frac{\sin(r/d_{core})}{r}, \tag{2.38}$$

with d_{core} given by (2.25):

$$d_{core} = \sqrt{\frac{\lambda_{fiss}^{core}\lambda_{trans}^{core}}{3\left(-\alpha + v - 1\right)}}, \tag{2.39}$$

while that in the tamper is given by (2.36) and (2.37).

The physical question is: "What boundary conditions apply in order that we have a physically reasonable solution?" Let the core have radius R_{core} and let the outer radius of the tamper be R_{tamp}; we assume that the inner edge of the tamper is snug against the core. First consider the core/tamper interface. If no neutrons are created or lost at this interface then it follows that both the density and flux of neutrons across the interface must be continuous. That is, we must have

$$N_{core}(R_{core}) = N_{tamp}(R_{core}) \tag{2.40}$$

and, from (6.72) of Appendix G,

$$\lambda_{trans}^{core}\left(\frac{\partial N_{core}}{\partial r}\right)_{R_{core}} = \lambda_{trans}^{tamp}\left(\frac{\partial N_{tamp}}{\partial r}\right)_{R_{core}}. \tag{2.41}$$

Equation (2.41) accounts for the effect of any neutron reflectivity of the tamper via λ_{trans}^{tamp}.

In addition, we must consider what is happening at the outer edge of the tamper. If there is no "backflow" of neutrons from the outside, then the situation is analogous to the boundary condition of (2.29) that was applied to the outer edge of the untampered core:

$$N_{tamp}\left(R_{tamp}\right) = -\frac{2}{3}\lambda_{trans}^{tamp}\left(\frac{\partial N_{tamp}}{\partial r}\right)_{R_{tamp}}. \tag{2.42}$$

Applying (2.40)–(2.42) to (2.36)–(2.39) results, after some tedious algebra, in the following constraints:

$$\left[1 + \frac{2R_{thresh}\lambda_{trans}^{tamp}}{3R_{tamp}^2} - \frac{R_{thresh}}{R_{tamp}}\right]\left[\left(\frac{R_{thresh}}{d_{core}}\right)\cot\left(\frac{R_{thresh}}{d_{core}}\right) - 1\right]$$
$$+ \frac{\lambda_{trans}^{tamp}}{\lambda_{trans}^{core}} = 0, \quad (\delta = 0) \tag{2.43}$$

and, for $\delta > 0$,

$$e^{2(x_{ct}-x_t)} \left[\frac{x_c \cot x_c - 1 - \lambda (x_{ct}-1)}{R_{tamp} + 2\lambda_{trans}^{tamp}(x_t-1)/3} \right] = \left[\frac{x_c \cot x_c - 1 + \lambda (x_{ct}+1)}{R_{tamp} - 2\lambda_{trans}^{tamp}(x_t+1)/3} \right], \qquad (2.44)$$

where

$$\left. \begin{array}{l} x_{ct} = R_{core}/d_{tamp} \\ x_c = R_{core}/d_{core} \\ x_t = R_{tamp}/d_{tamp} \\ \lambda = \lambda_{trans}^{tamp}/\lambda_{trans}^{core} \end{array} \right\}. \qquad (2.45)$$

It is also necessary to demand that $\alpha = \delta$, else the fact that (2.40)–(2.42) must also hold as a function of *time* would be violated. Some comments on these results follow.

(i) Equation (2.43) corresponds to *tamped threshold criticality*, where $\alpha = \delta = 0$. Once values for the d's and λ's are given, the only unknown is R_{thresh}, the threshold critical radius for a tamped core.

(ii) To use (2.44) and (2.45), proceed as follows: (i) Decide on the number of tamped threshold critical masses C (>1) of material for your bomb core. This will have radius $R_{core} = C^{1/3}R_{thresh}$, where R_{thresh} comes from solving (2.43). (ii) Pick a value for R_{tamp}, the *outer* radius of the tamper. (iii) Solve (2.44) numerically for α ($=\delta$), which enters the d's and x's of (2.44) and (2.45) through (2.37) and (2.39).

The value of knowing α will become clear when the efficiency and yield calculations of Sects. 2.4 and 2.5 are developed; for the present, our main concern is with R_{thresh}.

A special-case application of (2.43) can be used to get an approximate sense of how dramatically the presence of a tamper decreases the threshold critical mass. Suppose that the tamper is very thick, $R_{tamp} \gg R_{thresh}$. In this case (2.43) reduces to

$$(R_{thresh}/d_{core}) \cot (R_{thresh}/d_{core}) = 1 - \left(\lambda_{trans}^{tamp}/\lambda_{trans}^{core} \right). \qquad (2.46)$$

Now consider two sub-cases. The first is that the tamper is in fact a vacuum. Since empty space would have essentially zero cross-section for neutron scattering, this is equivalent to specifying $\lambda_{trans}^{tamp} = \infty$, in which case (2.46) becomes

$$(R_{thresh}/d_{core}) \cot (R_{thresh}/d_{core}) = -\infty. \qquad (2.47)$$

This can only be satisfied if

$$\left(\frac{R_{thresh}}{d_{core}} \right)_{vacuum\ tamper} = \pi. \qquad (2.48)$$

The second sub-case is more realistic in that we imagine a thick tamper with a non-zero transport mean free path. For simplicity, assume that $\lambda_{trans}^{core} \sim \lambda_{trans}^{tamp}$, that is, that the neutron-scattering properties of the tamper are much like those of the core. In this case (2.46) becomes

$$(R_{thresh}/d_{core}) \cot (R_{thresh}/d_{core}) = 0. \tag{2.49}$$

The solution in this case is

$$\left(\frac{R_{Thresh}}{d_{core}}\right)_{thick\ tamper\ finite\ cross-section} = \frac{\pi}{2}, \tag{2.50}$$

one-half the value of the vacuum-tamper case. To summarize: With an infinitely-thick tamper of finite transport mean free path, the threshold critical radius is one-half of what it would be if no tamper were present at all. A factor of two in radius means a factor of eight in mass, so the advantage of using a tamper is dramatic, even aside from the issue of any retardation of core expansion. This factor of two is predicated on an unrealistic assumption for the tamper thickness and so we cannot expect such a dramatic effect in reality, but we will see that the effect is dramatic enough.

What sort of critical-mass reduction can one expect in practice? In a website devoted to design details of nuclear weapons, Sublette (2007) records that the Hiroshima *Little Boy* bomb used tungsten-carbide (WC) as its tamper material. Tungsten has five naturally-occurring isotopes, ^{180}W, ^{182}W, ^{183}W, ^{184}W, and ^{186}W, with abundances 0.0012, 0.265, 0.1431, 0.3064, and 0.2843, respectively. The KAERI table-of-nuclides site referenced in Appendix B gives elastic-scattering cross sections for the four most abundant of these as (in order of increasing weight) 4.369, 3.914, 4.253, and 4.253 bn. Neglecting the small abundance of ^{180}W, the abundance-weighted average of these is 4.235 bn. Adding the 2.352 bn elastic-scattering cross-section for ^{12}C gives a total of 6.587 bn; the cross-sections must be added, not averaged, since we are considering the tungsten-carbide molecules to be "single" scattering centers of atomic weight equal to the sum of the individual atomic weights for W and C, $183.84 + 12.00 = 195.84$. The bulk density of tungsten-carbide is 14.8 g/cm^3. Assuming an outer radius for the tamper of 17.5 cm (the choice of this value is explained below), (2.43) indicates that the tamped threshold critical radius of ^{235}U in this configuration is 6.20 cm, equivalent to a mass of 18.7 kg, about 60% less than the untamped value of 45.9 kg (Table 2.1). Figure 2.6 shows how the tamped threshold critical mass for a U-235 core depends on the outer radius of a surrounding tungsten-carbide tamper. The mass of the tamper would be about 38 kg for an outer radius of 10 cm and just over 950 kg for an outer radius of 25 cm.

A shell of tungsten carbide of outer radius 17.5 cm and thickness 11.3 cm has a mass of 317 kg. The 17.5 cm outer radius was chosen as Sublette records that the *Little Boy* tamper had a mass of about 311 kg and that its core comprised about 64 kg of ^{235}U in a cylindrical shape surrounded by a cylindrical WC tamper of diameter and length 13 in. (see also Coster-Mullen (2010)). Assuming for

simplicity spherical geometry, a 64-kg core at a density of 18.71 g/cm^3 would have an outer radius of 9.35 cm; a 311-kg tamper would then require an outer radius of about 18 cm. For the mass of its tamper, therefore, *Little Boy* utilized about 3.5 threshold critical masses of fissile material.

Spreadsheet **CriticalityAnalytic.xls** allows users to carry out these calculations for themselves. In addition to the core parameters entered for the calculations of Sect. 2.2, the user enters the density, atomic weight, scattering cross-section and outer radius of the tamper. The "Goal Seek" function is then to determine the tamped threshold critical radius and mass from (2.43).

Why was tungsten-carbide used as the *Little Boy* tamper material? As one of the purposes of the tamper is to briefly retard core expansion, denser tamper materials are preferable; tungsten-carbide is fairly dense and has a low neutron absorption cross-section. In this sense it would seem that depleted uranium, which the Manhattan Project possessed in abundance, would be an ideal tamper material. (*Depleted* is the term given to the uranium that remains after one has extracted its fissile U-235. The term may sound strange in that the remains are actually enriched in U-238, but the term is used in the sense of the material having been depleted of U-235.) The reason that it was not used may be that it has a fairly high spontaneous fission rate, about 675 per kg/s (see Sect. 4.2). Over the approximately 100 μs required to assemble the core of a Hiroshima gun-type bomb, a 300 kg depleted-U tamper would have a fairly high probability of suffering a spontaneous fission and hence of initiating a predetonation. Further, as discussed in Sect. 1.9, U-238 has a significant inelastic-scattering cross-section: fast neutrons striking it tend to be slowed to the point that they become likely to be captured and hence lost to the possibility of being reflected back into the core. Former weapons designer Theodore Taylor has pointed out that beryllium is one of the best neutron reflectors known: its fission-spectrum
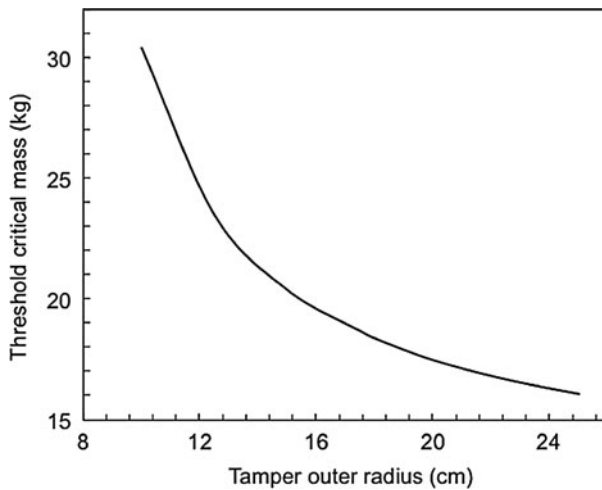

Fig. 2.6 Threshold tamped critical mass of a pure ^{235}U core as a function of the outer radius of a tamper of tungsten-carbide ($A = 195.84$ g/mol, $\rho = 14.8$ g/cm^3, $\sigma_{elastic} = 6.587$ bn)

averaged elastic scattering cross section is about 2.7 bn, while its inelastic-scattering cross-section is only about 40 μbn (McPhee 1974).

2.4   Estimating Bomb Efficiency: Analytic

Material in this section is adopted from a publication elsewhere by the author (Reed 2007).

In the preceding sections we examined how to estimate the critical mass for bare and tamped cores of fissile material. The analysis in Sect. 2.2 revealed that the threshold bare critical mass of ^{235}U is about 46 kg. In Sect. 1.6, however, we saw that complete fission of 1 kg of ^{235}U liberates energy equivalent to that of about 17 kt of TNT. Given that the *Little Boy* uranium bomb that was dropped on Hiroshima used about 64 kg of ^{235}U and is estimated to have had an explosive yield of only about 13 kt, we can infer that it must have been rather inefficient. The purpose of this section is to explore what factors dictate the efficiency of a fission weapon and to show how one can estimate that efficiency.

This section is the first of two devoted to the question of weapon efficiency and yield. In this section these issues are examined purely analytically. The advantage of an analytic approach is that it is helpful for establishing a sense of how the efficiency depends on the various parameters involved: the mass and density of the core and the various nuclear constants. However, conditions inside an exploding bomb core evolve very rapidly as a function of time, and this evolution cannot be fully captured with analytic approximations, elegant as they may be. To do so, one really needs to numerically integrate the core conditions as a function of time, tracking core size, expansion rate, pressure, neutron density and energy release along the way. Such a numerical integration is the subject of the next section; these two sections therefore closely complement each other and should be read as a unit. In the present section, we consider only *untamped* cores for sake of simplicity; tamped cores are considered in the following section.

To begin, it is helpful to appreciate that the efficiency of a nuclear weapon involves three distinct time scales. The first is mechanical in nature: the time required to assemble the subcritical fissile components into a critical assembly before fission is initiated. In principle, this time can be as long as desired, but in practice it is constrained by the occurrence of spontaneous fission. We do not want spontaneous fissions to be likely during the time required to assemble the core lest stray neutrons trigger a predetonation.

What is the order of magnitude of the assembly time? In a simple "gun-type" bomb, the idea is that a "projectile" piece of fissile material is fired like a shell inside an artillery barrel toward a mating "target" piece of fissile material, as sketched in Fig. 2.7. In World War II, the highest velocity that could be achieved for an artillery shell was about 1,000 m/s. If a projectile piece of length ~ 10 cm is shot toward a mating target piece at this speed, the time required for it to become fully engaged with the target piece from the time that the leading edge of the projectile meets the target piece will be ~ (10 cm)/(10^5 cm/s) ~ 10^{-4} s ~ 100 μs.

This type of assembly mechanism was used in the Hiroshima *Little Boy* bomb, which explains its cylindrical shape as illustrated in the photograph in Fig. 2.8. As shown in the cross-sectional schematic in Fig. 2.9, the projectile piece was fired from the tail end of the bomb and traveled most of the approximately 10-foot length of the weapon toward the nose.

As we will see in a more detailed analysis presented in Sect. 4.2, spontaneous fission was not an issue for assembling a uranium bomb over a time of 100 μs, but was such a serious issue with plutonium that it necessitated development of the implosion mechanism for triggering those weapons. So far as the present section is concerned, however, the essential idea is that if the spontaneous fission probability can be kept negligible during the assembly time (which we assume), the efficiency of the weapon is dictated by the other two time scales.

The first of these other two time scales is nuclear in nature. Once fission has been initiated, how much time is required for all of the fissile material to be consumed? This time we call $t_{fission}$. The other is again mechanical. As soon as fissions have been initiated, the core will begin to expand due to the extreme gas pressure of the fission fragments. As we will see, this expansion leads after a time $t_{criticality}$ to loss of criticality, after which the reaction rate will diminish. Weapon efficiency will depend on how these times compare: if $t_{criticality} > t_{fission}$ then in principle all of the core material will undergo fission and the efficiency would be 100%.
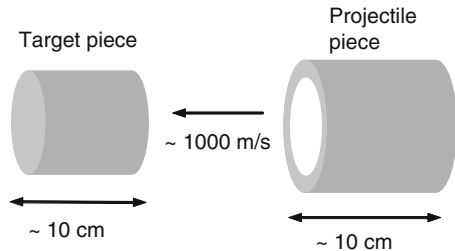

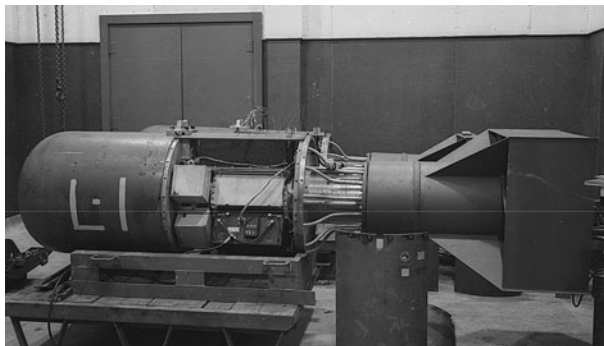**Fig. 2.7** Assembly timescale for a gun-type fission weapon

Fig. 2.8 *Little Boy* test units. *Little Boy* was 126 in. long, 28 in. in diameter, and weighed 8,900 pounds when fully assembled (Sublette 2007). Photo courtesy Alan Carr, Los Alamos National Laboratory
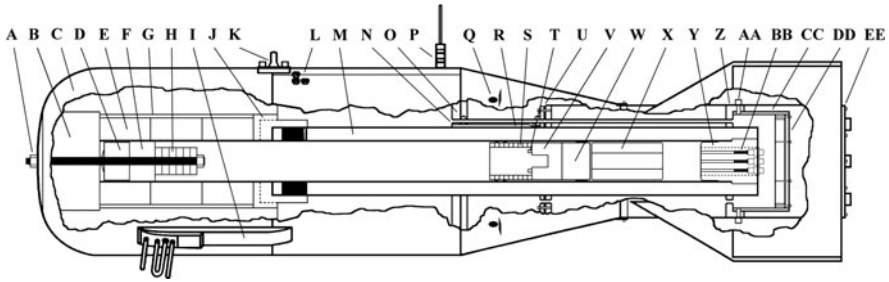
Fig. 2.9 Cross-section drawing of Y-1852 *Little Boy* showing major components. Not shown are radar units, clock box with pullout wires, barometric switches and tubing, batteries, and electrical wiring. Numbers in parentheses indicate quantity of identical components. Drawing is to scale. Copyright by and used with kind permission of John Coster-Mullen

A. Front nose elastic locknut attached to 1-in. diameter Cd-plated draw bolt

B. 15.125-in. diameter forged steel nose nut

C. 28-in. diameter forged steel target case

D. Impact-absorbing anvil with shim

E. 13-in. diameter 3-piece WC tamper liner assembly with 6.5-in. bore

F. 6.5-in. diameter WC tamper insert base

G. 14-in. diameter K-46 steel WC tamper liner sleeve

H. 4-in. diameter U-235 target insert discs (6)

I. Yagi antenna assemblies (4)

J. Target-case to gun-tube adapter with four vent slots and 6.5-in. hole

K. Lift lug

L. Safing/arming plugs (3)

M. 6.5-in. bore gun

N. 0.75-in. diameter armored tubes containing priming wiring (3)

O. 27.25-in. diameter bulkhead plate

P. Electrical plugs (3)

Q. Barometric ports (8)

R. 1-in. diameter rear alignment rods (3)

S. 6.25-in. diameter U-235 projectile rings (9)

T. Polonium–beryllium initiators (4)

U. Tail tube forward plate

V. Projectile WC filler plug

W. Projectile steel back

X. 2-pound Cordite powder bags (4)

Y. Gun breech with removable inner breech plug and stationary outer bushing

Z. Tail tube aft plate

(AA) 2.25-in. long 5/8–18 socket-head tail tube bolts (4)

(BB) Mark-15 Mod 1 electric gun primers with AN-3102-20AN receptacles (3)

(CC) 15-in. diameter armored inner tail tube

(DD) Inner armor plate bolted to 15-in. diameter armored tube

(EE) Rear plate with smoke puff tubes bolted to 17-in. diameter tail tube

First consider $t_{criticality}$. This involves two key ideas: (i) that a fissioning bomb core will rapidly (within about a microsecond) heat up, melt, vaporize, and thereafter behave as an expanding gas with the expansion driven by the gas pressure in a $P\Delta V$ manner, and (ii) that the vast majority of energy liberated in fission reactions can be assumed to go into the kinetic energy of the fission products. Our approach here will be to establish the range of radius (and hence time) over which the core can expand before the expansion lowers the density of the fissile material to subcriticality. Fission reactions will continue to happen after this time, of course, but it is this "criticality shutdown timescale" that fundamentally sets the efficiency scale of the weapon.

As in the preceding sections, let $N(r, t)$ represent the number density of neutrons within the core; our concern here is with the time-dependence of this quantity. From (2.22), the time-evolution of the number-density of neutrons within the core is given by

$$N(t) = N_o e^{(\alpha/\tau)\, t}, \tag{2.51}$$

where N_o is the neutron density at $t = 0$. N_o is set by the number of neutrons released by some "initiator" at the bomb core, and α is given by solving (2.25), (2.30), and (2.31) for the core at hand. Recall that for threshold criticality $\alpha = 0$ and that for a core of more than one critical mass we will have $\alpha > 0$, an issue to which we will return in a moment.

On average, a neutron will cause another fission after traveling for a time given by $\tau = \lambda_f / v_{neut}$ where λ_f is the mean free path for fission and v_{neut} is the average neutron velocity. Inverting this, we can say that a single neutron will lead to a subsequent fission at a *rate* of $1/\tau$ per second. Hence the rate of fissions as a function of time is given by

$$fissions/\text{sec} = \left(\frac{N_o V}{\tau}\right) e^{(\alpha/\tau)\, t}. \tag{2.52}$$

Equation (2.52) is actually more complicated than it looks because α is really a function of time. To see this, consider a core of some general radius r and density ρ. Both r and ρ will vary in time as the core expands. In Sect. 2.2 we saw that the condition for criticality can be expressed as $\rho r \geq K$ where K is a constant characteristic of the material being used, and that, for a core of some mass M, this condition is expressible as $\rho r \propto M/r^2$. As the core expands, the value of ρr will decrease and must eventually fall below the level needed to maintain criticality; we call this situation "criticality shutdown." This is also known in the technical literature as *second criticality*. For a single critical mass of normal-density material, this will happen as soon as the expansion begins. One way to (briefly) circumvent this is to provide a tamper to momentarily retard the expansion and so to give the reaction time to build up to a significant degree. Another is to start with a core of more than one critical mass of material of normal density, and this is what is

assumed here. The effect of a tamper and the detailed time-evolution of $\alpha(t)$ is dealt with in the following section.

Thus, assume that we have a core of $C \, (> 1)$ *untamped* threshold critical masses of material of normal density; the initial radius of such a core will be $r_i = C^{1/3} R_o$. We can then solve the diffusion-theory criticality equations, (2.30) and (2.31), for the value of α that just satisfies those equations upon setting the radius to be $C^{1/3}$ times the threshold critical radius determined in Table 2.1. But as the core expands due to the momentum acquired by fission fragments, α will decline from this initial value down to zero at the moment of criticality shutdown, hence the remark above that α is a function of time. To avoid having to deal with this complexity, we take α to be an "effective" α given by the average of these two extreme values, that is, $\alpha_{initial}/2$; this is done automatically in the **CriticalityAnalytic.xls** spreadsheet. This assumption is not strictly valid as the core expands exponentially as opposed to linearly in time, but the intent here is to get a sense of how the efficiency depends on the various parameters at hand.

Now consider the energy released by these fissions. If each fission liberates energy E_f, then the rate of energy liberation throughout the entire volume V of the core will be

$$\frac{dE}{dt} = \left(\frac{N_o V E_f}{\tau}\right) e^{(\alpha/\tau)\, t}. \tag{2.53}$$

Integrating this from time $t = 0$ to some general time t gives the energy liberated to that time:

$$E(t) = \left(\frac{N_o V E_f}{\tau}\right) \int_0^t e^{(\alpha/\tau)\, t} dt = \left(\frac{N_o V E_f}{\alpha}\right) e^{(\alpha/\tau)\, t}, \tag{2.54}$$

where it has been assumed that $e^{(\alpha/\tau)t} >> 1$ for the timescale of interest, an assumption to be investigated *a posteriori*. The *energy density* corresponding to $E(t)$ is given by $U(t) = E(t)/V$, and corresponding to this, we know from thermodynamics that there will be a growth in pressure given by $P(t) = \gamma \, U(t)$. The choice of γ depends on whether gas pressure ($\gamma = 2/3$) or radiation pressure ($\gamma = 1/3$) is dominant; in the case of a "gas" of uranium nuclei of standard density of that metal, radiation pressure dominates for per-particle energies greater than about 2 keV (see Problem 2.12). Thus

$$P(t) = \left(\frac{\gamma N_o E_f}{\alpha}\right) e^{(\alpha/\tau)\, t} = P_o \, e^{(\alpha/\tau)\, t}, \tag{2.55}$$

where $P_o = \left(\gamma N_o E_f / \alpha\right)$ is the pressure at $t = 0$.

For simplicity, we model the bomb core as an expanding sphere of radius $r(t)$ with every atom in it moving at speed v. Do not confuse this velocity with the

average neutron speed, which enters into τ. If the sphere is of density $\rho(t)$ and total mass M, its total kinetic energy will be

$$K_{core} = \frac{1}{2}Mv^2 = \left(\frac{2\pi}{3}\right)\rho\, v^2 r^3. \tag{2.56}$$

Now invoke the work-energy theorem in its thermodynamic formulation $W = P(t)\, dV$ and equate the work done by the gas (or radiation) pressure in changing the core volume by dV over time dt to the change in the core's kinetic energy over that time:

$$P(t)\frac{dV}{dt} = \frac{dK_{core}}{dt}. \tag{2.57}$$

To formulate this explicitly, write $dK_{core}/dt = (2\pi/3)\rho r^3(2v\,dv/dt)$, $dV/dt = 4\pi r^2(dr/dt)$, and incorporate (2.55) to give

$$\frac{dv}{dt} = \left(\frac{3P_o}{\rho\, r}\right)e^{(\alpha/\tau)\,t}. \tag{2.58}$$

To solve this for the radius of the core as a function of time we face the problem of what to do about the fact that both ρ and r are functions of time. We deal with this by means of an approximation.

Review the discussion about core expansion following (2.52) above. As the core expands, its density when it has any general radius r will be $\rho(r) = C\rho_o(R_o/r)^3$, and criticality will hold until such time as $\rho r = \rho_o R_o$, or, on eliminating ρ, $r = C^{1/2}R_o$. We can then define Δr, the range of radius over which criticality holds:

$$\Delta r = \left(C^{1/2} - C^{1/3}\right)R_o, \tag{2.59}$$

a result we will use in a moment.

Now, since $r_i = C^{1/3}R_o$, $(\rho r)_{initial} = C^{1/3}(\rho_o R_o)$. For $C = 2$ (for example), this gives $(\rho r)_{initial} = 1.26(\rho_o R_o)$. At criticality shutdown we will have $(\rho r)_{crit} = (\rho_o R_o)$, so $(\rho r)_{crit}$ and $(\rho r)_{initial}$ do not differ greatly. In view of this, we assume that the product ρr in (2.58) can be replaced with a mean value given by the average of the initial and final (loss-of-criticality) radii:

$$\langle \rho r \rangle = \frac{1}{2}\left(1 + C^{1/3}\right)\rho_o R_o. \tag{2.60}$$

We can now integrate (2.58) from time $t = 0$ to some general time t to determine the velocity of the expanding core at that time:

$$v(t) = \left(\frac{3P_o}{\langle \rho \, r \rangle}\right) \int_0^t e^{(\alpha/\tau)\,t}\,dt = \left(\frac{3P_o \, \tau}{\langle \rho \, r \rangle \, \alpha}\right) e^{(\alpha/\tau)\,t}, \qquad (2.61)$$

where it has again been assumed that $e^{(\alpha/\tau)t} \gg 1$.

The stage is now set to compute the amount of time that the core will take to expand through the distance Δr of (2.59). Writing $v = dr/dt$ and integrating (2.61) from r_i to $r_i + \Delta r$ for time $= 0$ to $t_{criticality}$ gives

$$t_{crit} \sim \left(\frac{\tau}{\alpha}\right) \, \ln \left[\frac{\Delta r \, \alpha^2 \, \langle \rho \, r \rangle}{3 P_o \tau^2}\right] = \left(\frac{\tau}{\alpha}\right) \, \ln \left[\frac{\Delta r \, \alpha^3 \, \langle \rho \, r \rangle}{3 \, \gamma \, \tau^2 N_o E_f}\right], \qquad (2.62)$$

again assuming $e^{(\alpha/\tau)t} \gg 1$ and using $P_o = \gamma N_o E_f / \alpha$. Notice that we cannot determine t_{crit} without knowing the initial neutron density N_o.

We now define efficiency. Equation (2.54) gives the total energy liberated up to time t. If all of the nuclei were to fission, then total energy $E_f \, n \, V$ would be liberated, where n and V are the initial nuclear number density and volume of the core. We define efficiency as the ratio of the total energy liberated up to time t_{crit} to the total possible that can be liberated if all nuclei fission:

$$Efficiency = \frac{\left(\frac{E_f N_o V}{\alpha}\right)}{\left(E_f \, n \, V\right)} \exp \left[(\alpha/\tau)\,t_{crit}\right] = \frac{\Delta r \, \alpha^2 \, \langle \rho \, r \rangle}{3 \, \gamma \, n \, \tau^2 E_f}, \qquad (2.63)$$

where we again substituted for P_o. *Note that the efficiency does not depend on the initial neutron density.*

The yield of the weapon is given by the product of this efficiency times the core mass (in kilograms) times the energy liberated per kilogram of fissioned nuclei, $E_f N_A (1000/A)$, where A is the atomic weight in g/mol.

To help determine what value of γ to use, we can compute the total energy liberated to time t_{crit} as in (2.63), and then compute the energy per particle by dividing by the number of nuclei in the core, nV. The result is

$$\left(\begin{array}{c} energy \; per \; nucleus \\ at \; time \; t_{crit} \end{array}\right) = (efficiency)E_f. \qquad (2.64)$$

Even if the efficiency is very low, say 0.1%, then for $E_f = 180$ MeV the energy per nucleus would be 180 keV, much higher than the ~2 keV per-particle energy where radiation pressure dominates over gas pressure; it would thus seem reasonable to take $\gamma = 1/3$.

Further, it can be shown by substituting (2.62) into (2.55) and (2.61) that at the time of criticality shutdown the core velocity is given by

$$v\left(t_{crit}\right) = \frac{\alpha \, \Delta r}{\tau}, \qquad (2.65)$$

and that the pressure within the core is given by

$$P(t_{crit}) = \frac{\alpha^2 \, \Delta r \, \langle \rho r \rangle}{3 \, \tau^2}. \tag{2.66}$$

Curiously, this pressure does not depend on the value of γ.

To determine t_{crit} explicitly requires adopting a number of "initial" neutrons to be distributed throughout the volume of the core. But since t_{crit} depends logarithmically on N_o, it is not particularly sensitive to the choice made for that number; presumably the *minimum* sensible value is one initial neutron.

We can also estimate the timescale to fission the entire core by demanding that the integral of (2.52) from time zero to time t_{fiss} equals the total number of nuclei within the core, nV:

$$nV = \left(\frac{N_o V}{\tau}\right) \int_0^{t_{fiss}} e^{(\alpha/\tau)\,t} dt \Rightarrow t_{fiss} = \left(\frac{\tau}{\alpha}\right) \ln\left[\frac{\alpha\, n}{N_o}\right]. \tag{2.67}$$

Numbers for uranium and plutonium cores of $C = 2$ bare threshold critical masses appear in Table 2.2. Secondary neutrons are assumed to have $E = 2$ MeV, and it is assumed that the initial number of neutrons is one.

The timescales and pressures involved in the detonation process are remarkable: Neutrons travel for a time of only $\tau \sim 1/100$ μs between fissions, and criticality shuts down after only 1–2 μs. A pressure of 10^{15} Pa is equivalent to about 10 *billion* atmospheres. In the case of ^{235}U, changing the initial number of neutrons to 1,000 changes the fission and criticality timescales by only about 10%, down to 1.81 and 1.64 μs, respectively. Since $(\alpha/\tau)t_{crit} \sim 50$, the assumption that $e^{(\alpha/\tau)t} \gg 1$ is quite reasonable. Even though $t_{crit}/t_{fiss} \sim 0.9$, the efficiencies are low: small changes in an exponential argument lead to large changes in the results.

Spreadsheet **CriticalityAnalytic.xls** carries out the efficiency and yield calculations for an untamped core as developed above. In addition to the parameters already entered for the calculations of the preceding two sections, the user need only

Table 2.2 Criticality and efficiency parameters for $C = 2$, $E_f = 180$ MeV, $\gamma = 1/3$. Initial number of neutrons = 1. Secondary neutron energy = 2 MeV

Quantity	Unit	Physical meaning	^{235}U	^{239}Pu
$\alpha_{initial}/2$	–	Effective value of α	0.246	0.304
R_O	cm	Threshold critical radius	8.37	6.346
τ	ns	Neutron travel time between fissions	8.64	7.23
Δr	cm	Expansion distance to crit shutdown	1.29	0.98
Efficiency	%	Efficiency	1.34	1.71
$P(t_{crit})$	10^{15} Pa	Pressure at crit shutdown	6.20	6.47
Yield	kt	Explosive yield	21.7	9.9
t_{fiss}	μs	Time to fission all nuclei	2.08	1.39
t_{crit}	μs	Time to crit shutdown	1.93	1.29

additionally specify an initial number of neutrons, a value for γ, and the mass of the core. The "Goal Seek" function is then run a third time, to solve (2.30) and (2.31) for the value of α. The spreadsheet then computes and displays quantities such as the expansion distance to second criticality, the fission and criticality timescales, the pressure within and velocity of the core at second criticality, and the efficiency and yield.

When applied to a 64 kg ^{235}U core ($C = 1.39$), **CriticalityAnalytic.xls** indicates that the expansion distance to second criticality is $\Delta r = 0.53$ cm and that the yield will be only 1.6 kt. This is not directly comparable to the ~13 kt yield of *Little Boy*, however, as that device was tamped; a more realistic simulation of *Little Boy* is given in the next section.

It is important to emphasize that the above calculations cannot be applied to a tamped core; that is, one cannot simply solve (2.44) and (2.45) for a core of some specified mass and tamper of some size (outer radius) and use the value of α so obtained in the time and efficiency expressions established above. The reason for this has to do with the distance through which the core can expand before second criticality, (2.59) above:

$$\Delta r = \left(C^{1/2} - C^{1/3} \right) R_o. \tag{2.68}$$

This expression derived from the fact that the criticality equation for the untamped case involves the density and radius of the core in the combination ρr; in the tamped case the criticality condition admits no such combination of parameters, so the subsequent calculations of criticality timescale and efficiency do not simply transform to using a tamped critical radius. Efficiency in the case of a tamped core can only be established numerically, which is the subject of the next section, where we will see that, typically, $\Delta r_{tamped} > \Delta r_{bare}$.

2.5   Estimating Bomb Efficiency: Numerical

In this section, a numerical approach to estimating weapon efficiency and yield is developed. The essential physics necessary for this development was established in the preceding three sections; what is new here is how that physics is used. The analysis presented in this section is adopted from a publication elsewhere by the author (Reed 2010).

The approach taken here is one of standard numerical integration: The parameters of a bomb core and tamper are specified, along with a timestep Δt. At each timestep, the energy released from the core is computed, from which the acceleration of the core at that moment can be computed. The velocity and radius of the core can then be tracked until such time as second criticality occurs, after which the rate of fissions will drop drastically and very little additional energy will be liberated.

The simulation developed here is realized via a spreadsheet where rows correspond to time steps and the columns are used to track various quantities.

This spreadsheet, **CriticalityNumerical.xls**, is very similar to that developed in the preceding sections, **CriticalityAnalytic.xls**.

Specifically, the integration process involves eight steps:

(i) Fundamental parameters are specified: the mass of the core, its atomic weight, initial density, and nuclear characteristics σ_f, σ_{el}, and v. For the tamper, its atomic weight, density, initial outer radius (effectively, its mass) and elastic-scattering cross-section are specified. The energy release per fission E_f and gas/radiation pressure constant γ are also specified. A timestep Δt also needs to be set; from the discussion in the preceding section, this will be on the order of nanoseconds.

(ii) Elapsed time, the speed of the core, and the total energy released are initialized to zero; the core radius is initialized according as its mass and initial density.

(iii) The exponential neutron-density growth parameter α is determined by numerical solution of (2.44) and (2.45).

(iv) The rate of fissions at a given time is given by (2.52):

$$fissions/\sec = \left(\frac{N_o V}{\tau}\right) e^{(\alpha/\tau)\,t}. \tag{2.69}$$

(v) The amount of energy released during time Δt is computed from (2.53):

$$\Delta E = \left(\frac{N_o V E_f}{\tau}\right) e^{(\alpha/\tau)\,t}(\Delta t). \tag{2.70}$$

(vi) The total energy released to time t is updated, $E(t) \to E(t) + \Delta E$, and the pressure at time t is given by [see the discussion preceding (2.55)]

$$P_{core}(t) = \frac{\gamma E(t)}{V_{core}(t)}. \tag{2.71}$$

I use the core volume here on the rationale that the fission products which cause the gas/radiation pressure will likely largely remain within the core.

(vii) A key step is computing the change in the speed of the core over the elapsed time Δt due to the energy released during that time. In the discussion leading up to (2.58), this was approached by invoking the work-energy theorem:

$$P(t) \frac{dV_{core}}{dt} = \frac{dK_{core}}{dt}. \tag{2.72}$$

To improve the veracity of the simulation, it is desirable to account, at least in some approximate way, for the retarding effect of the tamper on the expansion of

the core. To do this, I treat the dK/dt term in (2.72) as involving the speed of the core but with the mass involved being that of the core *plus* that of the tamper. The dV/dt term is taken to apply to the core only. I treat the tamper as being of constant density but with an outer radius that is recomputed at each step to keep its mass as specified at the outset; the inner edge of the tamper is assumed to remain snug against the expanding core. With r as the radius and v the speed of the core, we have

$$\frac{\gamma E(t)}{V_{core}(t)} \left(\frac{dV_{core}}{dt} \right) = \frac{dK_{total}}{dt}$$

$$\Rightarrow \frac{\gamma E(t)}{V_{core}(t)} \left(4\pi r^2 \frac{dr}{dt} \right) = \frac{1}{2} M_{c+t} \left(2v \frac{dv}{dt} \right),$$

from which we can compute the change in expansion speed of the core over time Δt as

$$\Delta v = \left[\frac{4\pi r^2 \gamma E(t)}{V_{core} M_{c+t}} \right] (\Delta t). \tag{2.73}$$

With this, the expansion speed of the core and its outer radius can be updated according as $v(t) \rightarrow v(t) + \Delta v$ and $r(t) \rightarrow r(t) + v(t)\Delta t$. The outer radius of the tamper is then adjusted on the assumption that its density and mass remain constant.

(viii) Return to step (iii) to begin the next timestep; continue until second criticality is reached when $\alpha = 0$.

The assumption that the density of the tamper remains constant is probably not realistic: nuclear engineers speak of the "snowplow" effect, where high-density tamper material piles up just ahead of the expanding core/tamper interface. But the point here is an order-of-magnitude pedagogical model.

CriticalityNumerical.xls consists of three interlinked sheets. The first is essentially a copy of **CriticalityAnalytic.xls**, where the user inputs the fundamental data of step (i) above. As before, the Excel "Goal Seek" function is then run three times, to establish values for (1) the bare threshold critical radius, (2) the tamped threshold critical radius, and (3) the value of α corresponding to the chosen core mass. The radii (and corresponding masses) in (1) and (2) are computed for reference; the tamped threshold critical radius is also used in computing a "normalized" radius as described below.

A significant complexity in carrying out this simulation is that one apparently needs to solve (2.44) and (2.45) for the value of α at each time-stepped core radius: the fission rate, energy generation rate, and pressure all depend on α as a function of time. I have found, however, that α is usually quite linear as a function of core radius. This behavior can be used to greatly simplify the programming of the simulation. Sheet 2 of the spreadsheet allows the user to establish parameters for this linear behavior for the values of the various parameters that were input on Sheet 1. Sheet 2 consists of rows representing radii running from the initial core radius to 1.4 times the value of the second-criticality radius for a *bare* core of the mass chosen by

the user on Sheet 1; this range appears to be suitable to establish the behavior of α. For convenience, Sheet 2 utilizes a "normalized" radius defined as

$$r_{norm} = \frac{r - C^{1/3} R_{tamp}^{thresh}}{\left(C^{1/2} - C^{1/3}\right) R_{tamp}^{thresh}}, \qquad (2.74)$$

where C is now defined as the number of tamped threshold critical masses. r_{norm} = 1 corresponds to the second criticality radius one would compute from (2.59) if it applied as well to a tamped core. Sheet 2 tracks the changing mass density, nuclear number density, and fission and total mean free paths within the core as a function of r. By running the Goal Seek function on each of 28 radii between 1.0 and 1.4 normalized radii, the user adjusts α in each case to render (2.44) equal to zero. The behavior of $\alpha(r)$ is displayed in an automatically-generated graph. On a separate line with α fixed to a value very near zero (10^{-10} is built-in), the user adjusts the radius to once again render (2.44) equal to zero, thus establishing the radius of second criticality for the parameters of the system. The slope and intercept of a linear $\alpha(r)$ fit are then automatically computed in preparation for the next step. While one could use just the initial and final radii to establish the linear relationship, it is probably wise to check the extent of linearity with all 28 radial points.

The actual time-dependent simulation occurs on Sheet 3. The simulation is set up to involve 500 timesteps, one per row. The initial core radius is transferred from Sheet 1 for $t = 0$. Because much of the energy release in a nuclear weapon occurs during the last few generation of fissions before second criticality, Sheet 3 allows the user to set up two different timescales: an "initial" one (dtinit) intended for use in the first few rows of the Sheet when a larger timestep can be tolerated without much loss of accuracy, and a later one (dtlate), to be chosen considerably smaller and used for the majority of the rows. In this way a user can optimize the 500 rows to both capture sufficient accuracy in the last few fission generations while arranging for $\alpha(r)$ to just approach zero at the last steps of the process. Typical choices for dtinit and dtlate might be a few tenths of a microsecond and a few tenths of a nanosecond, respectively. At each radius, Sheet 3 computes the value of $\alpha(r)$ from the linear approximation of Sheet 2, the core volume, mass density, nuclear number densities and mean free paths within the core, τ, rates of fission and energy generation, pressure, and total energy liberated to that time. The core speed and radius are updated depending upon the timestep in play, and the updated radius is transferred to the subsequent row to seed the next step. The user is automatically presented with graphs of $\alpha(r)$, the fission rate, pressure, and total energy liberated (in kilotons equivalent) as functions of time.

2.5.1 A Simulation of the Hiroshima Little Boy Bomb

Using the parameters for the *Little Boy* bomb given in Sect. 2.3 (64 kg core of radius 9.35 cm plus a 311 kg tungsten-carbide tamper of outer radius 18 cm), the following results were obtained with **CriticalityNumerical.xls**.

Figure 2.10 shows the run of $\alpha(r)$ for this situation: it is sensibly linear over the expansion of the core to second criticality at a radius of 12.31 cm, with $\alpha(r) \sim -18.53r + 2.28$. This represents an expansion distance of $\Delta r = 2.96$ cm from the initial core radius of 9.35 cm; for an *untamped* 64 kg core, (2.59) predicts a value for Δr of only 0.53 cm; the effect of the tamper is significant.

Figures 2.11 and 2.12 show α, the integrated energy release, and the fission rate and pressure as functions of time. The number of initial neutrons is taken to be one. Notice that α actually remains close to its initial value until just before second criticality. The brevity and violence of the detonation are astonishing. The vast majority of the energy is liberated within an interval of about 0.1 μs. The pressure peaks at close to 5×10^{15} Pa, or about 50 *billion* atmospheres, equivalent to about one-fifth of that at the center of the Sun. The fission rate peaks at about 3.6×10^{31} per second. The core acceleration peaks at about 1.4×10^{12} m/s^2 at $t \sim 0.9$ μs, and second criticality occurs at $t \sim 1.07$ μs, at which time the core expansion velocity is about 270 km/s. These graphs dramatically illustrate what Robert Serber wrote in *The Los Alamos Primer*: "Since only the last few generations will release enough energy to produce much expansion, it is just possible for the reaction to occur to an interesting extent before it is stopped by the spreading of the active material".

The predicted yield of *Little Boy* from this simulation is 11.9 kt. This result is in surprisingly good agreement with the estimated ~12-kt yield published by Penney et al. (1970). At a fission yield of 17.59 kt/kg of pure U-235 (at 180 MeV/fission), this represents an efficiency of only about 1.1% for the 64-kg core. While some of this agreement must be fortuitous in view of the approximations incorporated in the present model, it is encouraging to see that it gives results of the correct order of magnitude. That the yield estimate needs to be taken with some skepticism is demonstrated by the fact that increasing the initial number of neutrons to 10 increases the yield to 12.5 kt. However, this change does not much affect the
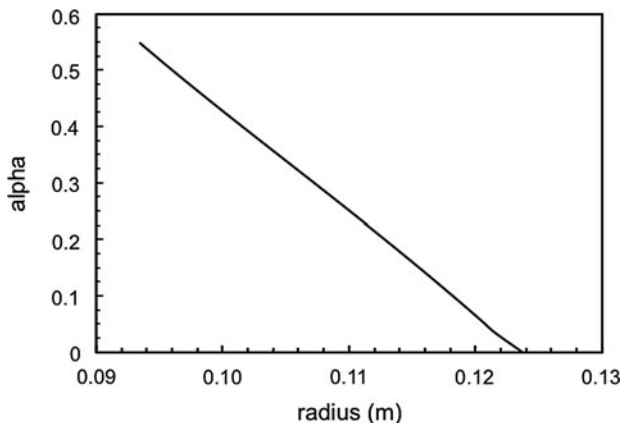

Fig. 2.10 Neutron density exponential growth parameter α vs. core radius for a simulation of the *Little Boy* bomb: 64 kg core plus 311 kg tungsten-carbide tamper
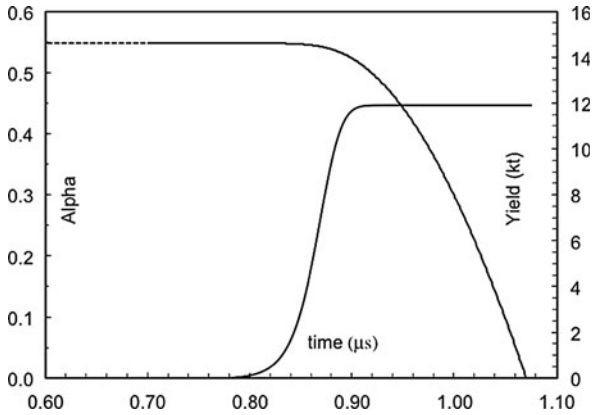
Fig. 2.11 Neutron density exponential growth parameter α (*descending curve*, *left scale*) and integrated energy release in kilotons (*ascending curve*, *right scale*) vs. time for a simulation of the *Little Boy* bomb
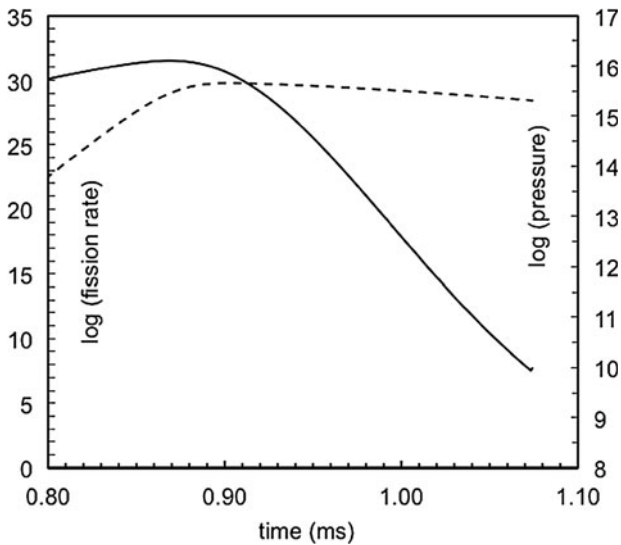

Fig. 2.12 Logarithm (base 10) of fission rate (*solid curve*, left scale) and logarithm of pressure (*dashed curve*, right scale) vs. time for a simulation of the *Little Boy* bomb

timescale or the peak pressure and fission rates. A 1952 Los Alamos report on the yield of the Hiroshima bomb, http://www.fas.org/sgp/othergov/doe/lanl/la-1398. pdf, gives a yield of 18.5 ± 5 kt for *Little Boy*; published yield estimates are clearly subject to considerable uncertainty.

Figure 2.13 shows how the simulated yield of the 64-kg core varies as a function of tamper mass; the points are the results of simulations for initial tamper outer radii
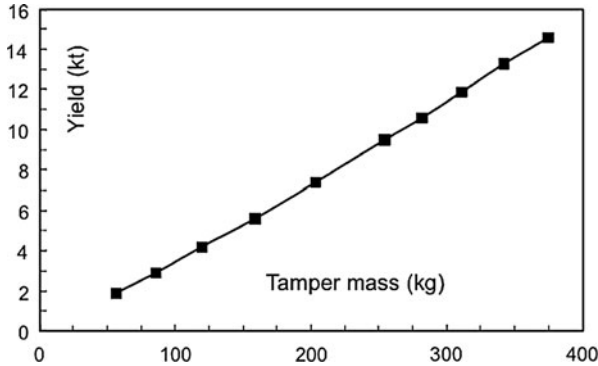
Fig. 2.13 Yield of a 64-kg U-235 core vs. mass of surrounding tungsten-carbide tamper. The curve is interpolated. The *Little Boy* tamper had a mass of about 310 kg

of 12, 13, ... 17, 17.5, 18, 18.5, and 19 cm. In the latter case the mass of the tamper would be about 375 kg, or just over 800 pounds. As the tamper mass increases so does the efficiency of the weapon as measured by the number of kilotons of yield per kilogram of fissile material.

2.6   Another Look at Untamped Criticality: Just One Number

In Sect. 2.2, we saw that the criticality condition for an untamped core is

$$x \cot(x) + \gamma x - 1 = 0, \tag{2.75}$$

where, for threshold criticality ($\alpha = 0$),

$$\gamma = \frac{1}{2} \sqrt{\frac{3\lambda_f}{\lambda_t(v-1)}} = \frac{1}{2} \sqrt{\frac{3\sigma_t}{\sigma_f(v-1)}}. \tag{2.76}$$

Once the nuclear parameters σ_f, σ_{el}, and v are set, (2.75) is solved numerically for x, from which the critical radius R follows from (again with $\alpha = 0$)

$$R = dx = \sqrt{\frac{\lambda_f \lambda_t}{3(v-1)}} x = \frac{1}{n} \sqrt{\frac{1}{3\sigma_f \sigma_t(v-1)}} x, \tag{2.77}$$

where n is again the nuclear number density. The critical radius is fundamentally set by σ_f, σ_{el}, v, and n; our concern here will be with the first three of these variables.

Since these quantities will be different for different fissile isotopes, it would appear that there is no "general" statement one can make regarding critical radii.

The purpose here, however, is to show how σ_f, σ_{el}, and v can be combined into one convenient dimensionless variable that largely dictates the critical radius in any particular case – the "just one number" of the title of this section.

As formulated, (2.75) and (2.76) are convenient in that both x and γ are dimensionless, but are awkward in that γ is not conveniently bounded: if v is very large γ will approach zero, but as $v \to 1$, it will diverge to infinity. It would be handy to some combination of σ_f, σ_{el}, and v that is finitely bounded.

Such a combination was developed by Peierls (1939), in a paper which was the first published in English to explore what he termed "criticality conditions in neutron multiplication." He defined a quantity ξ given by

$$\xi^2 = \frac{\sigma_f(v-1)}{\sigma_{el} + v\,\sigma_f}. \tag{2.78}$$

For $1 \leq v \leq \infty$, $0 \leq \xi \leq 1$. Note that it is the elastic-scattering cross-section σ_{el} that appears in the denominator of the definition of ξ, not the transport cross-section $\sigma_t = \sigma_{el} + \sigma_f$.

If (2.76) and (2.78) are both solved for $(v-1)$ and the results equated, the relationship between γ and ξ emerges as

$$\gamma = \sqrt{\frac{3}{4}\left(\frac{1}{\xi^2} - 1\right)}. \tag{2.79}$$

Similarly, if the definition of d in (2.77) is solved for $(v-1)$, then one finds

$$d = \sqrt{\frac{1}{3}\left(\frac{1}{\xi^2} - 1\right)}\,\lambda_t. \tag{2.80}$$

A general formulation of critical radii can now be made as follows: For a range of values of ξ between zero and one, (2.75) and (2.79) can be solved for x. For each solution, (2.77) and (2.80) then show that the value of R/λ_t is purely a function of ξ:

$$\frac{R}{\lambda_t} = x(\xi)\,d = x(\xi)\sqrt{\frac{1}{3}\left(\frac{1}{\xi^2} - 1\right)}. \tag{2.81}$$

In other words, a graph of $x(\xi)\,d(\xi) \equiv R/\lambda_t$ vs. ξ can be used to immediately indicate the ratio of the untamped threshold critical radius to the transport mean free path for any fissile isotope whose σ_f, σ_{el}, and v values are specified. The advantage of this approach is that the graph need only be constructed once.
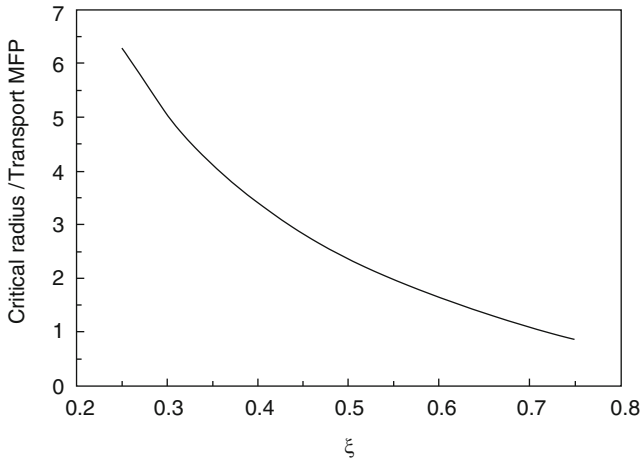
Fig. 2.14 Ratio of untamped threshold critical radius to transport mean free path as a function of Peierls' ξ parameter of (2.78)

Figure 2.14 shows R/λ_t as a function of ξ. For ^{235}U and ^{239}Pu, $\xi \sim 0.5084$ and 0.6221, and $R/\lambda_t \sim 2.33$ and 1.54, respectively. It is intuitively sensible that for small values of ξ (that is, for $\nu \rightarrow 1$), the critical radius will be large, and vice-versa.

References

Bernstein, J.: Hitler's Uranium Club: The Secret Recordings at Farm Hall. Copernicus Books, New York (2001)

Bernstein, J.: Heisenberg and the critical mass. Am. J. Phys. **70**(9), 911–916 (2002)

Coster-Mullen, J.: Atom bombs: the top secret inside story of little boy and fat man. Self-published (2010)

Hyde, E.K.: The Nuclear Properties of the Heavy Elements III. Fission Phenomena. Prentice-Hall, Englewood Cliffs, NJ (1964)

Logan, J.: The critical mass. Am. Sci. **84**, 263–277 (1996)

McPhee, J.: The Curve of Binding Energy. Farrar Strauss, and Giroux, New York, p. 92 (1974)

Peierls, R.: Critical conditions in neutron multiplication. Proc. Cam. Philos. Soc. **35**, 610–615 (1939)

Penney, W., Samuels, D.E.J., Scorgie, G.C.: The nuclear explosive yields at Hiroshima and Nagasaki. Philos. Trans. R. Soc. Lond. **A266**(1177), 357–424 (1970)

Reed, B.C.: Arthur Compton's 1941 Report on explosive fission of U-235: a look at the physics. Am. J. Phys. **75**(12), 1065–1072 (2007)

Reed, B.C.: Rudolf Peierls' 1939 analysis of critical conditions in neutron multiplication. Phys. Soc. **37**(4), 10–11 (2008)

Reed, B.C.: A brief primer on tamped fission-bomb cores. Am. J. Phys. **77**(8), 730–733 (2009)

Reed, B.C.: Student-level numerical simulation of conditions inside an exploding fission-bomb core. Nat. Sci. **2**(3), 139–144 (2010)

Serber, R.: The Los Alamos Primer: The First Lectures on How To Build An Atomic Bomb. University of California Press, Berkeley (1992)

Sublette, C: Nuclear Weapons Frequently Asked Questions: http://nuclearweaponarchive.org/Nwfaq/Nfaq8.html (2007)

Chapter 3
Producing Fissile Material

Abstract All of the theories and calculations underlying nuclear weapons would be of no value unless one can devise ways of obtaining sufficient fissile material: uranium-235 and plutonium-239. This chapter analyses some of the methods that were used for securing these materials during the Manhattan Project: the development of reactors to synthesize plutonium, and the use of electromagnetic and gaseous enrichment methods for uranium.

The vast majority of the manpower and funding of the Manhattan Project were devoted to producing fissile material. ^{235}U had to be laboriously separated from natural uranium, and plutonium had to be synthesized in nuclear reactors. In this chapter we examine some of the physics behind these techniques. Historically, the first major step along these lines was when Enrico Fermi and his collaborators achieved the first operation of a self-sustaining chain-reaction on December 2, 1942, with their CP-1 ("Critical Pile 1") reactor. This proved that a chain-reaction could be created and controlled, and opened the door to the design and development of the massive plutonium-producing reactors located at Hanford, WA. We thus look first at issues of reactor criticality (Sects. 3.1 and 3.2), and then examine plutonium production (Sect. 3.3). Sections 3.4 and 3.5 are devoted to analyzing techniques of uranium enrichment.

3.1 Reactor Criticality

The key quantifier in achieving a self-sustaining chain reaction is what is known as the "criticality factor" or "reproduction factor", designated as k. This dimensionless number is defined in such a way that if $k \geq 1$ then the reaction will be self-sustaining, whereas if $k < 1$ the reaction will eventually die out. In fact, if $k > 1$ the reaction rate will grow exponentially; reactors are equipped with control mechanisms that can be adjusted to maintain $k = 1$. k is analogous to the secondary neutron number v that was central to the discussion of critical mass and efficiency in the preceding chapter.

Achieving a chain reaction with uranium of natural isotopic composition involves several competing factors. The small fraction of ^{235}U present is inherently extremely fissile when bombarded by slow neutrons, and for each neutron consumed in fissioning a ^{235}U nucleus some 2.4 are on average released; these can go on to initiate other fissions. On the other hand, the vastly more abundant ^{238}U nuclei tend to capture neutrons without fissioning, removing them from circulation.

When a nucleus is struck by a neutron, one of three things will in general happen: (i) the nucleus may fission, (ii) the nucleus may capture (or "absorb") the neutron without fissioning, and (iii) the neutron may simply scatter from the nucleus. This last process serves only to redirect neutrons within the reactor and can be ignored if the reactor is sufficiently large that a neutron has a good chance of being involved in a fission or absorption before being scattered through the surface of the reactor and lost. We will be concerned with processes (i) and (ii).

The likelihood of each process is quantified by a corresponding cross-section. We will be concerned with fission (f) and capture (c) cross-sections for ^{235}U and ^{238}U. In self-evident notation we write these as σ_{f5}, σ_{c5}, σ_{f8}, and σ_{c8}. Numerical values for these quantities are listed in Table 3.1 for both isotopes for both "fast" and "slow" neutrons, also known as "unmoderated" and "moderated" neutrons, respectively. For the latter, the cross-sections refer to neutrons of kinetic energy 0.0253 eV; the origin of this curious number is explained in Sect. 3.2. Sources for these values are given in Appendix B. Also shown are the average secondary-neutron numbers for each isotope for both fast and slow-neutron induced fissions. Two important things to notice here are (i) the large fission cross-section for *slow* neutrons in the case of ^{235}U, and (ii) the non-zero *capture* cross-section for *slow* neutrons for the same isotope: upon absorbing a slow neutron, a ^{235}U nucleus actually has about a one-in-seven chance of *not* fissioning.

The number given in Table 3.1 for the capture cross-section of ^{238}U for fast neutrons, 2.661 bn, is the sum of this isotope's *true* capture cross-section for fast neutrons (0.0664 bn) plus its inelastic scattering cross-section for fast neutrons (2.595 bn). The rationale for this is that when neutrons inelastically scatter from ^{238}U they lose so much of their energy as to fall below the fission threshold for that isotope and are virtually guaranteed to be captured should they strike another ^{238}U nucleus; inelastic scattering by ^{238}U is therefore effectively capture by it (see Sect. 1.9). To simplify matters we assume that no neutrons are lost due to capture by fission products or by escape from the reactor; in reality, these are not trivial problems.

Table 3.1 Fissility parameters

Parameter	Fast neutrons	Slow neutrons
σ_{f5} (bn)	1.235	584.4
σ_{c5} (bn)	0.08907	98.81
v_5	2.637	2.421
σ_{f8} (bn)	0.3084	0
σ_{c8} (bn)	2.661	2.717
v_8	2.655	2.448

Suppose that our reactor consists of a mixture of ^{235}U and ^{238}U isotopes. For each isotope we write a total cross section as the sum of the cross-sections for all individual processes involving that isotope:

$$\sigma_5 = \left(\sigma_{f5} + \sigma_{c5}\right) \tag{3.1}$$

and

$$\sigma_8 = \left(\sigma_{f8} + \sigma_{c8}\right). \tag{3.2}$$

Let the fractional abundance of ^{235}U be designated by F; $0 \leq F \leq 1$. For neutrons created in fissions or otherwise supplied, the total cross-section for them to suffer *some* subsequent process is given by the abundance-weighted sum of the cross-sections for the individual isotopes:

$$\sigma_{total} = F\,\sigma_5 + (1 - F)\,\sigma_8. \tag{3.3}$$

Now imagine following a single neutron as it flies about within the reactor until it is consumed in causing a fission or by being captured. The reproduction factor k is defined as the average number of neutrons that this one original neutron subsequently gives rise to. We derive an expression for k by separately computing the number of secondary neutrons created by fissions with ^{235}U and ^{238}U and then adding the two results.

The probability of our neutron striking a nucleus of ^{235}U is given by the ratio of the total cross-section for ^{235}U to that for the total cross-section for all processes and isotopes, weighted by the abundance fraction of that isotope: $(F\sigma_5/\sigma_{total})$. Once the neutron has struck the ^{235}U nucleus the probability that it initiates a fission will be (σ_{f5}/σ_5). Hence, by the usual multiplicative process for combining independent probabilities, the overall probability that the neutron will fission a ^{235}U nucleus will be the product of these factors, $(F\sigma_5/\sigma_{total})(\sigma_{f5}/\sigma_5) = (F\sigma_{f5}/\sigma_{total})$. If fission of a ^{235}U nucleus liberates on average v_5 secondary neutrons, then the average number of neutrons created by our one neutron from fissioning a ^{235}U nucleus will be $v_5(F\sigma_{f5}/\sigma_{total})$. Likewise, fissions of ^{238}U nuclei will give rise, on average, to $v_8(1 - F)(\sigma_{f8}/\sigma_{total})$ secondary neutrons. The total number of secondary neutrons created by our one initial neutron will then be

$$k = \frac{F\,v_5\,\sigma_{f5} + (1 - F)v_8\,\sigma_{f8}}{\sigma_{total}}. \tag{3.4}$$

In natural uranium, $F = 0.0072$; we ignore here the very small natural abundance of ^{234}U. Notice that as $F \to 1$, $k \to v_5$.

We first apply this to the possibility for a chain reaction with *unmoderated* (fast) neutrons in natural uranium:

$$\sigma_{total} = F\left(\sigma_{f5} + \sigma_{c5}\right) + (1 - F)\left(\sigma_{f8} + \sigma_{c8}\right)$$

$$= (0.0072)(1.32407) + (0.9928)(2.9694) = 2.958. \qquad (3.5)$$

Hence

$$k_{fast} = \frac{F\,v_5\,\sigma_{f5} + (1 - F)v_8\,\sigma_{f8}}{\sigma_{total}}$$

$$= \frac{(0.0072)(2.637)(1.235) + (0.9928)(2.655)(0.3084)}{2.958} = 0.283. \quad (3.6)$$

Since $k_{fast} < 1$, a self-sustaining chain reaction using unmoderated neutrons with natural uranium is impossible. This is why a lump of ordinary uranium of any size is perfectly safe against a spontaneous chain reaction; a nuclear weapon cannot be constructed using uranium of natural isotopic composition.

Figure 3.1 shows k_{fast} as a function of F; k_{fast} does not exceed unity until $F \sim 0.53$. One must therefore undertake a significant enrichment effort to construct a uranium bomb. Bomb-grade uranium is usually considered to be 90% [235]U.

In the case of moderated neutrons the story is different. Here we have

$$\sigma_{total} = (0.0072)(584.4 + 98.81) + (0.9928)(0 + 2.717) = 7.617. \qquad (3.7)$$

Hence

$$k_{slow} = \frac{F\,v_5\,\sigma_{f5} + (1 - F)v_8\,\sigma_{f8}}{\sigma_{total}}$$

$$= \frac{(0.0072)(2.421)(584.4) + 0}{7.617} = 1.337. \qquad (3.8)$$

Here $k > 1$, which means that a self-sustaining reaction with moderated neutrons is possible. This slow-neutron reproduction factor is the premise underlying CP-1 and all commercial power-producing reactors. In situations where a commercial reactor would be impractical, such as in a naval vessel, smaller reactors are used that are fueled with uranium significantly enriched in [235]U.

3.2 Neutron Thermalization

Fermi's CP-1 reactor used graphite (crystallized carbon) as a *moderator* to slow neutrons emitted from fissioning [235]U nuclei to so-called "thermal" speeds to take advantage of the large fission cross-section of that isotope for neutrons of such
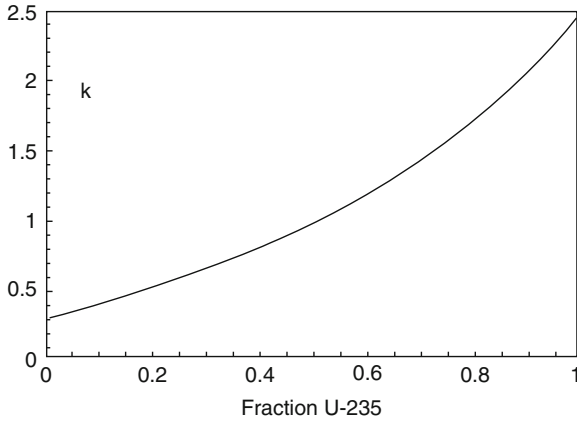
Fig. 3.1 Fast-neutron reproduction factor k vs. ^{235}U abundance fraction

energy. Graphite was used as it has a low capture cross-section for neutrons. We can estimate the typical distance a neutron will travel while this is happening, and hence get an understanding of why the lumps of uranium in CP-1 were distributed as a cubical lattice with a spacing of 8.25 in. (21 cm). A detailed description of CP-1 was published in Fermi (1952).

It is first necessary to quantify more precisely what is meant by a thermal neutron. From Maxwellian statistical mechanics, the most probable velocity of a particle of mass m at absolute temperature T is given by

$$v_{mp} = \sqrt{\frac{2kT}{m}}, \tag{3.9}$$

where k is Boltzmann's constant. Thermalization is taken to correspond to $T = 298$ K, that is, room temperature. For neutrons, this evaluates to

$$v_{mp} = \sqrt{\frac{2\left(1.381 \times 10^{-23} J/K\right)\left(298K\right)}{\left(1.675 \times 10^{-27} kg\right)}} = 2217 m/s. \tag{3.10}$$

The kinetic energy of such a neutron is

$$E = \frac{1}{2}mv_{mp}^2 = 4.115 \times 10^{-21} J = 0.025 eV. \tag{3.11}$$

In technical nuclear physics literature, "thermal" neutrons are defined to have $v = 2,200$ m/s, which corresponds to an energy of 0.0253 eV. This energy is a far cry from the typical ~2 MeV with which a secondary neutron emerges from a fission. The premise here is that since the nuclei of the moderating material will be

randomly moving with energies characteristic of at least room temperature, neutrons cannot be slowed to speeds less than this.

Consider a neutron of mass m_n that has initial speed v_o as it emerges from a fissioning nucleus. From classical conservation of momentum, if this neutron strikes an initially stationary carbon atom of mass m_C head-on, then the neutron will recoil from the collision with speed v given by

$$v = \left| \frac{m_n - m_C}{m_n + m_C} \right| v_o. \tag{3.12}$$

A carbon atom is about 12 times heavier than a neutron, so

$$v \sim \left(\frac{11}{13} \right) v_o. \tag{3.13}$$

If the neutron goes on to strike another carbon nucleus, its speed will be reduced by a further factor of 11/13. After N such collisions its final speed will be

$$v \sim \left(\frac{11}{13} \right)^N v_o. \tag{3.14}$$

Energy is proportional to speed squared, so the ratio of the final kinetic energy of the neutron to its initial kinetic energy will be

$$\frac{E}{E_o} \sim \left(\frac{11}{13} \right)^{2N}. \tag{3.15}$$

For $E_o = 2\,\text{MeV}$ and $E = 0.0253\,\text{eV}$, $N \sim 54$, a not very large number. In reality we should expect to need a somewhat larger number of collisions to achieve thermalization as not all of them will be head-on as assumed here, but even a factor of two increase in N would not change our final conclusion drastically.

How far will a neutron travel during these 50-odd scatterings? In Sect. 2.1 a derivation was given of the average distance a bombarding particle can be expected to penetrate through a medium before suffering some sort of reaction. In application to the present case we can write this as a *characteristic scattering length*

$$\lambda_s = \frac{1}{\sigma_s n}, \tag{3.16}$$

where σ_s is the scattering cross-section and n is the number density of nuclei. Strictly, this applies only for neutrons scattering through a medium of infinite extent, but since any sensible reactor will have a size considerably greater than λ_s, this is not a problem.
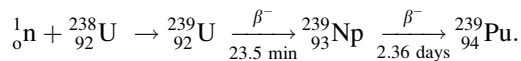
The density of graphite is 1.62 g/cm^3, for which $n \sim 8.13 \times 10^{28}$ m^{-3}. For thermal neutrons, the elastic scattering cross-section for ^{12}C is 4.746 bn; this number is taken from the KAERI site referenced in Appendix B. These figures give

$$\lambda_s \sim 2.6 \text{ cm.} \tag{3.17}$$

This is equivalent to about 1 in. Now, we know from statistical mechanics that if a particle takes N randomly-directed steps of length λ meters from some starting point, then the resulting average displacement from the starting point will be $\sqrt{N}\,\lambda$ meters. In the present case the neutron displacement will be $\sqrt{N}\,\lambda_s$ $\sim \sqrt{54}(2.6cm) \sim 19cm$, a figure very close to CP-1's 21-cm lattice spacing. Even if $N = 100$, we would have a mean displacement of only about 26 cm. Fermi designed CP-1 to occupy the minimum volume possible while achieving effective neutron thermalization.

3.3 Plutonium Production

The three giant graphite-moderated, water-cooled plutonium production piles constructed for the Manhattan Project in Hanford, Washington, were vastly scaled-up, much more complex versions of Fermi's CP-1 Chicago pile. Fueled with natural uranium, these reactors were designed to utilize a controlled slow-neutron chain-reaction as described in the preceding two sections to synthesize ^{239}Pu from neutron absorption and β-decay of ^{238}U according as the reaction:

$$^{1}_{0}\text{n} + {}^{238}_{92}\text{U} \;\rightarrow\; {}^{239}_{92}\text{U} \;\xrightarrow[23.5 \text{ min}]{\beta^-}\; {}^{239}_{93}\text{Np} \;\xrightarrow[2.36 \text{ days}]{\beta^-}\; {}^{239}_{94}\text{Pu.}$$

The important question is the rate of plutonium production, say in units of grams per day. The answer to this can be gleaned from knowledge of the power output of the reactor, the isotopic composition of the fuel, and the fission and capture (absorption) cross-sections for the isotopes involved. The analysis presented in this section is adopted from a publication elsewhere by this author (Reed 2005).

Commercial power-producing reactors are usually rated by their net electrical power output, so many "megawatts electrical", which we designate by the symbol P_e. However, this quantity reflects power output after accounting for the inevitable thermal (Carnot) inefficiencies involved. The power output "within" the plant itself – the number of "megawatts thermal" – is given by $P_t = P_e/\eta$, where η is the thermal efficiency of the plant. Typically, $\eta \sim 0.3$–0.4. In the case of a reactor the power created derives from mass-energy liberated in the fissioning of ^{235}U atoms. Various fission reactions are possible, but we can simplify the situation by assuming that each liberates, on average, energy E. If E is given in MeV (typically,

$E \sim 180$ MeV), then the reaction rate necessary to sustain thermal power production P_t is

$$\text{fissions per second} = \frac{10^6 P_t}{\left(1.6022 \times 10^{-13}E\right)}, \qquad (3.18)$$

where the numerical factors arise from converting megawatts to watts and MeV to Joules.

Each fissioning ^{235}U atom liberates secondary neutrons; call this number v as we did in the discussions of critical mass and reactor criticality. For our purposes, such secondary neutrons subsequently suffer one of three fates: (i) they can strike another ^{235}U atom and cause it to fission, (ii) they can be absorbed by an atom of ^{235}U without causing fission, or (iii) they can be absorbed by an atom of ^{238}U. Process (i) is necessary to keep the reaction going, while process (iii) is what ultimately produces Pu. Process (ii) is parasitic, serving only to remove neutrons from circulation. As in Sect. 3.1, designate the cross-sections for these processes as σ_{f5}, σ_{c5}, and σ_{c8}, respectively. We adopt $(\sigma_{f5}, \sigma_{c5}, \sigma_{c8}) = (584, 99, 2.7)$ bn (see Appendix B; $\sigma_{f8} = 0$ for thermal neutrons). These figures are for "thermalized" or "moderated" neutrons such as one has in a reactor, not the fast neutrons one has in a bomb. To simplify matters, we assume that no neutrons are lost due to capture by fission products or by diffusion and escape through the surface of the reactor. Also, as before, we can neglect neutron scattering as this just redirects neutrons within the reactor.

The other factor we need is the fractional abundance F of ^{235}U in the fuel rods. In natural uranium, $F = 0.0072$. For various reasons, power-producing reactors in the United States use fuel enriched to $F \sim 0.03$. As before, the total effective cross-section for a reaction of any sort to occur is then given by the abundance-weighted sum of each possibility:

$$\sigma_{tot} = F\left(\sigma_{f5} + \sigma_{c5}\right) + (1 - F)\,\sigma_{c8}. \qquad (3.19)$$

Now, of the v neutrons liberated in each fission, the number subsequently absorbed by ^{238}U (and hence the number of atoms of ^{239}Pu produced per fission) is given by v times the ratio of the effective absorption cross-section for ^{238}U to σ_{tot}:

$$\text{neutrons absorbed by } ^{238}\text{U per } ^{235}\text{U fission } = v\left[\frac{(1 - F)\,\sigma_{c8}}{\sigma_{tot}}\right]. \qquad (3.20)$$

This expression is a central part of the story, but left as it is would result in seriously overestimating the rate of Pu production. To appreciate this, consider the analogous expression for the number of subsequent fission events created by each secondary neutron:

neutrons causing subsequent ^{235}U fission per ^{235}U fission

$$= v \left[\frac{F \, \sigma_{f5}}{\sigma_{tot}} \right]. \tag{3.21}$$

As in the discussion of reactor criticality, this number is known as the "repro-duction factor" k. In a reactor fueled with uranium enriched to $F = 0.03$, the above cross-sections give $k = 1.835$ for $v = 2.421$ (Table 3.1). If left uncontrolled, the number of fissions would multiply by a factor of nearly 2 in each generation and rapidly lead to a catastrophic meltdown. To achieve a steady reaction rate, control rods are used to absorb a sufficient number of neutrons in order to have $k = 1$. Hence, we need to correct (3.20) by dividing by k, that is, by dividing by (3.21):

$$\text{neutrons absorbed by} \, ^{238}\text{U per} \, ^{235}\text{U fission} \, = \left[\frac{(1 - F) \, \sigma_{c8}}{F \, \sigma_{f5}} \right]. \tag{3.22}$$

The rate of production of Pu is then given by multiplying this result by the fission rate, (3.18):

Atoms of Pu produced per second

$$= \left[\frac{10^6 P_t}{(1.6022 \times 10^{-13} E)} \right] \left[\frac{(1 - F) \, \sigma_{c8}}{F \, \sigma_{f5}} \right]. \tag{3.23}$$

On accounting for the atomic mass of ^{239}Pu ($239.05u = 3.970 \times 10^{-25}$ kg) and the number of seconds in a day, we can transform (3.23) into an expression for the number of grams of Pu produced per day:

$$\text{Pu production (gr/day)} = 214.1 \left[\frac{P_t \, (1 - F) \, \sigma_{c8}}{E F \, \sigma_{f5}} \right]. \tag{3.24}$$

Notice that the rate of Pu production is independent of the number of neutrons liberated per fission; this is because the reactor is controlled to ensure that only one second-generation fission is created per first-generation fission, no matter what the value of v.

For a plant producing electric power at a rate of 1 GW fueled at $F = 0.03$ and operating at efficiency $\eta = 0.3$ (hence, $P_t = 3.33$ GW), (3.24) gives a plutonium production rate of 593 g/day = 216 kg/year, assuming $E = 180$ MeV/fission. Given that there are some 100 commercial reactors in operation in the United States we can thus estimate the annual production of plutonium to be on the order of 20,000 kg, enough for more than 2,000 Nagasaki-type bombs. The rate of Pu production is very sensitive to small changes in the enrichment factor in view of this parameter appearing in the denominator of (3.24). A 1 GW-electrical reactor of the same efficiency but fueled with natural uranium (such as the Canadian CANDU system) will produce some 920 kg of Pu per year.

The Hanford reactors were fueled with natural uranium ($F = 0.0072$) and operated at a thermal power MW/η = 250 MW. For these figures, (3.24) gives a production rate of 190 g/day. Three reactors operating at this power would yield 570 g/day. To get enough Pu to construct a bomb core of 6 kg would therefore require about 11 days of steady-state operation. Fuel slugs were left in the Hanford reactors for typically 100 days of neutron bombardment; after being withdrawn they had to be cooled, and time allowed for dangerous short-lived fission products to decay. A discussion of the design of these reactors appears in Weinberg (2002).

Since commercial-reactor fuel rods in the US are not as a rule reprocessed, the Pu created remains locked up in them. Ironically, ^{239}Pu α-decays back to ^{235}U with a half-life of about 24,000 years; our distant descendants will find a fresh supply of "enriched" fuel rods awaiting them!

Fuel rods typically remain in commercial reactors for periods much longer than 100 days. A result of this is that some of the ^{239}Pu atoms that are formed have time to absorb neutrons to become ^{240}Pu; some 25% of the Pu in spent fuel rods is this isotope (Kazimi 2003). Section 5.3 of the present book develops a numerical simulation of reactor operation to show how to estimate the production rate of ^{240}Pu, but we will see that the essential overall scale of plutonium production is not much affected. As we explore in Sect. 4.2, this isotope is characterized by an extremely high spontaneous fission rate, a situation that presents a dangerous challenge for anyone who seeks to construct a nuclear weapon from such spent fuel. An excellent treatment of issues in civilian nuclear power generation appears in Garwin and Charpak (2001).

3.4 Electromagnetic Separation of Isotopes

The Manhattan Project's Oak Ridge, Tennessee, facility was devoted to separating uranium isotopes for use in the *Little Boy* bomb. Three separate techniques were involved in this effort: (i) electromagnetic separation, (ii) gaseous (barrier) diffusion, and (iii) liquid thermal diffusion. The first two of these can be examined on the basis of undergraduate-level physics and are so treated in this and the following sections. The physics of liquid thermal diffusion is extremely complex, however, so we do not consider that process further. Readers interested in the technical details of liquid thermal diffusion are urged to consult the classic paper "The Separation of Isotopes by Thermal Diffusion" by Jones and Furry (1946).

We first deal with electromagnetic separation of isotopes. Barrier diffusion is taken up in Sect. 3.5.

The electromagnetic separation facility at Oak Ridge was code-named Y-12, and utilized "calutron" separators designed by Ernest Lawrence; the name is a contraction of "California University Cyclotron". The design of these separators was predicated on the phenomenon that an ion directed into a magnetic field perpendicular to the ion's initial velocity will subsequently travel in a circular orbit whose radius is dictated by the strength of the field, the magnitude of the initial velocity, the

extent of ionization, and the mass of the ion. Isotopes of different masses consequently travel in different orbits and so can be separated. As with any isotope separation technique, this method depends on the very slight mass difference between the isotopes involved. In the case of ^{235}U and ^{238}U the mass difference is very small, so this technique is extremely difficult to realize in practice.

To analyze this we use a coordinate system where the x and y axes are in the plane of the page and the z-axis comes out of the page as shown in Fig. 3.2.

Assume that a uniform magnetic field $\vec{B} = B\hat{z}$ emerges perpendicularly from the page. An ion of mass m and net charge q (usually positive) moves under the influence of the field. According to the Lorentz force law, the force on the ion at any time will be

$$\vec{F} = q\left(\vec{v} \times \vec{B}\right) = qB\left(v_y\hat{x} - v_x\hat{y}\right). \tag{3.25}$$

Newton's Second law holds that $\vec{F} = m\vec{a}$, so we can write

$$qB\left(v_y\hat{x} - v_x\hat{y}\right) = m\left(\frac{dv_x}{dt}\hat{x} + \frac{dv_y}{dt}\hat{y} + \frac{dv_z}{dt}\hat{z}\right), \tag{3.26}$$

from which we have

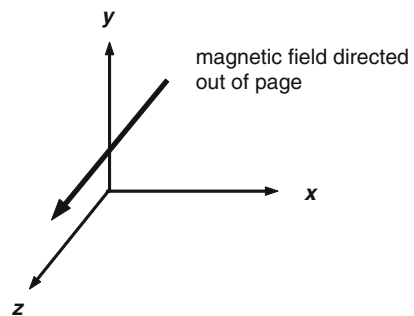$$\frac{dv_x}{dt} = \alpha v_y \tag{3.27}$$

and

$$\frac{dv_y}{dt} = -\alpha v_x, \tag{3.28}$$

where

$$\alpha = \frac{qB}{m}. \tag{3.29}$$

Fig. 3.2 Coordinate system for analyzing motion of charged particles in a magnetic field. The x and y axes are in the plane of the page; the z-axis emerges from the page, as does the magnetic field

Equations (3.27) and (3.28) are *coupled* differential equations: the rate of change of v_x depends on v_y and vice-versa. Note that we must have $dv_z/dt = 0$; if the ion enters the magnetic field with $v_z = 0$, its subsequent motion will be restricted to the xy plane, the case assumed here.

Equations (3.27) and (3.28) can be separated by the following trick. Differentiate (3.27) with respect to time:

$$\frac{d^2 v_x}{dt^2} = \alpha \, \frac{dv_y}{dt}. \tag{3.30}$$

Now substitute (3.28) into the right side of (3.30) to eliminate dv_y/dt:

$$\frac{d^2 v_x}{dt^2} = -\alpha^2 \, v_x. \tag{3.31}$$

What we have gained here is a differential equation that involves only the x-component of the velocity. Likewise, differentiating (3.28) and using (3.27) gives

$$\frac{d^2 v_y}{dt^2} = -\alpha^2 \, v_y. \tag{3.32}$$

Both v_x and v_y are governed by the same differential equation. The general solutions are

$$\left. \begin{aligned} v_x &= A \, \cos(\alpha t) + C \, \sin(\alpha t) \\ v_y &= D \, \cos(\alpha t) + E \, \sin(\alpha t) \end{aligned} \right\}, \tag{3.33}$$

where A, C, D, and E are constants of integration (B is reserved for the magnetic field strength); we use different constants in the x and y directions as we eventually impose different boundary conditions on them.

Integrating (3.33) with respect to time gives the equations of motion for the ion:

$$\left. \begin{aligned} x &= \frac{1}{\alpha} [A \, \sin(\alpha t) - C \, \cos(\alpha t)] + K_x \\ y &= \frac{1}{\alpha} [D \, \sin(\alpha t) - E \, \cos(\alpha t)] + K_y \end{aligned} \right\}, \tag{3.34}$$

where K_x and K_y are further constants of integration.

Not all of A, C, D, and E are independent. This can be seen by back-substituting (3.33) into (3.27) (or into (3.28) – the result is the same):

$$\frac{dv_x}{dt} = \alpha \, v_y$$

$$\Rightarrow \quad -A \, \sin(\alpha t) + C \, \cos(\alpha t) = D \, \cos(\alpha t) + E \, \sin(\alpha t), \tag{3.35}$$

which shows that we must have $D = C$ and $E = -A$. These constraints simplify (3.33) and (3.34) to

$$
\left.
\begin{aligned}
v_x &= A\,\cos(\alpha t) + C\,\sin(\alpha t) \\
v_y &= C\,\cos(\alpha t) - A\,\sin(\alpha t)
\end{aligned}
\right\}
\tag{3.36}
$$

and

$$
\left.
\begin{aligned}
x &= \frac{1}{\alpha}[A\,\sin(\alpha t) - C\,\cos(\alpha t)] + K_x \\
y &= \frac{1}{\alpha}[C\,\sin(\alpha t) + A\,\cos(\alpha t)] + K_y
\end{aligned}
\right\}.
\tag{3.37}
$$

We now set some initial conditions and impose them on (3.36) and (3.37). Assume that at $t = 0$ the positively-charged ion enters the magnetic field at $r_{initial} = (0, 0)$ while moving straight upward (in the positive-y direction) with velocity $v_{initial} = (0, v)$. This initial velocity can be supplied by passing the ions through an accelerating voltage before they are introduced into the magnetic field. The initial situation is sketched in Fig. 3.3.

The initial-velocity condition requires $A = 0$ and $C = v$ from (3.36); these results and the initial-position condition, when substituted into (3.34), demand $K_x = v/\alpha$ and $K_y = 0$. The velocity and position equations hence become:

$$
\left.
\begin{aligned}
v_x &= v\,\sin(\alpha t) \\
v_y &= v\,\cos(\alpha t)
\end{aligned}
\right\}
\tag{3.38}
$$

and

$$
\left.
\begin{aligned}
x &= \frac{v}{\alpha}[1 - \cos(\alpha t)] \\
y &= \frac{v}{\alpha}\,\sin(\alpha t)
\end{aligned}
\right\}.
\tag{3.39}
$$

Fig. 3.3 A positively-charged ion is launched with initial velocity in the y direction; the magnetic field emerges from the plane of the page
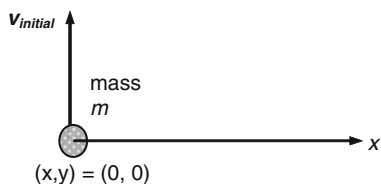
Equations (3.38) indicate that an ion's speed remains unchanged once it enters the magnetic field; a magnetic field can do no work on a charged particle. That (3.39) corresponds to circular motion can be appreciated by transforming to a new ("primed") coordinate system where the origin is displaced along the x-axis by an amount v/α:

$$\left.\begin{array}{l} x' = x - v/\alpha \\ y' = y \end{array}\right\}. \tag{3.40}$$

In this coordinate system, equations (3.39) transform to

$$\left.\begin{array}{l} x' = -\dfrac{v}{\alpha}\cos(\alpha t) \\ y' = +\dfrac{v}{\alpha}\sin(\alpha t) \end{array}\right\}. \tag{3.41}$$

These expressions correspond to clockwise circular motion of radius v/α. The resulting motion is illustrated in Fig. 3.4.

From the definition of α, the orbital radius will be

$$R = \frac{v}{\alpha} = \frac{mv}{qB}. \tag{3.42}$$

The initial velocity v is usually created by accelerating the ions through a potential (voltage) V_{acc} before injecting them into the magnetic field. The resulting speed is given by

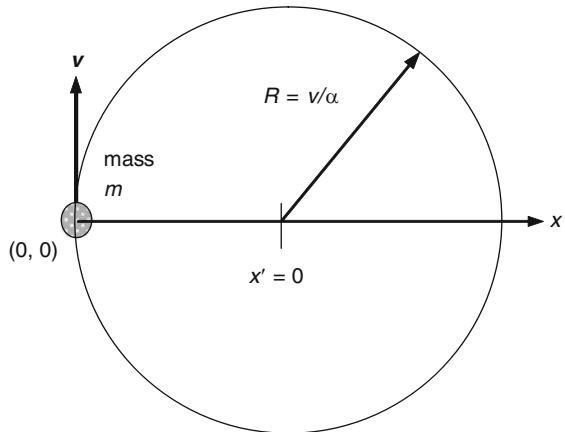$$\frac{1}{2}mv^2 = qV_{acc} \Rightarrow v = \sqrt{\frac{2qV_{acc}}{m}}. \tag{3.43}$$

Fig. 3.4 Motion of a positively-charged particle in a magnetic field which emerges perpendicularly from the page. v is the velocity of the particle at the moment shown

The orbital *diameter* 2R is

$$D = \sqrt{\frac{8V_{acc}}{qB^2}} \sqrt{m}. \tag{3.44}$$

Heavier ions will have larger orbital radii; two ions of different mass entering the magnetic field will follow paths as shown in Fig. 3.5.

The ions will be maximally separated when they return to the *x*-axis after one-half of an orbit. The separation will be the difference of the diameters:

$$s = K \left(\sqrt{m_{heavy}} - \sqrt{m_{light}} \right), \quad K = \sqrt{\frac{8V_{acc}}{qB^2}}. \tag{3.45}$$

Hewlett and Anderson (1962; pp. 142–145) state that the Y-12 magnets at Oak Ridge produced a field of 0.34 T and that uranium tetrachloride (UCl_4) ion beams were accelerated to 35,000 V before being injected into the field. If the UCl atoms were singly ionized, (3.45) gives $K \sim 3.89 \times 10^{12}$ m/kg$^{1/2}$. The molecular weights of $^{235}UCl_4$ and $^{238}UCl_4$ are 375 and 378 mass units, respectively. Either of these values when substituted into (3.44) gives a beam diameter of 3.07 m, and (3.45) gives a separation between the light and heavy beams of 1.23 cm, about half an inch.

For various reasons, the ion beam current represented by the stream of $^{235}UCl_4$ ions in the Y-12 magnets had to be held to only a few hundred *micro*amperes (Parkins 2005). A beam current of 500 μA would correspond to collecting some 3.12×10^{15} ions per second. With a per-atom mass of 3.90×10^{-25} kg for ^{235}U, this means that one could collect some 1.22×10^{-9} kg of ^{235}U per second, or about 105 mg/day. To collect 50 kg at this rate would require some 1,300 years of operation! It is thus understandable why the Y-12 facility eventually involved 1,152 magnet "tanks," each utilizing two or four ion sources.
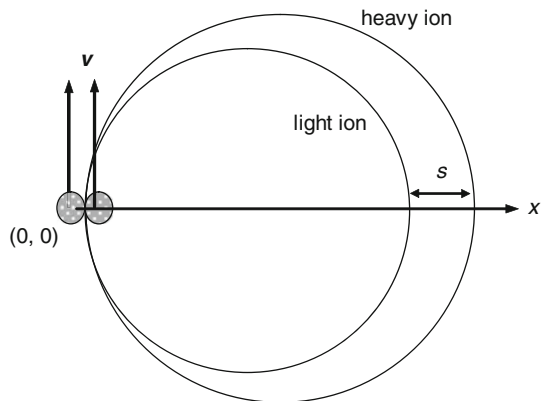

Fig. 3.5 As Fig. 3.4 but for ions of different masses

As described elsewhere by this author (Reed 2009), some of the Y-12 magnets were square coils of about 30 windings and side lengths of 3 m. The field at the center of such a coil is

$$B = \frac{2\sqrt{2}\,\mu_o Ni}{\pi L}, \qquad (3.46)$$

where $\mu_o = 4\pi \times 10^{-7}$ (Tesla-meter)/amp, L is the side length, i is the current, and N is the number of windings. With $L = 3$ m and $N = 30$, the current required to generate a field of 0.34 T is

$$i = \frac{\pi B L}{2\sqrt{2}\,\mu_o N} = \frac{\pi(0.34\,T)\,(3\,\mathrm{m})}{2\sqrt{2}\big(4\pi \times 10^{-7}T - \mathrm{m/amp}\big)(30)} \sim 30{,}000 \text{ amp}. \qquad (3.47)$$

The Y-12 electromagnets were enormously consumptive of electricity. By July 1945 the Y-12 facility had consumed some 1.6 billion kWh of electricity to enrich uranium for the *Little Boy* bomb. This amount of electrical energy corresponds to about 1,400 kt of TNT – some 100 times the yield of *Little Boy* itself!

3.5   Gaseous (Barrier) Diffusion

Like electromagnetic separation, gaseous diffusion played a central role in enriching uranium for the *Little Boy* fission bomb. The physical principal utilized in this facility, code-named K-25, was that when a gas of mixed isotopic composition is pumped against a barrier made of a mesh of millions of tiny holes, atoms of the lighter isotope will tend to *diffuse* through the barrier slightly more readily than those of the heavier one. (Strictly, the correct name for this process is *effusion*.) The gas on the other side of the barrier is collected with a vacuum pump and is said to be *enriched* in the lighter isotope as a result. However, the enrichment realizable through any one stage of barrier is limited by the relative masses of the two isotopes; the process must be repeated hundreds or thousands of times to achieve significant overall enrichment. In the case of uranium this is particularly so as the isotopes differ in mass by only about 1.3%. In fact, the input material to the K-25 plant was uranium hexafluoride gas, for which the isotopes differ by <1% in mass: $^{235}UF_6$ has atomic weight 349 while that of $^{238}UF_6$ is 352.

In view of the importance of gaseous diffusion to the success of the Manhattan Project, the basic physics of this process is derived here from first principles.

It is helpful to start with a result from classical thermodynamics. Suppose that we have a gas of atoms each of mass m trapped in a container at absolute temperature T. According to the Maxwell–Boltzmann distribution, the mean speed of an atom is given by

$$\langle v \rangle = \sqrt{\frac{8\,k\,T}{\pi\,m}}. \tag{3.48}$$

We can imagine all atoms to have this speed, racing about in all possible directions. As shown in Fig. 3.6, imagine an abstract three-dimensional space where the axes are the (x, y, z) components of an atom's velocity. The magnitude of the velocity vector v shown in the diagram is v and its direction is given by spherical coordinates (θ, ϕ).

If there is no preferred direction of motion, then any direction of travel (θ, ϕ) must be as probable as any other. From solid geometry we know that the solid angle subtended by angular limits θ to $\theta + d\theta$ and ϕ to $\phi + d\phi$ is $d\Omega = sin\theta\,d\theta\,d\phi$; if (θ, ϕ) are measured in radians then the solid angle is said to be measured in steradians. Integrating overall all possible directions $[\theta = (0, \pi); \phi = (0, 2\pi)]$ shows that the total available solid angle is 4π steradians.

The probability that any atom chosen at random is moving in the direction of a particular solid angle $d\Omega$ is then given by $P(d\Omega) = d\Omega/4\pi$, that is,

$$P\,(d\Omega) = \frac{1}{4\pi}\,\sin\theta\,d\theta\,d\phi. \tag{3.49}$$

We now consider the diffusion process itself. Figure 3.7 shows a small portion of a diffusion barrier with a single hole of area S. In reality there would be millions of such holes, but analyzing one of them will get us what we need. Atoms are pumped against the lower side of the barrier. All atoms are presumed to be moving at speed $\langle v \rangle$, and, at the moment shown, atom number 3 is just escaping through the hole. The fundamental problem is to compute the number of atoms that escape through the hole over some elapsed time Δt.

Over time Δt an atom moving at speed $\langle v \rangle$ would travel distance $\langle v \rangle \Delta t$. As can be imagined with the aid of Figs. 3.7 and 3.8, any atom moving in the same direction as
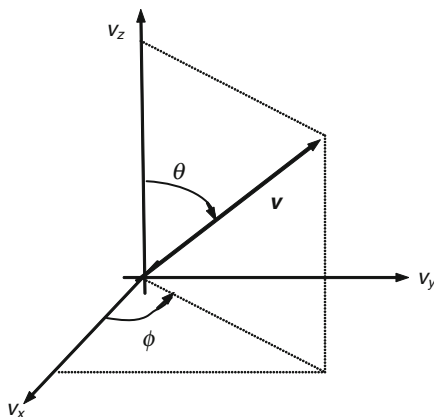

Fig. 3.6 Spherical coordinates. The axes are the components of the velocity vector v

#3 and that is within an "escape cylinder" of slant length $\langle v \rangle \Delta t$ that projects back from the hole along the direction of $\boldsymbol{v}$, that is, along a direction given by (θ, ϕ), must escape within time Δt.

The number of atoms contained within the cylinder shown in Fig. 3.8 would be the volume of the cylinder times the number density of atoms $\rho_N = N/V$ where N is the number of atoms in the gas and V is the volume of the container. To make number density a meaningful concept we have to assume that the density of the gas stays constant; as atoms fly in and out through the sides of the cylinder we presume that for each one that leaves the escape cylinder one arrives to take its place.

The volume of a cylinder of top area S, slant length $\langle v \rangle \Delta t$ and tilt angle θ is given by

$$V_{cyl} = S \langle v \rangle (\Delta t) \cos \theta. \qquad (3.50)$$

The number of atoms in the escape cylinder will then be

Fig. 3.7 Atoms moving in the vicinity of a hole of area S. Atom #3 is just escaping through the hole
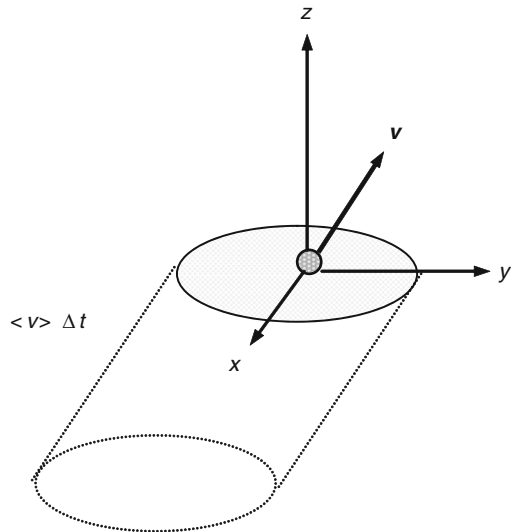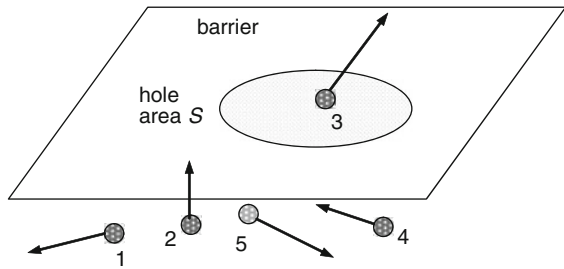

Fig. 3.8 Escape cylinder for a particle with velocity v

$$N_{cyl} = \rho_N \, S \, \langle v \rangle \, (\Delta t) \, \cos \theta. \tag{3.51}$$

Now, not all of these N_{cyl} atoms will be moving in the correct direction (θ, ϕ) to achieve escape. To account for this, we have to multiply (3.51) by the probability of an atom having its velocity so directed, which is given by (3.49):

$$N_{esc}(\Delta t, \theta, \phi) = N_{cyl} \, P \, (d\Omega) = \frac{\rho_N S \, \langle v \rangle (\Delta t)}{4\pi} \, \cos \theta \, \sin \theta \, d\theta \, d\phi. \tag{3.52}$$

We can account for all possible directions of escape by integrating (3.52) over the relevant angles:

$$N_{esc}(\Delta t) = \frac{\rho_N S \, \langle v \rangle \, (\Delta t)}{4\pi} \int\limits_{0}^{\pi/2} \sin \theta \, \cos \theta \, d\theta \int\limits_{0}^{2\pi} d\phi. \tag{3.53}$$

Notice that that the limits on θ here run from 0 to only $\pi/2$; we want to account for only *outward*-moving atoms. Since the diffusion barrier is packed with millions of holes practically edge-to-edge, it will not matter if an atom is offset from the one shown in the figures; any outward-moving atom will find a hole to escape through.

The integrals appearing in (3.53) are standard, and evaluate to $1/2$ and 2π. Combining these with (3.48) gives the important result

$$N_{esc} \, (\Delta t) = \frac{1}{4} \rho_N \, S \langle v \rangle (\Delta t) = C \left(\frac{\rho_N}{\sqrt{m}} \right), \tag{3.54}$$

where

$$C = (S \, \Delta t) \sqrt{\frac{kT}{2\pi}}. \tag{3.55}$$

Equation (3.54) is the central result for understanding barrier diffusion; it tells us that the number of atoms destined to escape through a hole of area S over time Δt is proportional to their density but, through the mean speed, inversely proportional to the square root of their mass. S could as well represent the area of all of the holes in the barrier.

First consider a gas consisting of a single-isotope species. All stages of the diffusion mechanism are presumed to have the same volume V, the same hole area S, and to operate at the same temperature T for the same time Δt; that is, that the constant C is presumed to be the same for each stage of the diffusion cascade. Let ρ_o be the number density of the feedstock to the first stage of the cascade. From (3.54) the number of atoms that will escape from the first stage of the diffuser will be

$$N_1 = C \left(\frac{\rho_o}{\sqrt{m}} \right). \tag{3.56}$$

The number density of atoms in the second stage will then be N_1/V or

$$\rho_{enter\ stage\ 2} = \frac{N_1}{V} = \frac{C}{V} \left(\frac{\rho_o}{\sqrt{m}} \right). \tag{3.57}$$

With this input number density for stage 2, the number of atoms that escape through stage 2 is given by re-applying (3.54):

$$N_2 = C \left(\frac{\rho_{enter\ stage\ 2}}{\sqrt{m}} \right) = \frac{C^2}{V} = \frac{\rho_o}{(\sqrt{m})^2}. \tag{3.58}$$

Propagating this logic shows that after a total of n successive stages the number of atoms that emerge from the n'th stage will be

$$N_n = \frac{C^n}{V^{n-1}} \frac{\rho_o}{(\sqrt{m})^n}. \tag{3.59}$$

If the gas consists of a mixture of two isotopes, say ^{235}U and ^{238}U, (3.59) will apply to each according as the relevant vales of ρ_o and m. If we designate the two isotopes with subscripts 5 and 8, then the final ratio of the number of 235 atoms to the number of 238 atoms can be written as

$$\frac{N_5}{N_8} = \left(\frac{\rho_{o5}}{\rho_{o8}} \right) \left(\frac{m_8}{m_5} \right)^{n/2}. \tag{3.60}$$

Even if different stages of the cascade have different values of V, S, T or Δt, (3.60) will still be correct as it expresses a ratio and those quantities will cancel at each stage as they apply equally to each isotope.

Since $m_8 > m_5$, (3.60) indicates that the ratio N_5/N_8 grows with each stage. However, the amount of enrichment achieved at each stage is tiny: If we start with uranium of natural isotopic composition and ignore the small natural abundance of ^{234}U, $\rho_{o5}/\rho_{o8} = 0.0072/0.9928 = 7.25 \times 10^{-3}$, and, with uranium hexafluoride, $m_8/m_5 = 1.0086$.

The extent of enrichment is usually quantified by the percentage of ^{235}U. If we define $x = N_5/N_8 = \rho_5/\rho_8$, then

$$\% (235) = 100 \left(\frac{x}{x+1} \right). \tag{3.61}$$

Bomb grade ^{235}U is usually considered to be reached at 90% enrichment ($x = 9$), which requires $n = 1,665$. In the case of 1,000 stages, 34% enrichment can be realized, whereas 50% enrichment requires $n = 1,151$. Rhodes (1986,
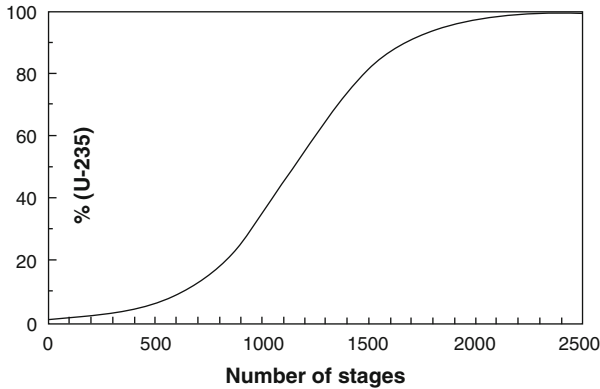
Fig. 3.9 ^{235}U enrichment as a function of number of diffusion stages. The initial isotopic abundance is assumed to be that of natural uranium

p. 495) relates that the original design criteria for the K-25 plant called for 2,892 stages, which would theoretically have realized 99.94% enrichment. In the actual K-25 facility, the feedstock was not input to the first stage of the cascade, as "depleted" uranium hexafluoride from each stage was recycled to preceding stages.

Figure 3.9 shows the run of percent ^{235}U as a function of the number of diffusion stages as predicted by (3.61), assuming that one starts with uranium of natural isotopic composition.

A website on uranium enrichment published by Kennesaw State University, available at http://chemcases.com/nuclear/nc-07.htm, indicates that uranium enriched to 0.86% ($x = 0.008673$) by the S-50 liquid thermal diffusion process served as the feed material to K-25, which produced as output 7%-enriched ($x = 0.07527$) material to be fed to the calutrons. For these figures, (3.60) gives $n \sim 505$ enriching stages. Of course, one has to expect losses in such a complex process: material will inevitably become stuck in valves, pumps, and the miles of pipes involved in such a facility.

References

Fermi, E.: Experimental production of a divergent chain reaction. Am. J. Phys. **20**, 536–558 (1952)

Garwin, R.L., Charpak, G.: Megawatts and Megatons: A Turning Point in the Nuclear Age? Alfred A. Knopf, New York (2001)

Hewlett, R.G., Anderson, O.E.: The New World 1939/1946: Volume I of a History of the United States Atomic Energy Commission. The Pennsylvania State University Press, University Park, PA (1962)

Jones, R.C., Furry, W.H.: The separation of isotopes by thermal diffusion. Rev. Mod. Phys. **18**, 151–224 (1946)

Kazimi, M.S.: Thorium fuel for nuclear energy. Am. Sci. **91**, 408–415 (2003)

Parkins, W.E.: The Uranium Bomb, the calutron, and the space-charge problem. Phys. Today **58** (5), 45–51 (2005)

Reed, B.C.: Understanding plutonium production in nuclear reactors. Phys. Teach. **43**, 222–224 (2005)

Reed, B. C.: Bullion to B-Fields: the Silver Program of the Manhattan Project. Michigan Academician **XXXIX**(3), 205–212 (2009)

Rhodes, R.: The Making of the Atomic Bomb. Simon and Schuster, New York (1986)

Weinberg, A.M.: Eugene Wigner. Nuclear engineer. Phys. Today **55**(10), 42–46 (2002)

Chapter 4
Complicating Factors

Abstract A number of controllable and uncontrollable factors can act to thwart efforts to make nuclear weapons or to secure fissile material. This chapter analyses three of the most serious of these. First, the reactors used to synthesize plutonium during the Manhattan Project used graphite as a moderating agent to slow neutrons. However, if the graphite is contaminated with even a small fraction of a neutron-absorbing element such as boron, the presence of such a contaminant can effectively poison the operation of the reactor. This chapter examines how much contaminant is tolerable. Second, within a bomb core itself, the fissile material will inevitably suffer some level of spontaneous fissions, which, if too great, can cause a predetonation. This problem led to the immensely difficult engineering challenge of implosion during the Manhattan Project. This chapter presents a detailed analysis of the spontaneous fission issue and how one can estimate the probability that a bomb will function correctly in the face of this problem. Finally, the presence of even a small amount of light-element contaminants within the core can lead to predetonation via what are called "α-n" reactions; this possibility sets stringent limits on the purity of the core material. Estimates of the tolerable levels of light-element impurities are developed.

A number of factors can thwart efforts to make nuclear weapons. In this chapter we explore three of these. The first (Sect. 4.1) involved being able to operate large-scale plutonium-production reactors in the face of neutron-absorbing impurities in the graphite that was used as a moderating medium. The other two (Sects. 4.2 and 4.3) involve the problem that if stray neutrons should be present during the brief time that one is assembling sub-critical pieces of fissile material to form a super-critical core, one runs the risk that such neutrons could initiate a premature and hence low-efficiency explosion. Some of these "background" neutrons arise from the fissile material itself and are fundamentally uncontrollable (Sect. 4.2), while others can be controlled, albeit with difficulty (Sect. 4.3).

4.1 Boron Contamination in Graphite

The presence of impurities in the graphite used as a moderator in the CP-1 and
Hanford reactors was a matter of serious concern in the Manhattan Project. Since
the purpose of the graphite was to slow and scatter neutrons without absorbing
them, it was important that it be as free as possible of any neutron-absorbing
impurities. The commercially-produced graphite of the time often contained trace
amounts of boron, which has a voracious appetite for neutron absorption. Indeed, it
was unappreciated boron contamination of their graphite that led German research-
ers to conclude that only heavy water could serve as an adequate moderator, a
situation that was at least in part responsible for their failure to achieve a self-
sustaining chain-reaction. In this section we examine the severity of this effect.

Two isotopes of boron occur naturally: ^{10}B (19.9%) and ^{11}B (80.1%). The
problem is that boron-10 has a huge cross-section – over 3,800 bn – for capture
of thermal neutrons by the reaction

$$_0^1n + {}_5^{10}B \rightarrow {}_2^4He + {}_3^7Li, \tag{4.1}$$

for which $Q = 2.79$ MeV. In view of this, the presence of even a small amount of
boron-10 can quickly suppress the desired chain reaction.

Table 4.1 lists the relevant cross-sections; we assume that the graphite is a
mixture of carbon-12 and boron. These cross-sections are for thermal neutrons
and are adopted from the KAERI site listed in Appendix B. While other reactions
are possible between these isotopes and thermal neutrons, the point here is a simple
model which emphasizes the difference in behavior between ^{10}B and ^{11}B versus ^{12}C
in response to thermal neutron bombardment.

The figures given in the last row of the table are computed on the basis of
assigning the total cross-section for ^{10}B to neutron capture, and the sum of the (n, α)
and radiative capture cross-sections for ^{11}B and ^{12}C to neutron capture.

Suppose that we are willing to tolerate a total neutron-capture cross section of
$\sigma_{capture}^{total}$. The question is: What maximum fraction by number can boron constitute of
the graphite?

Let the number fractions of the three isotopes ^{10}B, ^{11}B and ^{12}C be f^{10}, f^{11}, and
f^{12}, respectively. With obvious notation for the cross-sections, $\sigma_{capture}^{total}$ can be
written as

$$\sigma_{capture}^{total} = f^{10}\sigma_{capture}^{10} + f^{11}\sigma_{capture}^{11} + f^{12}\sigma_{capture}^{12}, \tag{4.2}$$

Table 4.1 Boron and carbon cross-sections (barns)

Cross-section	^{10}B	^{11}B	^{12}C
σ (total)	3,840	5.050	4.750
σ (n, α)	3,837	0.03138	0.07265
σ (elastic)	2.144	5.045	4.746
σ (radiative capture)	0.500	0.005075	0.003530
σ (capture, adopted)	3,840	0.036455	0.076180

where we must have

$$f^{10} + f^{11} + f^{12} = 1. \tag{4.3}$$

The abundance ratio of ^{10}B to ^{11}B is 19.9 to 80.1%. Define this ratio as α, that is,

$$\alpha = \frac{f^{10}}{f^{11}} = \frac{0.199}{0.801} = 0.248. \tag{4.4}$$

With this definition, (4.2) and (4.3) become

$$\sigma_{capture}^{total} = f^{11}\left(\alpha\,\sigma_{capture}^{10} + \sigma_{capture}^{11}\right) + f^{12}\sigma_{capture}^{12} \tag{4.5}$$

and

$$f^{11}(\alpha + 1) + f^{12} = 1. \tag{4.6}$$

Solving (4.6) for f^{11} and substituting the result into (4.5) gives

$$f^{12} = \frac{\sigma_{capture}^{total} - \beta}{\sigma_{capture}^{12} - \beta}, \tag{4.7}$$

where

$$\beta = \frac{\alpha\sigma_{capture}^{10} + \sigma_{capture}^{11}}{1 + \alpha}. \tag{4.8}$$

Equations (4.7) and (4.8) give the number fraction of the graphite that must be in the form of ^{12}C. Suppose we are willing to tolerate $\sigma_{capture}^{total} = 0.1$ bn, a value not much greater than the adopted ^{12}C capture cross section. With the numbers given in Table 4.1, we find $\beta = 763.106$ bn and $f^{12} = 0.9999688$. This means that the graphite must be >99.996% pure to keep the neutron-capture cross-section to the modest figure of 0.1 bn. Put another way, the total boron number fraction cannot exceed 0.0000312, that is, no more than one atom in 32,000 in the graphite can be boron! According to a U.S. Department of energy history of the Hanford reactors, the Boron in the graphite blocks in those reactors was held to a purity of 0.4 parts per million (DOE 2001).

Is 0.1 bn for the total neutron capture cross-section a reasonable number? To check this, we can use the results of the analysis of neutron thermalization in Sect. 3.2 to make a very rough estimate of what fraction of neutrons would survive their scatterings through the graphite. To simplify matters, let us assume that the total cross-section for ^{10}B is ascribed to neutron capture ($\sigma_{total}^{10} = 3,840$ bn), while the totals for ^{11}B and ^{12}C, ($\sigma_{total}^{11}, \sigma_{total}^{12}$) = (5.050 bn, 4.750 bn), are ascribed purely to elastic scattering. The total interaction cross-section is then

$$\sigma_{total} = f^{10}\sigma_{total}^{10} + f^{11}\sigma_{total}^{11} + f^{12}\sigma_{total}^{12}, \tag{4.9}$$

where the f's are again the isotopic number fractions. The probability that a neutron will survive an interaction with a nucleus in the graphite, that is, the probability that it will *not* be captured upon striking a nucleus, will be the cross-section for scattering only, $f^{11}\sigma_{total}^{11} + f^{12}\sigma_{total}^{12}$, divided by σ_{total}. For N independent successive scatterings the probability of survival will be

$$P_{survive} = \left(\frac{f^{11}\sigma_{total}^{11} + f^{12}\sigma_{total}^{12}}{\sigma_{total}}\right)^N. \tag{4.10}$$

We saw in Sect. 3.2 that on the order of 50 or so scatterings are required to thermalize a neutron of initial energy 2 MeV. For the isotopic fractions corresponding to $\sigma_{capture}^{total} = 0.1$ bn as used above, $\sigma_{total} = 4.7738$ bn, and the probability of surviving 50 interactions is about 0.779. If $\sigma_{capture}^{total}$ is increased to 0.12 bn (about one boron atom per 17,000) the survival probability for 50 interactions drops to 0.631; for 70 interactions it would be only 0.525. In this latter case, of every 2.5 neutrons emitted per "average" fission, only a little more than one would on average survive thermalization to go on to contribute to the next generation of fissions. These numbers make clear that even a fraction of a percent of boron impurity would be disastrous.

To be fair, this calculation overstates the case in that it takes no account of the fact that the (n, α) cross-section for ^{10}B is a strong function of energy; the cross-section is small for energetic neutrons (a few tenths of a barn at 1 MeV) but increases exponentially with decreasing energy. It is really only in its last few scatterings to thermalization a neutron faces a significant probability of capture by ^{10}B, whereas we have assumed that the 3,840 bn figure applies for all energies. Nevertheless, these numbers do give one a sense of why it is so important to reduce neutron-absorbing contaminants to essentially negligible levels.

Spreadsheet **Boron.xls** can be used to examine the calculations presented in this section. The user sets the value for the total tolerable capture cross-section of (4.5) and the number of successive scatterings N; the spreadsheet computes the tolerable boron fraction and the probability that a neutron will survive N scatterings.

4.2 Spontaneous Fission of ^{240}Pu, Predetonation, and Implosion

Material in this section is adopted from a publication elsewhere by this author (Reed 2010).

Emilio Segrè's discovery in December 1943 that ^{235}U has a very low spontaneous fission (SF) rate cleared the way for use of the "gun assembly" mechanism of the *Little Boy* bomb. Conversely, his later discovery that reactor-produced plutonium has a very high SF rate meant that gun assembly would be far too slow for the *Trinity* and *Fat Man* bombs. The problem was not with the ^{239}Pu to be used as fissile material for the bombs, but rather that some ^{240}Pu was inevitably formed in the Hanford reactors as a consequence of already-formed ^{239}Pu nuclei absorbing

neutrons; ^{240}Pu has an extremely high SF rate. Only implosion could trigger a Plutonium bomb quickly enough to prevent a SF from causing a premature detonation. In this section we examine the probability of predetonation. How one can estimate the amount of ^{240}Pu created in a reactor is analyzed in Sect. 5.3.

Let N_A designate Avogadro's number, and let A be the atomic weight (g/mol) of some spontaneously fissioning material. The number of atoms in 1 kg of material will be $10^3 (N_A/A)$. For any decay process characterized by a half-life $t_{1/2}$ seconds, the average lifetime of a nucleus against decay is $t_{1/2}/(ln\ 2)$. Consequently, the average spontaneous fission rate F (number per kilogram per second) is given by the number of atoms divided by their average lifetime:

$$F = 10^3 \left(\frac{N_A}{A} \right) \left(\frac{\ln 2}{t_{1/2}} \right) \left(\text{kg}^{-1}\text{sec}^{-1} \right). \tag{4.11}$$

Recommended values for SF half-lives for heavy isotopes have been published by Holden and Hoffman (2000). Numbers for four isotopes of interest are given in Table 4.2; see also Table 2.1. The spontaneous fission rates in the fourth column in Table 4.2 are quoted in spontaneous fissions per kilogram of material per 100 μs. The secondary-neutron v values for U-238 and Pu-240 represent the number of neutrons emitted in spontaneous fissions of these nuclides; these are adopted from Table 1.33 of Hyde (1964).

The reason for quoting the rates SF's in this way this was discussed in Sect. 2.4. If we assume that the core of a bomb is on the order of 10 cm in size and that the gun method is capable of accelerating projectiles to 1,000 m/s, then about 100 μs will be required to complete the assembly. During this time, a 50-kg ^{235}U assembly would suffer some 2.81×10^{-5} spontaneous fissions, a negligibly small number; the probability of predetonation would be miniscule (although not zero). From the point of view of spontaneous fission, then, contamination of a few percent ^{238}U in a ^{235}U core will not present a significant hazard. A 10-kg plutonium core contaminated with even only 1% ^{240}Pu, however, is likely to suffer some five spontaneous fissions in this brief time; the core pieces are not likely to reach their fully assembled configuration before a spontaneous fission causes a pre-detonation. The only option aside from the virtually impossible task of trying to remove the offending ^{240}Pu is to speed up the assembly process to on the order of a microsecond or less. For a *pure* 10-kg ^{239}Pu core the rate is about 0.007 spontaneous fissions per 100 μs.

While the above numbers give a sense of the potential magnitude of the possibility of a spontaneous-fission-induced predetonation, a more careful analysis is necessary to fully quantify this risk. Because spontaneous fission is

Table 4.2 Spontaneous fission parameters

Nuclide	$t_{1/2}$ (year)	A (g/mol)	SF (kg 100 μs)$^{-1}$	v
^{235}U	1.0×10^{19}	235.04	5.627×10^{-7}	2.637
^{238}U	8.2×10^{15}	238.05	6.776×10^{-4}	2.1
^{239}Pu	8×10^{15}	239.05	6.916×10^{-4}	3.172
^{240}Pu	1.14×10^{11}	240.05	48.33	2.257

fundamentally a random phenomenon, one is restricted to speaking in terms of probabilities: the physics of the situation will dictate a certain probability that a predetonation may happen. It is then a question of judgment as to the acceptability of that risk.

The approach taken here is based on a probabilistic model of neutrons traveling through a bomb core, and should be understandable to readers familiar with concepts such as multiplying together independent probabilities to generate an overall probability. I do not discuss the much more complex question of estimating the yield of a weapon in the event of predetonation (Mark 1993).

Random processes are described by Poisson statistics. To calculate the predetonation probability we have to treat two effects: the probabilities that 0, 1, 2, . . . spontaneous fissions occur during the assembly time, and the probability that the secondary neutrons so released travel to the edge of the core and escape without causing secondary fissions.

Imagine a spherical bomb core containing mass M of spontaneously fissioning material, and let F be the rate of spontaneous fissions as given by (4.11). We assume an already spherical geometry for the bomb core while it is being assembled – an obviously somewhat unrealistic model for a gun-type bomb. The average number of spontaneous fissions during the assembly time $t_{assemble}$ is

$$\mu = MFt_{assemble}. \tag{4.12}$$

From Poisson statistics, the probability P_k ($k = 0$, 1, 2, ...) that exactly k spontaneous fissions occur during this time is given by

$$P_k = \frac{\mu^k}{k!}e^{-\mu}. \tag{4.13}$$

If each spontaneous fission releases on average v neutrons, then k spontaneous fissions will release kv neutrons. For no predetonation to occur, all of these neutrons must escape. If P_{escape} represents the probability that an individual neutron escapes without causing a fission, then the probability that all will escape is $\left(P_{escape}\right)^{kv}$; how P_{escape} is determined is described below. Hence, the probability that both k spontaneous fissions occur and all of the emitted neutrons escape is $P_k\left(P_{escape}\right)^{kv}$.

To determine the probability of no predetonation we have to account for all possible number of occurrences of spontaneous fissions:

$$P_{\text{no predet}} = \sum_{k=0} P_k\left(P_{\text{escape}}\right)^{kv}. \tag{4.14}$$

In principle, the sum in (4.14) goes to infinity, but in practice the first few terms will suffice.

The next part of the argument is to determine P_{escape}, the overall escape probability for one neutron.

Neutrons can escape the core in one of two ways: they may escape directly by traveling in a straight line from their point of origin to the edge of the sphere, or they can scatter one or more times before escaping. For a given neutron, it is impossible to predict how many times it will scatter before escaping, but we can develop an expression for the probability that it will escape following a specified number of scatterings; adding these probabilities gives P_{escape}. It is useful to imagine that S_{max}, the maximum possible number of scatterings before escape, is known in advance. How S_{max} is treated is discussed following (4.19) below.

If π_j represents the probability that a neutron escapes following j successive scatterings, the overall total probability of escape is

$$P_{escape} = \pi_0 + \pi_1 + \pi_2 + \cdots + \pi_{S_{\max}}. \tag{4.15}$$

Do not to confuse these probabilities with those of (4.13), which are the probabilities of a given number of spontaneous fissions.

To determine the π_j, recall the expression from Sect. 2.1 for the probability that a neutron will penetrate through a linear distance x of material: $P(x) = \exp(-\sigma_{tot} n x)$, where n is the number density of nuclei in the material, and σ_{tot} is the total reaction cross-section for neutrons in the material. As in the calculation of critical mass, σ_{tot} is given by the sum of the scattering and fission cross sections. We ignore any possibility of non-fission neutron capture, which for any reasonably pure fissile material should be small. Now, this $P(x)$ refers to neutrons penetrating through a linear distance x. If the neutrons are emitted in random directions within the bomb core, we need to average $P(x)$ over all possible directions of neutron emission from all points within the sphere. So as not to disturb the flow of the present argument, this issue is examined in Appendix F, where it is shown that the appropriate average, $\langle P_{sph} \rangle$, can be expressed as a double integral which can readily be computed within the spreadsheet for the predetonation calculation.

The probability that a neutron will not directly escape is $1 - \langle P_{sph} \rangle$. These neutrons must first interact with a nucleus either by causing a fission (f) or by being scattered (s). The respective probabilities of these competing processes are σ_f/σ_{total} and σ_s/σ_{total}. Hence, the probability that a neutron will suffer one scattering is given by

$$P_{one} = \left(\frac{\sigma_s}{\sigma_{total}} \right) \left(1 - \langle P_{sph} \rangle \right) \equiv g. \tag{4.16}$$

The probability that such a once-scattered neutron will then escape, that is, π_1 of (4.15), is given by P_{one} times $\langle P_{sph} \rangle$:

$$\pi_1 = \left(\frac{\sigma_s}{\sigma_{total}} \right) \left(1 - \langle P_{sph} \rangle \right) \langle P_{sph} \rangle = g \langle P_{sph} \rangle. \tag{4.17}$$

Similarly, the probability that a neutron that has already undergone one scattering will experience a second scattering is given by P_{one} of (4.16) times the

probability of suffering a further interaction, $\left(1 - \langle P_{sph} \rangle\right)$, times the probability of that interaction being a scattering, σ_s/σ_{total}, that is, $P_{two} = g^2$. The probability of escape after two scatterings is thus $\pi_2 = g^2 \langle P_{sph} \rangle$. Carrying on this logic and assuming that scatterings are independent events, the probability that a neutron will suffer j successive scatterings and then escape is given by

$$\pi_j = g^j \langle P_{sph} \rangle. \tag{4.18}$$

Hence we have

$$P_{escape} = \langle P_{sph} \rangle \left(\sum_{j=0}^{S_{max}} g^j \right) = \langle P_{sph} \rangle \left[\frac{1 - g^{S_{max}+1}}{1 - g} \right]. \tag{4.19}$$

Equation (4.19) follows from the fact that the summation is the partial sum of a geometric series. Note that we have assumed that the neutrons are randomly redirected at each scattering.

What about the maximum number of scatterings S_{max}? For a reaction characterized by the cross-section σ, the mean free path between reactions (Sect. 2.1) is $\lambda = 1/\sigma n$. For U-235 and Pu-239 the mean free paths are about 4 cm, which is of the same order as the untamped critical radii, 8.4 and 6.3 cm, respectively. Many neutrons might not scatter at all, while some might suffer a few scatterings. As described in the results given below, however, the calculated predetonation probabilities are fairly insensitive to changes in S_{max}. The worst case scenario, which maximizes the predetonation probability, is $S_{max} = 0$. As shown below, for a model of the *Little Boy* U-235 core the predetonation probability changes by less than 1% for reasonable choices of S_{max}. For the *Fat Man* Pu-239 core the sensitivity is greater, up to a few percent, but the value of S_{max} is not a determining factor in whether or not implosion is necessary. Thus, the choice of S_{max} is left to the user to be assigned as desired. (That the worst-case scenario is $S_{max} = 0$ may seem counterintuitive, as one would expect more neutron–nucleus interactions would lead to more chances for fissions. But recall that some neutrons may escape even after a very large number of scatterings; setting $S_{max} = 0$ means that we forgo accounting for such escapees, leading to an overestimate of the predetonation probability.)

Equations (4.11)–(4.14) and (4.19) can be used to predict the no-predetonation probability once the nuclear constants, core and contaminant masses, and assembly time scale are specified. Spreadsheet **PreDetonation.xls** has been developed to carry out this calculation. The user enters the core and contaminant masses and their atomic weights, the relevant cross-sections, the SF half-life and secondary neutron number for the spontaneously fissile material, the maximum number of scatterings to be considered, and the assembly timescale. The spreadsheet then computes the non-predetonation probability; see also the description of computing the escape probability in Appendix F. To calculate the sum in (4.14) the spreadsheet takes an upper limit of $k = 20$, which is entirely sufficient for any reasonable situation.

4.2.1 Little Boy Predetonation Probability

As described in Sect. 2.3, the Hiroshima *Little Boy* core comprised about 64 kg of uranium in a cylindrical configuration, of which about 80% was U-235 and 20% (12.8 kg) was U-238. The half-life of U-238 for spontaneous fission, 8.2×10^{15} year, is about 1,200 times shorter than that of U-235, rendering the latter isotope almost negligible as far as the predetonation probability is concerned. As in Sect. 2.3, I model the core of *Little Boy* as being spherical; a 64 kg sphere of density 18.71 g/cm^3 has a radius of 9.35 cm. The effect of a surrounding tamper on escaping neutrons is ignored. In this case, even for a 200 μs assembly time, the non-predetonation probability is about 98.4% for $S_{max} = 0$. For $S_{max} = 5$ (probably too large), this rises slightly to 98.9%. At worst, fizzles could be expected to occur in about two such bombs out of every one hundred. For a 200 μs assembly time there is a 98.3% probability that no spontaneous fission will occur. The spherically averaged direct escape probability $\langle P_{sph} \rangle$ for this 64 kg core is 0.268; for $S_{max} = 5$, P_{escape} of (4.15) is 0.609. For a 100 μs assembly time, the mean number of spontaneous fissions is only about 0.009.

4.2.2 Fat Man Predetonation Probability

The untamped critical mass of Pu-239 is about 17 kg. However, the *Trinity* and *Fat Man* bombs used cores of mass about 6.2 kg due the greater efficiency afforded by implosion (Sublette 2007). For a 6.2 kg core of pure Pu-239, an assembly time of 200 μs yields a no-predetonation probability of 99.2% ($S_{max} = 0$). Although this would appear to be better odds than the U-238 contaminated *Little Boy* device, the comparison is misleading because a non-imploded Pu core of this mass would be subcritical. In reality, the 6.2 kg cores contained about 1.2% Pu-240 (0.0744 kg), which makes the outcome very different. Figure 4.1 shows the $S_{max} = 0$ non-predetonation probability for this case as a function of the assembly time. For $S_{max} = 0$ and a time of 100 μs the non-predetonation probability is only 5.8% (12.0% for $S_{max} = 1$); there is no realistic hope of successfully assembling such a core in a time scale characteristic of the gun design. Here $\langle P_{sph} \rangle = 0.497$, and, for $S_{max} = 5$, $P_{escape} = 0.771$. Although these numbers do not differ much from those of the *Little Boy* calculation, the mean number of spontaneous fissions is enormously greater in the case of the Pu-240 contaminated *Fat Man* device: over 100 μs, for example, this number is 3.6 in contrast to 0.009.

We can make a rough estimate of the real *Trinity* non-predetonation probability as follows. Neglecting the neutron initiator housed at its center, the core would have a radius of about 4.56 cm for a density of 15.6 g/cm^3. If the implosion is to crush the core to a density twice as great as this value, the final radius would be about 3.62 cm. If this is done at a speed of, say, 2,000 m/s, some 4.7 μs would elapse. Modeling the core as having a mass 6.2 kg at a density midway between these values, 23.4 g/cm^3, gives a $S_{max} = 0$ non-predetonation probability of 86.5% (88.9% for $S_{max} = 1$; the
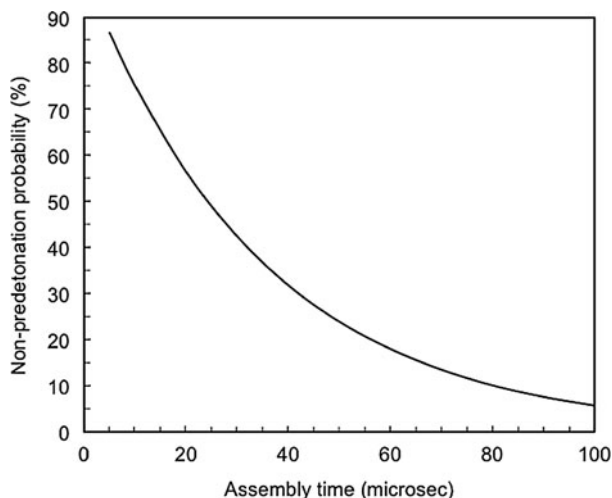
Fig. 4.1 Non-predetonation probability for a non-imploded 6.2-kg Pu core contaminated with 1.2% Pu-240 as a function of assembly time. The maximum number of scatterings is assumed to be zero

altered density makes little difference to the probabilities: at 15.6 g/cm^3 they are respectively 87.5 and 90.5%). Implosion is the only means to achieve such short assembly times. Former Los Alamos Theoretical Division Director Carson Mark, working from figures given in a letter from Robert Oppenheimer to Manhattan Engineer District Commander General Leslie Groves, reported that Oppenheimer estimated a 88% chance of a "nominal" 20 kt yield from the *Trinity* device (Mark 1993); we can conclude that the present model is reasonable.

Given that plutonium synthesized in fuel rods in commercial reactors comprises about 20% Pu 240, we can appreciate the difficulties faced by terrorists who would plan to steal spent fuel rods and use them to create a workable plutonium bomb. Mark concluded, however, that even a 0.5 kt "fizzle yield" for a terrorist bomb based on reactor-grade plutonium would still produce a severely damaging explosion. Such an explosion would be equivalent to about 200 of the truck bombs used to destroy the Murrah Federal Building in Oklahoma City in 1995 (Bernstein 2008). Thus, while an efficient *Trinity*-like terrorist weapon based on purloined fuel rods is highly unlikely, the issue of fuel supply and security will remain a pressing one for years to come.

Figure 4.2 shows a photograph of the *Trinity* test device; Fig. 4.3 shows the Nagasaki *Fat Man* bomb; the bulbous casing enclosed the implosion assembly within and provided stable flight characteristics when dropped.

To end this section, we ask: "How can one obtain an *implosion*?" After all, explosions are normally seen to be outwardly-directed phenomena. This was done by using an assembly of *implosion lenses*. The fundamental idea is sketched in Fig. 4.4, which shows a single lens in cross-section; in three dimensions imagine a roughly pyramidal-shaped block that would fit comfortably on your lap. The block is composed of two explosive castings that mate precisely together. The outer casting is of a fast-burning explosive (technically known as "Composition B", or just Comp B),
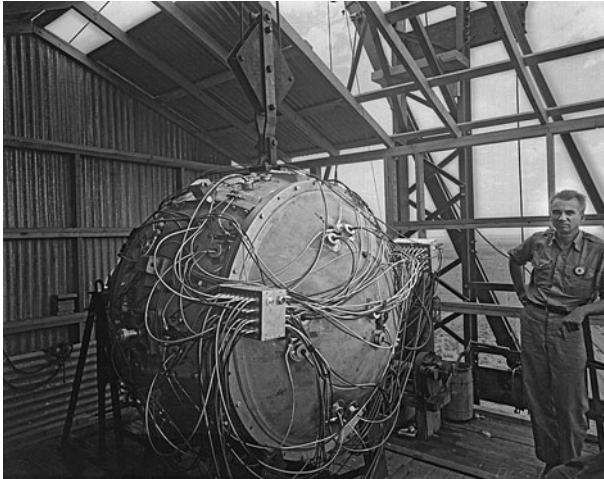
Fig. 4.2 The *Trinity* device atop its test tower on July 15, 1945. Norris Bradbury (1909–1997), who served as Director of the Los Alamos Laboratory from 1945 to 1970, stands to the right. The *spherical shape* of this implosion device is clearly visible; the cables feeding from the box halfway up the device go to the implosion-lens detonators discussed in the text. Photo courtesy Alan Carr, Los Alamos National Laboratory

Fig. 4.3 The Nagasaki *Fat Man* plutonium implosion weapon shortly before its mission. *Fat Man* was 12 feet long, 5 feet in maximum diameter, and weighed 10,300 pounds when fully assembled (Sublette 2007). Photo courtesy Alan Carr, Los Alamos National Laboratory

Fig. 4.4 Schematic
illustration of implosion
lens segment
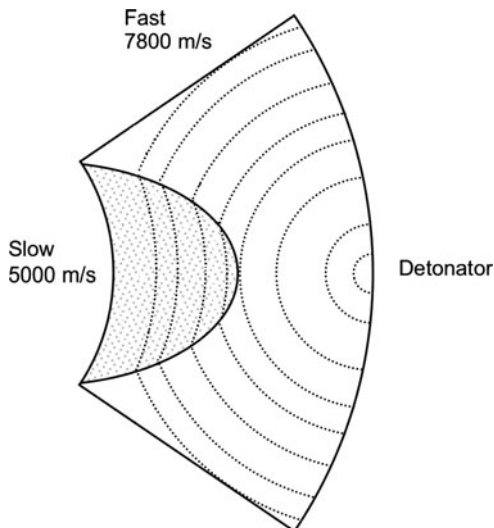
while the inner, lens-shaped one is a slower burning material known as Baratol,
a mixture of barium nitrate and TNT. A detonator at the outer edge of the Comp
B initiates an outward-expanding detonation wave. When the detonation wave hits the
Baratol, it too begins exploding. If the interface between the two is of just the right
shape, the two waves can be arranged to combine as they progress along the interface
in such as way as to create an inwardly-directed converging wave in the Baratol; the
dashed lines in Fig. 4.4 illustrate the right-to-left progression of the detonation. As
sketched in Fig. 4.5, 32-such "binary explosive" assemblies were fitted together to
create imploding spheres inside the *Trinity* and *Fat Man* devices. Within the Baratol
lenses resided another spherical assembly of 32 blocks of Comp B, which are
detonated by the Baratol to achieve a high-speed symmetric crushing of tamper
spheres that lay within them. A fascinating and very readable personal reminiscence
of casting and machining the implosion lenses was published by Hull and Bianco
(2005); for a more technical history, see Hoddeson et al. (1993).

4.3   Tolerable Limits for Light-Element Impurities

Beyond the uncontrollable issue of predetonation caused by spontaneous fission,
another danger for weapons designers, particularly in the case of plutonium bombs,
is that a chain reaction can be initiated by the natural α-decay of the fissile material
if that material contains even a small percentage of light-element impurities.
A particular danger in this regard is the presence of any beryllium in a Pu core.
^{239}Pu has a fairly short half-life for α-decay, about 24,100 years, or 7.605×10^{11} s.
From the decay-rate formula given in the preceding section this leads to an
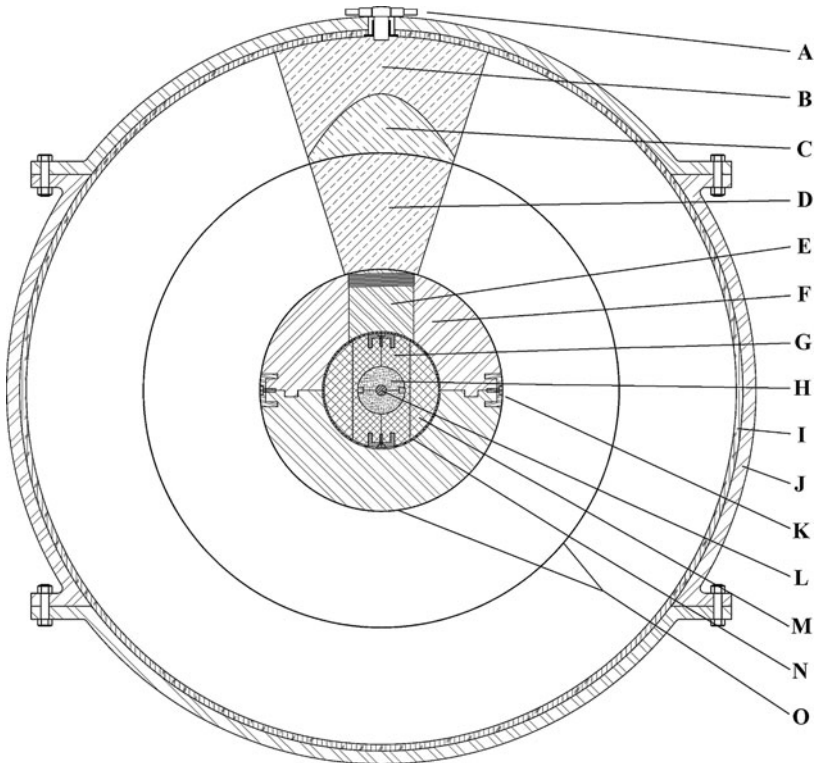enormous rate of α-decays:

Fig. 4.5 Cross-section drawing of the Y-1561 *Fat man* implosion sphere showing major components. Only one set of 32 lenses, inner charges, and detonators is depicted. Numbers in parentheses indicate quantity of identical components. Drawing is to scale. Copyright by and used with kind permission of John Coster-Mullen. (A) 1773 EBW detonator inserted into brass chimney sleeve (32) (B) Comp B component of outer polygonal lens (32) (C) Cone-shaped Baratol component of outer polygonal lens (32) (D) Comp B inner polygonal charge (32) (E) Removable aluminum pusher trap-door plug screwed into upper pusher hemisphere (F) 18.5-in. diameter aluminum pusher hemispheres (2) (G) 5-in. diameter Tuballoy (U-238) two-piece tamper plug (H) 3.62-in. diameter Pu-239 hemisphere with 2.75-in. diameter jet ring (I) 0.5-in. thick cork lining (J) 7-piece Y-1561 Duralumin sphere (K) Aluminum cup holding pusher hemispheres together (4) (L) 0.8-in. diameter Polonium–beryllium initiator (M) 8.75-in. diameter Tuballoy tamper sphere (N) 9-in. diameter boron plastic shell (O) Felt padding layer under lenses and inner charges
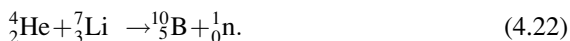
$$R_\alpha = 10^3 \left(\frac{N_A}{A}\right) \left(\frac{\ln 2}{t_{1/2}}\right) = 10^3 \left(\frac{6.022 \times 10^{23}}{239}\right) \left(\frac{\ln 2}{7.605 \times 10^{11}}\right)$$

$$= 2.296 \times 10^{12} \text{kg}^{-1}\text{sec}^{-1}. \tag{4.20}$$

This rate is much greater than the rate of spontaneous fissions for ^{240}Pu. For a 10-kg core we would have an α-decay rate of some 2.3×10^{13} s^{-1}. If some of these alphas should find a beryllium nucleus to react with during the time that the bomb

core is being assembled, the result will be a neutron which could go on to initiate a premature chain reaction in the plutonium. Recall Chadwick's (α, n) reaction for producing neutrons by α-bombardment of beryllium (Sect. 1.4):

$$_2^4\text{He} + {}_4^9\text{Be} \rightarrow {}_6^{12}\text{C} + {}_0^1\text{n}. \tag{4.21}$$

A similar effect happens with α bombardment of lithium:

$$_2^4\text{He} + {}_3^7\text{Li} \rightarrow {}_5^{10}\text{B} + {}_0^1\text{n}. \tag{4.22}$$

This issue is a serious one; as described by Bernstein (2007), plutonium metal at room temperature is rather brittle and difficult to form into desired shapes unless alloyed with another metal. A light alloying metal such as aluminum, however, cannot be used because of this (α, n) problem; one has to use a heavier metal. Los Alamos metallurgists alloyed plutonium with gallium to achieve desirable malleability properties. For impurities heavier than calcium the issue is moot as the alphas cannot mount the Coulomb barrier of the nucleus (Serber 1992).

Chemical processing of the plutonium will inevitably introduce some level of impurities. What level of impurity can one tolerate if the resulting rate of neutron production is to be kept below, say, one per 100 μs? For simplicity, we develop the analysis assuming that only one impurity is present.

To address this issue requires appreciating two empirical ideas from experimental nuclear physics: (i) the *yield* of a reaction, and (ii) the *range* of a particle within a given material. We discuss these first and then develop a formula for predicting the neutron-generation rate for some impurity. We have in mind here beryllium as the impurity for sake of definiteness.

The yield y of a reaction can be understood as follows. Suppose that one has a well-mixed sample of Be and an α emitter such as plutonium, radium, or polonium. Not all of the emitted alphas will find a Be nucleus to react with; atoms are mostly empty space. The yield of the reaction is the number of neutrons produced per α emitted. From figures given by Fermi (1949, p. 179), 1 Curie (*Ci*) of radium well-mixed with beryllium yields about 10–15×10^6 neutrons per second, and 1 *Ci* of polonium well-mixed with Be yields some 2.8×10^6 neutrons per second. Both Ra and Po are α-emitters. On recalling that 1 *Ci* = 3.7×10^{10} s^{-1}, these figures correspond to yields of 2.7–4.1×10^{-4} and 7.6×10^{-5}, respectively. Radium and polonium alphas respectively have energies of about 4.8 and 5.3 MeV; curiously, the more energetic alphas give a lower yield. The reason for this is that a higher-energy particle will have a longer *range* of travel in some material before being consumed in a reaction, thus lowering the yield; this is discussed further in the next paragraph. Plutonium alphas have energies of about 5.2 MeV, so we might expect a yield for Pu-alphas on Be somewhere between these two results, say $y \sim 10^{-4}$. This is in the ballpark: West & Sherwood (1982) give the neutron yield of 5.2-MeV alphas on ^{9}Be as 6.47×10^{-5}.

The *range* of an energetic particle in some material is a measure of how far it will travel before being stopped by a nucleus of that material. Empirically, the

Bragg-Kleeman rule (Evans 1955, p. 652) states that range is proportional to the square root of the atomic weight A of the material being traversed and inversely proportional to its mass density:

$$R \propto \frac{\sqrt{A}}{\rho}. \tag{4.23}$$

The *stopping power S* of a material is defined to be inversely proportional to the range. Suppose that one has a mixture of two materials, A and B, each with different ranges for α particles. If $R_A > R_B$, then $S_A < S_B$, and one would expect an α to have a greater probability of reacting with a nucleus of material B than one of material A, presumably in the proportion S_B/S_A. We thus use stopping power as a measure of relative amounts of "reactivity" of the two materials:

$$S \propto \frac{\rho}{\sqrt{A}}. \tag{4.24}$$

In considering the presumably small amount of some impurity in a bomb core, the density to be used here for the impurity will not be its "normal" density, but rather that given by its small mass distributed throughout the volume of the core.

Now consider a bomb core of heavy fissile material of atomic weight A_H and density ρ_H along with an admixture of some light-element impurity of atomic weight A_L and density ρ_L (as defined above). We presume that the amount of impurity is so slight that ρ_H will be essentially the "normal" value for that material. Also let the nuclear number densities of the two materials be n_H and n_L, respectively; the goal here is to get an expression for the tolerable limit on n_L/n_H. If V is the volume of the core, the mass of the impurity will be $n_L A_L V/N_A$, and its mass density will be $n_L A_L/N_A$. This will give a stopping power S_L according as

$$S_L \propto \frac{\rho}{\sqrt{A}} \propto \frac{n_L A_L}{N_A \sqrt{A_L}} \propto \frac{n_L \sqrt{A_L}}{N_A}, \tag{4.25}$$

and similarly for the heavy fissile material.

Let R_n be the rate of neutron production (neutron/s) caused by the impurity. If the fissile material has no neutron yield for α bombardment (Coulomb barrier too great), we can express R_n as

$$R_n = R_\alpha y \begin{pmatrix} \text{fraction of total stopping} \\ \text{power due to impurity} \end{pmatrix}$$

$$= R_\alpha y \left(\frac{n_L \sqrt{A_L}}{n_L \sqrt{A_L} + n_H \sqrt{A_H}} \right), \tag{4.26}$$

where R_α is the rate of α-decay as in (4.20). Unless one has very poor chemical separation techniques we would expect $n_L \ll n_H$, so we can simplify this to

$$R_n = R_\alpha \, y \left(\frac{n_L}{n_H}\right) \left(\sqrt{\frac{A_L}{A_H}}\right). \tag{4.27}$$

Since we presumably know a tolerable maximum neutron rate R_n, it is more convenient to write this as a constraint on the ratio of number densities:

$$\left(\frac{n_L}{n_H}\right) < \frac{1}{y} \left(\frac{R_n}{R_\alpha}\right) \sqrt{\frac{A_H}{A_L}}. \tag{4.28}$$

Assuming beryllium as the contaminant in a 10-kg Pu core, adopting the West and Sherwood yield, and taking $R_n = 10^{-4} \, \text{s}^{-1}$ (=1 per 100 μs) gives

$$\left(\frac{n_L}{n_H}\right) < \frac{1}{(6.47 \times 10^{-5})} \left(\frac{10^4}{2.3 \times 10^{13}}\right) \sqrt{\frac{239}{9}} \sim 3.5 \times 10^{-5}. \tag{4.29}$$

This means that no more than about 1 atom in 29,000 can be one of beryllium.

In the case of a ^{235}U core the situation is much more favorable; one can tolerate a very high degree of impurity if necessary. The α-decay half life for ^{235}U is about 7.0×10^8 years, or ~2.2×10^{16} s. This gives $R_\alpha \sim 8.0 \times 10^7 \, \text{kg}^{-1} \, \text{s}^{-1}$, or about $4.0 \times 10^9 \, \text{s}^{-1}$ for a 50-kg core. For a yield of 5×10^{-5}, (4.28) gives $n_L/n_H < 0.26$. Incidentally, ^{238}U has an α-decay rate equal to about 0.16 of that of ^{235}U while that of ^{240}Pu is about 3.7 times that of ^{239}Pu, further reasons to minimize their presence in bomb cores. Of course, the spontaneous fission and α-decay effects are additive.

An interesting application of the yield concept is to the question of initiating a nuclear explosion. This was accomplished by using a device placed within the core known as an *initiator*. According to Sublette (2007), this was an approximately golfball-sized sphere that contained polonium and beryllium, which were initially separated by a metal foil. Upon implosion or by being crushed by an incoming projectile piece of fissile material, the Po and Be mix; alphas from the Po then strike Be nuclei, liberating neutrons to initiate the detonation. Sublette records that the Manhattan Project initiators used 50 *Ci* of polonium. This is equivalent to a mass of about 11 mg, and a rate of α emission of $1.85 \times 10^{12} \, \text{s}^{-1}$. If we suppose a yield of 10^{-4}, this corresponds to some 185 neutrons during the critical ~1 μs of assembly time. Re-running the time-dependent simulation of a *Little Boy* 64-kg ^{235}U core plus 310-kg tamper described in Sect. 2.3 with the initial number of neutrons equal to 200 gives a yield of 13.8 kt, a quite reasonable result.

References

Bernstein, J.: Plutonium: A History of the World's Most Dangerous Element. Joseph Henry Press, Washington (2007)

Bernstein, J.: Nuclear Weapons: What You Need to Know. Cambridge University Press, New York (2008)

DOE: Historic American Engineering Record: B Reactor (105-B Building), HAER No. WA-164. See particularly p. 72. Available at http://www.cfo.doe.gov/me70/history/NPSweb/DOE-RL-2001-16.pdf (2001)

Evans, R.D.: The Atomic Nucleus. McGraw-Hill, New York (1955)

Fermi, E.: Nuclear Physics. University of Chicago Press, Chicago (1949)

Hoddeson, L., Henriksen, P.W., Meade, R.A., Westfall, C.: Critical Assembly: A Technical History of Los Alamos during the Oppenheimer Years, 1943–1945. Cambridge University Press, Cambridge, UK (1993)

Holden, N.E., Hoffman, D.C.: Spontaneous fission half-lives for ground-state nuclides. Pure Appl. Chem. **72**(8), 1525–1562 (2000)

Hull, M., Bianco, A.: Rider of the Pale Horse: A Memoir of Los Alamos and Beyond. University of New Mexico Press, Albuquerque (2005)

Hyde, E.K.: The Nuclear Properties of the Heavy Elements III. Fission Phenomena. Prentice-Hall, Englewood Cliffs, NJ (1964)

Mark, J.C.: Explosive properties of reactor-grade plutonium. Sci. Glob. Secur. **4**(1), 111–128 (1993)

Reed, B. C.: Predetonation probability of a fission-bomb core. Am. J. Phys. **78**(8), 804–808 (2010)

Serber, R.: The Los Alamos Primer: The First Lectures on How to Build an Atomic Bomb. University of California Press, Berkeley (1992)

Sublette, C.: Nuclear Weapons Frequently Asked Questions. http://nuclearweaponarchive.org/Nwfaq/Nfaq8.html (2007)

West, D., Sherwood, A.C.: Measurements of thick target (α, n) yields from light elements. Ann. Nucl. Energ. **9**, 551–577 (1982)

This page intentionally left blank

Chapter 5
Miscellaneous Calculations

Abstract This chapter explores a few interesting miscellaneous issues: Would the core of a nuclear weapon actually feel warm to the touch? How bright did the 1945 *Trinity* test appear to the naked eye? Could it have been seen from the Moon? How can one estimate the production in a reactor of trace elements that are of such concern in predetonation issues?

In this final chapter we take up some miscellaneous but interesting issues associated with fission weapons. One often reads that a bomb core is warm to the touch, and in Sect. 5.1 we investigate this claim. Section 5.2 quantifies just how bright a nuclear explosion appears to the naked eye. Finally, Sect. 5.3 develops a numerical simulation for estimating the production of trace isotopes such as ^{240}Pu in a reactor.

5.1 How Warm is It?

Would a lump of plutonium feel warm to the touch? ^{239}Pu is an alpha emitter with a half-life of 24,110 years. As seen in the preceding section, this corresponds to some 2.3×10^{12} alpha-decays per second per kilogram of material. With alphas of energy 5.2 MeV, the power generated by alpha-decay in a 1-kg mass of ^{239}Pu amounts to $P \sim 1.912$ W!

We can make a crude estimate of how much hotter the surface of such a mass would be than the surrounding air by assuming that this power is radiated away in accordance with the Stefan–Boltzmann law. If the material is considered to act like a blackbody, then the power radiated is given by

$$P = A\,\sigma\left(T_{sphere}^4 - T_{ambient}^4\right), \tag{5.1}$$

where A is the surface area of the mass and σ is the Stefan–Boltzmann constant, 5.67×10^{-8} W/(m^{2}K^4). For a 6.2-kg *Trinity/Fat Man* core, these numbers

correspond to a power output of 11.85 W. If spherical, this mass would have a radius of 4.56 cm and a surface area of 2.61×10^{-2} m². For an ambient temperature of 20°C (293 K), these numbers correspond to an equilibrium temperature $T_{sphere} \sim 79$°C, warm indeed. Some of the heat generated would also be lost by convection to the outside air and so this result is likely an overestimate, but the claim of warmth is certainly credible.

5.2   Brightness of the *Trinity* Explosion

Much of the analysis presented in this section is adopted from a publication elsewhere by the author (Reed 2006).

Nuclear weapons release fantastic amounts of energy, only a small fraction of which is initially in the form of visible light. However, they rapidly ionize and heat the surrounding air to incandescence, creating extremely bright fireballs. Rhodes (1986, p. 672) remarks of the July 16, 1945, *Trinity* test that "Had astronomers been watching they could have seen it reflected from the moon, literal moonshine," an allusion to Ernest Rutherford's famous dismissal of the prospect of atomic energy. Investigating this impressive claim makes for an informative exercise in the physics of astronomical magnitudes and prompts other intriguing questions: Just how bright would the explosion have appeared to an observer on the Moon? What about an observer on Mars or otherwise located in the solar system? What fraction of the bomb's yield was in the form of visible light?

These questions can be addressed with the help of information published in a report on the *Trinity* test prepared by the test's director, Kenneth Bainbridge. His report, titled *Trinity*, was prepared soon after the test as Los Alamos report LA-1012. In 1976, a public version of this report was released as Los Alamos report LA-6300-H. This report is available from the History link of the Los Alamos National Laboratory website at http://www.lanl.gov/history/atomicbomb/trinity.shtml. On page 52 of this report appears a graph of the illumination created by the *Trinity* test in "Suns" equivalent as a function of time at a detector located 10,000 yd from the explosion. This is reproduced in Fig. 5.1. At $t = 10^{-4}$ s the illumination is approximately 80 Suns; it drops to about 0.1 Suns at $t \sim 0.04$ s, rises back to about 2 Suns at $t = 0.4$ s and then declines to about 0.4 Suns as $t \sim 10$ s.

In working the following analysis, it must be remembered that many *Trinity* diagnostic experiments were overwhelmed by the explosion and so yielded only approximate results; the following calculations should be regarded as "back-of-the-envelope" estimates at best. I interpret "Suns" of illumination to mean multiples of the solar constant, that is, the flux of solar energy at the Earth, about 1,400 W/m².

To determine the brightness of the *Trinity* explosion as it would have been seen from various vantage points, it is most convenient to work with its equivalent astronomical magnitude. For readers not familiar with the magnitude scale, details can be found in any good college-level astronomy textbook; the relevant relationships are briefly summarized here without extensive derivation.

Fig. 5.1 Brightness of the *Trinity* explosion as a function of time. Scales are logarithmic. The quality of the curve is somewhat erratic as this graph was produced by scanning a copy of Fig. 7 of Los Alamos report LA-6300; the original version contains numerous grid lines which have not been reproduced to avoid cluttering the diagram
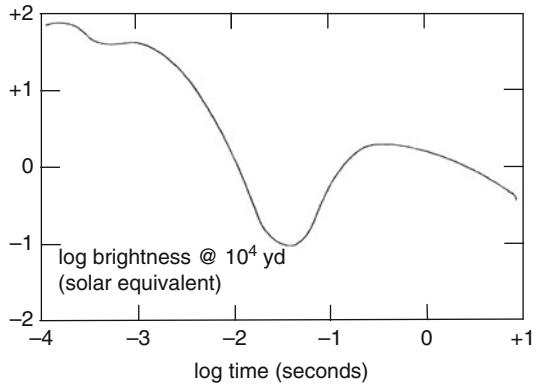
For various historical, physical, and physiological reasons, the scale of astronomical magnitudes is defined in terms of the common logarithm of the measured brightnesses of stars. The apparent magnitude m of a star is defined in terms of its measured brightness b (its energy flux in W/m^2) such that the difference between the apparent magnitudes of two stars A and B is given by

$$m_A - m_B = 2.5 \log(b_B/b_A). \tag{5.2}$$

In practice, this relationship is applied to a given star by measuring its brightness in comparison to that of a "standard" star of arbitrarily-assigned apparent magnitude; historically, the star Vega was taken to define $m = 0$.

The absolute magnitude M of a star is defined in analogy to (5.2) but with the measured brightnesses replaced by the true energy outputs (in Watts) of the stars. In astronomical parlance, energy outputs are known as luminosities and are traditionally designated by the symbol L:

$$M_A - M_B = 2.5 \log(L_B/L_A). \tag{5.3}$$

The apparent and absolute magnitudes of a star are related via its distance; the inverse-square law of light leads to the relationship

$$m - M = 5 \log(d_{pc}) - 5, \tag{5.4}$$

where d_{pc} designates the distance of the star in parsecs (pc). The apparent and absolute magnitudes for a star at a distance of 10 pc will by definition be equal. One parsec is defined as the distance a star must be from the Sun in order that it has a parallax of one second of arc when viewed from a baseline equal in length to the Earth's orbital radius of one Astronomical Unit (AU); 1 pc = 206,265 AU = 3.086 $\times 10^{16}$ m. One parsec is equivalent to about 3.26 light-years. The star nearest the Sun, Proxima Centauri, is about 4.2 light-years distant.

Equations (5.2)–(5.4) reflect the historical definition of astronomical magnitude as originally developed by Hipparchus in about the second century BC, who defined the brightest stars visible to the naked eye to have $m = +1$ and the faintest as having $m = +6$. Numerically *lower* magnitudes are associated with *brighter* objects. Sirius has $m \sim -1.4$, whereas Venus, at its brightest, appears at $m \sim -4.5$. The full moon has $m \sim -12.7$ and the Sun $m \sim -27$.

We now apply these concepts to the *Trinity* (*TR*) explosion by comparing it to the Sun (*S*). From (5.3), the absolute magnitudes of these two sources of illumination are related to their luminosities according as

$$M_{TR} = M_S + 2.5 \log(L_S/L_{TR}). \tag{5.5}$$

Now, let N represent the equivalent number of Suns of *Trinity* illumination incident at some moment on a detector at a distance of 10,000 yd from the explosion (as Fig. 5.1). Define the solar constant to be C. For a spherically symmetric explosion, *Trinity's* total power (in Watts) will be $L_{TR} = 4\pi r^2 CN$ where r designates 10,000 yd. Hence

$$M_{TR} = M_S + 2.5 \log(L_S/4\pi r^2 CN). \tag{5.6}$$

The measured absolute magnitude and luminosity of the Sun are $+4.82$ and 3.83×10^{26} W, respectively. (Strictly, these numbers apply for light emitted in the visible part of the electromagnetic spectrum). Putting $C = 1,400$ W/m^2 and $r = 10,000$ yd $= 9,144$ m, (5.6) gives

$$M_{TR} = 40.86 - 2.5 \log(N). \tag{5.7}$$

By combining (5.4) and (5.7), we can derive an expression for the apparent magnitude of *Trinity* as viewed from distance d_{pc} parsecs:

$$m_{TR} = 35.86 + 5 \log(d_{pc}) - 2.5 \log(N). \tag{5.8}$$

For practical purposes, solar-system distances are more conveniently measured in AUs: $d_{pc} = d_{AU}/206{,}265$. With this conversion, (5.8) becomes

$$m_{TR} = 9.29 + 5 \log(d_{pc}) - 2.5 \log(N). \tag{5.9}$$

We are now ready to compute *Trinity* apparent magnitudes. Consider first an observer located on the Moon, with $d = 384{,}400$ km $= 2.57 \times 10^{-3}$ AU. With $N = 80$, we find $m_{TR} = -8.4$. Neglecting any effects due to atmospheric absorption and cloud cover, *Trinity* would momentarily have appeared *over 30 times brighter than Venus* to an observer located on the Moon; apply (5.2) in the sense of comparing the brightnesses of the two. Not until the fireball cooled to $N \sim 2.2$

a few tenths of a second after the explosion would it have diminished to the brightness of Venus for our lunar observer, and, even after 10 s ($N \sim 0.4$, $m \sim -2.7$) would still have outshone Jupiter ($m \sim -2$). In actuality on the day of the *Trinity* test, the moon was at first-quarter phase and set about 1 AM New Mexico time, some four and one-half hours before the test.

Figure 5.2 shows curves of *Trinity* apparent magnitude as a function of distance in AUs for various values of N. At the time of the test, Mercury, Venus, and Mars were respectively 0.97, 0.88, and 1.65 AUs from the Earth. When $N = 80$, *Trinity* would have appeared brighter than $m = +6$ for observers residing on all three of these planets, although only Venus and Mars were actually above the horizon at the time.

Could astronomers actually have detected the light of *Trinity* as reflected from the Moon? The Moon is seen by reflected sunlight, so the key issue is how the flux of *Trinity* light on the Moon would have compared with that from the Sun. In his LA-6300 report, Bainbridge remarks that the total radiant energy density received at 10,000 yd was 12,000 J/m^2. If we presume that all of this light was emitted over 1 μs, such an energy density corresponds to a flux of 6.8 W/m^2 at the distance of the Moon. The solar flux at the Moon will be essentially same as that at the Earth, about 1,400 W/m^2, some 200 times greater. The idea of reflected *Trinity* light being visible from Earth is thus probably literary license.

Finally, we can estimate what fraction of *Trinity's* yield was in the form of visible light. Various estimates of the yield can be found in the literature; we use 15 kt TNT equivalent. Explosion of one ton of TNT liberates 4.2×10^9 J of energy; 15 kt would be equivalent to 6.3×10^{13} J. An energy density of 12,000 J/m^2 at 10,000 yd corresponds to a total energy of 1.26×10^{13} J if the energy of the explosion radiated uniformly in all directions, or approximately 20% of the total. In other words, some four-fifths of *Trinity's* energy release was in forms *in*visible to the human eye.

Fig. 5.2 Apparent magnitude of the Trinity explosion as a function of distance in Astronomical Units for times when the explosion was equivalent to 80, 20, 5, and 1 times the solar illumination for a detector located at 10,000 yd. Apparent magnitudes below the dashed line are visible to the naked eye. On this scale, the Moon would be located at the extreme left edge of the plot
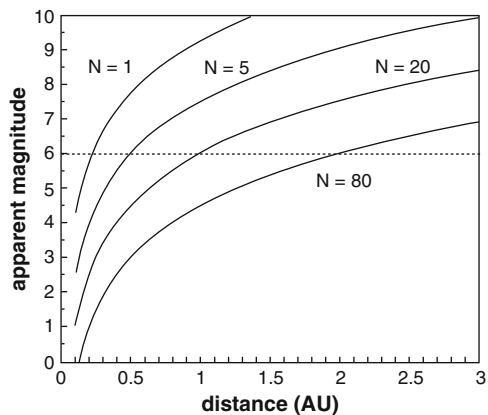
5.3   Model for Trace Isotope Production in a Reactor

In Sect. 3.3 we examined the production of Pu-239 in a reactor via calculations that involved only the isotopes U-235, U-238, and Pu-239; no account was taken of other isotopes that are produced along with the Pu-239. In Sect. 4.2, however, we saw that even a small amount of Pu-240 can lead to significant predetonation issues because of its high spontaneous fission rate. It was remarked in that section that formation of Pu-240 in a reactor is inevitable on account of neutron absorption by already-synthesized atoms of Pu-239. The purpose of this section is to develop a numerical simulation to approximately quantify the production rate of Pu-240.

The idea here is to simulate the time-evolution of the abundances of a few key isotopes in a reactor of given thermal power output and fuel load. Reactor engineering is an extremely complex discipline, so a number of simplifying assumptions have to be made for purposes of a pedagogical model. The simulation, **Reactor.xls**[1], can be found at the companion website.

In developing any reactor simulation the first issue to decide is that of what isotopes are to be tracked. Figure 5.3 shows the isotopes tracked and reactions considered in the present case. U-236 can be formed from neutron capture by U-235. U-236 has a small thermal neutron-capture cross-section of its own, but as this is only about 5 bn it is neglected; U-236 is assumed to simply accumulate as an end product. For simplicity, I assume that the creation of Pu-239 via neutron absorption by U-238 is an instantaneous process; no account is taken of the 23-min and 2.9-day beta-decay half lives of the intervening U-239 and Np-239 nuclei. This is a quite reasonable assumption since the model will typically be run for tens or hundreds of simulated days. The neutron capture cross sections for Pu-239, Pu-240, and Pu-241 are all fairly large, so these species are tracked; Pu-242 is assumed to accumulate like U-236. U-235, Pu-239, and Pu-241 all have appreciable fission cross-sections, so those processes must be tracked as well; of course, the vast majority of the energy generated comes from fission of U-235.

The simulation is predicated on a constant number of atoms within the reactor's fuel load, so I assume that when a nucleus fissions it gives rise to a single atom of "fission product." The simulation is actually programmed to track two fission products should the user desire. Since fission products can absorb neutrons, provision is made for assigning a neutron-capture cross section for the production of fission product "2" from fission product "1". The results discussed below assumed a zero-cross section for this process, but this can easily be changed by the user. In reality, most fission products have half-lives of but a few hours and so decay quickly.

I also assume that no fresh fuel is loaded into the reactor during the span of the simulation. (Many reactors can be refueled when on-line; the Hanford reactors had this capability.) Some smaller cross-sections, such as that for fission of U-238, are neglected, and no alpha or beta-decays are presumed to occur.

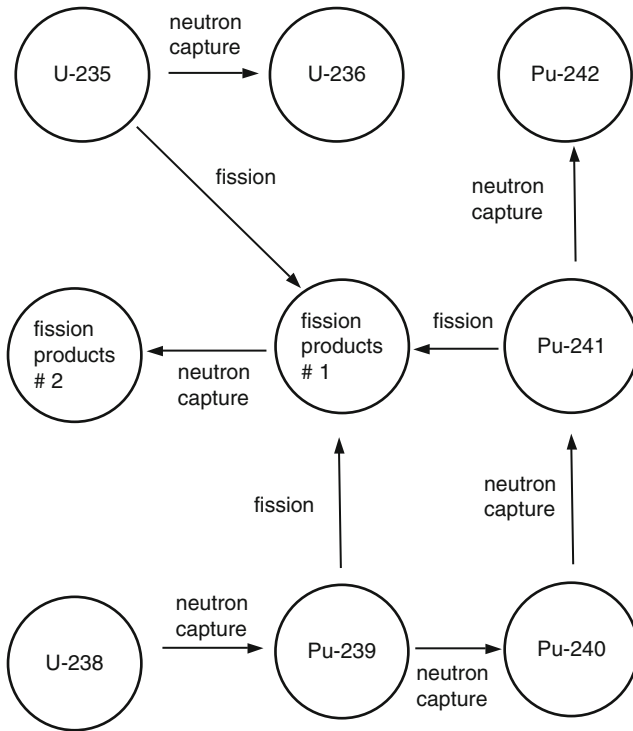[1]All Excel sheets are available at http://www.manhattanphysics.com

Fig. 5.3 Flowchart for species tracked in reactor simulation. The relevant cross-sections appear in Table 5.1

To formulate the simulation, we can begin with a result that was established in Sect. 3.3. From (3.18), if P is the *thermal* power generated by the reactor in megawatts and E_f is the average energy per fission in MeV, then the number of fissions *per day* is given by

$$\text{fissions/day} = R = \left[\frac{(86400)(10^6)P}{1.6022 \times 10^{-13}E_f} \right]. \tag{5.10}$$

The unit of time in the simulation is take to be 1 day, but the user can set the timestep Δt as desired. Over such a timestep, we will have

$$\text{fissions per } \Delta t \text{ days} = R\,\Delta t. \tag{5.11}$$

As in Sect. 3.3, let v be the number of neutrons released per fission. The number of neutrons released over time Δt will then be

$$\text{neutrons released per } \Delta t \text{ days} = v\,R\,\Delta t. \tag{5.12}$$

Fundamentally, the simulation operates by tracking the fractional abundances of isotopes as a function of time. For a given isotope i, let $F^i(t)$ be the fractional abundance of that isotope in the fuel at time t. (F is used here for fractional abundance as opposed to the f of Sect. 4.1, as that symbol is used here to represent fission.) If N is the total number of atoms of fuel loaded into the reactor, then the number of atoms of isotope i at time t will be $N^i(t) = N F^i(t)$.

Now consider some process p that a nucleus can suffer under neutron bombardment; this will be either fission (f) or absorption (a) of the neutron. No other processes are allowed to occur, and all free neutrons are assumed to either cause a fission or be absorbed during a given timestep. The total cross-section available for all processes over all isotopes at any time is given by the abundance-weighted sums of all individual-process cross-sections in play:

$$
\begin{aligned}
\sigma_{total}(t) &= \sum_{i,p} \sigma_p^i N^i(t) \\
&= N \left\{ F^{235}\left(\sigma_f^{235} + \sigma_a^{235}\right) + F^{238}\left(\sigma_a^{238}\right) + F^{239}\left(\sigma_f^{239} + \sigma_a^{239}\right) \right. \\
&\quad \left. + F^{240}\left(\sigma_a^{240}\right) + F^{241}\left(\sigma_f^{241} + \sigma_a^{241}\right) \right\}.
\end{aligned}
\tag{5.13}
$$

The total fission cross-section at any time will be

$$
\sigma_{fiss}(t) = N \left\{ F^{235}\left(\sigma_f^{235}\right) + F^{239}\left(\sigma_f^{239}\right) + F^{241}\left(\sigma_f^{241}\right) \right\}.
\tag{5.14}
$$

The probability of a neutron causing a subsequent fission will be $\sigma_{fiss}/\sigma_{total}$; the total number of atoms N will cancel when taking this ratio. The number of fissions that occur over Δt will then be the number of neutrons available over that interval times the probability of their causing fissions:

$$
\textit{fissions occurring over } \Delta t \textit{ days} = v R \Delta t \left(\frac{\sigma_{fiss}}{\sigma_{total}}\right).
\tag{5.15}
$$

Now, if the power output of the reactor is to remain steady, this number of fissions must just equal $R\Delta t$ of (5.11), which sets a constraint on v:

$$
v = \left(\frac{\sigma_{total}}{\sigma_{fiss}}\right).
\tag{5.16}
$$

Since the cross-sections will vary in time due to the varying abundance fractions, v will also vary; it has to be computed afresh at each timestep. A steadily-increasing v value is the price we pay for demanding a constant power output from a fuel load whose abundance of U-235 steadily decreases.

The next step is to find out how many atoms of isotope i undergo a given process during elapsed time Δt. If all neutrons are involved in some event over time Δt, then

the number of events that are of process type p with isotope i is given by the total number of events involved times the ratio of the total cross-section for that process with isotope i to the total available cross-section:

$$Events\,(i,\,p) = (v\,R\,\Delta t)\frac{\sigma_p^i\,N\,F^i(t)}{\sigma_{total}}. \tag{5.17}$$

We can now develop an expression for the change in the number of atoms of isotope i over time Δt; accumulation of fission products is dealt with separately as a special case below. Atoms of a given isotope can be created by neutron capture by a nucleus of *lower* weight if applicable, while simultaneously being lost due to fission and capturing neutrons themselves to produce isotopes of greater weight. The net change in the number of atoms of the isotope concerned will be the ratio of the aggregate cross-section for these effects to the total cross-section times the number of events $vR\Delta t$ that must be accounted for, that is,

$$N^i(t + \Delta t) = N^i(t) + \left(\frac{v\,R\,\Delta t}{\sigma_{total}}\right) N\left[F^{lower}\sigma_a^{lower} - F^i\sigma_f^i - F^i\sigma_a^i\right]. \tag{5.18}$$

The simulation actually tracks fractional abundances, that is, (5.18) divided by N. The factor of N in (5.18) thus disappears, but one factor of N still remains in σ_{total} as per (5.13). Because of this, we need to know the number of atoms in the fuel supply; I make the assumption that the fuel is all composed of U-238 initially. Given that the fuel in most reactors is enriched to only a few percent U-235, this will not be a drastic approximation.

What of the fission products? "Product 1" accumulates from fissions of the three fissile isotopes in the simulation, U-235, Pu-239 and Pu-241, but is lost according as its own abundance and capture cross-section for neutrons:

$$N^1(t + \Delta t) = N^1(t) + \left(\frac{v\,R\,\Delta t}{\sigma_{total}}\right) N\left[F^{235}\sigma_f^{235} + F^{239}\sigma_f^{239} + F^{241}\sigma_f^{241} - F^1\sigma_a^1\right]. \tag{5.19}$$

Similarly, product 2 accumulates from neutron capture by product 1; there is no loss mechanism for product 2:

$$N^2(t + \Delta t) = N^2(t) + \left(\frac{v\,R\,\Delta t}{\sigma_{total}}\right) N\left[F^1\sigma_a^1\right]. \tag{5.20}$$

To run the simulation, the user sets the cross-sections and initial abundance fractions at $t = 0$. Since the only isotopes present initially are presumed to be U-235 and U-238, the operator need only specify the initial fractional abundance of 235. The user also sets the power output P, the timestep Δt, and the total mass of fuel in kg. Initial values for the total and fission cross-sections and v are computed

from (5.13), (5.14), and (5.16). New fractional abundances for each isotope and the fission products at time $t + \Delta t$ are computed according as (5.18)–(5.20). The cross-sections and v are updated and the process iterated. Rows of the spreadsheet correspond to timesteps (250 altogether) and columns hold the abundances for the various isotopes. For practical purposes, it makes sense to run the simulation only to a time such that v remains less than the maximum value it could attain in reality, $v \sim 2.5$.

The simulation also tracks what is known to reactor engineers as the "burnup" or "fuel exposure" in megawatt-days per metric ton (MWd/MT). This is the cumulative amount of thermal energy produced by the reactor per metric ton of fuel. One metric ton is 1,000 kg, and a megawatt-day means literally one megawatt times 1 day: $(1.0 \times 10^6 \text{ J/s}) (86,400 \text{ s}) = 8.64 \times 10^{10}$ J. A burnup of 33,000 MWd/MT is characteristic of the spent fuel from commercial reactors (Mark 1993); this can also be quoted as 33 gigawatt-days per metric ton, or GWd/MT.

Relevant cross-sections are collected in Table 5.1.

We now apply this model to the Hanford reactors of the Manhattan Project. According to a Department of Energy publication (DOE 2001), these reactors consisted of 2004 "process tubes", each of which during normal operation contained 32 cylindrical slugs of natural uranium fuel ($^{235}F = 0.0072$, initially) measuring 1.44 in. in outside diameter by 8.7 in. long. At a density of 18.95 g/cm^3 this would correspond to just under 4.4 kg per slug, or a total fuel load of about 282,000 kg. I round this down to 275 MT for computational purposes as the slugs were jacketed in a layer of aluminum. The reactors operated at a thermal power output of 250 MW, and a given slug was irradiated for typically 100 days before being removed and processed.

Assuming 180 MeV per fission, the simulation shows that after 100 days a total of 18.57 kg of plutonium will have been produced, of which 99.66% is Pu-239 and 0.34% is Pu-240. This overall plutonium production rate agrees closely with that estimated in Sect. 3.3, 190 g/day. The burnup to 100 days is about 91 MWd/MT. The initial value of v is 1.801, and at 100 days is 1.807. The figure used for the Pu-240 abundance in the *Trinity* and *Fat Man* devices in Sect. 4.2 was 1.2%, but it must be remembered that the simulation developed here does not account for all processes going on within the reactor. If the *Fat Man* predetonation probability calculation of Sect. 4.2 is repeated for a 6.2 kg core containing 0.34% Pu-240 (0.0211 kg), the probability that the bomb will function correctly for a 100 μs

Table 5.1 Cross-sections for reactor simulation

Isotope	Fission	Absorption
^{235}U	585	99
^{236}U	0	0
^{238}U	0	2.68
^{239}Pu	750	271
^{240}Pu	0	290
^{241}Pu	1,010	361
^{242}Pu	0	0
Product 1	0	0

assembly time is only 44%; implosion would still required to achieve a sensibly high probability of avoiding predetonation. According to Mark (1993), the plutonium created in a modern commercial reactor that has generated a burnup of 33 GWd/MT will be 21% Pu-240.

References

DOE: Historic American Engineering Record: B Reactor (105-B Building), HAER No. WA-164. See particularly p. 34. Available at http://www.cfo.doe.gov/me70/history/NPSweb/DOE-RL-2001-16.pdf (2001)

Mark, J.C.: Explosive properties of reactor-grade plutonium. Sci. Global Secur. **4**(1), 111–128 (1993)

Reed, B.C.: Seeing the light: visibility of the July '45 trinity atomic bomb test from the inner solar system. Phys. Teach. **44**, 604–606 (2006)

Rhodes, R.: The Making of the Atomic Bomb. Simon and Schuster, New York (1986)

This page intentionally left blank

Chapter 6
Appendices

6.1 Appendix A: Selected Δ-Values and Fission Barriers

Δ-values for nuclides involved in every reaction in this book are listed below. These are adopted from Jagdish K. Tuli, *Nuclear Wallet Cards* (Brookhaven National Laboratory, April 2005.) The full publication is available at http://www.nndc.bnl.gov. Fission barriers quoted for selected heavy nuclides are taken from an online IAEA publication, http://www-nds.iaea.org/RIPL-2/fission/fis-barrier-exp.readme; the barrier values cited here are the larger of the "inner" and "outer" barriers listed in that document.

Nuclide	Δ (MeV)	Nuclide	Δ (MeV)	$E_{Barrier}$ (MeV)
$^{1}_{0}$n	8.071	$^{92}_{36}$Kr	−68.79	
$^{1}_{1}$H	7.289	$^{95}_{38}$Sr	−75.117	
$^{2}_{1}$H	13.136	$^{94}_{40}$Zr	−87.267	
$^{3}_{1}$H	14.950	$^{116}_{46}$Pd	−79.96	
$^{4}_{2}$He	2.425	$^{118}_{46}$Pd	−75.5	
$^{6}_{3}$Li	14.087	$^{139}_{54}$Xe	−75.64	
$^{7}_{3}$Li	14.908	$^{141}_{56}$Ba	−79.726	
$^{9}_{4}$Be	11.348	$^{150}_{66}$Dy	−69.317	
$^{10}_{5}$B	12.051	$^{206}_{82}$Pb	−23.785	
$^{12}_{6}$C	0.000	$^{208}_{82}$Pb	−21.749	
$^{13}_{6}$C	3.125	$^{210}_{84}$Po	−15.953	
$^{14}_{7}$N	2.863	$^{220}_{86}$Rn	10.613	
$^{16}_{8}$O	−4.737	$^{222}_{86}$Rn	16.374	
$^{17}_{8}$O	−0.809	$^{224}_{88}$Ra	18.827	
$^{17}_{9}$F	1.952	$^{226}_{88}$Ra	23.669	
$^{19}_{9}$F	−1.487	$^{231}_{91}$Pa	33.426	
$^{20}_{9}$F	−0.017	$^{232}_{91}$Pa	35.948	6.40
$^{20}_{10}$Ne	−7.042	$^{233}_{92}$U	36.920	5.55
$^{22}_{10}$Ne	−8.025	$^{235}_{92}$U	40.921	6.00
$^{26}_{10}$Ne	0.43	$^{236}_{92}$U	42.446	5.67
$^{25}_{12}$Mg	−13.193	$^{238}_{92}$U	47.309	6.30

(continued)

Nuclide	Δ (MeV)	Nuclide	Δ (MeV)	$E_{Barrier}$ (MeV)
$^{27}_{12}$Mg	-14.587	$^{239}_{92}$U	50.574	6.45
$^{27}_{13}$Al	-17.197	$^{237}_{93}$Np	44.873	6.00
$^{30}_{15}$P	-20.201	$^{239}_{93}$Np	49.312	
$^{31}_{15}$P	-24.441	$^{239}_{94}$Pu	48.590	6.20
$^{35}_{16}$S	-28.846	$^{240}_{94}$Pu	50.127	6.05
$^{56}_{26}$Fe	-60.605	$^{241}_{95}$Am	52.936	6.00
		$^{252}_{99}$Es	77.29	

6.2 Appendix B: Densities, Cross-Sections and Secondary Neutron Numbers

6.2.1 Thermal Neutrons (0.0253 eV)

Quantity	Unit	U-235	U-238	Pu-239
Density	g/cm^3	18.71	18.95	15.6
Atomic wt.	g/mol	235.04	238.05	239.05
$\sigma_{capture}$	bn	98.81	2.717	270.3
$\sigma_{fission}$	bn	584.4	0	747.4
$\sigma_{elastic\ scatter}$	bn	15.04	9.360	7.968
v	–	2.421	2.448	2.872

6.2.2 Fast Neutrons (2 MeV)

Quantity	Unit	U-235	U-238	Pu-239
Density	g/cm^3	18.71	18.95	15.6
$\sigma_{capture}$	bn	0.089	0.066	0.053
$\sigma_{fission}$	bn	1.235	0.308	1.800
$\sigma_{elastic\ scatter}$	bn	4.566	4.804	4.394
v	–	2.637	2.655	3.172

The density for ^{235}U is (235/238) that of natural uranium, 18.95 g/cm^3. Plutonium exhibits several different crystalline phases depending on temperature (Bernstein 2007, 2008); the so-called "delta" phase is the one used for weapons. The density figure for Pu is that for the delta-phase as quoted on page 144 of Bernstein (2008). The v value for U-238 for fission-energy neutrons is for neutrons of energy 2.9 MeV. Cross-sections are adopted from the Korean Atomic Energy Research Institute (KAERI) Table of Nuclides, http://atom.kaeri.re.kr/ton/index.htm. Cross-sections that are exceedingly small are recorded here as zero. For fast neutrons, cross-sections represent averaged values over the fission-energy spectrum. Secondary neutron numbers are adopted from ENDF files.

6.2.2.1   References

Bernstein, J.: Plutonium: A History of the World's Most Dangerous Element. Joseph Henry, Washington (2007)

Bernstein, J: Nuclear Weapons: What You Need to Know. Cambridge University Press, New York (2008)

6.3   Appendix C: Energy and Momentum Conservation in a Two-Body Collision

In many instances we have cause to examine reactions where an "incoming" nucleus strikes a second nucleus that is initially at rest, with two product nuclei emerging from the reaction. An example of this is the reaction used by Rutherford to first induce an artificial transmutation,

$$\,^{4}_{2}\mathrm{He}\ +\ ^{14}_{7}\mathrm{N}\ \rightarrow\ ^{1}_{1}\mathrm{H}\ +\ ^{17}_{8}\mathrm{O}.$$
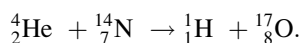
We are usually interested in the final kinetic energy and/or momentum of one of the product nuclei. (Often, the other product may remain stuck in the bombarded sample and so not easily studied.) In this section we develop formulae for these quantities, assuming that we have a head-on collision.

Figure 6.1 illustrates the situation. Let the *rest masses* of the nuclei be m_A, m_B, m_C, and m_D. Nucleus A is presumed to bring kinetic energy K_A into the reaction; the struck nucleus, B, is assumed to be at rest when struck. Products C and D emerge from the reaction with kinetic energies K_C and K_D. If no transmutation is involved we can set $C = A$ and $D = B$. We assume that it is desired to know the final kinetic energies and momenta of nuclei C and D.

Begin with energy conservation. From the definition of Q in Sect. 1.1 we can write energy conservation for our reaction as

$$K_A = K_C + K_D - Q, \tag{6.1}$$

where

$$Q = E_A + E_B - E_C - E_D, \tag{6.2}$$

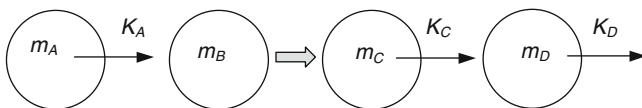and where the E's are the mc^2 rest energies of the various nuclei.

Fig. 6.1   Head-on collision of two nuclei producing two other nuclei

As for momentum conservation, any reaction we will have cause to examine will be such that none of the momenta are relativistic. This allows us to deal with momentum from a purely classical perspective, which greatly simplifies the algebra. In Newtonian mechanics the momentum p of a mass m which is moving with kinetic energy K is given by $p = \sqrt{2mK} = \sqrt{2EK}/c$, so we have, upon canceling factors of 2 and c,

$$\sqrt{E_A K_A} = \pm\sqrt{E_C K_C} + \sqrt{E_D K_D}. \qquad (6.3)$$

A $\pm$ sign has been put in front of the momentum for nucleus C as a reminder that it may be moving forward or backward after the collision; the direction of C will emerge automatically from the numbers. We assume that nucleus D is moving forward after the reaction.

The goal here is to solve (6.1) and (6.3) for K_D in terms of the known quantities K_A, E_A, E_B, E_C, E_D and Q. We need to eliminate K_C. To do this, first isolate the $\pm\sqrt{E_C K_C}$ term from (6.3) and then square the result, which will cause the $\pm$ sign to disappear. Then solve (6.1) for K_C and substitute into the result of manipulating (6.3). The result is a quadratic in $\sqrt{K_D}$:

$$\alpha K_D + \beta\sqrt{K_D} + \gamma = 0, \qquad (6.4)$$

where

$$\alpha = (E_C + E_D), \qquad (6.5)$$

$$\beta = -2\sqrt{E_A E_D\, K_A}, \qquad (6.6)$$

and

$$\gamma = (E_A K_A - E_C K_A - E_C\, Q). \qquad (6.7)$$

Solving the quadratic gives

$$\sqrt{K_D} = \frac{-\beta \pm \sqrt{\beta^2 - 4\alpha\gamma}}{2\alpha}. \qquad (6.8)$$

There are two possible solutions for K_D (provided that $\beta^2 - 4\alpha\gamma > 0$; see below), either or both of which may be valid. Their validities can be checked after the fact by computing K_C in two separate ways and checking for consistency: (i) from (6.1), and (ii) from conservation of momentum by first computing $p_D = \sqrt{2m_D K_D} = \sqrt{2E_D K_D}/c$, demanding $p_C = p_A - p_D$, and then evaluating $K_C = \left(p_C^2/2E_C\right)c^2$. (Recall that we are assuming that D is always moving forward after the reaction.)

It can be seen from (6.8) that a real solution for K_D will obtain only when $\beta^2 - 4\alpha\gamma > 0$. From (6.5)–(6.7), this demand reduces to

$$0 > K_A(E_A - E_C - E_D) - Q\,(E_C + E_D). \qquad (6.9)$$

Table 6.1 Rutherford alpha-bombardment reaction parameters

Reactant	Nuclide	A	Δ	Rest mass (MeV/c²)
A	$_2^4\mathrm{He}$	4	2.425	3728.401
B	$_7^{14}\mathrm{N}$	14	2.863	13043.779
C	$_8^{17}\mathrm{O}$	17	−0.809	15834.589
D	$_1^1\mathrm{H}$	1	7.289	938.783

Now, $(E_A - E_C - E_D)$ is likely to be less than zero, so let us write (6.9) as

$$0 > - K_A |E_A - E_C - E_D| - Q(E_C + E_D). \tag{6.10}$$

Consider (6.10) in two separate cases: (i) $Q > 0$ and (ii) $Q < 0$. If $Q > 0$ we can write $Q = +|Q|$, and (6.10) reduces to

$$|Q|(E_C + E_D) > - K_A |E_A - E_C - E_D|, \tag{6.11}$$

which is always true. This means that in cases where $Q > 0$ there is no constraint on K_A. On the other hand, if $Q < 0$, write $Q = -|Q|$, in which case we have

$$0 > - K_A |E_A - E_C - E_D| + |Q|(E_C + E_D), \tag{6.12}$$

which demands

$$K_A > \frac{|Q|(E_C + E_D)}{|E_A - E_C - E_D|}. \qquad (Q < 0) \tag{6.13}$$

This expression means that there is a *threshold* energy for K_A in cases where $Q < 0$.

We now apply this analysis to the Rutherford transmutation reaction. Identify A, B, C, and D as He, N, O, and H, respectively. The relevant numbers appear in Table 6.1. This reaction has a Q-value of -1.192 MeV. A conversion factor of $\varepsilon = 931.494$ MeV/amu was used to compute rest masses in MeV/c² via the relationship rest mass $= \varepsilon A + \Delta$.

Suppose that the alpha particle enters the reaction with $K_A = 5$ MeV. Then we find

$$\alpha = (E_C + E_D) = 16773.37 \qquad \text{(MeV)},$$

$$\beta = -2\sqrt{E_A E_D K_A} = -8366.79 \qquad \text{(MeV)}^{3/2},$$

and

$$\gamma = (E_A K_A - E_C K_A - E_C Q) = -41656.11 \qquad \text{(MeV)}^2.$$

The two solutions for K_D give 3.404 and 1.812 MeV, but only the first of these proves to be valid. The corresponding momentum of the proton is

$$p = \frac{\sqrt{2E_D K_D}}{c} = \frac{1}{c}\sqrt{2\,(938.783\ \text{MeV})\,(3.404\ \text{MeV})} = 79.94\,\frac{\text{MeV}}{c}.$$

The oxygen nucleus emerges from the reaction with kinetic energy $K_C = 0.404$ MeV and momentum 113.15 MeV/c.

Equation (6.13) gives a threshold energy of $K_A > 1.533$ MeV. This is larger than the 1.192 MeV one might expect on the basis of the Q-value alone. This is because *both* momentum and energy must be conserved; were nucleus A to strike nucleus B with only 1.192 MeV of kinetic energy, nuclei C and D would emerge form the reaction with no kinetic energy and hence no momentum, a situation inconsistent with A bringing momentum into the reaction in the first place.

These calculations are carried out in the spreadsheet **TwoBody.xls**.[1]

6.4 Appendix D: Energy and Momentum Conservation in a Two-Body Collision that Produces a Gamma-Ray

In Sect. 1.4, the Joliot–Curies' proposed gamma-producing reaction

$$_{2}^{4}\text{He} + {_{4}^{9}\text{Be}} \rightarrow {_{6}^{13}\text{C}} + \gamma \tag{6.14}$$
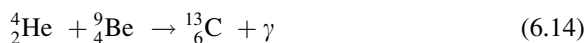
arose. The alpha-particle carries ~5.3 MeV of kinetic energy into the reaction and bombards the initially stationary Be nucleus. The quantities of interest in this reaction are the energy and momentum of the emergent gamma-ray. In this section we develop formulae for these quantities, assuming that the collision is head on and that the Be nucleus is initially stationary.

Figure 6.2 illustrates the situation. Let the *rest masses* of the three nuclei be m_A, m_B, and m_C. Nucleus A is presumed to bring kinetic energy K_A into the reaction. Product C emerges from the reaction with kinetic energy K_C and the gamma-ray with energy E_γ. (We do not refer to E_γ as a kinetic energy as that term is usually reserved for the motional energy of a particle of non-zero rest mass.)

Begin with energy conservation, accounting for the kinetic energies of the reactants as well as their relativistic rest energies:

$$K_A + (m_A + m_B)\,c^2 = K_C + m_C c^2 + E_\gamma. \tag{6.15}$$
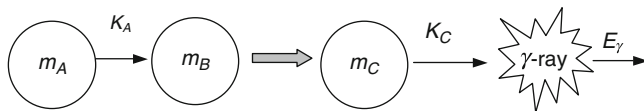

Fig. 6.2 Head-on collision of two massive particles leading to production of a massive particle and a gamma-ray

[1]All Excel sheets are available at http://www.manhattanphysics.com

For momentum conservation we take the Newtonian momentum $p = \sqrt{2mK}$ for the particles with mass, and, from Einstein, $p = E/c$ for the gamma-ray, giving

$$\sqrt{2m_A K_A} = \pm\sqrt{2m_C K_C} + E_\gamma/c, \qquad (6.16)$$

where the upper (lower) sign is to be taken if nuclide C is moving to the right (left) after being produced; we assume that the gamma-ray is moving forward after the reaction. The direction of C after the reaction is dictated by energy and momentum conservation. Let the rest energies mc^2 of the particles with mass be designated by E's, e.g, $E_A = m_A c^2$. If we replace the masses in (6.16) by these rest energies, a factor of c can be canceled, leaving

$$\sqrt{2E_A K_A} = \pm\sqrt{2E_C K_C} + E_\gamma. \qquad (6.17)$$

We desire to eliminate K_C between (6.15) and (6.17). Rearrange (6.17) to isolate the $\sqrt{2E_C K_C}$ term, square, and then solve for K_C. The $\pm$ sign vanishes and we get

$$K_C = \left(\frac{E_A}{E_C}\right) K_A - \frac{\sqrt{2E_A K_A}\, E_\gamma}{E_C} + \frac{E_\gamma^2}{2E_C}. \qquad (6.18)$$

Now rearrange (6.15) to the form

$$K_C = E_A + E_B + K_A - E_C - E_\gamma. \qquad (6.19)$$

Substitute (6.19) into (6.18) and rearrange; the result is a quadratic equation in E_γ:

$$\alpha E_\gamma^2 + \varepsilon E_\gamma + \delta = 0, \qquad (6.20)$$

where

$$\alpha = \frac{1}{2E_C}, \qquad (6.21)$$

$$\varepsilon = 1 - \frac{\sqrt{2E_A K_A}}{E_C}, \qquad (6.22)$$

and

$$\delta = \left(\frac{E_A}{E_C}\right) K_A - (E_A + E_B + K_A - E_C). \qquad (6.23)$$

Hence

$$E_\gamma = \frac{-\varepsilon \pm \sqrt{\varepsilon^2 - 4\alpha\delta}}{2\alpha}. \qquad (6.24)$$

There are two possible solutions for E_γ; often, one of these will be unphysical in that it leads to a negative value for K_C from (6.19).

These calculations are done in the spreadsheet **TwoBodyGamma.xls**.

6.5   Appendix E: Formal Derivation of the Bohr–Wheeler Spontaneous Fission Limit

6.5.1   E1: Introduction

Material in this section is adopted from a publication elsewhere by the author (Reed 2009).

In Sects. 1.7 and 1.10 we used a simplified model of a fissioning nucleus to get a sense of how the limit against spontaneous fission (SF), $Z^2/A = 2a_S/a_C \sim 48$ arises (Bohr and Wheeler 1939). Given the historic significance of this result, a formal derivation of it is justified, and is presented here.

Curiously, few texts actually present a full derivation of this work. Some offer partial treatments based on starting from "it-can-be-shown-that" expressions for the area and self-energy of an ellipsoid of variable eccentricity (see, for example, Cottingham and Greenwood 2001), a derivation of which from first principles appears in Bernstein and Pollock (1979). However, the ellipsoidal model does not really reflect the approach taken by B&W, who used a sum of Legendre polynomials to describe the shape of the surface of a nucleus as it distorts. To be sure, if the SF limit is a matter of instability against slight distortions then it should be irrelevant how the distortion is modeled, but it seems unfortunate that pedagogical tendency has shifted away from the "true" historical approach.

This situation is no doubt due to the fact that some of the mathematics of the B&W analysis *is* tricky, even if one is facile with multivariable calculus and properties of Legendre polynomials. B&W published virtually none of the algebraic details of their work, which they referred to as a "straightforward calculation." Present and Knipp (1940a, b) pointed out that that there is an internal inconsistency in B&W and that they changed the definition of some of their surface-distortion parameters part-way through their derivation. In a paper that now seems all but forgotten, Plesset (1941) reconstructed the details of the B&W derivation, but his work is difficult to follow in view of some tangled notation and the fact that he carried through his algebra to higher orders of perturbation than are necessary to understand the SF limit.

In reconstructing the B&W derivation, one faces the question of what level of detail to present. To lay out every step of the algebra would result in a manuscript that is far too lengthy for sensible publication. Conversely, the danger of brevity is that subtle but important points can get overlooked. Here I try to tread a middle path by setting down benchmark steps in the calculations between which most readers should be able fill in the intervening gaps. A supporting document with all of the

algebraic details is available online at the companion website for this book. No treatment is given here of the much more complex question of the fission *barrier*, which requires carrying the algebra to higher orders of perturbation.

This derivation is rather lengthy. In Sect. E2, the Legendre-polynomial model of a distorted nucleus is described, and the calculation of the volume of the nucleus is carried out. The surface area energy is calculated in Sect. E3. Section E4 deals with the lengthy and somewhat tricky calculation of the Coulomb self-energy of the nucleus, which, when combined with the results of the preceding sections, leads to understanding how the SF limit arises.

6.5.2 E2: Nuclear Surface Profile and Volume

Bohr and Wheeler began by imagining an initially spherical nucleus of radius R_O undergoing a distortion expressible as a sum of Legendre polynomials:

$$r(\theta) = R_O\{1 + \alpha_0 + \alpha_2 P_2(\cos\theta) + ...\}, \tag{6.25}$$

where $P_2(cos\ \theta)$ is the second-order Legendre polynomial, $P_2(cos\ \theta) = (3\ cos^2\theta - 1)/2$. θ is the polar angle in the usual spherical coordinate system. Such a perturbation, greatly exaggerated, is sketched schematically in Fig. 6.3, where the nucleus has been perturbed into a dumbbell shape along the polar axis.
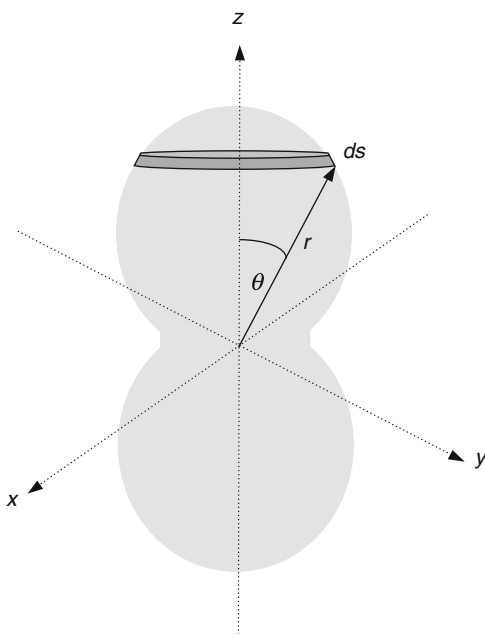
Fig. 6.3 The surface of a distorted nucleus is described by the function $r(\theta)$ of (6.25). A ribbon of surface of edge length ds and area $dA = 2\pi r \sin\theta\,ds$ at colatitude θ is shown

The perturbation coefficients α_0 and α_2 are presumed to be small; using only two coefficients is enough to derive the SF limit. Coefficient α_2 dictates the non-spherical shape of the nucleus; α_0 is necessary to be able to ensure volume conservation as the distortion occurs. It is conventional to consider α_2 as the "independent" coefficient, and ultimately express both the area and Coulomb energies as functions of it alone. The essence of the Bohr–Wheeler calculation is to compare the total energy of the deformed nucleus ($\alpha_2 \neq 0$) to that which it had in its initial spherical condition ($\alpha_0 = \alpha_2 = 0$), and then determining what circumstance must hold so that *any* perturbation, no matter how slight, will lead yield a lower-energy configuration. The lowest-order contributions to these energies both prove to be of order α_2^2, so it is not necessary to carry through terms to any higher orders than that. Some texts do not emphasize that the volume of the nucleus is assumed to be conserved, that is, that nuclei are considered to be incompressible.

Note that there is no "first-order" term $\alpha_1 P_1$ in (6.25). The reason for this is sometimes stated as being that such a term (or, indeed, any odd-parity perturbation) creates only a displacement of the center of mass of the nucleus along the z-axis, but this is not quite true: such a term would introduce a distortion of the shape of the nucleus, rendering it somewhat flattened at the "south pole" ($\theta = \pi$). Incorporating only even-order Legendre polynomials simplifies the situation to having a nucleus whose centre of mass remains at the coordinate origin and which is symmetric about the xy plane. Because $r(\theta)$ contains no dependence on the azimuthal angle ϕ, the nucleus remains axially symmetric about the polar axis. The sign of α_2 dictates the nature of the distortion. If $\alpha_2 > 0$, the nucleus becomes squeezed at the equator and elongated at the poles, as suggested in Fig. 6.3; $\alpha_2 < 0$ produces the opposite effect, rendering the nucleus somewhat doughnut-shaped in the equatorial plane.

At this point, one might well ask: "Why Legendre polynomials?" The surface of the nucleus could presumably be described by any arbitrarily-chosen function of the spherical coordinates (θ, ϕ), subject only to the condition that it contains enough parameters to be able to ensure volume conservation. The value of Legendre polynomials, and particularly of the Associated Legendre polynomials and spherical harmonics built up from them, is that they constitute an orthogonal set of functions over (θ, ϕ) with a particularly simple orthogonality relationship, namely (6.28) below. Consequently, they form a natural family of functions for describing perturbations from circularity or sphericity.

The first task is to ensure conservation of volume. The volume of the distorted nucleus is given by

$$V = \int\limits_{\theta=0}^{\pi} \int\limits_{r=0}^{r(\theta)} \int\limits_{\phi=0}^{2\pi} r^2 \sin\theta \, d\phi \, dr \, d\theta \qquad (6.26)$$

Note carefully here the order of integrations over r and θ. Because the upper limit of r is a function of θ, the integral over r must be done first, then that over θ. The integral over ϕ gives 2π directly. Hence we have

$$V = \frac{2\pi}{3} \int\limits_{\theta=0}^{\pi} r^3(\theta) \, \sin\theta \, d\theta. \tag{6.27}$$

Be sure to understand the distinction between the integrands in (6.26) and (6.27): in the former, r is a variable whose limits are 0 and $r(\theta)$; the $r^3(\theta)$ in (6.37) means a function of θ given by the cube of (6.25).

The B&W calculation involves numerous integrals of the form of (6.27), with different powers of $r(\theta)$ and sometimes other functions of θ in the integrand. It is convenient to make a change of variable $x = cos\theta$, which renders $sin\theta \, d\theta$ as $-dx$, with limits $x = (1, -1)$. The limits can be flipped, with the result that the negative sign in $-dx$ can be dropped. In terms of this new variable, the orthonormalization relation for Legendre polynomials,

$$\int\limits_{-1}^{1} P_i P_j \, dx = \frac{2\,\delta_i^j}{i+j+1}, \tag{6.28}$$

is also extremely valuable.

The evaluation of the volume integral is described briefly here; most other integrals are left to the reader as exercises. Transforming to x and substituting (6.25) into (6.27) gives

$$V = \left(\frac{2\,\pi R_O^3}{3}\right) \int\limits_{-1}^{1} [1 + \alpha_0 + \alpha_2 P_2]^3 \, dx. \tag{6.29}$$

Treating the square bracket as $(1 + \alpha_0) + \alpha_2 P_2$ and cubing gives

$$V = \left(\frac{2\,\pi R_O^3}{3}\right) \left\{ (1 + \alpha_0)^3 \int\limits_{-1}^{1} dx + 3\,(1 + \alpha_0)^2 \alpha_2 \int\limits_{-1}^{1} P_2 \, dx \right.$$

$$\left. + 3\,(1 + \alpha_0)\alpha_2^2 \int\limits_{-1}^{1} P_2^2 dx + \alpha_2^3 \int\limits_{-1}^{1} P_2^3 dx \right\}. \tag{6.30}$$

The first integral gives 2, the second vanishes by (6.28) (why?), the third gives 2/5 by (6.28), and the last is dropped as I retain terms only to order α_2^2. The volume integral thus evaluates as

$$V = \left(\frac{4\,\pi R_O^3}{3}\right) \left\{ (1 + \alpha_0)^3 + \frac{3}{5}\,(1 + \alpha_0)\,\alpha_2^2 + ... \right\}. \tag{6.31}$$

If volume is to be conserved, then the contents of the brace bracket in (6.31) must equal unity. If α_0 and α_2 are presumed small, then the $\alpha_0 \alpha_2^2$ and α_0^3 terms can be dropped; what remains is a quadratic equation in α_0 whose solution is

$$\alpha_0 \sim -\frac{1}{5}\alpha_2^2. \tag{6.32}$$

This result will prove valuable in computing the area and Coulomb energies.

6.5.3   E3: The Area Integral

Figure 6.3 shows a "ribbon" of surface area at co-latitude θ and angular width $d\theta$ that goes all the way around the nucleus. The area of the ribbon will be its arc length times its circumference, which is $r \, sin\theta$. But the deformed nucleus does not have a spherical profile, so the arc length is not simply $r \, d\theta$. Rather, we have to compute it by using the general expression for arc-length in spherical coordinates for a trajectory running along a line of constant "longitude" ϕ:

$$ds^2 = dr^2 + r^2 d\theta^2. \tag{6.33}$$

Since r is a function of θ, we can write this as

$$ds^2 = dr^2 + r^2 d\theta^2 = r^2 d\theta^2 \left[1 + \frac{1}{r^2}\left(\frac{dr}{d\theta}\right)^2 \right]. \tag{6.34}$$

The area of the ribbon is then

$$dA = 2\pi r \sin\theta \, ds = 2\pi r^2 \sin\theta \sqrt{1 + \frac{1}{r^2}\left(\frac{dr}{d\theta}\right)^2} \, d\theta. \tag{6.35}$$

If the nucleus is not greatly distorted, then $dr/d\theta$ will be small. We can then invoke a binomial expansion,

$$\sqrt{1 + \frac{1}{r^2}\left(\frac{dr}{d\theta}\right)^2} \sim 1 + \frac{1}{2}\frac{1}{r^2}\left(\frac{dr}{d\theta}\right)^2 - \frac{1}{8}\frac{1}{r^4}\left(\frac{dr}{d\theta}\right)^4 + ... \tag{6.36}$$

From (6.25), $(dr/d\theta) = \alpha_2 R_O (dP_2/d\theta)$, so, to retain terms to order α_2^2, we need only carry two terms in the expansion in (6.36):

$$dA = 2\pi \, \sin\theta \left\{ r^2 + \frac{1}{2}\left(\frac{dr}{d\theta}\right)^2 + ... \right\} d\theta. \tag{6.37}$$

To this level of approximation, the surface area of the deformed nucleus comprises two contributions:

$$A = 2\pi \left\{ \int_0^\pi r^2 \sin\theta \, d\theta + \frac{1}{2} \int_0^\pi \left(\frac{dr}{d\theta}\right)^2 \sin\theta \, d\theta + \dots \right\}. \tag{6.38}$$

These integrals are fairly straightforward, and reduce to

$$A \sim 4\pi R_O^2 \left\{ (1+\alpha_0)^2 + \frac{4}{5}\alpha_2^2 + \dots \right\}. \tag{6.39}$$

Substitute into this the result of volume conservation, $\alpha_0 \sim -\alpha_2^2/5$. Also invoke the usual nuclear radius approximation $R_O \sim a_o A^{1/3}$ ($a_o \sim 1.2$ fm), and write the factor which converts surface area to equivalent energy as Ω. U_S can then be written as

$$U_S \sim \left(a_S A^{2/3}\right) \left\{ 1 + \frac{2}{5}\alpha_2^2 + \dots \right\}, \tag{6.40}$$

where $a_S = 4\pi\Omega a_o^2 \sim 18\text{MeV}$. The areal energy *increases* upon perturbation of the nucleus from its initially spherical shape; this is understandable in that a sphere is the surface of minimum area which encloses a given volume.

6.5.4 E4: The Coulomb Integral and the SF Limit

Figure 6.4 illustrates the geometry of computing the Coulombic self-potential of the distorted nucleus.

The nucleus is divided into elements of volume $d\tau$ throughout which the protons are assumed to be uniformly distributed. By considering pairs of volume elements labeled as "1" and "2", the electrostatic self energy is computed from

$$U_C = \frac{1}{2}\left(\frac{\rho^2}{4\pi\varepsilon_o}\right) \int_{(1)} \int_{(2)} \frac{d\tau_1 \, d\tau_2}{r_{12}}; \tag{6.41}$$

where ρ is the charge density and r_{12} is the distance between the two volume elements. Each volume element is three-dimensional, so (6.41) is actually a *sextuple integral*. As in the computation of the surface area, integrals over r must be done before those over θ. Care must be taken to keep track of the "1" and "2" integrals and coordinates.

To treat the factor of r_{12} in the denominator of (6.41), invoke the identity

Fig. 6.4 Geometry for computing the Coulomb self-energy of the distorted nucleus. The two volume elements are located at distances r_1 and r_2 from the origin, and are separated by distance r_{12}. The angle between them as viewed from the origin is θ_{12}
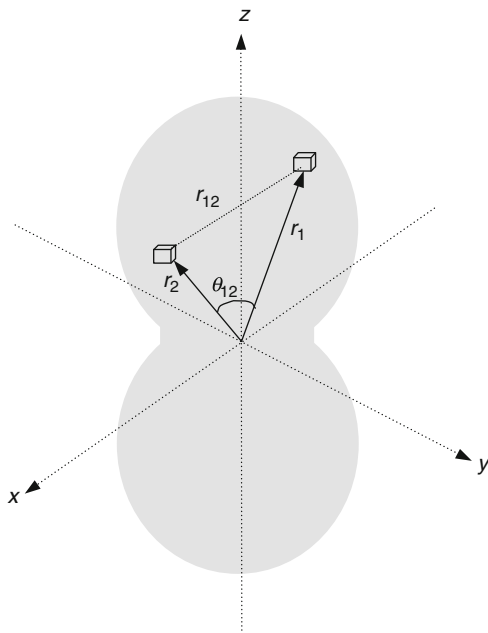
$$\frac{1}{r_{12}} = \begin{cases} \displaystyle\sum_{k=0} \left(\frac{r_2^k}{r_1^{k+1}}\right) P_k(\cos\theta_{12}), r_2 < r_1 \\[2em] \displaystyle\sum_{k=0} \left(\frac{r_1^k}{r_2^{k+1}}\right) P_k(\cos\theta_{12}), r_2 > r_1, \end{cases} \tag{6.42}$$

where θ_{12} is the angle between the directions from the origin to volume elements 1 and 2.

It is immaterial whether one integrates over the "1" or "2" coordinates first; I elect the latter and proceed by writing (6.41) as

$$U_C = \frac{\rho^2}{8\pi\varepsilon_o} \int\limits_{(1)} \left\{ \int\limits_{(2)} \frac{d\tau_2}{r_{12}} \right\} d\tau_1. \tag{6.43}$$

Call the inner integral U_2. To proceed, break it into two regimes, one for $r_2 = 0$ to r_1 (for which $r_2 < r_1$), and another from $r_2 = r_1$ to $r_2(\theta_2)$ (for which $r_2 > r_1$), and use (6.42):

$$U_2 = \int\limits_{(2)} \frac{d\tau_2}{r_{12}} = \sum_k \int\limits_0^{r_1} \left(\frac{r_2^k}{r_1^{k+1}}\right) P_k \, d\tau_2 + \sum_k \int\limits_{r_1}^{r_2(\theta_2)} \left(\frac{r_1^k}{r_2^{k+1}}\right) P_k \, d\tau_2. \tag{6.44}$$

Note that P_k still means $P_k(\cos \theta_{12})$. As these integrals are over the "2" coordinates, factors of r_1 can be extracted from within them but must remain within the sums. Writing the volume elements explicitly as $d\tau = r^2 dr\, d\Omega$ then gives

$$U_2 = \sum_k \frac{1}{r_1^{k+1}} \int\limits_{\theta,\phi} \int\limits_0^{r_1} r_2^{k+2} P_k dr_2\, d\Omega_2 + \sum_k r_1^k \int\limits_{\theta,\phi} \int\limits_{r_1}^{r_2(\theta_2)} r_2^{1-k} P_k dr_2\, d\Omega_2 \quad (6.45)$$

The first integral over r_2 is trivial and gives $r_1^{k+3}/(k+3)$; the second requires care in the case of $k = 2$, where a logarithmic term arises:

$$U_2 = r_1^2 \sum_k \int\limits_{\theta,\phi} \frac{P_k}{(k+3)} d\Omega_2 + \sum_{k \neq 2} \frac{r_1^k}{(2-k)} \int\limits_{\theta,\phi} r_2^{2-k}(\theta) P_k d\Omega_2$$

$$-r_1^2 \sum_{k \neq 2} \frac{1}{(2-k)} \int\limits_{\theta,\phi} P_k d\Omega_2 + r_1^2 \int\limits_{\theta,\phi} \ln\left(\frac{r_2(\theta)}{r_1}\right) P_2\, d\Omega_2. \quad (6.46)$$

Now, from the addition theorem for spherical harmonics, the $P_k(\cos \theta_{12})$ can be written in terms of products of Associated Legendre polynomials whose arguments are the cosines of the *individual* direction angles of the volume elements:

$$P_k(\cos \theta_{12}) = \sum_{m=-k}^{k} \frac{(k-m)!}{(k+m)!} P_k^m(\cos \theta_1) P_k^m(\cos \theta_2) \exp[\imath m(\phi_1 - \phi_2)]. \quad (6.47)$$

Imagine (6.47) substituted into (6.46). In integrating over ϕ_1 and ϕ_2, only $m = 0$ will give non-zero contributions. The Associated Legendre polynomials consequently reduce to regular Legendre polynomials, which I designate as $P_{k(1)}$ and $P_{k(2)}$. Thus, for example, $P_{k(1)}$ designates the k'th-order Legendre polynomial for coordinate set "1". Then we have

$$U_2 = r_1^2 \sum_k \frac{P_{k(1)}}{(k+3)} \int\limits_{\theta,\phi} P_{k(2)} d\Omega_2 + \sum_{k \neq 2} \frac{r_1^k P_{k(1)}}{(2-k)} \int\limits_{\theta,\phi} r_2^{2-k}(\theta) P_{k(2)} d\Omega_2$$

$$-r_1^2 \sum_{k \neq 2} \frac{P_{k(1)}}{(2-k)} \int\limits_{\theta,\phi} P_{k(2)} d\Omega_2 + r_1^2 P_{2(1)} \int\limits_{\theta,\phi} \ln\left(\frac{r_2(\theta)}{r_1}\right) P_{2(2)}\, d\Omega_2. \quad (6.48)$$

The first and third integrals in (6.48) vanish except when $k = 0$ in view of (6.28); for $k = 0$ they respectively give $4\pi r_1^2/3$ and $-2\pi r_1^2$, for a total of $-2\pi r_1^2/3$. The second and third integrals in (6.48) are a little more involved and involve further series expansions of the $r(\theta)$ terms; details are given in the available

web-based document. A crucial manipulation in carrying along expansions to correct orders in these two integrals is to factor terms of the form $r^p(\theta)$ as

$$\left\{1 + \alpha_0 + \alpha_2 P_{2(k)}\right\}^p = (1 + \alpha_0)^p \left\{1 + \frac{\alpha_2 P_{2(k)}}{(1 + \alpha_0)}\right\}^p, \tag{6.49}$$

and then undertake a binomial expansion of the brace bracket to order α_2^2. The overall result for U_2 is

$$U_2 = -\frac{2\pi}{3} r_1^2 + 2\pi R_O^2 (1 + \alpha_0)^2 + \frac{4\pi}{5} P_{2(1)} \frac{r_1^2 \alpha_2}{(1 + \alpha_0)}$$

$$+ \pi \alpha_2^2 R_O^2 \sum_k P_{k(1)} \left(\frac{r_1}{R_O}\right)^k \frac{(1 - k)}{(1 + \alpha_0)^k} \{k, 2, 2\}, \tag{6.50}$$

where $\{i, j, k\}$ designates the integral of the product of three Legendre polynomials over $x = \cos\theta$:

$$\{i, j, k\} = \int_{-1}^{1} P_i P_j P_k \, dx. \tag{6.51}$$

At this point, (6.50) goes back into (6.43) and (6.44) to give the Coulomb energy as

$$U_C = \frac{\rho^2}{8\pi\varepsilon_o} \left\{ -\frac{2\pi}{3} \int_{\theta,\phi} \int_0^{r_1(\theta)} r_1^4 dr_1 d\Omega_1 + 2\pi R_O^2 (1 + \alpha_0)^2 \int_{\theta,\phi} \int_0^{r_1(\theta)} r_1^2 dr_1 d\Omega_1 \right.$$

$$+ \frac{4\pi}{5} \frac{\alpha_2}{(1 + \alpha_0)} \int_{\theta,\phi} \int_0^{r_1(\theta)} P_{2(1)} r_1^4 dr_1 d\Omega_1$$

$$\left. + \pi \alpha_2^2 R_O^2 \sum_k \frac{(1 - k)\{k, 2, 2\}}{R_o^k (1 + \alpha_0)^k} \int_{\theta,\phi} \int_0^{r_1(\theta)} r_1^{k+2} P_{k(1)} \, dr_1 d\Omega_1 \right\}. \tag{6.52}$$

The third integral in (6.52) is done here as an example; complete solutions for the others are detailed in the web document. Integrating over r_1 and ϕ and transforming to x renders the integral as

$$\frac{8\pi^2}{25} \frac{\alpha_2}{(1 + \alpha_0)} \int_{-1}^{1} P_{2(1)} r_1^5(\theta) \, dx. \tag{6.53}$$

Put $r_1(\theta) = R_o[(1 + \alpha_0) + \alpha_2 P_2]$. In expanding r_1 to the fifth power, keep only terms to order α_2^2, which gives

$$\frac{8\pi^2}{25} \frac{\alpha_2 R_O^5}{(1 + \alpha_0)} \int_{-1}^{1} P_{2(1)} \left[(1 + \alpha_0)^5 + 5(1 + \alpha_0)^4 \alpha_2 P_{2(1)} \right.$$
$$\left. + 10(1 + \alpha_0)^3 \alpha_2^2 P_{2(1)}^2 + ... \right] dx. \tag{6.54}$$

Note the presence of the factor of $P_{2(1)}$ in front of the square bracket within the integrand. The first term within the square bracket will make no contribution to the integral since the integral of $P_{2(1)}$ over $-1 \leq x \leq 1$ is zero. We can ignore the last term within the square bracket as it will lead to a term of order α_2^3 when combined with the factor of α_2 outside the integral. Only the second term gives a surviving contribution:

$$\frac{8\pi^2}{5} R_O^5 (1 + \alpha_o)^3 \alpha_2^2 \int_{-1}^{1} P_{2(1)}^2 \, dx = \frac{16\pi^2}{25} R_o^5 (1 + \alpha_o)^3 \alpha_2^2. \tag{6.55}$$

Upon carrying out the other integrals in (6.52), the result, again to order α_2^2, is

$$U_C = \frac{\rho^2}{8\pi\varepsilon_o} \pi^2 R_O^5 \left\{ \frac{32}{15} (1 + \alpha_0)^5 + \frac{128}{75} (1 + \alpha_0)^3 \alpha_2^2 \right\}. \tag{6.56}$$

On writing the charge density as $\rho = 3Ze/4\pi R_O^3$, again invoking $R_O \sim a_o A^{1/3}$, and substituting the volume-conservation condition $\alpha_0 \sim -\alpha_2^2/5$, U_C reduces to

$$U_C \sim a_C \left(\frac{Z^2}{A^{1/3}} \right) \left\{ 1 - \frac{1}{5} \alpha_2^2 + ... \right\}. \tag{6.57}$$

where $a_C = (3e^2/20\pi\varepsilon_o a_o) \sim 0.72$ MeV is the Coulomb energy parameter. The Coulomb self-energy *decreases* upon perturbation of the nucleus from its initially spherical shape.

We can now determine the limiting condition for stability against spontaneous fission. If the nucleus becomes slightly distorted, that is, if $\alpha_2 \neq 0$, then fission will proceed spontaneously if the total energy of the deformed nucleus is less than what it was in its initial undeformed spherical shape ($\alpha_2 = 0$), that is, if $\Delta E = (U_S + U_C)_{deformed} - (U_S + U_C)_{undeformed} < 0$. On substituting (6.40) and (6.57), ΔE emerges as

$$\Delta E = \left(\frac{2}{5} a_S A^{2/3} \alpha_2^2 \right) \left\{ 1 - \frac{1}{2} \left(\frac{a_C}{a_S} \right) \left(\frac{Z^2}{A} \right) \right\}. \tag{6.58}$$

Clearly, whatever the value of α_2, ΔE will be negative so long as

$$\frac{Z^2}{A} > 2 \left(\frac{a_S}{a_C} \right), \tag{6.59}$$

the Bohr and Wheeler SF condition. With $a_S \sim 18$ MeV and $a_C \sim 0.72$ MeV, the limiting Z^2/A evaluates to about 50. Readers seeking expressions for U_S and U_C to higher orders of perturbation are urged to consult Present and Knipp (1940a, b) and Plesset (1941).

With empirically-known values for a_S and a_C, the Z^2/A limit provides an understanding of why nature stocks the periodic table with only about 100 elements: nuclei have $A \sim 2Z$, so $Z^2/A \sim 50$ corresponds to a limiting Z of about 100. In extending their analysis to higher orders of perturbation, B&W also provided the first real understanding as to why only a very few isotopes at the heavy end of the periodic table are subject to fission by slow neutrons: yet heavier ones are too near the Z^2/A limit to remain stable for long against SF, while for lighter ones the fission barrier is too great to be overcome by the binding energy released upon neutron absorption.

6.5.5 References

Bernstein, J., Pollock, F.: The calculation of the electrostatic energy in the liquid drop model of nuclear fission – a pedagogical note. Physica **96A**, 136–140 (1979)

Bohr, N., Wheeler, J.A.: The mechanism of nuclear fission. Phys. Rev. **56**, 426–450 (1939)

Cottingham, W.N., and Greenwood, D.A.: An Introduction to Nuclear Physics. Cambridge University Press, Cambridge, 2nd edn, p. 84 (2001)

Plesset, M.S.: On the classical model of nuclear fission. Am. J. Phys. **9**, 1–10 (1941)

Present, R.D., Knipp, J.K.: On the dynamics of complex fission. Phys. Rev. **57**, 751 (1940a)

Present, R.D., Knipp, J.K.: On the dynamics of complex fission. Phys. Rev. **57**, 1188–1189 (1940b)

Reed, B.C.: The Bohr–Wheeler spontaneous fission limit: an undergraduate-level derivation. Eur. J. Phys. **30**, 763–770 (2009)

6.6 Appendix F: Average Neutron Escape Probability from Within a Sphere

We derive here the mean escape probability for neutrons emitted from within a sphere, the quantity $\langle P_{sph} \rangle$ of Sect. 4.2 This is based on extending the semi-empirical linear expression

$$P(x) = \exp\left(-\sigma_{tot}\, n\, x\right) \tag{6.60}$$

to three dimensions.

Figure 6.5 shows an element of volume dV at radius r within a sphere of radius R. We can put this volume element somewhere along the z-axis without any loss of generality.

The vector $\boldsymbol{r}$ goes from the center of the sphere to dV, that is, $r = r\,\hat{z}$. The vector $\boldsymbol{d}$ represents the straight-line path of a neutron emitted from dV in a direction that

reaches the surface of the sphere, and $\mathbf{R} = \mathbf{r} + \mathbf{d}$ is a vector from the center of the sphere to where the neutron reaches the surface, as shown in Fig. 6.6.

To specify the direction of $\mathbf{d}$, we use the usual spherical coordinate angles (θ, ϕ) originating at dV:

$$d = (d \sin \theta \cos \phi)\hat{x} + (d \sin \theta \sin \phi)\hat{y} + (d \cos \theta)\hat{z}. \tag{6.61}$$

From $\mathbf{R} \bullet \mathbf{R} = R^2 = |r + d|^2$ and (6.61), we can obtain an expression for the magnitude of $\mathbf{d}$:

$$d(w, \theta) = R \left(-w \cos \theta + \sqrt{1 - w^2 \sin^2 \theta} \right), \tag{6.62}$$

where $w = r/R$ is a dimensionless radial variable.

If neutrons emitted from dV travel in random directions, then the probability of any one of them being emitted into the solid angle defined by the angular limits θ to $\theta + d\theta$ and ϕ to $\phi + d\phi$ is
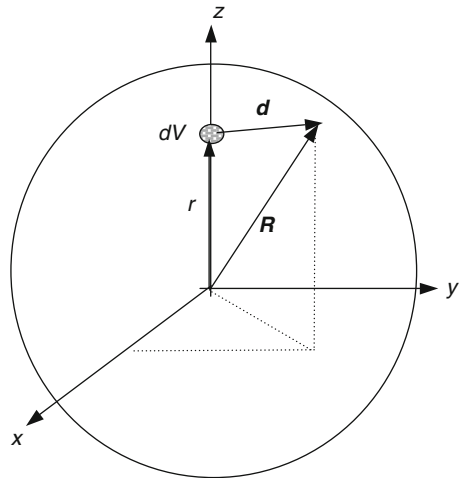
Fig. 6.5 Neutrons escaping from a small volume dV within a bomb core. A neutron begins at position $\mathbf{r}$. $\mathbf{R}$ is its position when it reaches the surface of the core. $\mathbf{d}$ goes from the volume element to the edge of the sphere in a direction defined in Fig. 6.6 below
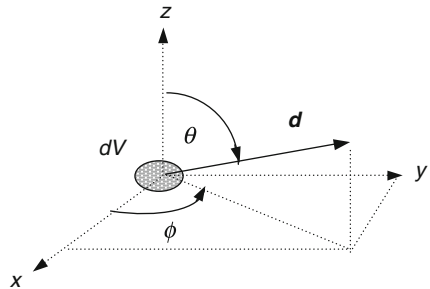
Fig. 6.6 Detailed view of vector $\mathbf{d}$ of Fig. 6.5

$$P\left(d\Omega\right) = \frac{1}{4\pi}\,\sin\theta\,d\theta\,d\phi. \tag{6.63}$$

The probability that a neutron emitted into $d\Omega$ will escape is $P(x)$ times $P(d\Omega)$, where the distance d of (6.62) replaces x in the expression for $P(x)$ in (6.60). By invoking a second set of spherical coordinates (θ', ϕ') measured with respect to the origin, we can write dV as $dV = r^2 \sin\theta'\,d\theta'\,d\phi'\,dr$. If the number of neutrons emitted per unit volume is constant, we can obtain the overall average escape probability by weighting $P(x)$ times $P(d\Omega)$ times dV, integrating over all directions of emission θ and over the entire volume of the sphere, and then dividing by the volume of the sphere:

$$\left\langle P_{sph}\right\rangle = \frac{3}{4\pi R^3}$$
$$\times \int_{\theta=0}^{\pi}\int_{\phi=0}^{2\pi}\int_{r=0}^{R}\int_{\theta'=0}^{\pi}\int_{\phi'=0}^{2\pi} e^{-\sigma n d(w,\theta)}\left(\frac{\sin\theta d\theta d\phi}{4\pi}\right)\left(r^2 \sin\theta'\,d\theta'\,d\phi'\,dr\right) \tag{6.64}$$

The integrals over θ, θ', and ϕ' can be carried out directly and yield $8\pi^2$. Transforming the integral over r into one over w gives

$$\left\langle P_{sph}\right\rangle = \frac{3}{2}\int_{w=0}^{1}\int_{\theta=0}^{\pi} w^2 \sin\theta e^{-\sigma n d(w,\theta)}\,d\theta dw. \tag{6.65}$$

This integral is incorporated into the spreadsheet **PreDetonation.xls** discussed in Sect. 4.2. The spreadsheet actually comprises two "Sheets". In Sheet 1 the user enters cross-sections, core and contaminant masses, and spontaneous fission data. The integral is done in Sheet 2, with 100 columns for w (from 0 to 1 in steps of 0.01) and 100 rows for θ (0 to π in steps of $\pi/100$). The result of the integral is automatically transferred to the first Sheet for use in calculating the predetonation probability for a given assembly time.[2]

6.7   Appendix G: The Neutron Diffusion Equation

The analysis of critical mass presented in Sect. 2.2 was developed from the diffusion equation for neutrons. This equation is a differential equation for the time and space-dependence of the number density of neutrons within a bomb core. Fundamentally, it expresses a competition between neutron gain and loss.

---

[2]Note added in proof: (6.65) can be solved analytically. See S. Croft, Nucl. Instr. and Meth. in Phys. Res. **A288**, 589–592 (1990).

Imagine isolating a small volume of material within the core. The volume concerned will gain neutrons both from fissions happening within it and from neutrons that enter from surrounding material. At the same time, it will lose neutrons as they are consumed in causing fissions and as they fly out into surrounding material or to the outside world. The quantity of interest is the number density of neutrons in the volume at hand, N, which has units of neutrons/m^3 and is presumed to be a function of both position and time. In anticipation of modeling a spherical core we write the neutron number density as $N(r, t)$. In words, the net rate of change of neutron density can be expressed as

$$\frac{dN}{dt} = \begin{pmatrix} net\ rate\ of\ neutron\ density\ gain \\ from\ fissions\ per\ unit\ volume \end{pmatrix}$$
$$+ \begin{pmatrix} net\ rate\ of\ neutron\ density\ gain\ by\ neutron \\ transport\ through\ boundary,\ per\ unit\ volume \end{pmatrix}. \tag{6.66}$$

The derivation given here is motivated by that appearing in Serber (1992); readers seeking more details are urged to consult Liverhant (1960) or any similar text on reactor engineering.

We approach the development of the diffusion equation in two steps, with each corresponding to one of the terms on the right side of (6.66). The first term can be explained fairly easily, so we examine it first.

Assume that that, on average, neutrons have speed $\langle v \rangle$. From the development in Sect. 2.1 we know that the average distance a neutron will travel before causing a fission is given by $\lambda_f = 1/n\sigma_f$ where n is the number density of fissile nuclei and σ_f their fission cross-section. The time that a neutron will travel before causing a fission is then $t = \lambda_f/\langle v \rangle$. On average, then, individual neutrons will cause fissions at a rate $\langle v \rangle/\lambda_f$ per second. If each fission produces v secondary neutrons, then the net rate of secondary neutron production per "average" neutron will be $(v-1)\langle v \rangle/\lambda_f$ per second; the "-1" appears because the neutron causing the fission is consumed in doing so. Now apply this argument to a volume V where the number density of neutrons is N. The total number of neutrons will be NV and the rate of secondary neutron production will consequently be $NV(v-1)\langle v \rangle/\lambda_f$ per second. The rate of change of the density of neutrons caused by fissions is given by this quantity divided by V, or

$$\left(\frac{\partial N}{\partial t} \right)_{fission} = \frac{\langle v \rangle}{\lambda_f} (v-1) N. \tag{6.67}$$

The second term in (6.66) involves neutrons entering and leaving the volume as they fly about. This step is trickier and is most easily dealt with in two sub-steps.

To begin, an important quantity here is the *transport mean free path*, the average distance a neutron will travel before suffering any interaction. In a bomb core the

important interactions are fission and elastic scattering; again appealing to Sect. 2.1 we can write this as

$$\lambda_t = \frac{1}{n\sigma_{total}} = \frac{1}{n\left(\sigma_{fission} + \sigma_{elastic}\right)}. \tag{6.68}$$

We are assuming that the only important processes are fission and elastic scattering.

Imagine neutrons flying about in a spherical bomb core of radius R as sketched in Fig. 6.7. The first sub-step here is to get an expression for the net rate at which neutrons flow from the inside to the outside through an imaginary surface at radius r.

This derivation makes use of a result established in Sect. 3.5, where we examined the effusion of particles through holes in a barrier. In deriving equation (3.54), we found that the effusion rate of particles through a hole of area A is given by

$$effusion\ rate = \frac{1}{4}NA\langle v\rangle. \tag{6.69}$$

The unit of this expression is neutrons/s, or simply s^{-1}. In our case A will be the area of the imaginary surface at radius r, namely $4\pi r^2$.

Apply (6.69) to the imaginary surface at radius r. Unlike the barrier diffusion issue taken up in Sect. 3.5, here we have neutrons passing through the surface that have come from both "within" (radii $< r$) and "outside" (radii $> r$) the surface. Suppose that those that come from within have come from a region where the average neutron number density is $N_<$, while those that pass through from the outside have come from a region where the neutron number density is $N_>$.
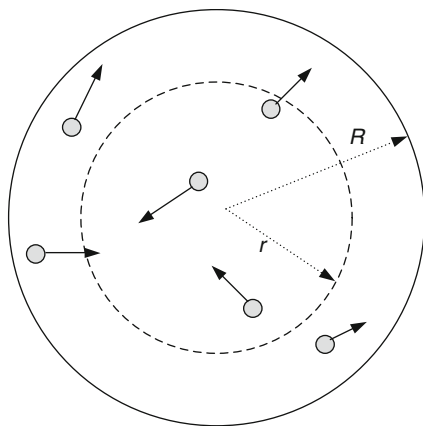
Fig. 6.7 Schematic representation of a fissioning spherical bomb core of radius R. The small circles represent neutrons. The neutron number density $N(r, t)$ is presumed to be a function both position and time within the core

The net neutron flux from the inside to the outside through the imaginary surface will then be

$$\left(\begin{array}{c} \textit{net effusion rate} \\ \textit{inside to outside} \\ \textit{at radius } r \end{array}\right) = \frac{1}{4} A \langle v \rangle \left(N_< - N_> \right). \tag{6.70}$$

While the neutrons will on average travel distance λ_t of (6.68) between interactions, they will be flying about in random directions. In specifying the locations of $N_<$ and $N_>$ we should consequently use values corresponding to the average *radial* displacement that a neutron will undergo between its last collision and reaching the surface at r, that is, their average displacement perpendicular to the escape surface. This will presumably be less than λ_t due to the neutrons' random flights. For the moment, let us represent this average radial displacement as $\langle \lambda_r \rangle$; how this relates to λ_t is taken up following (6.81) below.

Now, reverse the order of the terms in (6.70) and both multiply and divide it by $2 \langle \lambda_r \rangle$:

$$\left(\begin{array}{c} \textit{net effusion rate} \\ \textit{inside to outside} \\ \textit{at radius } r \end{array}\right) = -\frac{1}{4} A \langle v \rangle \left[\frac{(N_> - N_<)}{2 \langle \lambda_r \rangle}\right] (2 \langle \lambda_r \rangle). \tag{6.71}$$

The square bracket in (6.71) is the change in N divided by the distance over which that change occurs, that is, the derivative of N with respect to radial distance:

$$\left(\begin{array}{c} \textit{net effusion rate} \\ \textit{inside to outside} \\ \textit{at radius } r \end{array}\right) = -\frac{1}{2} A \langle v \rangle \langle \lambda_r \rangle \left(\frac{\partial N}{\partial r}\right)_r = -2 \pi r^2 \langle v \rangle \langle \lambda_r \rangle \left(\frac{\partial N}{\partial r}\right)_r, \tag{6.72}$$

where we have substituted for the area of the sphere and used partial derivatives as a reminder that N is a function of both position and time.

Be sure to understand why factors of 2 were included with the factors of $\langle \lambda_r \rangle$ in (6.71): the surfaces of density $N_<$ and $N_>$ are each a distance $\langle \lambda_r \rangle$ from the surface at radius r and so the distance over which the change $(N_> - N_<)$ occurs is $2 \langle \lambda_r \rangle$.

We come now to the second sub-step of this part of the derivation. We desire an expression for the net rate of change of N per unit volume due to random neutron motions. To do this, apply (6.72) to a spherical shell within the core that extends from inner radius r to outer radius $r + dr$, as shown in Fig. 6.8:

$$\left(\begin{array}{c} \textit{rate of neutrons from} \\ \textit{within } r \textit{ entering shell} \end{array}\right) = -2 \pi r^2 \langle v \rangle \langle \lambda_r \rangle \left(\frac{\partial N}{\partial r}\right)_r. \tag{6.73}$$
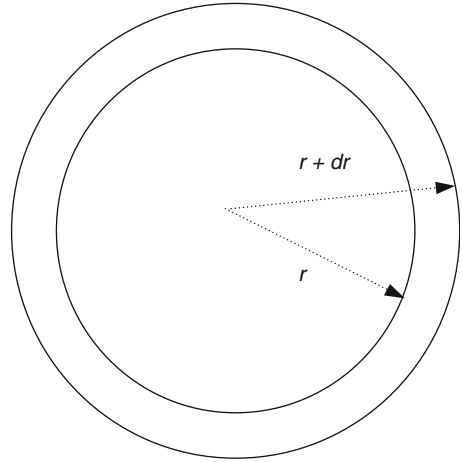
At the same time, neutrons exit the volume by passing through the surface at $r + dr$:

$$\begin{pmatrix} rate\ of\ neutrons\ exiting \\ shell\ from\ within\ shell \end{pmatrix} = -2\,\pi\,(r+dr)^2 \langle v \rangle\, \langle \lambda_r \rangle \left(\frac{\partial N}{\partial r} \right)_{r+dr}. \qquad (6.74)$$

Notice that in writing these expressions we evaluate $(\partial N/\partial r)$ at the inner and outer surfaces of the shell. It follows that the *net* rate of neutron flux into the shell is given by the entry rate, (6.73), minus the exit rate, (6.74); the overall result could in fact be a loss (and will be so at the outer surface of the core):

$$\begin{pmatrix} net\ rate \\ of\ neutrons \\ entering\ shell \end{pmatrix} = 2\,\pi\,\langle v \rangle\,\langle \lambda_r \rangle \left\{ (r+dr)^2 \left(\frac{\partial N}{\partial r} \right)_{r+dr} - r^2 \left(\frac{\partial N}{\partial r} \right)_r \right\}. \qquad (6.75)$$

Expanding out the factor of $(r+dr)^2$ and writing

$$\left(\frac{\partial N}{\partial r} \right)_{r+dr} = \left(\frac{\partial N}{\partial r} \right)_r + \left(\frac{\partial^2 N}{\partial r^2} \right)_r dr, \qquad (6.76)$$

one arrives at, after a few lines of algebra,

$$\begin{pmatrix} net\ rate\ of\ neutrons \\ entering\ shell \end{pmatrix} = 2\,\pi\,\langle v \rangle\,\langle \lambda_r \rangle \left\{ \left[r^2 \left(\frac{\partial^2 N}{\partial r^2} \right)_r + 2r \left(\frac{\partial N}{\partial r} \right)_r \right] dr \right.$$
$$\left. + 2r \left(\frac{\partial^2 N}{\partial r^2} \right)_r dr^2 + \left(\frac{\partial N}{\partial r} \right)_r dr^2 + \left(\frac{\partial^2 N}{\partial r^2} \right)_r dr^3 \right\}. \qquad (6.77)$$

Now recall the Laplacian operator in spherical coordinates:

$$\left(\nabla^2 N\right)_r = \frac{1}{r^2}\left[r^2\left(\frac{\partial^2 N}{\partial r^2}\right)_r + 2r\left(\frac{\partial N}{\partial r}\right)_r\right]. \tag{6.78}$$

But for a factor of $1/r^2$, this is exactly the square-bracketed term in (6.77), that is, we can write

$$\begin{pmatrix} net\ rate\ of \\ neutrons \\ entering\ shell \end{pmatrix} = 2\,\pi\,\langle v\rangle\,\langle\lambda_r\rangle\,\left\{r^2\left(\nabla^2 N\right)_r dr + 2r\left(\frac{\partial^2 N}{\partial r^2}\right)_r dr^2\right.$$

$$\left. + \left(\frac{\partial N}{\partial r}\right)_r dr^2 + \left(\frac{\partial^2 N}{\partial r^2}\right)_r dr^3\right\}. \tag{6.79}$$

Now, the volume of the shell is $4\pi\,r^2 dr$. If we divide (6.79) by this volume we will arrive at the rate of change of the density of neutrons within the volume due to neutrons flying into or out of it:

$$\left(\frac{\partial N}{\partial t}\right)_{neutron\,flight} = \frac{1}{2}\langle v\rangle\langle\lambda_r\rangle\left\{\left(\nabla^2 N\right)_r + \frac{2}{r}\left(\frac{\partial^2 N}{\partial r^2}\right)_r dr + \frac{1}{r^2}\left(\frac{\partial N}{\partial r}\right)_r dr + \frac{1}{r^2}\left(\frac{\partial^2 N}{\partial r^2}\right)_r dr^2\right\}. \tag{6.80}$$

If we let the shell become infinitesimally thin, that is, if $dr \rightarrow 0$, then the last three terms on the right side of (6.80) will vanish and we are left with

$$\left(\frac{\partial N}{\partial t}\right)_{neutron\ flight} = \frac{1}{2}\langle v\rangle\langle\lambda_r\rangle\left(\nabla^2 N\right), \tag{6.81}$$

where we drop the subscript r on $\nabla^2 N$ for brevity.

We now need to address the issue of expressing $\langle\lambda_r\rangle$ in terms of the transport cross-section of (6.68). To do this we again appeal to Sect. 3.5, where we looked at the rate of escape of particles from within a slanted "escape cylinder." From (3.52), the number of particles traveling in the range of spherical directions (θ, ϕ) to $(\theta + d\theta, \phi + d\phi)$ that escape in elapsed time Δt is given by

$$N_{esc}(\Delta t) = \frac{NA\,\langle v\rangle(\Delta t)}{4\pi}\,\cos\theta\,\sin\theta\,d\theta\,d\phi, \tag{6.82}$$

where N, A, and $\langle v\rangle$ are again respectively the neutron number density, the area of the surface of escape, and the average neutron speed.

In (6.82), $\langle v\rangle(\Delta t)$ corresponds to the average distance that a neutron travels while making good its escape, that is, $\langle v\rangle(\Delta t) = \lambda_t$. Since θ is measured from the z-axis

(review Figs. 3.6 and 3.8), the vertical component of this distance, that is, the average distance that a neutron travels in a direction perpendicular to the escape surface, will be $\lambda_t \cos\theta$. In the context of our spherical bomb core this perpendicular direction translates into the distance that a neutron will travel in the *radial* direction while escaping, which is what we are interested in. The total radial distance traveled by neutrons that escape in time Δt will then be

$$\begin{pmatrix} total\ radial\ distance \\ traveled\ by\ all\ neutrons \\ moving\ in\ directions\ (\theta, \phi) \\ that\ escape\ in\ time\ \Delta t \end{pmatrix} = \begin{pmatrix} number\ that\ escape \\ in\ time\ \Delta t \end{pmatrix}$$

$$\times \begin{pmatrix} average\ radial\ distance \\ traveled\ by\ each\ neutron \end{pmatrix}$$

$$= \frac{NA\,\lambda_t^2}{4\pi}\ \cos^2\theta\ \sin\theta\ d\theta\ d\phi. \qquad (6.83)$$

To account for all possible direction of escape we integrate over $0 \le \theta \le \pi/2$ and $0 \le \phi \le 2\pi$:

$$\begin{pmatrix} total\ radial\ distance \\ traveled\ by\ all\ neutrons \\ that\ escape\ in\ time\ \Delta t \end{pmatrix} = \frac{NA\,\lambda_t^2}{4\pi} \int\limits_{\phi=0}^{2\pi} \int\limits_{\theta=0}^{\pi/2} \cos^2\theta\ \sin\theta\ d\theta\ d\phi \qquad (6.84)$$

This double integral gives $2\pi/3$, so

$$\begin{pmatrix} total\ radial\ distance \\ traveled\ by\ all\ neutrons \\ that\ escape\ in\ time\ \Delta t \end{pmatrix} = \frac{NA\,\lambda_t^2}{6}. \qquad (6.85)$$

For use in (6.81) we need the *average* radial distance traveled, which we can get by dividing (6.85) by the total number that escape in time Δt. Equation (6.69) gives the *rate* of escape (neutrons/s), so the number that escape in time Δt will just be that rate times Δt:

$$\begin{pmatrix} average\ radial\ distance \\ traveled\ by\ all\ neutrons \\ that\ escape\ in\ time\ \Delta t \end{pmatrix} = \frac{\left(\frac{NA\,\lambda_t^2}{6}\right)}{\left(\frac{1}{4}NA\,\langle v\rangle \Delta t\right)} = \frac{2}{3}\lambda_t, \qquad (6.86)$$

where we used $\langle v \rangle (\Delta t) = \lambda_t$. This result, when substituted into (6.81) gives

$$\left(\frac{\partial N}{\partial t}\right)_{neutron\ flight} = \frac{1}{3}\langle v \rangle \lambda_t \left(\nabla^2 N\right). \tag{6.87}$$

We have now established two important results. These are (i) that within a unit volume of core material, (6.67) accounts for the rate of change of neutron density caused by neutrons created by fissions, and, (ii), that (6.87) accounts for that caused by neutrons entering or leaving the volume. The *total* rate of change of neutron density is the sum of these two effects:

$$\frac{dN}{dt} = \frac{v}{\lambda_f}\ (v-1)\,N + \frac{v\,\lambda_t}{3}\left(\nabla^2 N\right), \tag{6.88}$$

where we have dropped the angle brackets on the average neutron speed. This is the diffusion equation used in Sect. 2.3 to study critical mass.

Solving (6.88) can be approached by the usual separation-of-variables technique; this is done in Sect. 2.2. To actually determine a critical radius, however, requires a boundary condition, that is, some specification on $N(R)$. Establishing this condition requires being a little more careful with our derivation in (6.70) and (6.71) regarding the edge of the sphere. Consider first (6.70) applied to the surface of the core at radius R. Here there will be no "backflow" of neutrons from the outside; the only neutrons that pass through the surface of the core will be those which have come from a characteristic distance $\langle \lambda_r \rangle$ from within. In this case, (6.70) reduces to

$$\left(\begin{array}{c} net\ effusion\ rate \\ through\ core\ surface \end{array}\right) = \frac{1}{4}A\,\langle v \rangle\,(N_<). \tag{6.89}$$

Now consider (6.71) at the surface. The role of $N_>$ will be played by N_R, that is, the neutron density at the surface. In this case we have the change in N over only a distance of $\langle \lambda_r \rangle$ as opposed to the previous $2\langle \lambda_r \rangle$ since there is no inward flux from the outside:

$$\left(\begin{array}{c} net\ effusion\ rate \\ through\ core\ surface \end{array}\right) = -\frac{1}{4}A\,\langle v \rangle \left[\frac{(N_R - N_<)}{\langle \lambda_r \rangle}\right]\langle \lambda_r \rangle$$

$$= \frac{1}{4}A\,\langle v \rangle\,\langle \lambda_r \rangle \left(\frac{\partial N}{\partial r}\right)_R. \tag{6.90}$$

Demand consistency by equating (6.89) and (6.90); also invoke (6.86) for $\langle \lambda_r \rangle$. On approximating $N_< \sim N_R$, we find

$$N(R) = -\frac{2}{3}\, \lambda_t \left(\frac{dN}{dr}\right)_R. \tag{6.91}$$

This is the boundary condition used in Sect. 2.2 for determining critical mass.

6.7.1 References

Liverhant, S.E.: Elementary Introduction to Nuclear Reactor Physics. Wiley, New York (1960)
Serber, R.: The Los Alamos Primer: The First Lectures on How To Build An Atomic Bomb. University of California Press, Berkeley (1992)

6.8 Appendix H: Questions

1.1 Compute Q-values for the following reactions. Reaction (a) produces high-energy neutrons for use in so-called "boosted" fission weapons. Reaction (b) is important in the production of tritium for use in reaction (a). Reaction (c) is a hypothetical fission reaction. Reaction (d) is an example of how alpha-bombardment of a light element can release neutrons, an important consideration in avoiding pre-detonation in fission weapons.

(a) $^{2}_{1}\text{H} + ^{3}_{1}\text{H} \rightarrow ^{4}_{2}\text{He} + ^{1}_{0}\text{n}$

(b) $^{6}_{3}\text{Li} + ^{1}_{0}\text{n} \rightarrow ^{3}_{1}\text{H} + ^{4}_{2}\text{He}$

(c) $^{1}_{0}\text{n} + ^{238}_{92}\text{U} \rightarrow 2\left(^{118}_{46}\text{Pd}\right) + 3\left(^{1}_{0}\text{n}\right)$

(d) $^{4}_{2}\text{He} + ^{27}_{13}\text{Al} \rightarrow ^{30}_{15}\text{P} + ^{1}_{0}\text{n}$

1.2 To melt 1 g of ice at 0°C into 1 g of water at 0°C requires input of 80 cal of heat energy. If all of the energy involved in the alpha-decay of 1 g ^{226}Ra could directed into melting ice, how many grams of ice could be melted per day? The decay rate of ^{226}Ra is 3.7×10^{10} per g/s, and the emergent alphas have kinetic energies of 4.8 MeV.

1.3 Prove equation (1.20) (assume classical mechanics) and then apply it to the case of radium decay discussed in Sect. 1.2. What will be the kinetic energy of the emergent α-particle? How does your result compare to the value of 4.78 MeV quoted in the *Chart of the Nuclides*?

1.4 For each of the reactions below, compute the energy of the resulting γ-ray for both forward and backward motion. Assume that the target nucleus is stationary in each case.

(a) $^{1}_{1}\text{H} + ^{16}_{8}\text{O} \rightarrow ^{17}_{9}\text{F} + \gamma \quad (K_{\text{H}} = 4.9 \text{ MeV})$

(b) $^{4}_{2}\text{He} + ^{27}_{13}\text{Al} \rightarrow ^{31}_{15}\text{P} + \gamma \quad (K_{\text{He}} = 6.5 \text{ MeV})$

(c) $^{56}_{26}\text{Fe} + ^{94}_{40}\text{Zr} \rightarrow ^{150}_{66}\text{Dy} + \gamma \ (K_{\text{Fe}} = 50 \text{ MeV})$

1.5   For each of the reactions below, compute the Q-value of the reaction, the threshold energy (if any), and the kinetic energies and directions of motion of the products. Assume that the target nucleus is initially stationary in each case.

(a) $^{4}_{2}\text{He} + ^{27}_{13}\text{Al} \rightarrow ^{30}_{15}\text{P} + ^{1}_{0}\text{n}$ ($K_{\text{He}} = 5$ MeV)
(b) $^{2}_{1}\text{H} + ^{3}_{1}\text{H} \rightarrow ^{4}_{2}\text{He} + ^{1}_{0}\text{n}$ ($K_{\text{H}} = 3$ MeV)
(c) $^{4}_{2}\text{He} + ^{19}_{9}\text{F} \rightarrow ^{22}_{10}\text{Ne} + ^{1}_{1}\text{H}$ ($K_{\text{He}} = 2.75$ MeV)
(d) $^{4}_{2}\text{He} + ^{56}_{26}\text{Fe} \rightarrow ^{35}_{16}\text{S} + ^{25}_{12}\text{Mg}$ ($K_{\text{He}} = 30$ MeV)
(e) $^{16}_{8}\text{O} + ^{238}_{92}\text{U} \rightarrow ^{252}_{99}\text{Es} + ^{2}_{1}\text{H}$

1.6   Consider a γ-ray of energy Q and a classical, non-relativistic particle of mass m with the same kinetic energy. Both strike a classical, non-relativistic particle of mass M head on. Show that the ratio of the kinetic energy acquired by M when struck by the massive particle to that when struck by the γ-ray is

$$\frac{K_M^m}{K_M^\gamma} = \frac{2E_m}{Q\left(1 + E_m/E_M\right)^2},$$

where the E's designate rest masses and where it has been assumed that $Q \ll E_M$. Apply to an α-particle being struck by a γ-ray and a proton, where $Q = 10$ MeV.

1.7   Show that the kinetic energy of a nonrelativistic neutron moving with speed $v = \beta c$ is given by $E \sim 470\,\beta^2$ MeV.

1.8   In an environment of absolute temperature T, the motion of a particle is on average equivalent to kinetic energy $3kT/2$ where k is Boltzmann's constant. Show that if a neutron is moving at a nonrelativistic speed with kinetic energy E MeV, then the equivalent temperature is $T = (7.74 \times 10^9\,E)$ Kelvin. Energies of a couple MeV are characteristic of neutrons released in fission reactions.

1.9   See Fig. 6.9 below. A neutron of mass m and kinetic energy K (non-relativistic) strikes and is absorbed by a heavy nucleus of mass $2M \gg m$. The resulting compound nucleus flies off with kinetic energy K_C. Shortly thereafter the compound nucleus fissions into two equal halves, each of mass M. One fragment travels backward with kinetic energy K_B while the other continues forward with kinetic energy K_F. Energy $2Q$ is liberated in the fission, that is, $K_B + K_F - K_C = 2Q$. Show that to a good approximation, the difference in kinetic energies $\Delta Q = K_F - K_B$ between the forward and backward-moving fission fragments is given by
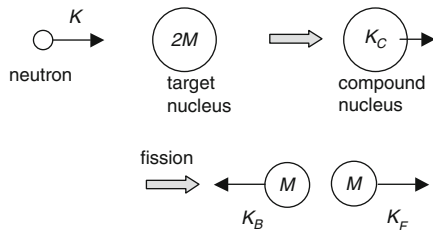

Fig. 6.9   Problem 1.9

$$\frac{\Delta Q}{Q} \sim 2\sqrt{\frac{Km}{QM}}.$$

Apply your result to a neutron with $K = 14$ MeV striking a ^{235}U nucleus; what is $\Delta Q/Q$ if $Q = 100$ MeV? HINTS: Conserve momentum in each reaction. Assume that $M \gg m$, $K \ll 2Q$, and that $\Delta Q/K_B$ (or $\Delta Q/K_A$) is small. Are these approximations justified in the 14-MeV neutron + ^{235}U reaction?

1.10 Suppose that all of the energy liberated in the explosion of a 20-kt fission weapon could be directed into raising 1 cubic kilometer of water in the Earth's gravitational field. How high could that cubic km of water be raised?

1.11 Use **BarrierCubic.xls** to carry out the calculations involved in Sect. 1.10 for fitting a cubic equation of the form $f_{smooth}(x) = Fx^3 + Bx^2 + Cx + D$ to model the fission barrier. If $a_C = 0.70$ MeV and $a_S = 16.5$ MeV, what are the parameters F, B, C, and D for a fission with mass ratio $f = 1.45$? What is the "offset" energy in this case for $A = 1$ if you adopt a (Z, A) fit of the form $Z \sim 0.60679\,A^{0.92383}$?

1.12 See Fig. 6.10. A nucleus containing Z_1 protons approaches a fixed target nucleus containing Z_2 protons and a total of A nucleons; the kinetic energy of the incoming nucleus is E MeV when it is far from the target nucleus. If nuclear radii are described empirically by $R \sim a_O A^{1/3}$ where $a_O = 1.2$ fm, show that the ratio of the distance d of closest approach of the nuclear centers to the radius of the target nucleus is given by

$$\frac{d}{R} = 1.2\left(\frac{Z_1 Z_2}{EA^{1/3}}\right),$$

Apply to an alpha-particle with $E = 5$ MeV approaching a U-235 nucleus.

2.1 Using the same nuclear-radius empirical expression as in the previous problem, estimate the geometrical cross-sectional area of a ^{235}U nucleus; give your result in barns. How does your result compare to the fission cross-section for fast neutrons for this isotope, $\sigma_f = 1.235$ bn?

2.2 Because cadmium-113 has an enormous cross-section for absorbing thermal neutrons, strips of cadmium metal are often used in control mechanisms in reactors. Given $\rho = 8.65$ g/cm^3, $A = 112.904$ g/mol and $\sigma_{absorb} = 20,600$,

Fig. 6.10 Problem 1.12

compute the probability that a neutron will penetrate through a strip of Cd-113 of thickness 0.05 mm.

2.3 Show that the time between fissions $\tau = \lambda_f / v_{neut}$ for neutrons traveling with speed v_{neut} corresponding to classical kinetic energy E MeV between nuclei in a material of atomic weight A g/mol, density ρ g/cm^3, and fission cross-section σ_f barns is given by

$$\tau = \frac{1.20A}{\sigma_f \rho \sqrt{E}} \text{ nanoseconds}$$

Compute τ for the case of 2-MeV neutrons in ^{235}U: $A = 235$, $\rho = 18.71$ g/cm^3 and $\sigma_f = 1.235$ bn.

2.4 Show that if the boundary condition in Sect. 2.2 for neutron escape from a spherical bomb core is simplified to $N(R_C) = 0$ (that is, if we demand that *no* neutrons escape from the surface), then the threshold critical radius can be expressed explicitly as

$$R_C = \frac{\pi}{\sqrt{3(v-1)}} \left(\frac{1}{n\sqrt{\sigma_f \sigma_t}} \right).$$

Evaluate this result numerically for a ^{235}U core using the fissility parameters given in Sect. 2.2. What is the resulting threshold critical mass?

2.5 In Sect. 2.2 we took the solution to the spatial part of the diffusion equation, (2.27), to be of the form $(sin\ x/x)$. But any second-order differential equation should have two solutions. The second solution in this case is $(cos\ x/x)$. This solution is usually rejected on the basis of a physical argument, however. What do you suppose this argument to be?

2.6 Working from the development of bomb efficiency in Sect. 2.4, show that the speed of the expanding core at the time of criticality shutdown is given by

$$v\left(t_{crit}\right) = \frac{\alpha\,\Delta r}{\tau}.$$

Evaluate $v\left(t_{crit}\right)$ explicitly in the case of a ^{235}U core with $C = 2$ using the values given in Table 2.2. How does $v\left(t_{crit}\right)$ compare to the average neutron speed?

2.7 Working from the development of bomb efficiency in Sect. 2.4, show that the pressure within the expanding core at the time of criticality shutdown is given by

$$P(t_{crit}) = \frac{\alpha^2\,\Delta r\,\langle \rho r \rangle}{3\,\tau^2}.$$

Evaluate $P(t_{crit})$ in the case of a ^{235}U core with $C = 2$. Express your result in atmospheres: 1 atm ~ 101,000 Pa.

2.8   Consider a fissile material with $\rho = 17.3$ g/cm^3, $A = 250$ g/mol, $\sigma_f = 1.55$ bn, $\sigma_{el} = 6$ bn, and $v = 2.95$. What are the bare threshold critical radius and mass of this material? What are the (analytic) effective α-value, Δr, efficiency, and yield for a core of $C = 3$ critical masses of this material if $E_f = 185$ MeV and if the secondary neutrons have $E = 2$ MeV? Take $\gamma = 1/3$. If the initial number of neutrons is taken to be one, what are the fission and criticality-shutdown timescales?

2.9   Consider a mass m of a pure fissile material whose normal density is ρ_o, with m being less than the bare threshold critical mass for the material. Show that this mass can be made critical by compressing it to a radius given by

$$r_{compress} \leq \sqrt{\frac{3m}{4\pi\rho_o R_o}},$$

where R_o is the threshold critical radius at normal density for the material. Show further that if C (<1) is the number of threshold critical masses represented by m, then the ratio of the density at this compressed radius to the initial density is given by

$$\frac{\rho_{compress}}{\rho_o} = \sqrt{\frac{1}{C}}.$$

Evaluate numerically for 100 g of ^{235}U.

2.10 The diffusion equation for neutrons in a bomb core, (2.18), can be applied in any coordinate system provided that the expression for $\nabla^2 N$ in that system is used. To this end, consider a *cubical* bomb core that extends from $0 \leq x \leq L$, $0 \leq y \leq L$, and $0 \leq z \leq L$. Solve the diffusion equation in Cartesian coordinates. Show that if the simplified boundary condition $N(L_C) = 0$ is used, then the side length for threshold criticality is given by

$$L_C = \frac{\pi}{\sqrt{v - 1}} \sqrt{\lambda_f \lambda_t},$$

where the symbols have the same meanings as in Sect. 2.2. Compare this result to that in Problem 2.4 to show that the critical mass for a cubical bomb core of a given material is $3^{5/2}/(4\pi) \sim 1.24$ times that for a spherical core of the same material. HINT: If you are familiar with quantum mechanics, the solution to this problem is very similar to that of a particle in a three-dimensional infinite potential box.

2.11 Consider a fission bomb made of a 60 kg core of pure ^{239}Pu (normal density) surrounded by a ^{238}U tamper (18.95 g/cm^3) of outer radius 17 cm. Use the numerical integration spreadsheet of Sect. 2.5 with the fissility parameters given in Appendix B for fast neutrons to determine the tamped threshold critical mass and yield of such a weapon. Take $\gamma = 1/3$, the average neutron energy to be 2 MeV, and the energy per fission to be 180 MeV.

2.12 It is remarked in Sect. 2.4 that in the case of a gas of uranium nuclei of normal density of that metal (18.95 g/cm^3), radiation pressure dominates gas pressure for per-particle energies greater than about 2 keV. This problem investigates this issue.

For a "gas" of photons, thermodynamics provides the following expression for the pressure:

$$P_{rad} = \left(\frac{8\pi^5 k^4}{45c^3 h^3}\right) T^4,$$

where k is Boltzmann's constant, c is the speed of light, h is Planck's constant and T is the absolute temperature. For a gas of "classical" particles, the ideal gas law can be cast as

$$P_{classical} = 10^6 \left(\frac{\rho N_A k}{A}\right) T,$$

where ρ and A are the density and atomic weight of the material in g/cm^3 and g/mol, respectively, and where N_A is Avogadro's number. Given that in the classical case the per-particle energy is $3kT/2$, show that radiation pressure will dominate over the gas pressure for per-particle energies satisfying

$$E > \frac{3}{2}\left(\frac{45 \times 10^6}{8\pi^5}\right)\left(\frac{ch}{e}\right)\left(\frac{\rho N_A}{A}\right)^{1/3} \sim (4.908 \times 10^{-5})\left(\frac{\rho N_A}{A}\right)^{1/3} \text{eV},$$

where e is the electron charge. Hence verify the ~2 keV figure for uranium.

3.1 See Fig. 6.11. A non-relativistic neutron initially traveling in the x-direction with kinetic energy K_n suffers a *completely elastic* collision with an initially stationary nucleus of rest mass m_A. The neutron scatters through angle θ while the struck nucleus scatters through angle ϕ as shown. After the collision the neutron and struck nucleus have kinetic energies K_n' and K_A, respectively. By conserving classical kinetic energy and momentum, eliminate ϕ and K_A to show that the initial and final neutron kinetic energies are related as

$$\sqrt{\frac{K_n'}{K_n}} = \frac{\cos\theta + \sqrt{\cos^2\theta + A^2 - 1}}{A + 1},$$
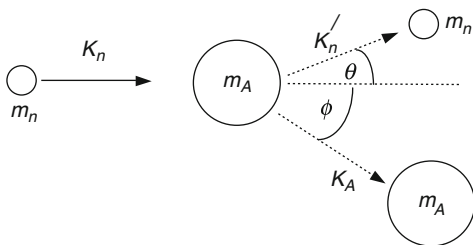
Fig. 6.11 Problem 3.1

where A is the mass ratio m_A/m_n. If a neutron strikes an initially stationary carbon nucleus ($A = 12$) and scatters through $\theta = 90°$, what will be the it's final speed in terms of its initial speed? Compare to the head-on case examined in Sect. 3.2.

3.2 Consider an ideal gas trapped within a sealed container at absolute temperature T. Working from the development in Sect. 3.5, show that the number of molecules that strike a square-meter area of the container wall per second is given by

$$\frac{P}{\sqrt{2 \pi m k T}},$$

where P is the pressure, m is the mass of an individual molecule, and k is Boltzmann's constant. HINT: Use the Boltzmann's-constant form of the Ideal Gas Law. Air is mostly diatomic nitrogen (N_2); standard atmospheric pressure is about 101,000 Pa. Evaluate your answer for $T = 300$ K.

3.3 Consider the first stage of a gaseous diffusion plant for separating uranium isotopes, where essentially all (139/140) of the atoms are ^{238}U. Suppose that vaporized pure uranium at $T = 300$ K and $P = 1$ atmosphere is pumped against a barrier; assume a vacuum on the other side. Working from your result in the previous problem, what total "hole area" S will you need if you want to process 140 kg of uranium per day? This would correspond to processing (although not isolating) 1 kg ^{235}U per day.

3.4 As in Problem 3.2, consider an ideal gas trapped within an initially sealed container at absolute temperature T. The wall of the container is punctured, resulting in a small hole of area A through which molecules of the gas can effuse; assume that the outside environment is a vacuum so that no molecules effuse from the outside back to the inside. Effusion represents a net *loss* of molecules from within the container.

(a) Working from the development in Sect. 3.5, show that, as a function of time, the pressure within the container will behave as

$$P = P_o e^{-t/\tau},$$

where P_o is the initial pressure and τ is a *characteristic effusion timescale* given by

$$\tau = \frac{4V}{A\langle v \rangle},$$

where V is the volume of the container and $\langle v \rangle$ is the average molecular speed. Assume that the temperature inside stays constant. The meaning of τ is that if the hole is not plugged, the pressure will drop to $1/e \sim 0.37$ of its initial value after τ seconds.

(b) A spacecraft cabin of volume 5 m^3 is punctured by a meteor, resulting in a hole of area 1 cm^2. If you model the atmosphere inside as pure diatomic nitrogen initially at standard atmospheric pressure and $T = 300$ K, what is the timescale τ in this case? Average molecular speed as a function of temperature is given by

$$\langle v \rangle = \sqrt{\frac{8\,k\,T}{\pi\,m}}.$$

3.5 A reactor fueled with uranium enriched to $F = 0.06$ produces electrical power at a rate of 750 MW with a thermal efficiency $\eta = 0.29$. What will be the rate of plutonium production in this reactor? Take $\sigma_{f5} = 584$ bn, $\sigma_{c8} = 2.7$ bn, and a fission energy of 180 MeV per reaction.

4.1 The half-life for spontaneous fission of $^{242}_{96}\text{Cm}$ is 7.0×10^6 year. What is the corresponding rate of spontaneous fissions per kg per second?

4.2 A rogue militia organization in an unstable country claims to have acquired 20 kg of Pu 239 of normal density and to have developed a crude gun-type bomb. The core contains 3% Pu 240. If they are to have a 50–50 chance of non-predetonation, what is the maximum tolerable assembly time? Take $S_{max} = 0$.

4.3 According to the publication of West & Sherwood cited in Sect. 4.3, the yield of 5.2 MeV alphas on ^{27}Al is 4.25×10^{-7}. If the number-density ratio of aluminum to the fissile material in a bomb core is held to 10^{-5}, what maximum rate of alpha-decays can be tolerated if the production of neutrons is to be kept to no more than 10^4 per second?

4.4 The purpose of this problem is to make a very crude estimate of the radioactivity produced by a fission weapon.
Suppose that fission of ^{235}U happens exclusively by the reaction

$$^{235}_{92}\text{U} + ^{1}_{0}\text{n} \rightarrow ^{141}_{56}\text{Ba} + ^{92}_{36}\text{Kr} + 3\left(^{1}_{0}\text{n}\right)$$
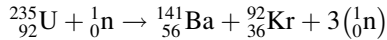
Assume that 1 kg of ^{235}U is fissioned in this way. ^{141}Ba and ^{92}Kr then both subsequently decay by beta-decay with half-lives of 18 min and 1.8 s, respectively. Use the decay rate expression of Sect. 4.2 to estimate the "immediate" beta-radioactivity so generated; ignore the neutrons released in the above reaction for sake of simplicity. If this radioactivity falls out over an area of 10 square miles, what will be the resulting immediate radioactivity in Curies per square meter? To put your result in perspective, household smoke detectors use 1 μCi alpha-emitters as ionization sources to help detect smoke particles.

6.9 Answers

1.1 (a) 17.59 MeV, (b) 4.78 MeV, (c) 182.2 MeV, (d) -2.64 MeV
1.2 7.34 g
1.3 4.784 MeV
1.4 (a) $E_\gamma = 5.24$ or 5.18 MeV
(b) $E_\gamma = 15.44$ or 15.21 MeV
(c) Reaction impossible; $E_\gamma = -48$ MeV forward; -46.5 MeV backward.

1.5 (a) Threshold 3.034; $Q = -2.642$; P & n energies 0.307, 2.051; both forward

    (b) No threshold; $Q = 17.59$; He & n energies 0.99, 19.60;
       He backward; n forward

    (c) No threshold; $Q = 1.674$; Ne & H energies
       0.068 and 4.356; both forward

    (d) Threshold 17.296; $Q = -16.141$; S & Mg energies 1.304
       and 12.56; S backward; Mg forward

    (e) Threshold 51.07; $Q = -47.85$; Es & D energies 2.816 and 9.330; both
       forward

1.6 $K_M^m / K_M^\gamma \sim 120$

1.7 $\Delta Q/Q \sim 0.07$; all approximations satisfied

1.8 8.57 m

1.9 $(F, B, C, D) = (0.3031, -0.3510, -0.2072, 0.2552)$; offset $= 4.183$ MeV

1.10 $d/R = 7.16$

2.1 $\sigma \sim 1.723$ bn

2.2 Penetration probability ~0.00863

2.3 8.63 ns

2.4 $R_C = 11.05$ cm; mass ~105.7 kg.

2.5 Diverges at $r = 0$.

2.6 $v(t_{crit}) \sim 3.68 \times 10^5$ m/s; ~ 1.9% neutron speed

2.7 $P(t_{crit}) \sim 6.20 \times 10^{15}$ Pa ~ 61 billion atmospheres

2.8 $R_o = 6.74$ cm; $M_o = 22.2$ kg. For $C = 3$, $\alpha_{eff} = 0.421$, $\Delta r = 1.95$ cm,
    efficiency $= 6.36\%$, yield $= 72$ kt (at 17 kt/kg), $t_{fiss} = 1.12$ μs, $t_{crit} = 1.07$ μs.

2.9 $r_{compress} = 3.91$ mm; $\rho_f = 21.15\,\rho_o$

2.10 Threshold tamped critical mass 10.26 kg; yield ~75 kt. The initial core radius
    is 9.72 cm; core radius at second criticality $= 14.41$ cm.

3.1 $v_{final}/v_{initial} = \sqrt{11/13}$

3.2 Strike rate ~2.904 $\times 10^{27}$ m^{-2}/s

3.3 4.12×10^{-6} m^2

3.4 About 7 min

3.5 223 g/day

4.1 7.806×10^9 kg^{-1}s^{-1}

4.2 2.70 μs

4.3 7.0×10^{15} s^{-1}

4.4 1.04×10^6 Ci/m^2

6.10 Appendix I: Further Reading

Apropos of the significance of the topic, an online search keyed on the phrase
"Manhattan Project" will typically return millions of hits, a number which will
surely grow as more and more previously classified material becomes publicly
available. Scientists and historians will continue to revisit both the technical and
human aspects of the project for years to come. While many of the sources that turn

up in an online search are interesting and well-researched, it can be difficult to sort through such a deluge of material for credible, objective information on the history, science, and personalities associated with the project. This appendix offers a brief, necessarily very limited, annotated bibliography of Manhattan Project books, journal articles, and websites. Some of the references listed here appear in various chapters in this book but are copied here for sake of completeness. A more complete bibliography can be found in the author's "Resource Letter MP-1: The Manhattan Project and related nuclear research", Am. J. Phys. **73**(9), 805–811 (2005).

The sources cited below are divided into four categories: general works, biographical and autobiographical works, technical works, and websites. Web addresses appear in *italic* font to discriminate them from surrounding text.

6.10.1 General Works

Coster-Mullen, J.: Atom Bombs: The Top Secret Inside Story of Little Boy and Fat Man (2010). This remarkable self-published work contains a trove of drawings, photographs, reproductions of documents, mission logs and reports and detailed descriptions of *Little Boy* and *Fat Man* and the Hiroshima and Nagasaki bombing missions. Available from online booksellers.

Fermi, R., Samra, E.: Picturing the Bomb: Photographs from the Secret World of the Manhattan Project. Harry N. Abrams, New York (1995). Beautifully reproduced and instructively captioned photographs of sites and artifacts associated with the MP. The first author is Enrico Fermi's granddaughter.

Gosling, F. G.: The Manhattan Project: Making the Atomic Bomb. U.S. Department of Energy (1999). A brief but very readable and well-illustrated summary. Available free from the DOE at *http://www.osti.gov/accomplishments/documents/fullText/ACC0001.pdf*.

Hersey, J.: Hiroshima. Knopf, New York (1985). Originally published in 1946, this compelling work of firsthand accounts of Hiroshima survivors is a "must read" for students of the MP. The edition cited here includes an additional chapter written 40 years later which brings the survivors stories up-to-date.

Hewlett, R.G., Anderson, O.E.: A History of the United States Atomic Energy Commission, Vol. 1: The New World, 1939/1946. Pennsylvania State University, University Park, PA (1962). Detailed history of the Manhattan Project prepared under the auspices of the Historical Advisory Committee of the U.S. Atomic Energy Commission. Full of facts, figures, dates, names, and places. Fully referenced to Manhattan Engineer District documents.

Jones, V.C.: United States Army in World War II. Special Studies. Manhattan: The Army and the Atomic Bomb. Center of Military History, United States Army, Washington, DC (1985). Comprehensive history of Army involvement in the Manhattan Project, fully referenced to Manhattan Engineer District documents. Unfortunately, this work no longer appears to be available through the Government Printing Office, but many libraries have copies.

Laurence, W.L.: Dawn Over Zero: The Story of the Atomic Bomb. Knopf, New York (1946). Laurence was a *New York Times* science reporter who was allowed to visit Los Alamos during the Project, witnessed the *Trinity* test, and rode aboard *Bockscar* on the Nagasaki bombing mission. This work was the one of the first serious popular accounts of the Project.

Rhodes, R.: The Making of the Atomic Bomb. Simon and Schuster, New York (1986). This remains the best current overall survey of the context, personalities, and science and engineering of the Manhattan Project. Some chapters are not directly germane to the Project, but Rhodes does a superb job of explaining the relevant physics in layman's language. Contains an extensive bibliography. A follow-on book, Dark Sun: The Making of the Hydrogen Bomb (Simon and Schuster, New York, 1995) details the development of the hydrogen bomb and is particularly interesting for its description of Soviet espionage in the United States during the Manhattan Project and afterward.

Smyth, H.D.: Atomic Energy for Military Purposes: The Official Report on the Development of the Atomic Bomb under the Auspices of the United States Government, 1940–1945. Princeton University Press, Princeton, NJ, (1948). This work was the first official report on the Manhattan Project. The edition cited here includes various appendices not included in the original 1945 edition. Various editions are readily available online.

Stoff, M.B., Fanton, J.F., Williams, R.H.: The Manhattan Project: A Documentary Introduction to the Atomic Age. McGraw Hill, New York (1991). This book includes reproductions of a number of official documents and memoranda concerning the Project. It is now somewhat dated because so much material is available online, but it is still worth perusing.

United States Department of Energy: The First Reactor (1982). This publication presents a brief, well-illustrated account of the first self-sustaining chain reaction. Available online at *http://www.osti.gov/accomplishments/documents/fullText/ACC0044.pdf*

6.10.2   *Biographical and Autobiographical Works*

Bernstein, J.: Hitler's Uranium Club: The Secret Recordings at Farm Hall. American Institute of Physics, New York (1996). At the end of the war, a number of leading German nuclear physicists including Werner Heisenberg were interned for 6 months at Farm Hall, an English country estate, and their conversations secretly recorded. Bernstein analyses the transcripts.

Bernstein, J.: Oppenheimer: Portrait of an Enigma. Ivan R. Dee, Inc., Chicago (2004). Engaging brief biography of Oppenheimer by one who knew him personally.

Bird, K., Sherwin, M.J.: American Prometheus: The Triumph and Tragedy of J. Robert Oppenheimer. Knopf, New York (2005). This book is likely to become the definitive biography of Oppenheimer. The authors particularly examine his

upbringing, ethical outlook, and postwar political activities. Descriptions of physics can be muddled in some places.

Cassidy, D.C.: Uncertainty: The Life and Science of Werner Heisenberg. W.H. Freeman, New York (1993). Published prior to release of the Farm Hall transcripts [see Bernstein (1996) above], this work continues to be the major scholarly biography of Heisenberg.

Cassidy, D.C.: J. Robert Oppenheimer and the American Century. Pi, New York (2005). A full scholarly biography of Oppenheimer. Cassidy devotes fairly little space to the well-trodden ground of Oppenheimer's Los Alamos years but gives a much more complete picture of his life and scientific work than many sources. Includes lists of Oppenheimer's publications and students.

Fermi, L.: Atoms in the Family: My Life with Enrico Fermi. University of Chicago Press, Chicago (1954). Fermi's life and work as related by his wife, Laura. Chapters 18–23 deal with the first chain-reacting pile and the Fermis' time at Los Alamos.

Frisch, O. What Little I Remember. Cambridge University Press, Cambridge (1979). Frisch helped to interpret fission, is generally credited with being the first experimenter to deliberately produce fission, and in collaboration with Rudolf Peierls estimated that the critical mass of U-235 might be on the order of kilograms.

Goodchild, P.: Robert Oppenheimer: Shatterer of Worlds. BBC, London, (1980). A well-illustrated treatment of the Manhattan Project and Oppenheimer's life.

Groves, L.R.: Now It Can Be Told: The Story of the Manhattan Project. Harper and Row, New York (1962). Now somewhat dated, but still valuable; the view from one who was there.

Howes, R.C., Herzenberg, C.C.: Their Day in the Sun: Women of the Manhattan Project. Temple University Press, Philadelphia (1999). Examines the lives and work of female physicists, chemists, biologists, technicians and others on the Project.

Norris, R.S.: Racing for the Bomb: General Leslie R. Groves, The Manhattan Project's Indispensable Man. Steerforth, South Royalton, VT (2002). Detailed account of the life and work of General Groves.

Pais, A., Crease, R.P.: J. Robert Oppenheimer: A Life. Oxford, New York (2006). Pais knew Oppenheimer from 1946 until the latter's death in 1967 and had completed about three-quarters of this work before his own passing in August 2000; it was completed by his widow and Robert Crease. The emphasis here is not so much on Oppenheimer's Los Alamos years but rather on his contributions to the growth of American theoretical physics, his postwar directorship of the Institute for Advanced Study, as a leader of conferences, and his service on numerous government committees.

Peierls, R.: Bird of Passage: Recollections of a Physicist. Princeton University Press, Princeton (1985). Memoirs of the other half of the Frisch-Peierls team; written with humor and warmth.

Segrè, E.: Enrico Fermi: Physicist. University of Chicago Press, Chicago (1970). Very readable biography by one of Fermi's closest collaborators.

6.10.3   Technical Works

Amaldi, E.: From the discovery of the neutron to the discovery of nuclear fission. Phys. Rep. **111** (1–4), 1–331 (1984). Masterful account of the development of nuclear physics during the 1930s; contains over 900 references. Amaldi's career began as a student of Fermi.

Bernstein, J.: Plutonium: A History of the World's Most Dangerous Element. Joseph Henry, Washington (2007). Reviews the history of the discovery of fission and plutonium, its bizarre chemical properties, and the crucial, often-overlooked contributions of metallurgists at Los Alamos.

Bernstein, J.: Nuclear Weapons: What You Need to Know. Cambridge University Press, Cambridge, UK (2008). This companion volume to the above entry summarizes the development of nuclear weapons from the discoveries of Thomson and Rutherford through the North Korean test of 2006. Full of interesting personal anecdotes and sidebar stories.

Brode, H.L.: Review of nuclear weapons effects. Annu. Rev. Nuc. Sci. **18**, 153–202 (1968). This article gives an advanced technical account of the fireball, shock, thermal, radiation, electromagnetic pulse, and fallout effects of nuclear explosions.

Broyles, A.A.: Nuclear explosions. Am. J. Phys. **50**(7), 586–594 (1982). An undergraduate-level account of the effects of nuclear explosions.

Fermi, E.: Experimental production of a divergent chain reaction. Am. J. Phys. **20** (9), 536–558 (1952). Description of Fermi's first critical pile, published on the tenth anniversary of that achievement.

Garwin, R.L., Charpak, G.: Megawatts and megatons: a turning point in the nuclear age? Knopf, New York (2001). Excellent treatment of nuclear power, nuclear weapons, radiation effects, waste disposal, and associated environmental and political issues.

Glasstone, S., Dolan, P.J.: The Effects of Nuclear Weapons, 3rd edn. United States Department of Defense and Energy Research and Development Administration, Washington (1977). This sobering volume summarizes technical analyses of the shock, blast, thermal, and radiation effects of nuclear explosions on structures and people. Available at a number of sites online; see, for example, *http://www. dtic.mil/cgi-bin/GetTRDoc? AD=ADA087568&Location=U2&doc=GetTRDoc.pdf*

Hawkins, D.: Project Y, The Los Alamos Story. Tomash, Los Angeles, (1983). Originally published as Los Alamos report LAMS-2532, Manhattan District History, Project Y, The Los Alamos Project. Now unfortunately out of print, this book gives a detailed technical and administrative history of Los Alamos from its inception through December 1946. However, the original Los Alamos report on which the book is based is available at *http://www.cfo.doe.gov/me70/ manhattan/publications/LANLMDHProjectYPart1.pdf*

Hoddeson, L., Henriksen, P.W., Meade, R.A., Westfall, C.: Critical Assembly: A Technical History of Los Alamos During the Oppenheimer Years, 1943–1945.

Cambridge University Press, Cambridge (1993). An authoritative technical history of Los Alamos during the war years.

Serber, R.: The Los Alamos Primer: The First Lectures on How To Build An Atomic Bomb. University of California Press, Berkeley (1992). The original lectures given by Serber to Los Alamos scientists in April 1943 are reproduced and supplemented by extensive annotations. Includes the March 1940 Frisch-Peierls memoranda that can be said to have started the Project.

6.10.4 Websites

Readers are cautioned that websites and addresses can change.

The Los Alamos National Laboratory's history website can be found at *http://www.lanl.gov/history*.

The *Bulletin of the Atomic Scientists* is a good source of up-to-date information on weapons deployments, treaties concerning nuclear weapons, and nuclear issues in general. *http://www.thebulletin.org*.

The National Science Foundation Digital Library on the Atomic Bomb at *www.atomicarchive.com* contains material on the history and science of the atomic bomb, and includes links to the full text of the Smyth report and the declassified version of Bainbridge's report on the Trinity test.

The office for history of science and technology at the University of California at Berkeley has created a website exploring Robert Oppenheimer's life. *http://ohst.berkeley.edu*.

The National Science Foundation-funded Alsos digital library for nuclear issues at *http://alsos.wlu.edu* provides links to a broad range of annotated references for the study of nuclear issues including books, articles, films, CDs and websites.

Carey Sublette maintains an extensive site on nuclear weapons at *http://nuclearweaponarchive.org/Nwfaq/Nfaq8.html*.

The homepage of the National Museum of Nuclear Science and History (Albuquerque, NM) can be found at *http://www.nuclearmuseum.org*.

The U.S. Department of Energy Office of History and Heritage Resources maintains an Interactive History website on the Manhattan Project at *http://www.cfo.doe.gov/me70/manhattan/index.htm*.

A number of National Nuclear Security Administration documents available under the Freedom of Information Act are available at *http://www.doeal.gov/opa/FOIAReadRmLinkst.aspx*.

The Nevada Site Office of the National Nuclear Security Administration offers an online collection of films of nuclear tests conducted between 1945 and 1962. *http://www.nv.doe.gov/library/films/testfilms.aspx*.

The Harry S. Truman Library and Museum makes available online a collection of documents, diary entries, letters and press releases relevant to President Truman's decision to use atomic bombs.

http://www.trumanlibrary.org/whistlestop/study_collections/bomb/large.

The Atomic Heritage Foundation is a non-profit organization dedicated to the preservation and interpretation of the Manhattan Project, and works with the Department of Energy and the former Manhattan Project communities to preserve historic resources and other aspects of the history. *http://www.atomicheritage.org*.

The Federation of American Scientists maintains a website where they make available copies of hundreds of Los Alamos Technical Reports and Publications. *http://www.fas.org/sgp/othergov/doe/lanl/index1.html*.

The B-Reactor Museum Association is a volunteer group that works with local, state and federal authorities to preserve the Hanford B reactor and turn it into a publicly-accessible museum. *http://www.b-reactor.org*.

I have prepared a spreadsheet-based timeline of the Manhattan Project, **MPTimeline.xls**; this is available at the companion website.

6.11   Appendix J: Useful Constants and Conversion Factors

Quantity	Symbol	Value	Unit
Speed of light	c	2.99792458×10^8	m/s
Electron charge	e	$1.602176462 \times 10^{-19}$	C
Planck's constant	h	$6.62606876 \times 10^{-34}$	Js
Permittivity constant	ε_O	$8.85418782 \times 10^{-12}$	C^2/Jm
Avogadro's number	N_A	$6.02214199 \times 10^{23}$	mol^{-1}
Atomic mass unit	u	$1.66053873 \times 10^{-27}$	kg
Boltzmann constant	k	$1.3806503 \times 10^{-23}$	J/K
Kiloton TNT	kt	4.2×10^{12}	J
Fission 1 kg ^{235}U		7.1×10^{13}	J
Fission 1 kg ^{235}U		~17	kt
Curie	Ci	3.7×10^{10}	$decay/s$
Calorie	cal	4.186	J

6.11.1   Rest Masses

	10^{-27} kg	amu	MeV
Proton	1.67262158	1.00727646688	938.271998
Neutron	1.67492716	1.00866491578	939.565330
Electron	0.000910938188	0.0005485799110	0.510998902
Alpha	6.64465598	4.0015061747	3727.37904

Index